ANALYSIS OF NON-LINEAR SELF-EXCITED VIBRATIONS FOR MULTIPLE DEGREES OF FREEDOM SYSTEMS

Md. Sayem Uddin

BANGLADESH UNIVERSITY OF ENGINEERING AND TECHNOLOGY

DHAKA-1000, BANGLADESH

ANALYSIS OF NON-LINEAR SELF-EXCITED VIBRATIONS FOR MULTIPLE DEGREES OF FREEDOM SYSTEMS

By

Md. Sayem Uddin

A Thesis

Submitted to the

Department of Mechanical Engineering

In partial fulfillment of the requirements for the degree of

MASTER OF SCIENCE IN MECHANICAL ENGINEERING

BANGLADESH UNIVERSITY OF ENGINEERING AND TECHNOLOGY

Dhaka-1000, Bangladesh

March 2010

ACKNOWLEDGEMENTS

The author wishes to express his deep gratitude and indebtedness to Dr. Muhammad Ashiqur Rahman, Professor, Department of Mechanical Engineering, Bangladesh University of Engineering and Technology (BUET), Dhaka-1000, Bangladesh for his supervision, constant guidance, invaluable suggestions and constructive criticism throughout the thesis and patiently reading the manuscript and suggesting the improvements. The author is grateful also to Mr. Ashraf Uddin Ahmed for his suggestions in developing the program code.

CONTENTS

ABSTRACT

Dynamics of nonlinear self-excited vibrations for both two degrees of freedom system (2DOFS) and three degrees of freedom system (3DOFS) using nonlinear springs and dampers is treated as a boundary value problem (BVP) considering the self-exciting force as a function of displacement, velocity or combination of both and nonlinear displacement terms. Four different cases have been considered for this analysis. Each case comprises of four different conditions depending on self-excited force function. For different cases, a comparative study is performed varying the values of parameters to find out whether the system is stable or not. Nonlinearity is also considered for both springs and dampers to check the effect on the system's response. A code has been developed to determine the response of the system. Some parameters for system's stability have been determined from the system's response obtained from the results of the developed code. It has also been tried to identify some parameters for which the system always tends to be unstable. The system's behavior has also been observed by changing the values of self-excited force coefficients. Numerical analysis using multi-segment integration technique also shows the various phase planes and limit cycles in case of Van der Pol equation for various values of damping term, μ. This validates the developed code in analyzing such problems.

CERTIFICATE OF APPROVAL

This thesis titled, **“Analysis of Non-linear Self-excited Vibrations for Multiple Degrees of Freedom Systems”**, submitted by **Md. Sayem Uddin,** Roll No. **040810016 F**, Session: **April 2008** has been accepted as satisfactory in partial fulfillment of the requirement for the Degree of MASTER OF SCIENCE IN MECHANICAL ENGINEERING on 8 March 2010.

BOARD OF EXAMINERS

____

Dr. M. Ashiqur Rahman — Chairman (Supervisor)
Professor
Department of Mechanical Engineering
BUET, Dhaka-1000, Bangladesh.

____

Dr. Md. Maksud Helali — Member
Professor
Department of Mechanical Engineering
BUET, Dhaka-1000, Bangladesh.

____

Dr. Muhammad Mahbubul Alam — Member (Ex-Officio)
Professor & Head
Department of Mechanical Engineering
BUET, Dhaka-1000, Bangladesh.

____

Dr. Muhammad Fazli Ilahi — Member (External)
Professor (Ex- VC, IUT, OIC)
House No. 13, Road No.1, Sector 11,
Uttara Model Town, Dhaka-1230.

DECLARATION

It is hereby declared that this thesis or any part of this has not been submitted elsewhere for the award of any degree or diploma.

Md. Sayem Uddin

TO

MY PARENTS

CHAPTER 1

INTRODUCTION

The force acting on a vibrating object is usually external to the system and independent of the motion. However, there are systems in which the exciting force is a function of the motion variables (displacement, velocity or acceleration) and thus varies with the motion it produces. Friction-induced vibration (in vehicle clutches and brakes, vehicle-bridge interaction) and flow-induced vibration (circular wood saws, CDs, DVDs, in machining, fluid-conveying pipelines) are examples of self-excited vibration.

When a mass supported by a spring is carried by a moving belt through friction, the friction coefficient at the mass and belt interface is a function of the relative velocity between the mass and the belt and hence the moving belt can sustain self-excited vibration.

Some mechanical systems have frictional joints where one surface slides on another with dry friction. Under certain conditions, the steady state sliding motion becomes unstable. The instability leads to the occurrence of stable limit-cycle type self-excited vibrations [D'Souza and Dweib (1990)].

Squeal is a form of self-excited vibrations induced in a structure such as a wheel or violin string by the action of a frictional driving force [McMillan (1997)]. Brake squeal noise is still an issue since it generates high warranty costs for the automotive industry and irritation for customers [Coudeyras et al. (2009)].

The conventional cantilever type of aircraft landing gear, when fitted with brakes, can exhibit two main forms of friction-induced self-excited vibration [Thorby (2008)]:

(1) When the brakes are working normally, if the coefficient of friction between the rubbing surfaces in the brakes tends to decrease as the velocity increases, negative damping may result, producing the vibration known as ‘brake judder’ or ‘brake chatter’, at low frequencies, or ‘brake squeal’ at high frequencies.

(2) When the brakes lock completely, perhaps because the anti-skid device, if fitted, does not always operate down to very low speeds, the friction characteristics between the tires and the runway can then provide the negative damping instead. Measurements of tire

friction show that the negative slope of μ versus v, necessary for instability, tends to occur when the runway is wet, and the speed is low.

In both cases, the oscillations of the gear, in the fore-and-aft direction, can be quite pronounced, and lead to possible fatigue damage.

Self-excited vibrations pervade all areas of design and operations of physical systems where motion or time-variant parameters are involved — aeromechanical systems (flutter, aircraft flight dynamics), aerodynamics (separation, stall, musical wind instruments, diffuser and inlet chugging), aerothermodynamics (flame instability, combustor screech), mechanical systems (machine-tool chatter), and feedback networks (pneumatic, hydraulic, and electromechanical servomechanisms).

The vibration that occurs in most machines, structures and dynamic systems is undesirable, not only because of the resulting unpleasant motions, the noise and the dynamic stresses which may lead to fatigue and failure of the structure or machine, but also because of the energy losses and the reduction in performance that accompany the self-excited vibrations. It is therefore essential to carry out an analysis of self-excited vibrations of any proposed system for importance of performance and efficiency.

There have been many cases of systems failing or not meeting performance targets because of resonance, fatigue or excessive vibration of one component or another. Because of the very serious effects that unwanted vibrations can have on dynamic systems, it is essential that vibration analysis be carried out as an inherent part of their design; when necessary modifications can most easily be made to eliminate vibration or at least to reduce it as much as possible [Beards (1996)].

All real systems dissipate energy when they vibrate. The energy dissipated is often very small, so that an undamped analysis is sometimes realistic; but when the damping is significant its effect must be included in the analysis, particularly when the amplitude of vibration is required. Energy is dissipated by frictional effects, for example that occurring at the connection between elements, internal friction in deformed members, and windage. The most common types of damping are viscous, dry friction and hysteretic. Hysteretic damping arises in structural elements due to hysteresis losses in the material. The type and amount of damping in a structure has a large effect on the dynamic response levels.

The effect of damping is mainly evident in the diminishing of the vibration amplitude with time. Normal mode vibrations are free undamped vibrations that depend only on the mass and stiffness of the system and how they are distributed. When vibrating at one of these normal modes, all points in the system undergo simple harmonic motion that passes through their equilibrium positions simultaneously. To initiate a normal mode vibration, the system must be given specific initial conditions corresponding to its normal mode. When excitation frequency coincides with one of the natural frequencies of the system, a condition of resonance is encountered with large amplitudes limited only by the damping. Again damping is generally omitted except when its concern is of importance in limiting the amplitude of vibration or in examining the rate of decay of the free oscillation.

Self-excited vibration is one of the major problems in the field of aerofoil, jet engines as well as modern industrial turbo machines. This type of vibration can occur due to friction or within a strong fluid flow. Asfar and Akour (2005) performed a numerical study for the suppression of self-excited vibrations using an impact viscous damper. Chatterjee (2007) introduced a new method of controlling friction-driven self-excited vibrations. Plaut and Limam (1991) studied a class of self-excited mechanical or structural systems subjected to parametric excitation using equations of motion that included weak quadratic and cubic non-linearities in the stiffness, small negative linear damping terms and small positive cubic damping terms and took in account the special cases of Van Der Pol's equation and Rayleigh's equation. Dohnal's (2007) investigations on vibration suppression were performed on systems with two and more degrees of freedom with linear spring and damping elements that were subjected to self-excitation as well as parametric excitation by simultaneous stiffness and damping variation. Pust and Tondl (2008) investigated a two-mass system consisting of a self-excited basic system which was mounted on a foundation subsystem consisting of a mass on a spring by means of analytical and numerical solution and made a comparison between phase plane trajectories gained by numerical solution and analytical solution. Tondl and Nabergoj (2004) figured out the effect of parametric excitation on a self-excited three-mass system and showed that the self-excitation could be fully or partly suppressed in a particular frequency interval. Rudowski (1982) applied analytical approximate methods to check the possibility of generating stable multi-frequency almost-periodic limit cycles in ***n***-degree-of-freedom self-excited systems.

In previous studies, different mathematical techniques like Runge-Kutta integration method, Bifurcation method [Asfar and Akour (2005) and Chatterjee (2007)], Univariate search optimization method [Asfar and Akour (2005)], Method of multiple scales [Asfar et al. (1982) and Asrar (1991)] and Singular perturbation method of first order [Dohnal (2007)] have been used to solve self-excited vibration problems. Any such numerical technique that makes the computation faster and yields reliable results under any practically possible boundary conditions (in terms of displacement, velocity etc. of the vibrating bodies) would be much desirable. Present study aims to develop a new model for studying self-excited vibrations especially for a multiple degrees of freedom system (MDOFS). Multi-segment method of integration (MSMI) is a powerful scheme originally developed to study the response of shells in terms of highly nonlinear boundary value problem (BVP) [Kalnins and Lestingi (1967)]. Since the present study also intends to incorporate BVP, MSMI has been tried to solve the nonlinear equations of self-excited vibration systems. For this analysis, self-developed code using programming language C has been used.

A couple of terms used in vibration problem analysis are discussed below:

1.1 Degrees of Freedom (DOF):

"Degrees of freedom" can be described simply as the number of coordinates that it takes to uniquely specify the position of a system. Degrees of freedom (DOF) are the set of independent displacements and/or rotations that specify completely the displaced or deformed position and orientation of the body or system. A degree-of-freedom for a system is analogous to an independent variable for a mathematical function.

The number of independent coordinates required to describe the motion of a system is called degrees of freedom of the system. The free particle undergoing general motion in space will have three degrees of freedom, and a rigid body will have six degrees of freedom, i.e., three components of position and three angles defining its orientation. Furthermore, a continuous elastic body will require an infinite number of coordinates (three for each point on the body) to describe its motion; hence its degrees of freedom must be infinite. However, in many cases, parts of such bodies may be assumed to be rigid, and the system may be considered to be dynamically equivalent to one having finite degrees of freedom. In fact, a surprisingly large number of vibration problems can be treated with sufficient accuracy by reducing the system to one having a few degrees of freedom.

1.2 Stability of a System:

A system is said to maintain stability if it can sustain a small disturbance from its equilibrium condition at any level of external cause in any form of displacements, velocity, force etc. It should be noted that sustaining the disturbance means the structure would oscillate with small amplitude about its equilibrium position. On the other hand, if the structure does not go back to its original position or vibrate with ever increasing amplitude due to the disturbance, then the structure is said to be in an unstable state at that level of external cause. A close assessment of the critical load for simple mechanical stability models reveals that the system maintains its state of equilibrium states as long as the work done due to internal resisting forces is greater than that due to the external load for any disturbance from the equilibrium position. In other words, it is the balance between the potential energy due to the internal resisting forces, called internal strain energy or simply strain energy, and the potential energy due to the external force.

1.3 Nonlinear Springs and Dampers:

In general nonlinear vibrations are not harmonic, and their frequencies vary with amplitude. Superposition principle cannot be applied to solve such type of problems. One important type of nonlinearity arises when the restoring force of a spring is not proportional to its deformation. A spring is called nonlinear when the force exerted by the spring is the nonlinear function of the displacement. For nonlinear spring,

$$\textit{Spring force} = kx \pm k'x^3 \qquad \text{………………} (1.1)$$

Where, k and k' are spring constants, x is the displacement of the spring. If positive (+) sign is used the spring is called hard. For soft spring, negative (–) sign is used.

The static load-displacement curve for hard spring shows the slope increases as the load increases. Similarly the load – displacement curve for a soft spring shows that the slope decreases as the load increases. Similarly for nonlinear dampers,

$$\textit{Damper force} = c\dot{x} \pm c'\dot{x}^2 \qquad \text{…………….} (1.2)$$

Where, c and c' are damping constants, $\dot{x}$ is the velocity of the moving body. Hard and soft dampers follow similar relations like hard and soft springs respectively [Timoshenko (1974)].

1.4 Van der Pol Equation

One of the interesting non-linear equations that has been studied extensively is the Van der Pol equation.

$$\frac{d^2x}{dt^2} - \mu(1 - x^2)\frac{dx}{dt} + x = 0$$

where x is the position coordinate — which is a function of the time t, and μ is a scalar parameter indicating the strength of the damping.

This equation somewhat resembles that of free vibration of a spring-mass system with viscous damping; however, the damping term of this equation is non-linear in that it depends on both the velocity and displacement.

Oscillation of the Van der Pol equation is one of many examples of self-excited vibration. In dynamics, the Van der Pol oscillator is a non-conservative oscillator with non-linear damping. It evolves in time according to the second order Van der Pol differential equation.

Two interesting regimes for the characteristics of the unforced oscillator are:

- When $\mu = 0$, i.e. there is no damping function, the equation becomes:

$$\frac{d^2x}{dt^2} + x = 0$$

  This is a form of the simple harmonic oscillator and there is always conservation of energy.

- When $\mu > 0$, the system will enter a limit cycle, where energy continues to be conserved. Near the origin $\dot{} = dx/dt = 0$ the system is unstable, and far from the origin the system is damped. Energy can be lost or gained, and work is done, if the system does not enter a limit cycle immediately.

1.5 Phase Plane

A phase plane is a visual display of certain characteristics of certain kinds of differential equations. In an autonomous system, time *t* does not appear explicitly in the differential equation of motion. Thus, only the differential of time, *dt* appears in such equation.

If the differential equation of an autonomous system be

$$\ddot{x} + f(x, \dot{x}) = 0$$

Where $f(x, \dot{x})$ can be a non-linear function of x and $\dot{x}$. In the method of state space, the differential equation is expressed in terms of two first-order differential equations as follow:

$$\dot{x} = y \quad \text{and} \quad \dot{y} = -f(x, y)$$

If *x* and *y* are Cartesian coordinates, the *xy*-plane is called the phase plane. The state of the system is defined by the coordinate *x* and $y = \dot{x}$, which represents a point on the phase plane. As the state of the system changes, the point on the phase plane moves, thereby generating a curve that is called the trajectory.

Phase planes are useful in visualizing the behavior of physical systems; in particular, of oscillatory systems such as Van der Pol oscillator. This "spiral in" towards zero, "spiral out" towards infinity, or reach neutrally stable situations called centers where the path traced out can be circular, elliptical, or ovoid, or some variant thereof. This is useful in determining if the dynamics are stable or not.

1.6 Isocline

An **Isocline** is a series of lines with the same slope. It is often used as a graphical method of solving ordinary differential equations. In an equation of the form $\dot{y} = f(x, y)$, the isoclines are lines in the (*x*, *y*) plane obtained by setting *f*(*x*,*y*) equal to a constant. This gives a series of lines (for different constants) along which the solution curves have the same gradient. By calculating this gradient for each isocline, the slope field can be visualized; making it relatively easy to sketch approximate solution curves as shown in the following figure.

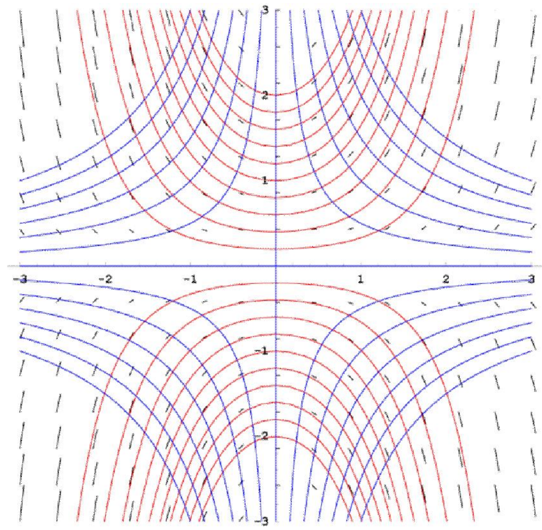

Figure 1.1 : Isoclines

1.7 Objectives with specific aims and possible outcomes:

In studies of non-linear self-excited vibrations, usually initial value problems were solved. But present work aims to solve both boundary and initial value problems for non-linear self-excited vibratory systems. Multi-segment integration technique [Kalnins and Lestingi (1967)] that helps to directly visualize the system's response with time would be very useful, in particular for the present study, when a boundary value problem is dealt with. Very recently Rahman and Ahmed (2009) and Ahmed (2009) used this method for stability analysis of vibration absorbers in terms of nonlinear boundary value problem. Therefore, objectives of this study can be described as below:

a) To study the nonlinear dynamic behavior of MDOFS varying the nonlinearity of self-excited vibrations. Similarly, springs and dampers can also be varied to incorporate different types of linear or nonlinear combinations.
b) To study the effect of changing boundary conditions on the system's response.
c) To investigate the deviation of the system from stable to unstable conditions and from unstable to stable conditions.
d) To find the response of the system for different mass ratios and spring constant ratios.
e) To find out the parameters that would make the self-excited vibrations unbounded and those that are beneficial. This will help to visualize the self-excited vibration suppression parameters.

f) Soundness of the code will be checked by comparing the available exact result for the case of self-excited vibrations given by Thomson and Dahleh (2003).

It will be possible to elaborately focus on the strategy to suppress the self-excited vibrations. Eventually this will be a handy tool for a self-excited vibration control scheme. Additionally, the effect of different types of nonlinearities on the stability of the system can be also studied. In future, the developed computer code can be extended to study self-excited vibrations of continuous systems.

1.8 Outline of Methodology:

A generalized computer code will be developed for nonlinear self-excited vibration analysis of a multiple degrees of freedom system having either linear or nonlinear springs and dampers. Computer coding will be done using Turbo *C*. Multi-segment method of integration developed by Kalnins and Lestingi (1967) will be used to solve the coupled nonlinear differential equations as boundary value problems. Specialty of this method is that the given interval of the independent variable is divided into finite number of segments. Next, initial value integration is performed over each segment followed by a solution of a system of matrix equations to ensure continuity of the dependent variables at all the nodal points. Steps are repeated until continuity of the dependent variables at the nodal points is achieved.

.

CHAPTER 2

LITERATURE REVIEW

Self-excited vibrations are often encountered in practice, with detrimental effects such as excessive wear of components, surface damage, fatigue failure and noise generation. To analyze the self-excited vibrations and to illustrate the effectiveness of the active vibration isolation in some linear self-excited systems (such as structures subject to flutter, rotor machines and tubes conveying fluid), various scholars tried in various ways.

Asfar and Akour (2005) presented a numerical study for the suppression of self-excited vibrations represented by a Rayleigh oscillator using an impact viscous damper. A systematic approach based on a univariate search optimization method was used to determine the best design parameters for suppressing self-excited vibrations and thus Optimum parameters for complete quenching of such vibrations were obtained. Their suggested system has been found to be effective in suppressing this type of vibration.

Chatterjee (2007) introduced a new method of controlling friction-driven self-excited vibration. The control law was primarily derived using the Lyapunov's second method. A single degree-of-freedom oscillator on a moving belt represented the primary model of the considered system. The control action was achieved by modulating the normal load at the frictional interface based on the state of the oscillatory system. The basic mechanism of the control action utilized subcritical Hopf bifurcation of the equilibrium followed by cyclic-fold bifurcation (of limit cycle oscillations) to globally stabilize the equilibrium. An approximate method for estimating the critical value of the control parameter that ensures global stability of the equilibrium was also proposed.

By using the method of multiple scales, various resonances were analyzed by Plaut and Limam (1991) to determine steady state response- amplitudes of a class of self-excited mechanical or structural systems having an arbitrary number of generalized co-ordinates and subjected to parametric excitation and were plotted as functions of a detuning parameter, excitation amplitudes. The equations of motion included weak quadratic and cubic non-linearities in the stiffness, small “negative” linear damping terms, and small “positive” cubic damping terms. Special cases were Van der Pol's equation and Rayleigh's equation. The parametric excitation included multiple frequencies

Stability investigations on vibration suppression employing the concept of actuators with variable stiffness and damping elements were presented by Dohnal (2007). Systems subjected to self-excitation as well as parametric excitation by simultaneous stiffness and damping variation with two and more degrees of freedom with linear spring- and damping-elements were considered.

Expressing the self-excitation in differential equations by a non-linear term of the second power, a two-mass system, consisting of a self-excited basic system was analyzed by Pust and Tondl (2008) to investigate the efficiency of the self-excited vibration suppressing of different positive damping components by means of analytical and numerical solution. Zhu et al. (2004) extensively studied nonlinear response of two degrees of freedom (2DOF) vibration system with nonlinear damping and nonlinear springs.

Tondl and Nabergoj (2004) examined a three-mass chain system in detail to deal with the quenching of self-excited vibrations by means of parametric excitation due to periodic variation of spring stiffness. They showed that the self-excitation can be fully or partly suppressed in a particular frequency interval.

A possibility of generating stable multi-frequency almost-periodic limit cycles in *n*-degree-of-freedom self-excited systems with non-linear forces was investigated by Rudowski (1982) using analytical approximate methods. He analyzed several examples of two-degree-of-freedom systems with Van der Pol terms in detail. He considered the effect of non-linear restoring forces and proved the possibility of occurrence of multi-frequency limit cycles through analytical methods and confirmed by analogue computer results.

Dweib and D'Souza (1990) conducted an experimental investigation in the laboratory to study self-excited vibrations induced by dry friction. They analyzed the waveforms of the self-excited vibrations and proposed a mathematical model of the contact, including non-linear contact stiffness and damping based on experimental data. This model of contact mechanics is necessary for stability analysis. They also conducted a parametric study to assess the influence of the system parameters on the stability of the steady state sliding motion. The method of triple-input describing functions is used with a non-linear model to analyze the resulting self-excited vibrations.

Dohnal (2007) investigated the **s**tability on vibration suppression employing the concept of actuators with variable stiffness and damping elements considering systems with two and more degrees of freedom with linear spring and damping elements and systems subjected to self-excitation as well as parametric excitation by simultaneous stiffness and damping variation. The general conditions for full vibration suppression were also derived analytically. Tondl (1975) presented an analysis of the possibility of initiation of two-frequency self-excited vibrations.

A novel nonlinear method called the Constrained Harmonic Balance Method (CHBM) was presented by Coudeyras et al. (2009) that works for nonlinear systems subject to flutter instability. By an analysis of disc brake squeal, they also performed both stability and non-linear analysis.

For the rolling slipping state of a main drive system, Wang and Wang (1998) established the nonlinear mechanical model of the main drive system and used the Krilov–Bogolubov method to produce the solution of the nonlinear mechanical model and ascertained the condition of generating self-excited vibration.

Analyzing the dynamic properties of the rotor on which the fluid force and the impact force (due to mass variation) act, the conditions of stable rotation were obtained by Cveticanin (1998) applying the direct Lyapunov theorem. The self-excited vibrations were determined analytically. Analyzing the amplitude of self-excited vibrations, the conditions of unstable motion were also defined.

Uczko (2002) introduced a geometrically non-linear model of the rotating shaft and this model was used to analyze the phenomenon of internal resonance and the influence of some of the system's parameters on the amplitude and frequency of self-excited vibration.

McMillan (1997) attempted to develop a dynamical system considering the phenomenon of squeal simplified the vibrating structure to that of a block resting on a moving conveyor belt restrained by a simple spring and dashpot to a rigid wall. Asfar et al. (1982) analyzed the response to multi-frequency excitation of a two-degree-of-freedom self-excited system by using the method of multiple scales. Steady state and stability analyses were carried out for each case and numerical results were presented showing the influences of the several parameters.

A universal active vibration isolation strategy was presented by Kravchenko (1994). The applications of this strategy to linear and parametrically self-excited structures were also investigated. Sinou and Jézéquel (2007) investigated qualitative aspects of mode-coupling instability of self-excited friction-induced oscillations in the presence of structural damping and a cubic nonlinearity examining the influence of structural damping on limit cycle amplitudes in order to achieve a complete design including not only the evolution of stable/unstable areas but also the evolution of limit cycle amplitudes as functions of the structural damping and nonlinear system parameter.

The time-dependent amplitude response of the self-excited harmonium reed vibrating at finite amplitudes was investigated by Hilaire (1976) both analytically and experimentally. Asrar (1991) used the method of multiple scales to study the response of two-degree-of-freedom systems with quadratic non-linearities under the simultaneous effects of a harmonic parametric excitation and self- excitation. The stability of the system was also studied and amplitude and frequency response curves were presented for both cases.

Practically self-excited vibration problems become nonlinear in nature as amplitude of oscillation becomes large [Ahmed (2009), Rahman et al. (2009)]. Nonlinear problems, usually having no closed form solutions, are always challenges for practicing engineers. Two widely used solution techniques are perturbation and iteration methods [Thomson and Dahleh (2003) and Zhu et al. (2004)] for the cases of nonlinear vibrations. Superposition principle cannot be applied and therefore different mathematical techniques are being tried to solve such problems. Any such numerical technique which makes the computation faster and yield reliable results under any practically possible boundary conditions (in terms of displacement, velocity etc., of the vibrating bodies), especially for MDOFS, would be much desirable.

Present work aims to solve both boundary and initial value problems for any system having MDOF undergoing self-excited vibration. A simple and direct method, like multi-segment integration technique, that helps to directly visualize the system's response with time, would be very useful, in particular for the present study, when a boundary value problem is dealt with.

Present investigation is to study the nonlinear dynamic behavior of self-excited vibration system having nonlinear spring with and without nonlinear damping but extensively varying the spring type for various values of self-exciting force factors. The solutions must be obtained solving highly nonlinear equations that are coupled. The problem is involved as the two boundary conditions are specified at two different times.

With the background of all relevant works as cited in the list of references [1]-[37], the present work is likely to yield new and interesting results.

CHAPTER 3

GOVERNING EQUATIONS AND METHOD OF SOLUTION

3.1 Governing Equations

Several methods can be used to set up the differential equation of motion for any system subjected to vibration. One of the methods is the inspection of the forces involved, using Newton's second law, with D'Alembert's principle, and the fundamental properties of mass, stiffness and damping. For purposes of demonstration and discussion, the necessary concepts will be introduced primarily by working through the solution of a 2DOFS. All these ideas transfer to larger systems, but with the 2DOF model we can demonstrate the key ideas without the complications of the major algebraic and numerical demands made by the larger systems.

For the system shown in Figure 3.1, we can derive the coupled equations of motion using Newton's Second Law of motion applied to a free body diagram for each mass, as shown in Figure 3.1. Governing equations of the system are derived from the free-body diagram [Thomson and Dahleh (2003), De Silva (2005)] given in Figure 3.1, considering nonlinear springs, nonlinear dampers and self-exciting forces acting on both masses. After rearranging and necessary transformation, 2nd order differential equations are converted to first order differential equations. By necessary partial differentiation with respect to initial conditions of the transformed variables, field equations for Multi-segment Integration Technique are formed.

3.1.1 Mathematical Models and Governing Equations

Following Fig. 3.1, we get

Spring force for the 1st spring = $k_1 x_1 + k_1' x_1^{\,3}$ ……... (3.1)

Spring force for the 2nd spring= $k_2(x_1 - x_2) + k_2'(x_1 - x_2)^3$ ………. (3.2)

Damping force for the 1st damper= $c_1 \dot{x}_1 + c_1' \dot{x}_1 x_1^2$ ………. (3.3)

Damping force for the 2nd damper= $c_2(\dot{x}_1 - \dot{x}_2) + c_2'(\dot{x}_1 - \dot{x}_2)(x_1 - x_2)^2$ ……… (3.4)

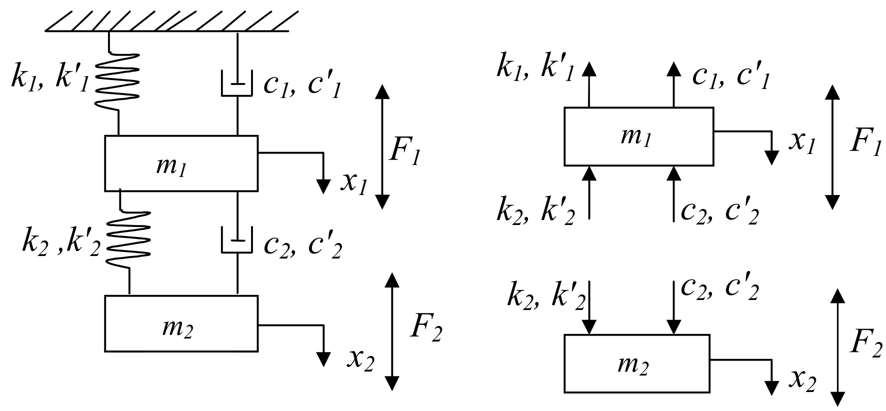

Fig.3.1 Arrangement of masses, springs and dampers for self-excited vibration of 2DOFS.

The equations of motion are as follows for m_1 and m_2 , respectively,

$$m_1\ddot{x}_1 + \left(k_1x_1 + k_1'x_1^3\right) + \left(c_1\dot{x}_1 + c_1'\dot{x}_1x_1^2\right) + \left\{k_2\left(x_1 - x_2\right) + k_2'(x_1 - x_2)^3\right\} + \left\{c_2\left(\dot{x}_1 - \dot{x}_2\right) + c_2'\left(\dot{x}_1 - \dot{x}_2\right)\left(x_1 - x_2\right)^2\right\} = F_1 \quad \text{……. (3.5)}$$

$$m_2\ddot{x}_2 - \left\{k_2\left(x_1 - x_2\right) + k_2'(x_1 - x_2)^3\right\} - \left\{c_2\left(\dot{x}_1 - \dot{x}_2\right) + c_2'\left(\dot{x}_1 - \dot{x}_2\right)\left(x_1 - x_2\right)^2\right\} = F_2 \quad \text{……. (3.6)}$$

Here F_1 and F_2 are the generalized self-excited forces of the considered system.

$$F_1 = \alpha_1 x_1 + \beta_1\dot{x}_1 + \gamma_1 x_1^2\dot{x}_1 \quad \text{………… (3.7)}$$

$$F_2 = \alpha_2 x_2 + \beta_2\dot{x}_2 + \gamma_2 x_2^2\dot{x}_2 \quad \text{………….. (3.8)}$$

If only α_1 & α_2 are nonzero, F_1 and F_2 are functions of displacements only. If only β_1 & β_2 are nonzero, F_1 and F_2 are functions of velocity only. If γ_1 & γ_2 are nonzero, F_1 and F_2 are functions of non-linear displacement term only.

Basic governing equations for 3DOFS are given in Appendix C. The developed code is given in Appendix D.

For using multi-segment method of integration, similar types of dependent variables will be of useful for forming systems of equations. So for transformations,

let $x_1 = y_1$, $\frac{dx_1}{dt} = \dot{x}_1 = y_2$, $x_2 = y_3$, and $\frac{dx_2}{dt} = \dot{x}_2 = y_4$

With those transformations, Equations 3.5 and 3.6 become,

$$m_1 \frac{dy_2}{dt} + \left(k_1 y_1 + k_1' y_1^3\right) + \left(c_1 y_2 + c_1' y_2 y_1^2\right) + \left\{k_2\left(y_1 - y_3\right) + k_2'\left(y_1 - y_3\right)^3\right\} + \left\{c_2\left(y_2 - y_4\right) + c_2'\left(y_2 - y_4\right)\left(y_1 - y_3\right)^2\right\} = F_1 = \alpha_1 y_1 + \beta_1 y_2 + \gamma_1 y_1^2 y_2 \quad \text{.........} \quad (3.9)$$

$$m_2 \frac{dy_4}{dt} - \left\{k_2\left(y_1 - y_3\right) + k_2'\left(y_1 - y_3\right)^3\right\} - \left\{c_2\left(y_2 - y_4\right) + c_2'\left(y_2 - y_4\right)\left(y_1 - y_3\right)^2\right\} = F_2 = \alpha_2 y_3 + \beta_2 y_4 + \gamma_2 y_3^2 y_4 \quad \text{.........} \quad (3.10)$$

Rearrangement of Equation (3.9) & (3.10) gives,

$$\frac{dy_2}{dt} = \frac{1}{m_1}\begin{bmatrix} F_1 - \left(k_1 y_1 + k_1' y_1^3\right) - \left(c_1 y_2 + c_1' y_2 y_1^2\right) - \left\{k_2\left(y_1 - y_3\right) + k_2'\left(y_1 - y_3\right)^3\right\} \\ - \left\{c_2\left(y_2 - y_4\right) + c_2'\left(y_2 - y_4\right)\left(y_1 - y_3\right)^2\right\} \end{bmatrix} \quad \text{.........} \quad (3.11)$$

$$\frac{dy_4}{dt} = \frac{1}{m_2}\left[F_2 + \left\{k_2\left(y_1 - y_3\right) + k_2'\left(y_1 - y_3\right)^3\right\} + \left\{c_2\left(y_2 - y_4\right) + c_2'\left(y_2 - y_4\right)\left(y_1 - y_3\right)^2\right\}\right] \quad \text{....} \quad (3.12)$$

The governing Equations (3.11) and (3.12) can now be rewritten as a set of four nonlinear first order ordinary differential equations (ODE) as follows:

$$\frac{dy_1}{dt} = y_2 \quad \text{..........} \quad (3.13)$$

$$\frac{dy_2}{dt} = \frac{1}{m_1}\begin{bmatrix} F_1 - \left(k_1 y_1 + k_1' y_1^3\right) - \left(c_1 y_2 + c_1' y_2 y_1^2\right) - \left\{k_2\left(y_1 - y_3\right) + k_2'\left(y_1 - y_3\right)^3\right\} \\ - \left\{c_2\left(y_2 - y_4\right) + c_2'\left(y_2 - y_4\right)\left(y_1 - y_3\right)^2\right\} \end{bmatrix} \quad \text{.........} \quad (3.14)$$

$$\frac{dy_3}{dt} = y_4 \quad \text{..........} \quad (3.15)$$

$$\frac{dy_4}{dt} = \frac{1}{m_2}\left[F_2 + \left\{k_2(y_1 - y_3) + k_2'(y_1 - y_3)^3\right\} + \left\{c_2(y_2 - y_4) + c_2'(y_2 - y_4)(y_1 - y_3)^2\right\}\right] \quad \text{…. (3.16)}$$

The additional field equations, needed for multi-segment method of integration are derived now from Equations 3.13-3.16. This is done by differentiating both sides of Equations 3.13-3.16, partially w.r.t. $y(a)$. For example, at first,

$\frac{\partial}{\partial y_1(a)}$ of Equation (11) gives

$$\frac{\partial}{\partial y_1(a)}\left\{\frac{dy_1}{dt}\right\} = \frac{\partial}{\partial y_1(a)}\{y_2\} \quad \text{or,} \quad \frac{d}{dt}\left\{\frac{\partial y_1(t)}{\partial y_1(a)}\right\} = \frac{\partial y_2(t)}{\partial y_1(a)}$$

The symbol Y has been used for the partial derivative term of $y(t)$ w.r.t. $y(a)$. So in general Y can be expressed as

$$Y_{mn} = \frac{\partial y_m(t)}{\partial y_n(a)}$$

Finally we get the additional field equations that are actually the governing differential Equations of Y, as follows:

$$\frac{d}{dt}(Y_{11}) = Y_{21} \quad \text{………. (3.17)}$$

Now $\frac{\partial}{\partial y_1(a)}$ of Equation (3.14)

$$\frac{\partial}{\partial y_1(a)}\left\{\frac{dy_2}{dt}\right\} = \frac{\partial}{\partial y_1(a)}\left\{\frac{1}{m_1}\left[\begin{array}{l} F_1 - (k_1 y_1 + k_1' y_1^3) - (c_1 y_2 + c_1' y_2 y_1^2) \\ -\left\{k_2(y_1 - y_3) + k_2'(y_1 - y_3)^3\right\} \\ -\left\{c_2(y_2 - y_4) + c_2'(y_2 - y_4)(y_1 - y_3)^2\right\} \end{array}\right]\right\} \quad \text{Or,}$$

$$\frac{d(Y_{21})}{dt} = -\frac{1}{m_1}\begin{bmatrix} -(\alpha_1 Y_{11} + \beta_1 Y_{21} + \gamma_1 y_1^2 Y_{21} + 2\gamma_1 y_1 y_2 Y_{11}) + (k_1 Y_{11} + 3k_1' y_1^2 Y_{11}) + (c_1 Y_{21} + c_1' y_1^2 Y_{21} + 2c_1' y_1 y_2 Y_{11}) \\ + \{k_2(Y_{11} - Y_{31}) + 3k_2'(y_1 - y_3)^2 (Y_{11} - Y_{31})\} \\ + \{c_2(Y_{21} - Y_{41}) + c_2'(y_1 - y_3)^2 (Y_{21} - Y_{41}) + 2c_2'(y_1 - y_3)(y_2 - y_4)(Y_{11} - Y_{31})\} \end{bmatrix}$$

…… (3.18)

Next, $\frac{\partial}{\partial y_1(a)}$ of Equation (3.15)

$$\frac{\partial}{\partial y_1(a)}\left\{\frac{dy_3}{dt}\right\} = \frac{\partial}{\partial y_1(a)}\{y_4\} \text{ or, } \frac{d}{dt}\left\{\frac{\partial y_3(t)}{\partial y_1(a)}\right\} = \frac{\partial y_4(t)}{\partial y_1(a)}$$

or,

$$\frac{d}{dt}(Y_{31}) = Y_{41}$$

…….. (3.19)

Finally, $\frac{\partial}{\partial y_1(a)}$ of Equation (3.16)

$$\frac{\partial}{\partial y_1(a)}\left\{\frac{dy_4}{dt}\right\} = \frac{\partial}{\partial y_1(a)}\left\{\frac{1}{m_2}\left[F_2 + \{k_2(y_1 - y_3) + k_2'(y_1 - y_3)^3\} + \{c_2(y_2 - y_4) + c_2'(y_2 - y_4)(y_1 - y_3)^2\}\right]\right\}$$

Or,

$$\frac{d(Y_{41})}{dt} = \frac{1}{m_2}\begin{bmatrix} (\alpha_2 Y_{31} + \beta_2 Y_{41} + \gamma_2 y_3^2 Y_{41} + 2 y_3 y_4 Y_{31}) + \{k_2(Y_{11} - Y_{31}) + 3k_2'(y_1 - y_3)^2 (Y_{11} - Y_{31})\} \\ + \{c_2(Y_{21} - Y_{41}) + c_2'(y_1 - y_3)^2 (Y_{21} - Y_{41}) + 2c_2'(y_1 - y_3)(y_2 - y_4)(Y_{11} - Y_{31})\} \end{bmatrix}$$

..….. (3.20)

Similarly $\frac{\partial}{\partial y_2(a)}$ of Equations (3.13), (3.14), (3.15), (3.16) will give

$$\frac{d}{dt}(Y_{12}) = Y_{22}$$

………. (3.21)

$$\frac{d(Y_{22})}{dt} = -\frac{1}{m_1}\begin{bmatrix} -(\alpha_1 Y_{12} + \beta_1 Y_{22} + \gamma_1 y_1^2 Y_{22} + 2\gamma_1 y_1 y_2 Y_{12}) + (k_1 Y_{12} + 3k_1' y_1^2 Y_{12}) + (c_1 Y_{22} + c_1' y_1^2 Y_{22} + 2c_1' y_1 y_2 Y_{12}) \\ + \{k_2(Y_{12} - Y_{32}) + 3k_2'(y_1 - y_3)^2 (Y_{12} - Y_{32})\} \\ + \{c_2(Y_{22} - Y_{42}) + c_2'(y_1 - y_3)^2 (Y_{22} - Y_{42}) + 2c_2'(y_1 - y_3)(y_2 - y_4)(Y_{12} - Y_{32})\} \end{bmatrix}$$

………….. (3.22)

$$\frac{d}{dt}(Y_{32}) = Y_{42}$$ ………….. (3.23)

$$\frac{d(Y_{42})}{dt} = \frac{1}{m_2}\begin{bmatrix} (\alpha_2 Y_{32} + \beta_2 Y_{42} + \gamma_2 y_3^2 Y_{42} + 2 y_3 y_4 Y_{32}) + \{k_2(Y_{12} - Y_{32}) + 3k_2'(y_1 - y_3)^2 (Y_{12} - Y_{32})\} \\ + \{c_2(Y_{22} - Y_{42}) + c_2'(y_1 - y_3)^2 (Y_{22} - Y_{42}) + 2c_2'(y_1 - y_3)(y_2 - y_4)(Y_{12} - Y_{32})\} \end{bmatrix}$$

…………. (3.24)

It can be seen that every column of the governing equations of Y has similar form. Thus, $\frac{\partial}{\partial y_3(a)}$ of Equations (3.13), (3.14), (3.15), (3.16) will give

$$\frac{d}{dt}(Y_{13}) = Y_{23}$$ …………. (3.25)

$$\frac{d(Y_{23})}{dt} = -\frac{1}{m_1}\begin{bmatrix} -(\alpha_1 Y_{13} + \beta_1 Y_{23} + \gamma_1 y_1^2 Y_{23} + 2\gamma_1 y_1 y_2 Y_{13}) + (k_1 Y_{13} + 3k_1' y_1^2 Y_{13}) + (c_1 Y_{23} + c_1' y_1^2 Y_{23} + 2c_1' y_1 y_2 Y_{13}) \\ + \{k_2(Y_{13} - Y_{33}) + 3k_2'(y_1 - y_3)^2 (Y_{13} - Y_{33})\} \\ + \{c_2(Y_{23} - Y_{43}) + c_2'(y_1 - y_3)^2 (Y_{23} - Y_{43}) + 2c_2'(y_1 - y_3)(y_2 - y_4)(Y_{13} - Y_{33})\} \end{bmatrix}$$

………… (3.26)

$$\frac{d}{dt}(Y_{33}) = Y_{43}$$ …………. (3.27)

$$\frac{d(Y_{43})}{dt} = \frac{1}{m_2}\begin{bmatrix} (\alpha_2 Y_{33} + \beta_2 Y_{43} + \gamma_2 y_3^2 Y_{43} + 2 y_3 y_4 Y_{33}) + \{k_2(Y_{13} - Y_{33}) + 3k_2'(y_1 - y_3)^2 (Y_{13} - Y_{33})\} \\ + \{c_2(Y_{23} - Y_{43}) + c_2'(y_1 - y_3)^2 (Y_{23} - Y_{43}) + 2c_2'(y_1 - y_3)(y_2 - y_4)(Y_{13} - Y_{33})\} \end{bmatrix}$$

..…….. (3.28)

Finally, $\frac{\partial}{\partial y_4(a)}$ of Equations (3.13), (3.14), (3.15), (3.16) will give

$$\frac{d}{dt}(Y_{14}) = Y_{24}$$ …………. (3.29)

$$\frac{d(Y_{24})}{dt} = -\frac{1}{m_1}\begin{bmatrix} -(\alpha_1 Y_{14} + \beta_1 Y_{24} + \gamma_1 y_1^2 Y_{24} + 2\gamma_1 y_1 y_2 Y_{14}) + (k_1 Y_{14} + 3k_1' y_1^2 Y_{14}) + (c_1 Y_{24} + c_1' y_1^2 Y_{24} + 2c_1' y_1 y_2 Y_{14}) \\ + \{k_2 (Y_{14} - Y_{34}) + 3k_2' (y_1 - y_3)^2 (Y_{14} - Y_{34})\} \\ + \{c_2 (Y_{24} - Y_{44}) + c_2' (y_1 - y_3)^2 (Y_{24} - Y_{44}) + 2c_2' (y_1 - y_3)(y_2 - y_4)(Y_{14} - Y_{34})\} \end{bmatrix}$$

…………… (3.30)

$$\frac{d}{dt}(Y_{34}) = Y_{44}$$ …………. (3.31)

$$\frac{d(Y_{44})}{dt} = \frac{1}{m_2}\begin{bmatrix} (\alpha_2 Y_{34} + \beta_2 Y_{44} + \gamma_2 y_3^2 Y_{44} + 2y_3 y_4 Y_{34}) + \{k_2 (Y_{14} - Y_{34}) + 3k_2' (y_1 - y_3)^2 (Y_{14} - Y_{34})\} \\ + \{c_2 (Y_{24} - Y_{44}) + c_2' (y_1 - y_3)^2 (Y_{24} - Y_{44}) + 2c_2' (y_1 - y_3)(y_2 - y_4)(Y_{14} - Y_{34})\} \end{bmatrix}$$

………….. (3.32)

These governing Equations (3.13 – 3.32) can be solved when the boundary conditions are specified. Equations of boundary conditions are described in the next section.

3.1.2 Boundary Conditions:

For different cases and chosen parameters, arbitrarily chosen boundary conditions and results are given in Tables 1-16. Among those, Tables 3 & 9 (for 2DOFS) and Table 11 (for 3DOFS) define the specific boundary conditions for BVP.

According to the multi-segment method of integration (MSMI), the boundary conditions for any boundary value problem are arranged in the following matrix form,

$$Ay(a) + By(b) = C \qquad \text{…… (3.33)}$$

The boundary conditions were chosen arbitrarily for this analysis since the devised program is capable to calculate the values of y for any specified boundary condition that is the primary objective of this analysis. For demonstrating the method of solution, a set of arbitrarily chosen data [Table 9] used for the boundary value problem analysis, are as below:

y_1 (a)= 0.01*m*; y_3 (a)= 0.02 *m*; y_2 (b)= 0.70 *m/s*; y_4 (b)= 0.80 *m/s*.

The above boundary conditions are used for both undamped and damped self-excited vibration analysis.

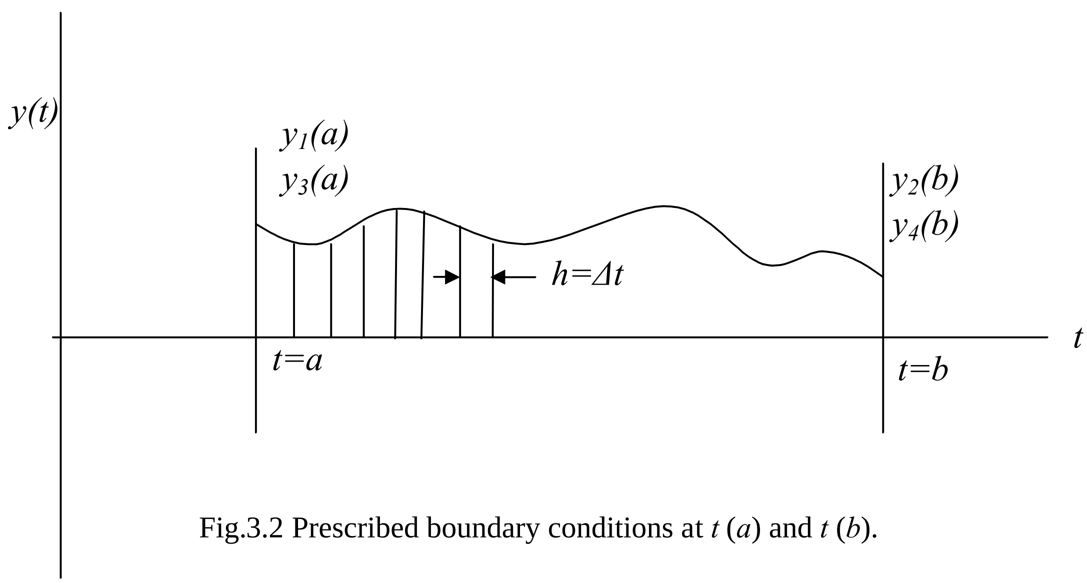

Fig.3.2 Prescribed boundary conditions at *t* (*a*) and *t* (*b*).

Fig. 3.2 specifies that it leads to a boundary value problem.

So the prescribed boundary conditions are, $\begin{bmatrix} y_1(a) \\ y_2(b) \\ y_3(a) \\ y_4(b) \end{bmatrix} = [C] = \begin{bmatrix} 0.01 \\ 0.70 \\ 0.02 \\ 0.80 \end{bmatrix}$

And, matrices of Equation 19 are then as follows:

$$\begin{bmatrix} 1 & 0 & 0 & 0 \\ 0 & 0 & 0 & 0 \\ 0 & 0 & 1 & 0 \\ 0 & 0 & 0 & 0 \end{bmatrix} \begin{bmatrix} y_1(a) \\ y_2(a) \\ y_3(a) \\ y_4(a) \end{bmatrix} + \begin{bmatrix} 0 & 0 & 0 & 0 \\ 0 & 1 & 0 & 0 \\ 0 & 0 & 0 & 0 \\ 0 & 0 & 0 & 1 \end{bmatrix} \begin{bmatrix} y_1(b) \\ y_2(b) \\ y_3(b) \\ y_4(b) \end{bmatrix} = \begin{bmatrix} y_1(a) \\ y_2(b) \\ y_3(a) \\ y_4(b) \end{bmatrix}$$

where, $[C]$ determines the arrangements of elements in matrices A and B. After deriving the governing Equations and the boundary condition (Equation 3.33) multi-segment integration technique is used to solve those equations as a boundary value problem.

Solutions of the boundary value problem with any arbitrarily chosen boundary conditions are possible by the present method.

Only for case (a) of self-excited vibration of 2DOFS, initial value problem (IVP) analysis has been performed. For this analysis, arbitrarily chosen boundary conditions for IVP are given in Table 5.

After deriving the governing Equations (3.13 – 3.32) and the boundary condition (Equation 3.33), multi-segment integration technique is used to solve those equations as a boundary value problem.
Multi-segment Method of Integration can also be used as an IVP where the boundary conditions are as defined in Table 5.

3.2 Method of Solution

Vibration problem would become quite complicated if all the boundary conditions are not specified at the same time reference. So along with conditions at initial time reference, some conditions are also specified at the final time reference. This type of problem needs to simultaneously solve a large number of nonlinear equations that depends on the number of intermediate grid points in between the two time references. Though, Newton-Raphson method can be used to solve that large number of equations, there are chances of non-convergence of solutions. Therefore Multi-segment Integration Technique developed by Kalnins and Lestingi (1967) has been used in the present study to solve the equations derived in previous section of this chapter.

3.2.1 Multi-segment Integration Technique

At first the m^{th} order ordinary differential equation (ODE) is reduced to '*m*' first order ODE. Then the scheme of multi-segment method of integration of a system of *m* first order ordinary differential equations is as follows:

$$\frac{dy(x)}{dx} = F\left(x, y^1(x), y^2(x), \ldots\ldots\ldots\ldots, y^m(x)\right) \qquad \ldots\ldots\ldots\ (3.34)$$

in the interval ($x_1 < x < x_{M+1}$) consists of

a. the division of the given interval into *M* segments;
b. (*m*+1) initial value integrations over each segment by fourth order Runge-Kutta method in this study ;
c. solution of a system of matrix equations to ensure continuity of the dependent variables at the nodal points;
d. repetition of (b) and (c) until continuity of the independent variables at the nodal points is achieved.

In Eq. (3.34) the symbol $y(x)$ denotes column matrix whose elements are *m* dependent variables, denoted by $y_j(x)$(j=1,2,3 …., *m*); *F* represents *m* functions arranged in a column matrix form; and *x* is the independent variable. Here for convenience the first *m*/2 elements of $y(x_1)$ and the last *m*/2 elements of $y(x_{M+1})$ are prescribed by the boundary conditions.

If at the initial point x_i of the segment S_i a set of values $y(x_i)$ is prescribed for the variables of Eqs. (3.34) then the variables at any *x* within S_i can be expressed as

$$y(x) = T[y^1(x_i), y^2(x_i), ..., y^m(x_j)] \qquad \text{……….} (3.35)$$

where the function T is uniquely dependent on x and the system of m first order ordinary differential equations. From Eqs. (3.35) the expressions for the small changes $\delta y(x)$ can be expressed, to a first approximation, by the following linear equations:

$$\delta y(x) = Y_i(x)\delta y(x_i) \qquad \text{……….} (3.36)$$

where,

$$Y_i(x) = \begin{bmatrix} \frac{\partial y^1(x)}{\partial y^1(x_i)} & \frac{\partial y^1(x)}{\partial y^2(x_i)} & .... & \frac{\partial y^1(x)}{\partial y^m(x_i)} \\ \frac{\partial y^2(x)}{\partial y^1(x_i)} & \frac{\partial y^2(x)}{\partial y^2(x_i)} & .... & \frac{\partial y^2(x)}{\partial y^m(x_i)} \\ . & . & . & . \\ . & . & . & . \\ . & . & . & . \\ . & . & . & . \\ \frac{\partial y^m(x)}{\partial y^1(x_i)} & \frac{\partial y^m(x)}{\partial y^2(x_i)} & .... & \frac{\partial y^m(x)}{\partial y^m(x_i)} \end{bmatrix} \qquad \text{………….} (3.37)$$

Expressing Eqs. (3.36) in finite difference form and evaluating them at $x = x_{i+1}$,

$$y^t(x_{i+1}) - y(x_{i+1}) = Y_i(x_{i+1})[y^t(x_i) - y(x_i)] \qquad \text{………….} (3.38)$$

where y^t denotes a trial solution state and y denotes an iterated solution state based on the condition of continuity of the variables at the nodal points. Eq. (3.38) is rearranged as

$$Y_i(x_{i+1})y(x_i) - y(x_{i+1}) = -Z_i(x_{i+1}) \qquad \text{……………..} (3.39)$$

where, $Z_i(x_{i+1}) = y^t(x_{i+1}) - Y_i(x_{i+1})y^t(x_i)$

In order to determine the coefficients $Y_i(x)$ in Eqs. (3.39) in the jth column of $Y_i(x)$ can be regarded as a set of new variables, which is solution of an initial value problem governed within each segment by a linear system of first order differential equations, obtained from Eqs. (3.34) by differentiation with respect to $y^j(x_i)$ in the form

$$\frac{d}{dx}\left[\frac{\partial y(x)}{\partial y^j(x_i)}\right] = \frac{\partial}{\partial y^j(x_i)}\left\{F\left[x, y^1(x), y^2(x), \ldots\ldots\ldots, y^m(x)\right]\right\} \qquad \ldots\ldots\ldots\ldots (3.40)$$

thus the columns of the matrix $Y_i(x)$ are defined as the solutions of m initial value problems governed in S_i by (3.40), with j=1, 2, ……..,m where the initial values, in view of Eqs. (3.36), are given by

$$Y_i(x_i) = I \qquad \ldots\ldots\ldots\ldots (3.41)$$

where I denotes the (m,m) unit matrix. to obtain the iterated solution $y(x_i)$ Eqs. (3.39) are rewritten as a partitioned matrix product of the form

$$\begin{bmatrix} y_1(x_{i+1}) \\ \ldots\ldots\ldots\ldots \\ y_2(x_{i+1}) \end{bmatrix} = \begin{bmatrix} Y_i^1(x_{i+1}) & \vdots & Y_i^2(x_{i+1}) \\ \cdots & \cdots & \cdots \\ Y_i^3(x_{i+1}) & \vdots & Y_i^2(x_{i+1}) \end{bmatrix} \begin{bmatrix} y_1(x_i) \\ \ldots\ldots\ldots \\ y_2(x_i) \end{bmatrix} + \begin{bmatrix} Z_i^1(x_{i+1}) \\ \ldots\ldots\ldots \\ Z_i^2(x_{i+1}) \end{bmatrix}$$

so that the known boundary conditions are separated from the unknowns and, therefore, turns into a pair of equations given by

$$Y_i^1(x_{i+1})y_1(x_i) + Y_i^2(x_{i+1})y_2(x_i) - y_1(x_{i+1}) = -Z_i^1(x_{i+1})$$

$$Y_i^3(x_{i+1})y_1(x_i) + Y_i^4(x_{i+1})y_2(x_i) - y_1(x_{i+1}) = -Z_i^1(x_{i+1}) \qquad \ldots\ldots\ldots\ldots (3.42)$$

The result is a simultaneous system of 2M linear matrix equations, in which the known coefficients $Y_1^j(x_{i+1})$ and $Z_1^j(x_{i+1})$ are (m/2,m/2) and (m/2,1) matrices, respectively, and the unknown, $y_j(x_i)$ are (m/2,1) matrices. Since $y_1(x_1)$ and $y_2(x_{M+1})$ are known, there are exactly 2m unknowns: $y_1(x_i)$, with i= 2,3,…..M+1, and $y_2(x_i)$, with i=1,2,….,M.

By means of Gaussian elimination, the system of equations (40) is first brought to the form

$$E_i y_2(x_i) - y_1(x_{i+1}) = A_i$$

$$C_i y_1(x_{i+1}) - y_2(x_{i+1}) = B_i \qquad \ldots\ldots\ldots\ldots (3.43)$$

for i=1,2,….,M. Using the notations Z_1^j and Y_1^j in place of symbols $Z_1^j(x_{i+1})$ and $Y_1^j(x_{i+1})$, the (m/2,m/2) matrices E_i and C_i in the Eqs. (41) are defined by

$$E_1 = Y_1^2, \qquad C_1 = Y_1^4 (Y_1^2)^{-1}$$

and $E_i = Y_i^2 + Y_i^1 C_{i-1}^{-1} \quad C_i = (Y_i^4 + Y_i^3 C_{i-1}^2) E_i^{-1}$

for i=2,3,……,M.

The (m/2, 1) matrices A_i and B_i are given by

$$A_1 = -Z_1^1 - Y_1^1 y_1(x_1),$$

$$B_1 = -Z_1^2 - Y_1^2 y_1(x_1) - Y_1^4 E_1^{-1} A_1,$$

$$A_i = -Z_i^1 - Y_1^1 C_{i-1}^{-1} B_{i-1},$$

$$b_i = -Z_i^2 - Y_i^3 C_{i-1}^{-1} B_{i-1} - (Y_i^4 + Y_i^3 C_{i-1}^{-1}) E_i^{-1} A_i,$$

for i=2,3,…..,M.

then the unknowns of (3.42) are obtained by

$$y_1(x_{M+1}) = C_{M-1}[B_M - y_2(x_{M+1})],$$

$$y_2(x_M) = E_{M-1}[y_1(x_{M+1}) + A_M],$$

and $$y_1(x_{M-i+1}) = C_{M-i}^{-1}[y_2(x_{M-i+1}) + N_{M-i}],$$

$$y_2(x_{M-i}) = E_{M-i}^{-1}[y_1(x_{M-i+1}) + A_{M-i}],$$

for i=2,3,…….,M-1.

Assuming $y(x_i)$ as the next trial solution $y^t(x_i)$ the process is repeated until the integration results of Eqs. (3.34) at x_{i+1}, as obtained from the integrations in segment S_i with the initial values $y(x_i)$, match with the elements of $y(x_{i+1})$ as obtained from (3.39) and also with the boundary conditions at x_{M+1}. But it is worth mentioning that number of segment, that is, M has been kept to one in this thesis to get the results and these are also reliable.

CHAPTER 4

RESULTS AND DISCUSSION

Self-excited vibration analysis is performed using the results obtained from the developed code using Turbo C for different cases considering self-excited force function and various combinations of springs and dampers. In section 4.1 soundness of the code is demonstrated by comparing the results for Van Der Pol's equation from Thompson and Dahleh (2003). Boundary conditions used for this validation are given in Table 1.

Sections 4.2-4.3 discuss self-excited linear vibrations while sections 4.4-4.7 & 4.9 discuss the effect of non-linearity on self-excited vibrations.

Three cases (cases (*a*) - (*c*) from Table 2) are considered to analyze 2DOFS undamped self-excited vibration. Using boundary conditions given in Table 3, boundary value problem (BVP) analysis method is applied to analyze undamped self-excited vibration taking eight different sets of data of various parameters from Table 4. So for every case, eight figures [(*i*) – *(viii)*] of the response are drawn according to eight sets of data from Table 4.

Initial value problem (IVP) analysis method is applied for only case (*a*). Boundary conditions and values of various parameters for this analysis are given in Table 5 and Table 6 respectively. For case (*a*), comparison is done between the responses of the system obtained from BVP and IVP analysis methods.

Choosing different combinations of mass, spring constant and self-excited force coefficients, figures [figures 4.8(*i*) - 4.8*(viii)*, 4.9, 4.10(*i*) - 4.10*(viii)*, 4.11(*i*) - 4.11*(viii)* and figures 1-7 of Appendix A] of the responses of undamped self-excited vibration of 2DOFS have been drawn for 100 seconds for ease of comparison. Comparison between various cases has been done by the system's amplitudes of vibration, frequency and phase planes.

In Table 7, ratios of mass to spring constant are shown for various cases considered for undamped self-excited vibration analysis of 2DOFS. This ratio gives an idea of the system's response for undamped case. For lower ratio, the system vibrates with higher amplitude and approaches to the more unstable condition.

Four cases (cases (*a*) - (*d*) from Table 2) are considered to analyze damped self-excited vibration of both 2DOFS and 3DOFS by only BVP analysis method. For analyzing both linear and non-linear damped self-excited vibration, four different combinations of springs and dampers depending on nonlinearity are chosen as given in Table 8. Boundary conditions for BVP analysis method are given in Table 9 (2DOFS) and Table 11 (3DOFS). Values of various parameters in analyzing damped self-excited vibration are given in Table 10 (2DOFS) and Table 12 (3DOFS).

For different combinations of mass, spring constant, damping constant, spring & damping nonlinearity and self-excited force coefficients, figures 4.12(a) – 4.12(d), 4.13(a) – 4.13(d), 4.14(a)-4.14(b), 4.15(a)-4.15(b), 4.16(a)-4.16(d), 4.17(a)-4.17(d) and figures 1-12 of Appendix B of the responses of self-excited vibration of 2DOFS have been drawn for 100 seconds considering two data sets. For data set 2 of Table 10, few curves [figures 4.13(d), 4.14(b), 4.15(b), 4.17(a) - 4.17(d) and figures 4-6, 8, 10-12 of Appendix B] have been drawn for 40 seconds as the developed code can't show the output due to the limitation of numerical solution through the code as only one segment is considered for calculation. For 3DOFS, responses have been drawn for 50 seconds. Comparison between various cases has been done by the system's amplitude of vibration, frequency and phase planes for various cases.

In Table 13, some particular values of various parameters are given for which the system maintains stability. This gives an idea of choosing various parameters to make the system stable in case of damped self-excited vibration. Table 14 and Table 15 recapitulate the responses of the self-excited vibration of 2DOFS and 3DOFS respectively as described later.

For damped self-excited vibration of 2DOFS, the system's instability has also been analyzed taking into account the boundary conditions given in Table 9. This has been done through trial and error method. Values of various parameters are chosen arbitrarily and then after running the code, the responses are drawn and checked from the figures of the responses whether the system becomes unstable or not. For the system's unstable conditions, few determined parameters are given in Table 16. This gives an outline of range of values of various parameters for system's design to control vibration.

4.1 Validity of the Code by Non-linear Analysis [Figures 4.1-4.7)]

To validate the developed code, Van der Pol's equation has been solved as SDOFS by means of non-linear BVP analysis method through the developed computer program written using the multi-segment method of integration for arbitrarily chosen boundary conditions given in Table 1. The time period for this analysis has been chosen to be 100 s from $t_a = 0$ s to $t_b = 100$ s.

Figure 4.1 shows the exact solution of Van der Pol's equation from Thomson and Dahleh (2003) when the damping term, μ is considered to be 1.0.

For different values of damping term μ, six different isoclines curves [figures 4.2-4.7] have been plotted and from these curves, limit cycles are found. Values of μ considered are 0.0, 0.25, 0.5, 1.0, 2.0 and 3.0. For μ = 0.0, figure 4.3 shows that the isocline curve becomes a circle.

Comparison between figure 4.1 and figure 4.2 clearly illustrates that multi-segment integration technique can present the proper result irrespective of chosen boundary conditions. This confirms the validity of the developed code.

From these isoclines curves it is evident that for small oscillations ($x < 1$), the damping is negative and the amplitude increases with time. For $x > 1$, the damping is positive and the amplitude diminishes with time. Form the exact result of Van der Pol's equation given in Thomson and Dahleh (2003), it is clear that if the system is initiated with x (0) and ˙(0), the amplitude will increase or decrease depending on whether x is small or large and it will finally reach a stable state known as limit cycle.

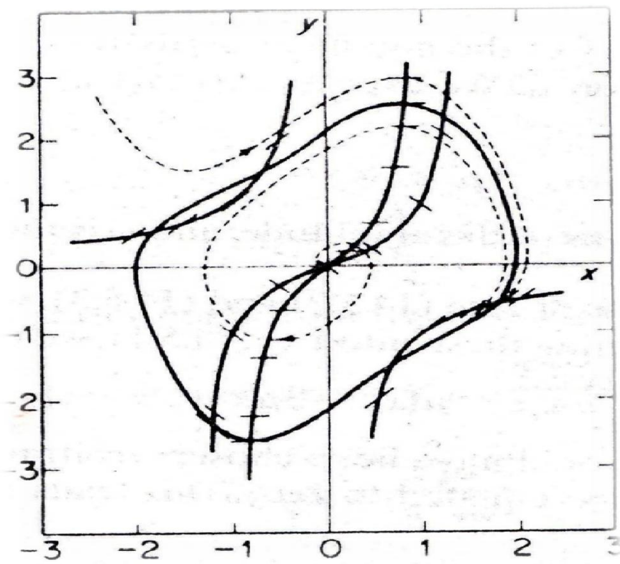

Fig. 4.1 Exact solution of Van der Pol’s equation for μ= 1.0 given in Thomson and Dahleh (2003)

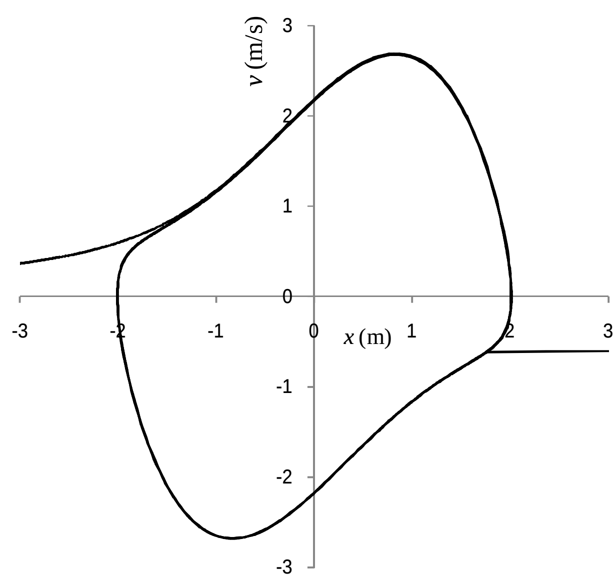

Fig. 4.2 Solution of Van der Pol’s equation for μ= 1.0 by BVP analysis method

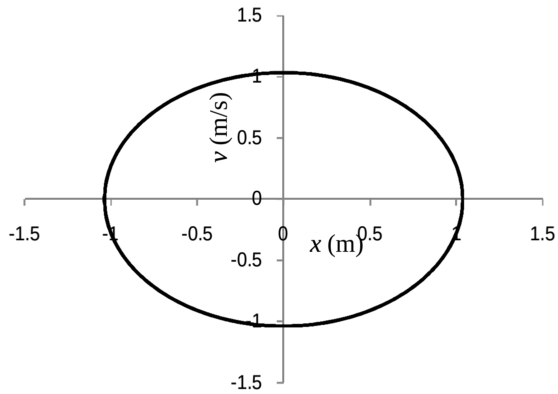

Fig. 4.3 Isocline curve for μ = 0.0

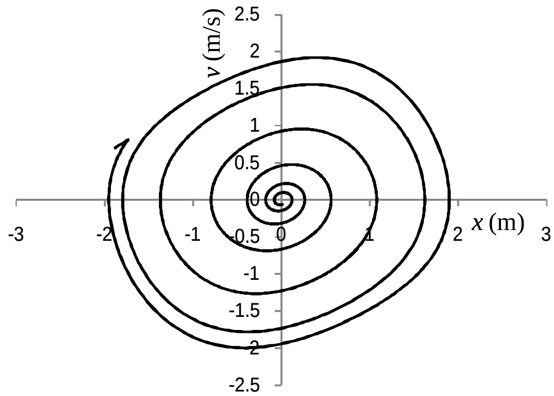

Fig.4.4 Isocline curve for μ = 0.25

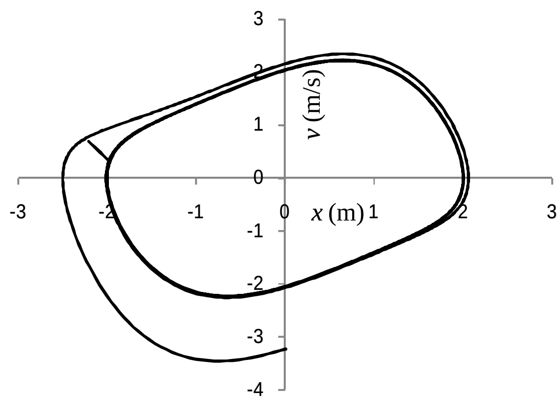

Fig. 4.5 Isocline curve for μ = 0.50

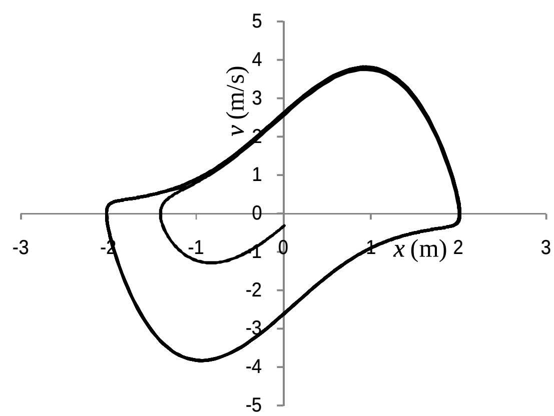

Fig. 4.6 Isocline curve for μ = 2.0

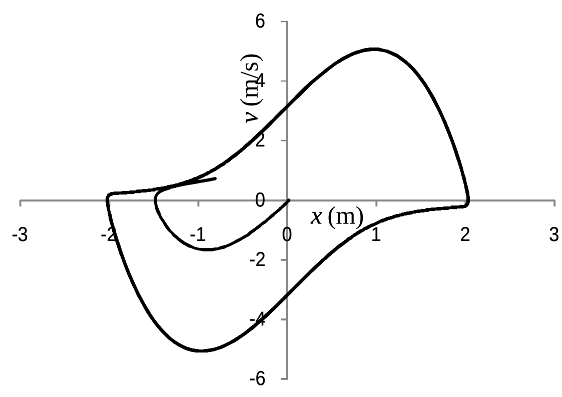

Fig. 4.7 Isocline curve for μ = 3.0

Fig. Solution of Van der Pol's equation by BVP analysis method [Figs. 4.3- 4.7]

4.2 BVP analysis of Undamped Linear Self-excited Vibration of 2DOFS

4.2.1 Self-excited force is function of only displacement

[Figures 4.8(*i*)-4.8*(viii)*]

Figure 4.8(*i*) for *f(d)* and data set (*i*), shows that the system (both m_1 and m_2) is vibrating with almost similar amplitude throughout the entire period and maintaining a regular fashion. However, due to the decrement of the value of spring constant in data sets *(ii)* and (*iii*), the system [figures 4.8(*ii*) & 4.8(*iii*)] starts to vibrate with lower amplitude and also with lower frequency. In figure 4.8(*iii*), amplitude decreases more with the decrement of self-excited force coefficients (α_1 & α_2) in data set (*iii*).

Again with increment of spring constant from 10 (N/m) to 100 (N/m) and lowering values of α_1 & α_2 in data set (*iv*) of Table 4, both amplitude and frequency increase as shown in figure 4.8(*iv*).

After the masses are increased in data sets *(v)* & *(vi)*, then amplitude and frequency for both m_1 and m_2 again decrease. These are shown in figures 4.8*(v)* & 4.8*(vi)*.

Again with higher values of k_1 & k_2 and lower values of α_1 & α_2 (as in data sets *(vii)*) amplitude decreases and frequency of vibration increases as shown in figure 4.8*(vii)*. But with the lower values of m_1 & m_2 in data set *(viii)*, figure 4.8*(viii)* shows that though amplitude decreases but frequency drastically increases.

4.2.2 Self-excited force is function of only velocity [*Figure 4.9*]

For this case when self-excited force is function of only velocity, response of the system for data set *(vii)* is given here and for other data sets *(i)* to *(vi)* and *(viii)*, the system's response are given in Appendix A (Figures A(1) – A(7)).

Figure 4.9 shows that the system continues steady state vibration for this case. So for data set *(vii)*, the system does not approach stability.

4.2.3 Self-excited force is function of both displacement and velocity

[*Figures 4.10(i)-4.10(viii)*]

Figures 4.10(*i*) – 4.10(*iv*) for *f(dv)* and data sets (*i*) to (*iv*) show that the system tends to be unstable over the period.

For increased values of m_1 and m_2 in data sets *(v)* to *(vii)*, figures 4.10*(v)*-4.10*(vii)* illustrate that the system vibrates at a stable manner.

For data set *(viii)* with higher values of both m_1 and m_2 and spring constants k_1 and k_2, the amplitude is much lower but gradually the system goes to unstable condition as shown in figure 4.10*(viii)*.

4.2.4 Comparison of responses of the system for BVP and IVP analysis method for undamped linear self-excited vibration of 2DOFS (*considering f(d)*).

The case (*a*) from Table 2 has been solved considering IVP analysis method. Boundary conditions for IVP and BVP are different. But the curves of the system's responses from IVP analysis [figures 4.11(*i*)-4.11*(viii)*] and from BVP analysis [figures. 4.8(*i*)-4.8*(viii)*] show that both IVP and BVP method give the similar result for various cases. There is no major change in output for these two methods. This indicates that the response of the vibratory system is independent of the chosen boundary conditions.

4.3 Comparison among the responses of undamped linear self-excited vibration of 2DOFS for cases (*a*)-(*d*)

4.3.1 Case (a) [Figures 4.8(*i*)-4.8*(viii)*]:

At first variation in vibration pattern is observed for undamped self-excited vibration for *f(d)*, that is, self-excited vibration is a function of only displacement for all the different data sets from Table 4.

Figure 4.8(*i*) for data set (*i*) shows that both m_1 and m_2 vibrate with higher frequency as for this case the values of spring constants are k_1 =100 N/m and k_2= 100 N/m. But for data set *(ii)* of Table 4, the masses vibrate with lower frequency as shown in figure 4.8*(ii)*. This implies that increment of spring constant without any change in mass decreases frequency of the system. This type of vibration with higher frequency is also seen in figures 4.8*(iv)*, 4.8*(vii)* and 4.8*(viii)*.

For both data set (iv) and *(v)*, spring constant is same, but figure 4.8(iv) for data set (iv) shows higher frequency of vibration than figure 4.8*(v)* for data set *(v)*. So pattern of vibration mostly depends on the ratio of both mass and spring constant. When the mass to spring constant ratio is very low (Table 7), frequency of vibration is much higher. This can be understood from figures 4.8*(i)*, 4.8*(iv)*, 4.8*(vii)* and 4.8*(viii)*. Their phase planes also show the proof of higher frequency of vibration.

For *f(d)*, both m_1 and m_2 maintain almost steady vibration throughout the entire considered period. So without damping, the system maintains steady vibration when the self-excited force is considered as of function of only displacement.

4.3.2 Comparison of case (a) [*Figures 4.8(i)-4.8(viii)]* with case (b) [Figure 4.9 and *Figures A(1)- A(7) of Appendix A*]:

When the self-excited force is taken as a function of velocity, the system shows rapid occurrence of instability (Figures A(1) – A(4)).

Figures A(1)-A(4) for data set *(i)* to *(iv)* and A(8) for data set *(viii)* from Table 4 show that vibration amplitudes of both m_1 and m_2 increase rapidly and approach to more unstable condition. Phase planes of figures A(2) to A(4) proves the system's greater instability. But figures

4.8(*v*)-4.8(*vii*), 4.9 and A(5)-A(6) for data sets *(v)*, *(vi)* and *(vii)* from Table 4, no significant variation of vibration pattern is seen between the two cases (*a*) and (*b*). Increase of mass with no significant increase of spring constant causes this similar type of vibration for *f(d)*. So if the mass to spring constant ratio approaches to unity (Table 7), the system shows steady vibration for the whole period.

4.3.3 Comparison of case (a), (b) and (c) [*Figures 4.10(i)-4.10(viii)]*:

For eight sets of data from Table 4 and for *f(dv)*, the system shows almost similar type of responses as the responses for *f(v)*. So it can be concluded that effect of displacement on self-excited force is not so dominant over velocity. That's why, the system presents alike vibration for both the cases when self-excited force is function of only velocity and of both displacement and velocity.

Figures of undamped self-excited vibration of 2DOFS (BVP)
Figs. 4.8(*i*) - 4.8(*viii*) drawn using data sets (*i*) - (*viii*) of **Table 4** for *f(d)* of **Table 2**

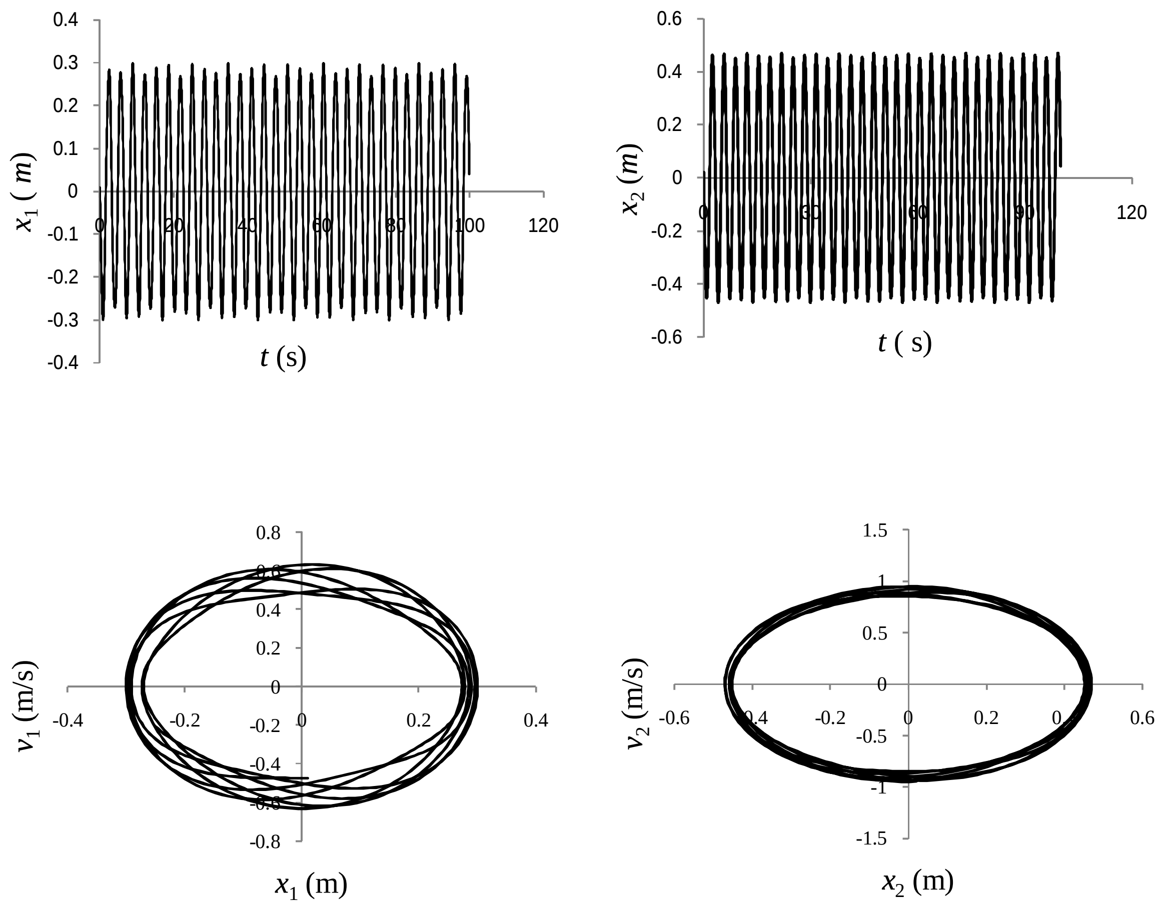

Fig. 4.8(*i*) *x* vs. *t* curves for 100 s and phase planes of m_1 and m_2 (for data set (*i*) and for *f(d)*)
[m_1=10kg, m_2= 10kg, k_1=100 N/m, k_2=100 N/m , α_1 = 0.3N/m , α_2=0.3N/m]

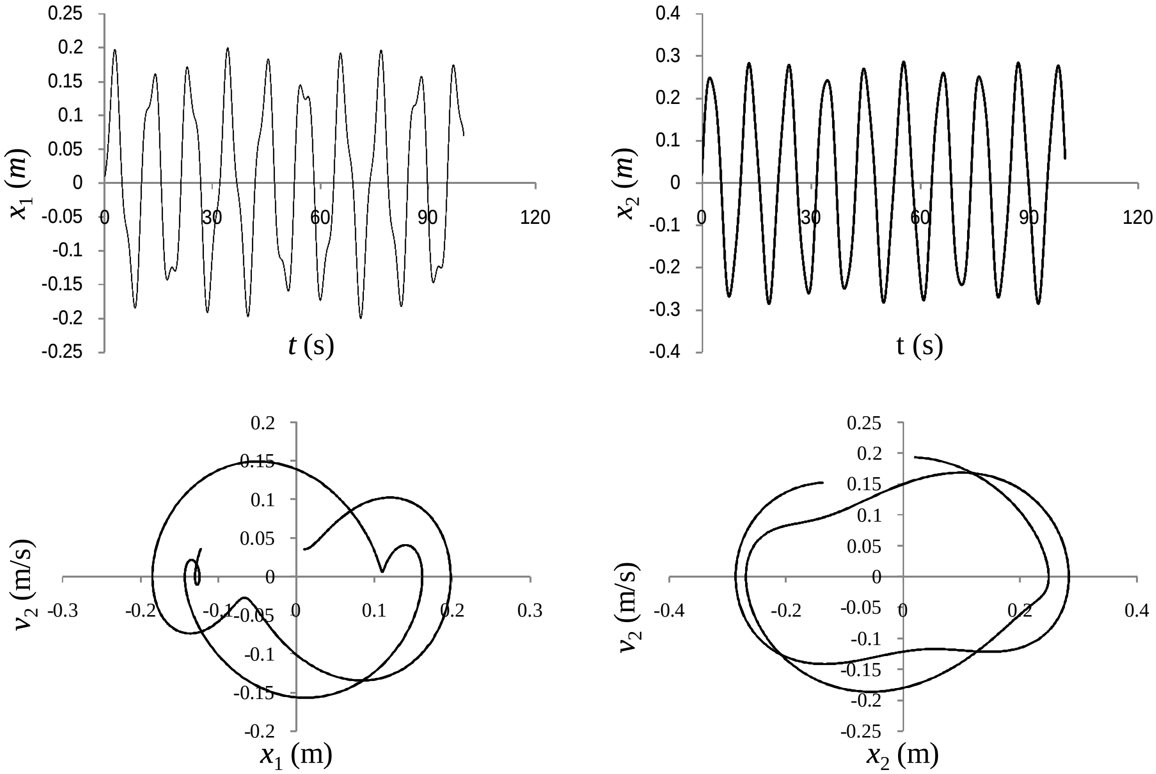

Fig. 4.8(*ii*) *x* vs. *t* curves for 100 s and phase planes of m_1 and m_2 (for data set (*ii*) and for *f(d))* *[*m_1*=10kg,* m_2*= 10kg,* k_1*=10 N/m,* k_2*=10 N/m,* α_1 *= 0.3 N/m ,*α_2*=0.3 N/m]*.

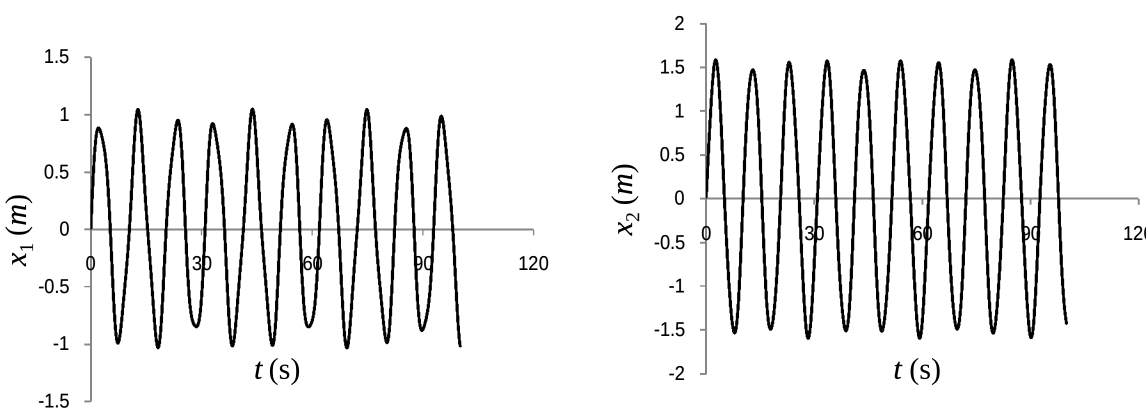

Fig. 4.8(*iii*) *x* vs. *t* curves of m_1 and m_2 (for data set (*iii*) and *f*(*d*)).
[m_1*=10kg,* m_2*= 10kg,* k_1*=10 N/m,* k_2*=10 N/m,* α_1 *= 0.1 N/m ,*α_2*=0.1 N/m*]

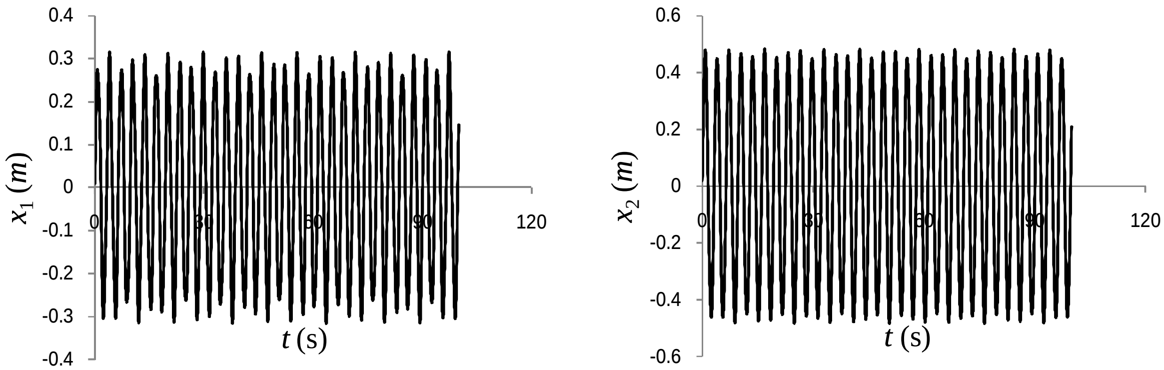

Fig. 4.8(*iv*) *x* vs. *t* curves of m_1 and m_2 (for data set (*iv*) and for *f(d)*)

[m_1=10kg, m_2= 10kg, k_1=100 N/m, k_2=100 N/m, α_1 = 0.1 N/m ,α_2=0.1 N/m]

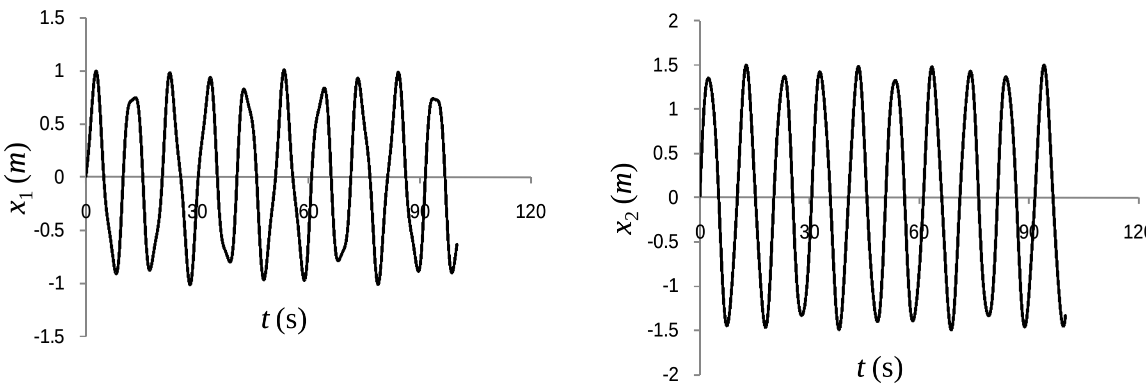

Fig. 4.8(*v*) *x* vs. *t* curves of m_1 and m_2 (for data set (*v*) and *f(d)*)

[m_1=100kg, m_2= 100kg, k_1=100 N/m, k_2=100 N/m, α_1 = 0.1 N/m ,α_2=0.1 N/m]

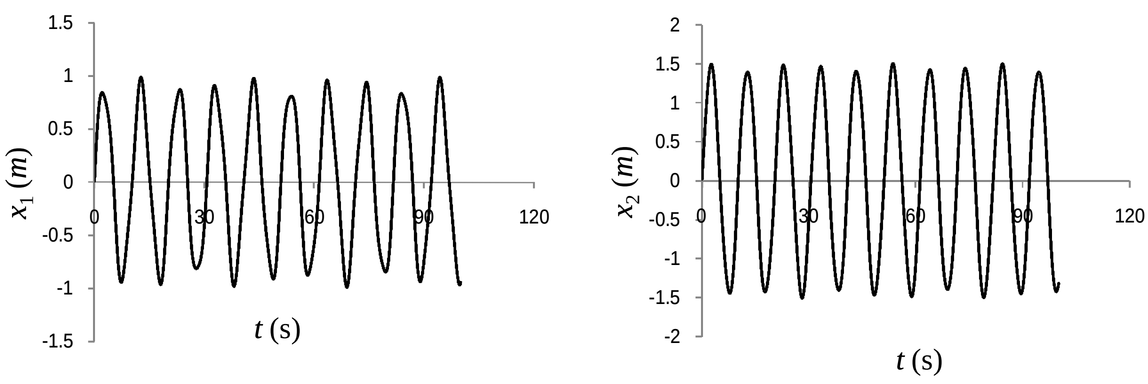

Fig. 4.8(*vi*) *x* vs. *t* curves of m_1 and m_2 (for data set (*vi*) and for *f(d)*)

[m_1=100kg, m_2= 100kg, k_1=100 N/m, k_2=100 N/m, α_1 = 0.3 N/m ,α_2=0.3 N/m]

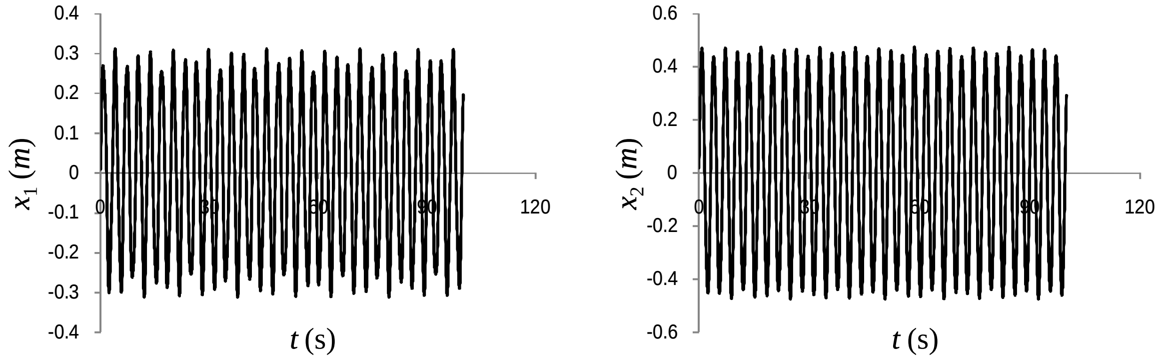

Fig. 4.8(*vii*) x vs. t curves of m_1 and m_2 (for data set (*vii*) and for *f(d)*)

[m_1=100kg, m_2= 100kg, k_1=1000 N/m, k_2=1000 N/m, α_1 = 0.1 N/m ,α_2=0.1 N/m]

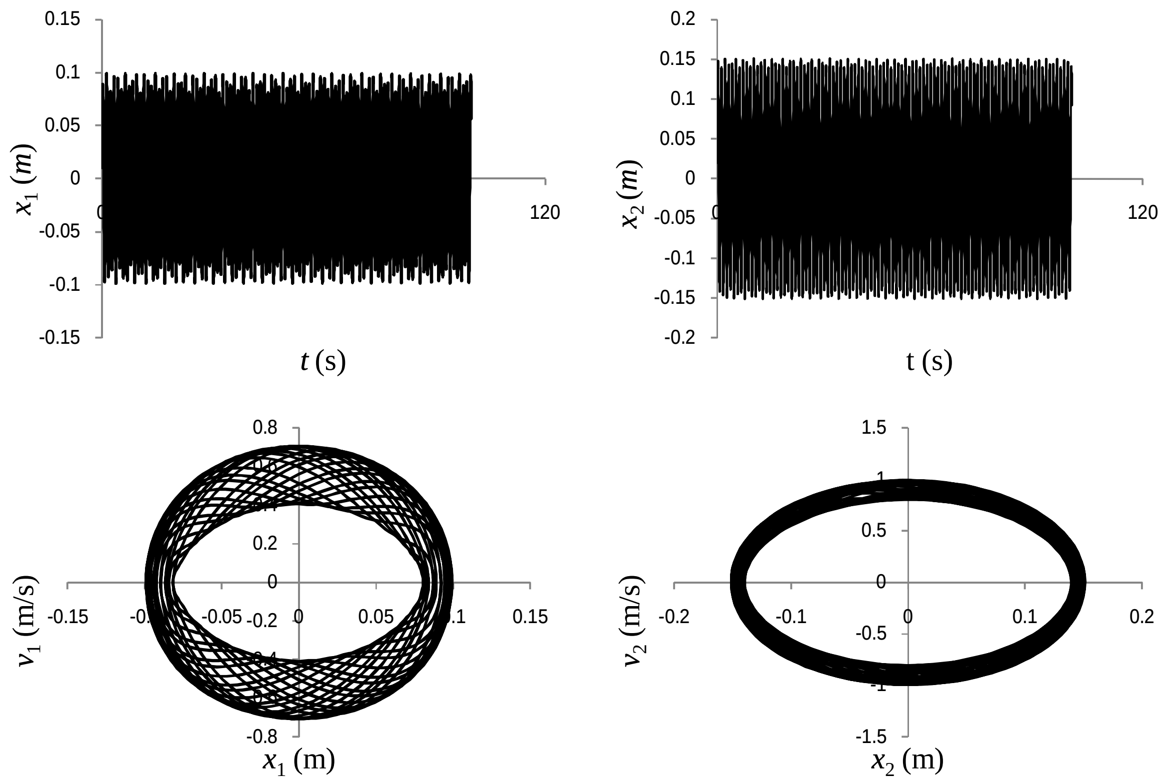

Fig. 4.8(*viii*) x vs. t curves and phase planes of m_1 and m_2 (for data set (*viii*) and for *f(d)*).

[m_1=10kg, m_2= 10kg, k_1=1000 N/m, k_2=1000 N/m, α_1 = 0.1 N/m ,α_2=0.1 N/m]

Figure of undamped self-excited vibration of 2DOFS (BVP)
Fig. 4.9 drawn using data set (*vii*) of **Table 4** for *f(v)* of **Table 2**

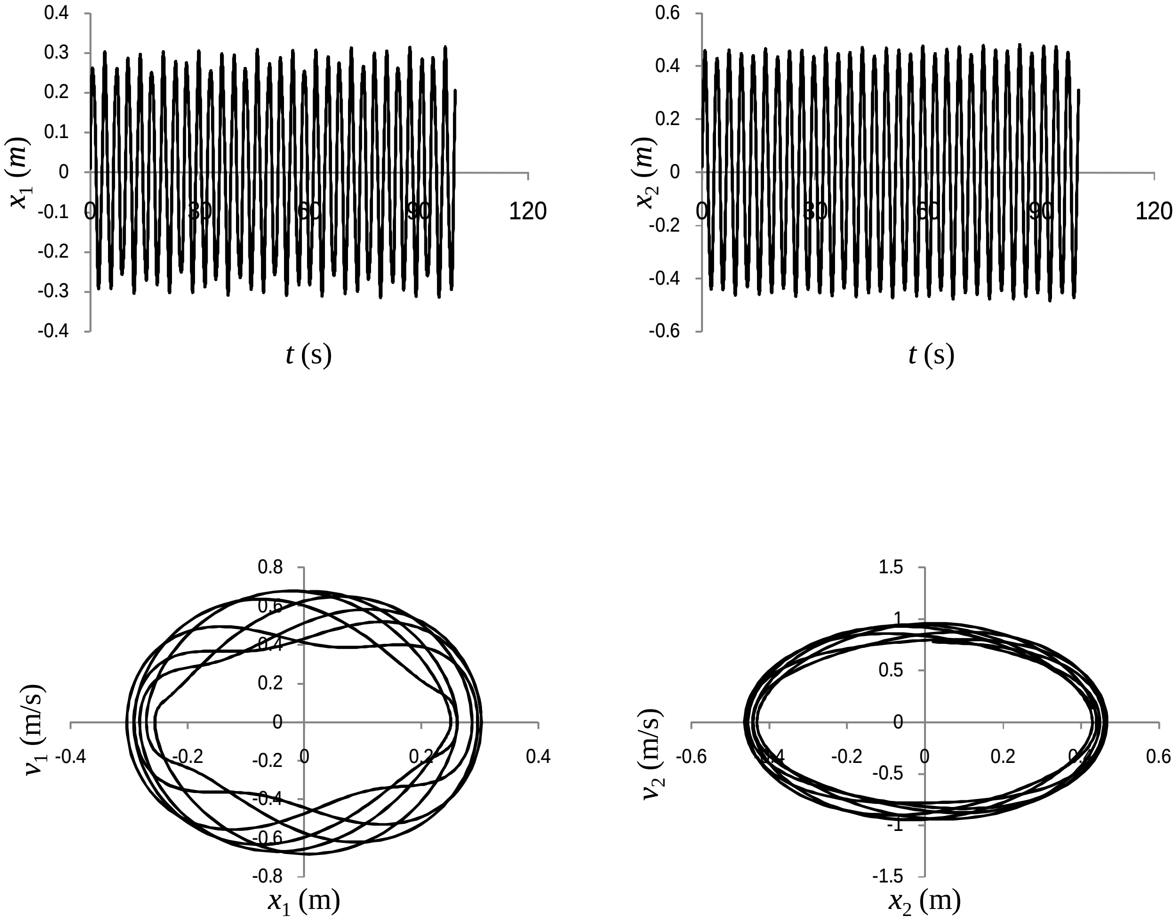

Fig. 4.9 x vs. t curves and phase planes of m_1 and m_2 (for data set (*vii*) and for $f(v)$.
[m_1=100kg, m_2= 100kg, k_1=1000 N/m, k_2=1000 N/m, β_1 = 0.1 Ns/m ,β_2=0.1 Ns/m]

Figures of undamped self-excited vibration of 2DOFS (BVP)
Figs. 4.10(*i*) - 4.10(*viii*) drawn using data sets (*i*) - (*viii*) of Table 4 for *f(dv)* of Table 2

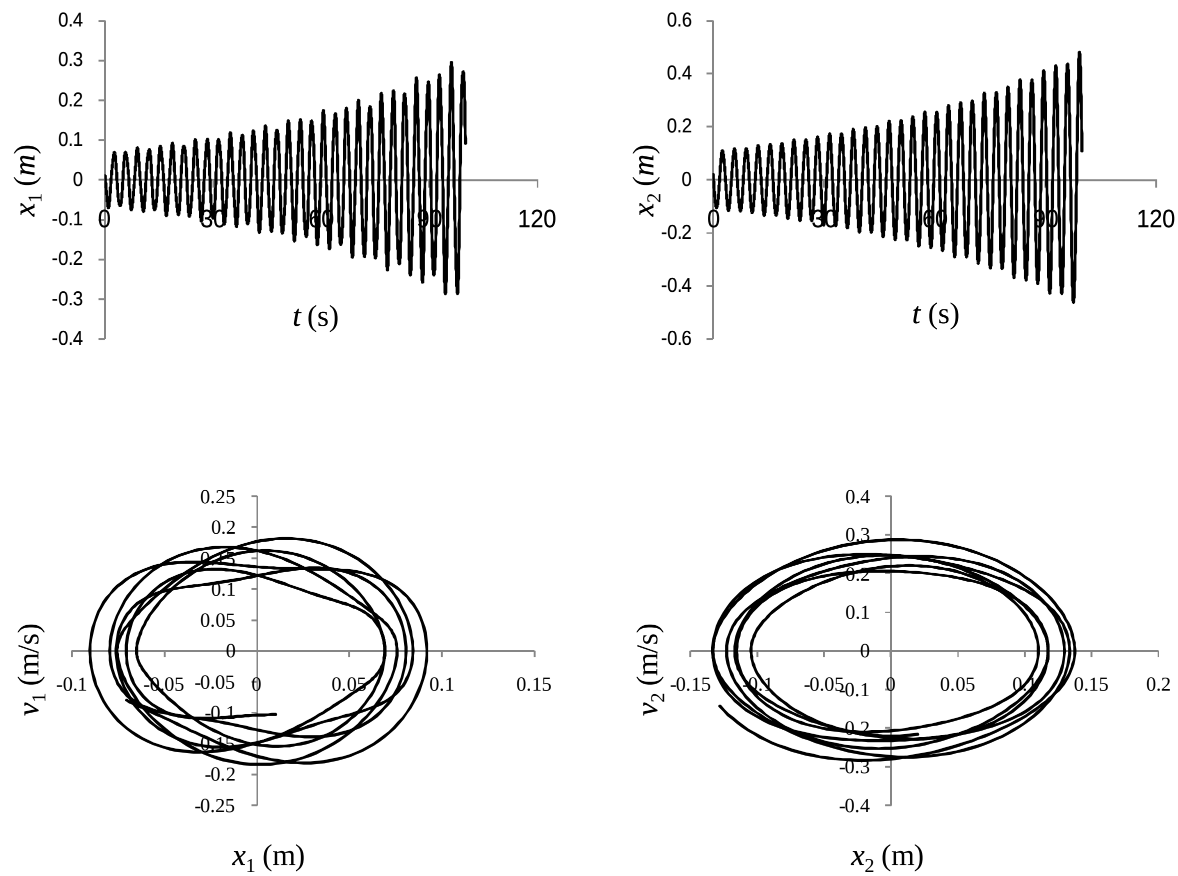

Fig. 4.10(*i*) x vs. t curves and phase planes of m_1 and m_2 (for data set (*i*) and *f(dv)*).
[m_1=10kg, m_2= 10kg, k_1=100 N/m, k_2=100 N/m, α_1=0.3 N/m, α_2=0.3 N/m, β_1 = 0.3 Ns/m , β_2=0.3 Ns/m]

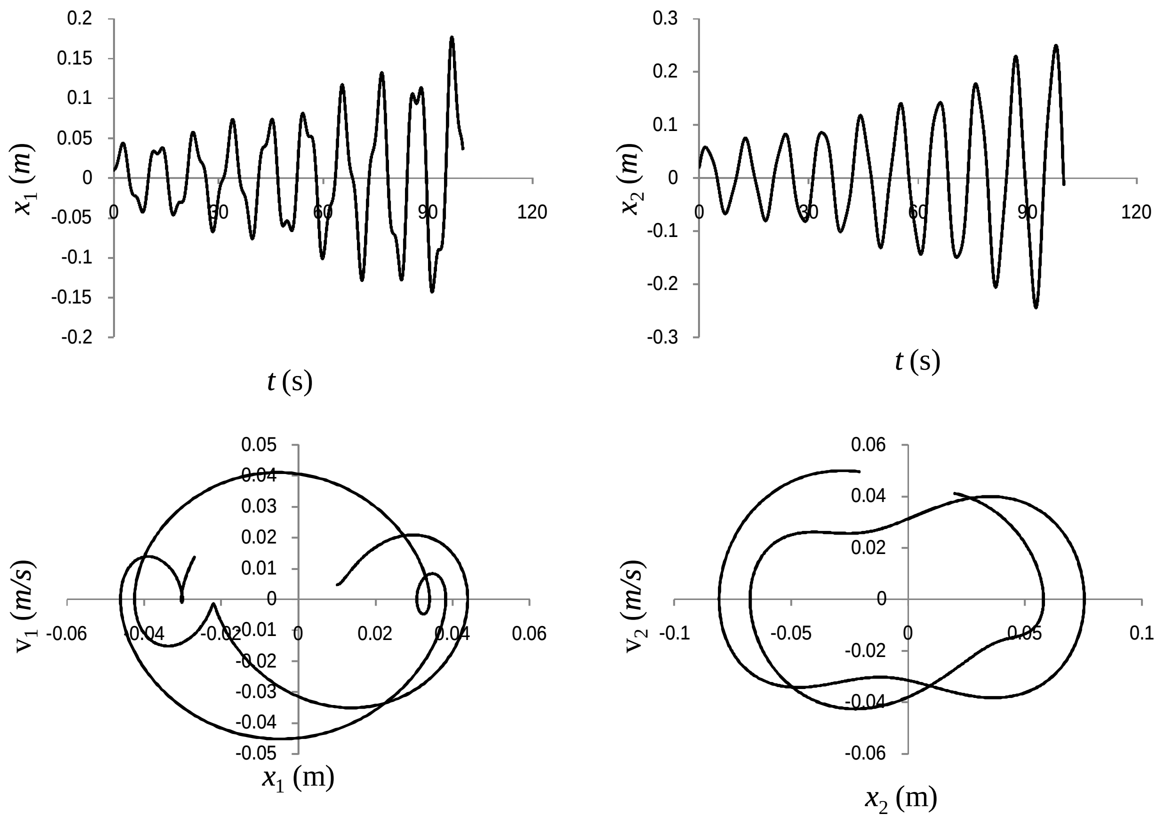

Fig. 4.10(*ii*) *x* vs. *t* curves and phase planes of m_1 and m_2 (for data set (*ii*) and for *f(dv)*).
[m_1=10kg, m_2= 10kg, k_1=10 N/m, k_2=10 N/m, α_1=0.3 N/m, α_2=0.3 N/m, β_1 = 0.3 Ns/m , β_2=0.3 Ns/m]

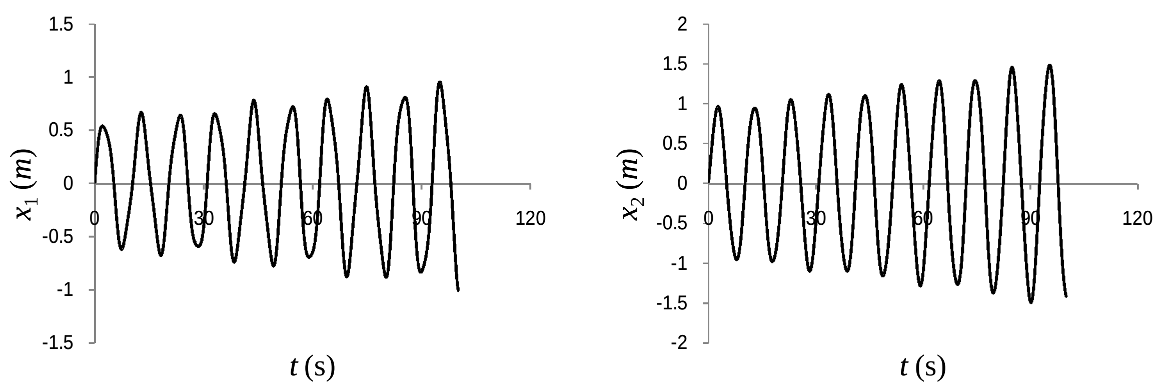

Fig. 4.10 (*iii*) *x* vs. *t* curve for m_1 and m_2 (for data set (*iii*) and for *f(dv)*)
[m_1=10kg, m_2= 10kg, k_1=10 N/m, k_2=10 N/m, α_1=0.1 N/m, α_2=0.1 N/m, β_1 = 0.1 Ns/m , β_2=0.1 Ns/m]

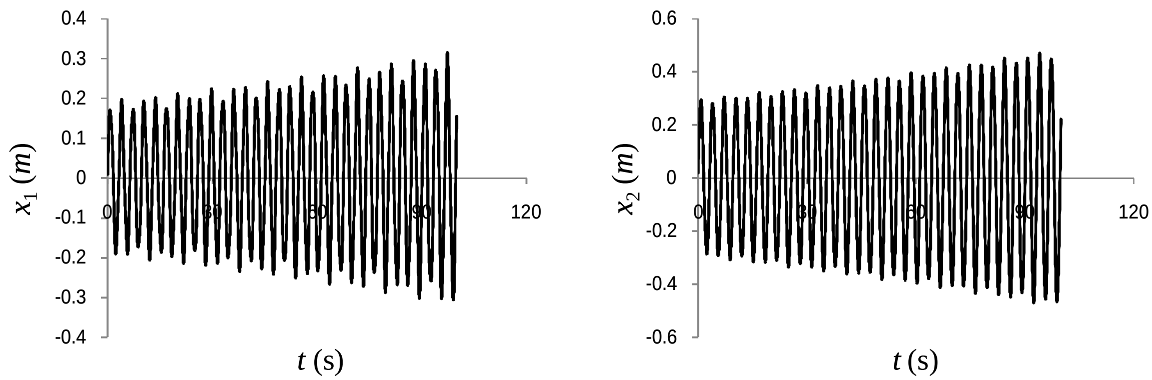

Fig. 4.10(*iv*) x vs. t curves of m_1 and m_2 (for data set (*iv*) and for *f(dv)*) [m_1=10kg, m_2= 10kg, k_1=100 N/m, k_2=100 N/m, α_1=0.1 N/m, α_2=0.1 N/m, β_1 = 0.1 Ns/m, β_2=0.1 Ns/m]

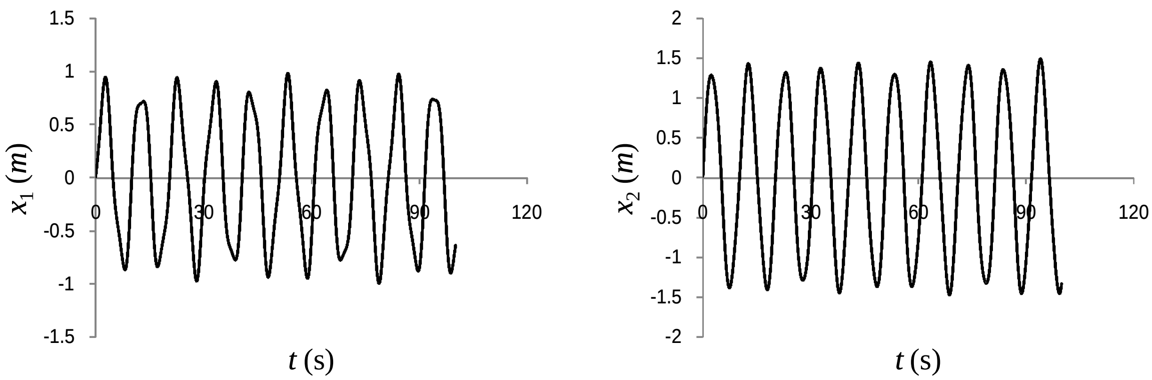

Fig. 4.10(*v*) x vs. t curves of m_1 and m_2 (for data set (*v*) and for *f(dv)*) [m_1=100kg, m_2= 100kg, k_1=100 N/m, k_2=100 N/m, α_1=0.1 N/m, α_2=0.1 N/m, β_1 = 0.1 Ns/m, β_2=0.1 Ns/m]

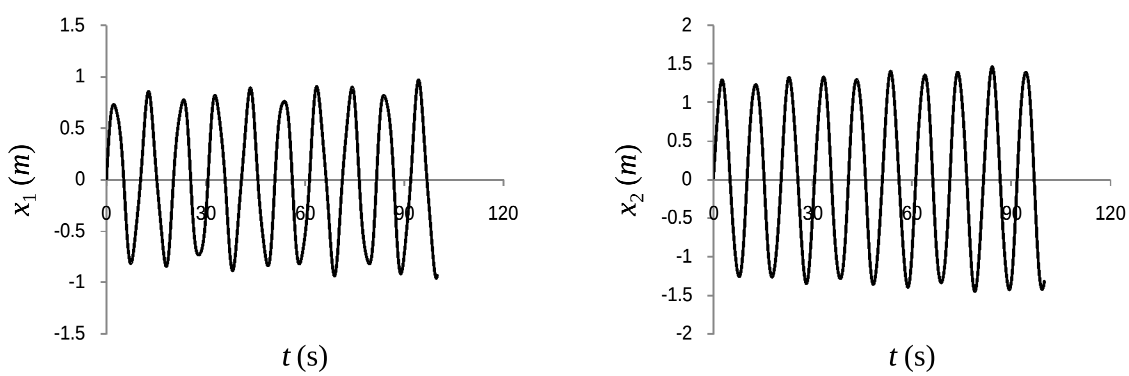

Fig. 4.10(*vi*) x vs. t curve for m_1 and m_2 (for data set (*vi*) and for *f(dv)*) [m_1=100kg, m_2= 100kg, k_1=100 N/m, k_2=100 N/m, α_1=0.3 N/m, α_2=0.3 N/m, β_1 = 0.3 Ns/m, β_2=0.3 Ns/m]

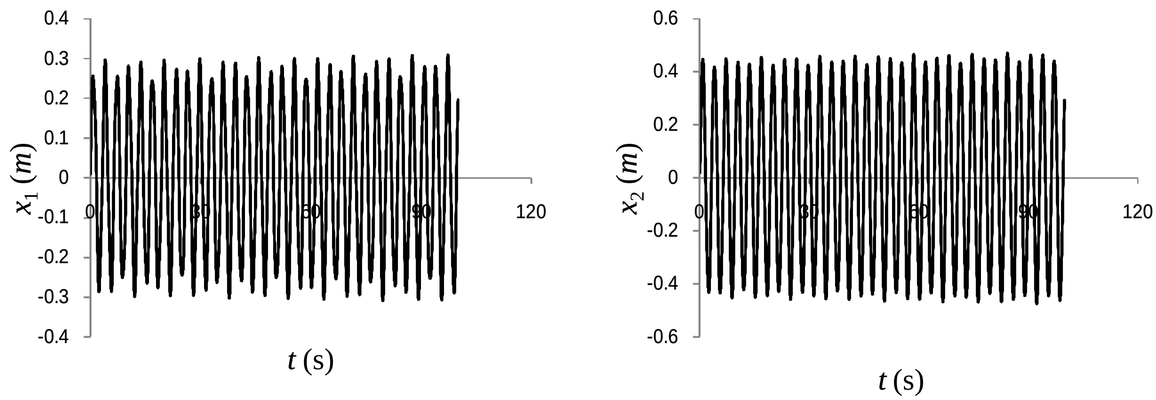

Fig. 4.10(*vii*) *x* vs. *t* curve for m_1 and m_2 (for data set (*vii*) and for *f(dv)*) [$m_1=100kg$, $m_2=100kg$, $k_1=1000$ N/m, $k_2=1000$ N/m, $\alpha_1=0.1$ N/m, $\alpha_2=0.1$ N/m, $\beta_1 = 0.1$ Ns/m, $\beta_2=0.1$ Ns/m]

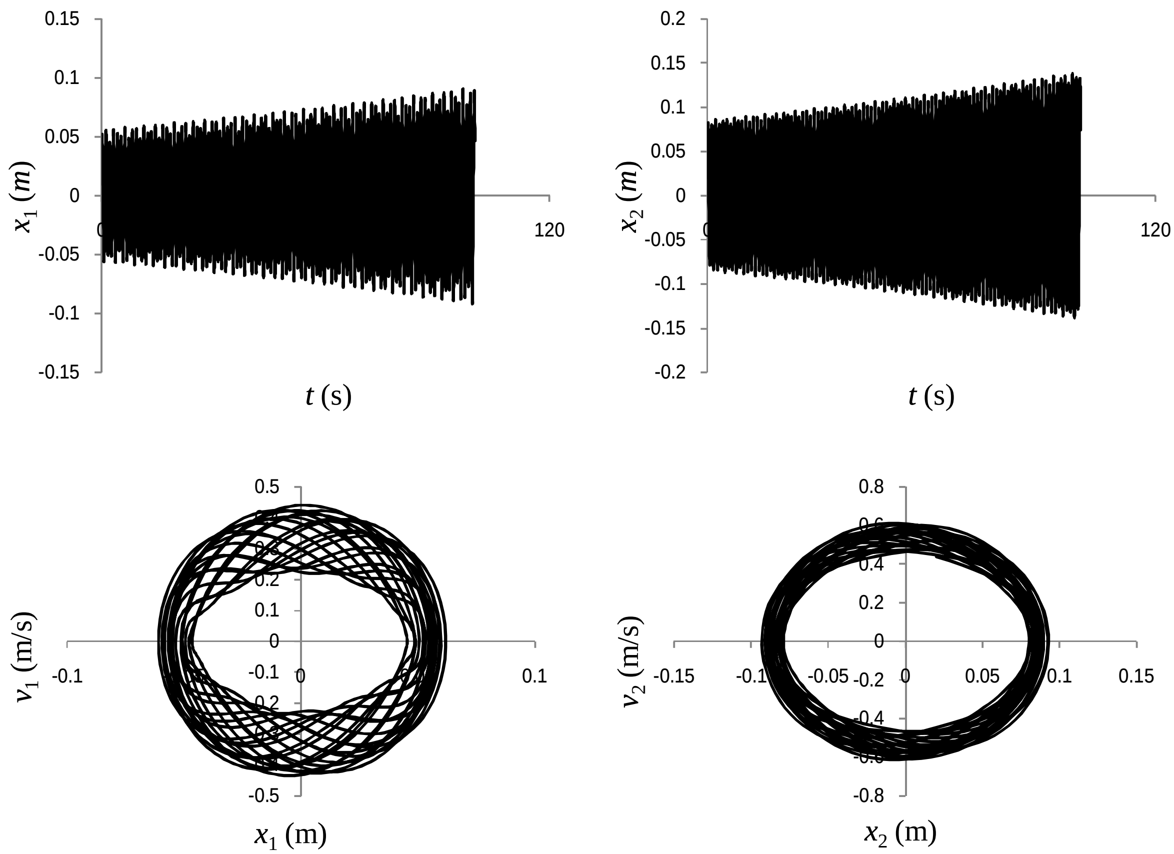

Fig. 4.10(*viii*) *x* vs. *t* curve and phase planes for m_1 and m_2 (for data set (*viii*) and for *f(dv)*) [$m_1=10kg$, $m_2= 10kg$, $k_1=1000$ N/m, $k_2=1000$ N/m, $\alpha_1=0.1$ N/m, $\alpha_2=0.1$ N/m, $\beta_1 = 0.1$ Ns/m, $\beta_2=0.1$ Ns/m]

.

Figures of undamped self-excited vibration of 2DOFS (**IVP**)
Figs. 4.11(*i*) - 4.11(*viii*) drawn using data sets (*i*) - (*viii*) of **Table 6** for *f(d)* of **Table 2**

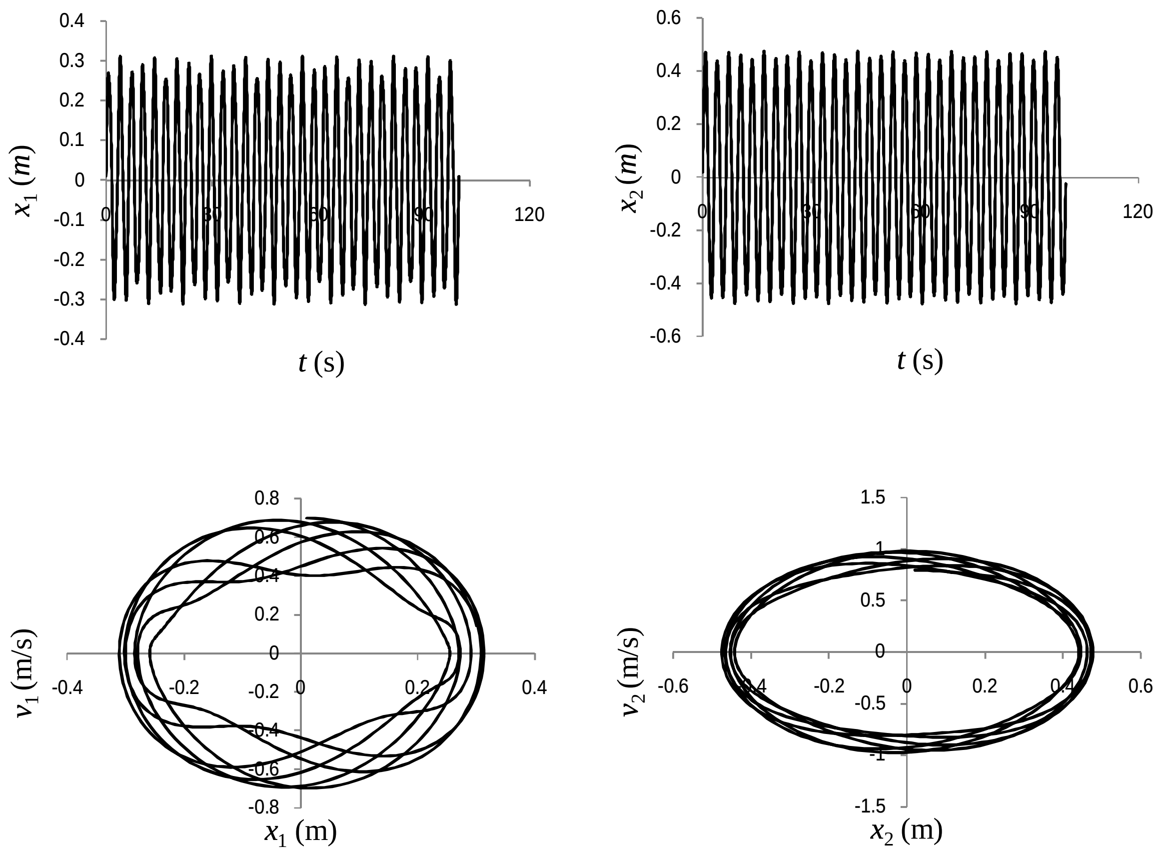

Fig. 4.11(*i*) x vs. t curves and phase planes of m_1 and m_2 (for data set (*i*) and for *f(d)*).
[m_1=10kg, m_2= 10kg, k_1=100 N/m, k_2=100 N/m, α_1=0.3 N/m, α_2=0.3 N/m]

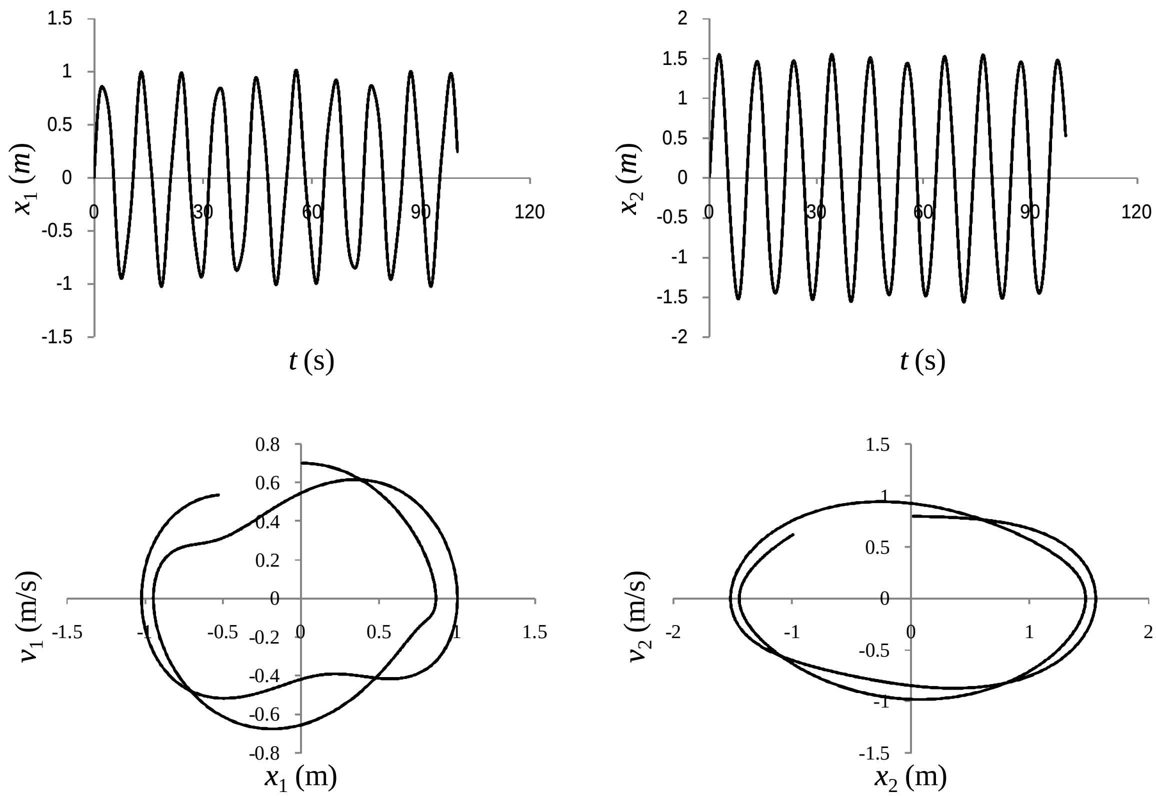

Fig. 4.11(*ii*) *x* vs. *t* curve and phase planes for m_1 and m_2 (for data set (*ii*) and for *f(d)*).
[m_1=10kg, m_2= 10kg, k_1=10 N/m, k_2=10 N/m, α_1=0.3 N/m, α_2=0.3 N/m]

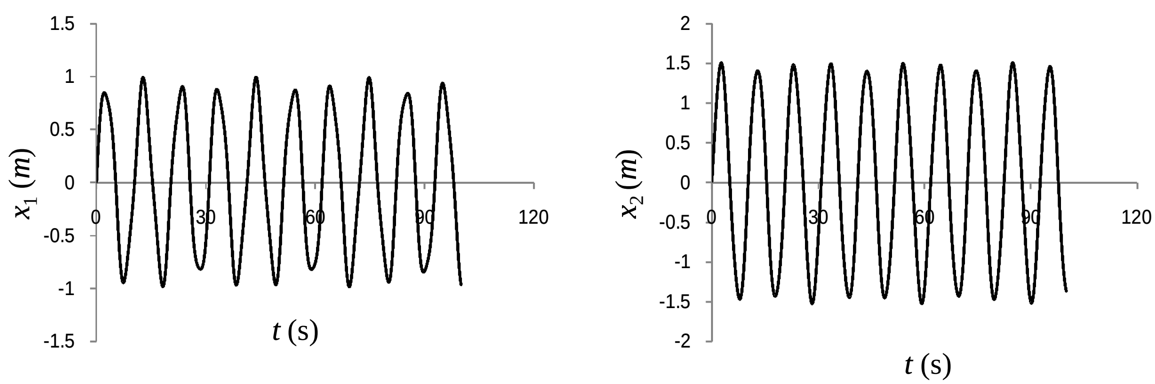

Fig. 4.11(*iii*) *x* vs. *t* curve for m_1 and m_2 (for data set (*iii*) and for *f(d)*)
[m_1=10kg, m_2= 10kg, k_1=10 N/m, k_2=10 N/m, α_1=0.1 N/m, α_2=0.1 N/m]

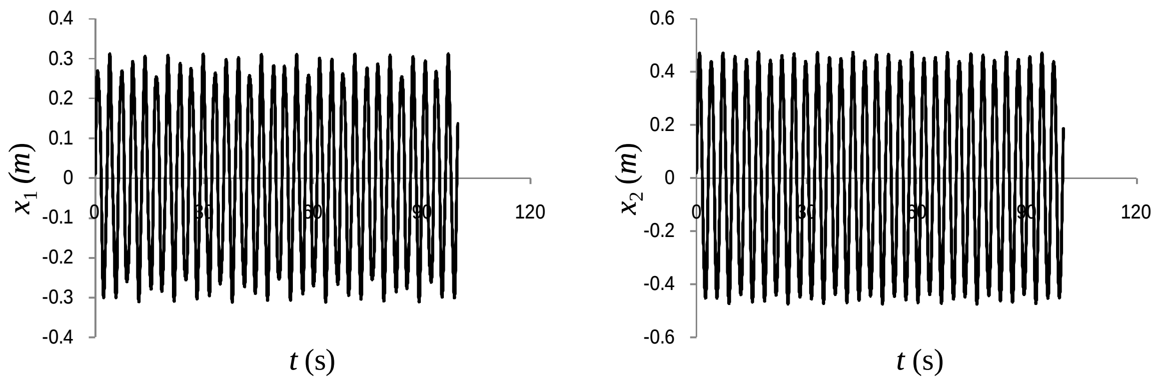

Fig. 4.11(*iv*) *x* vs. *t* curves of m_1 and m_2 (for data set (*iv*) and for *f(d)*)

[m_1=10kg, m_2= 10kg, k_1=100 N/m, k_2=100 N/m, α_1=0.1 N/m, α_2=0.1 N/m]

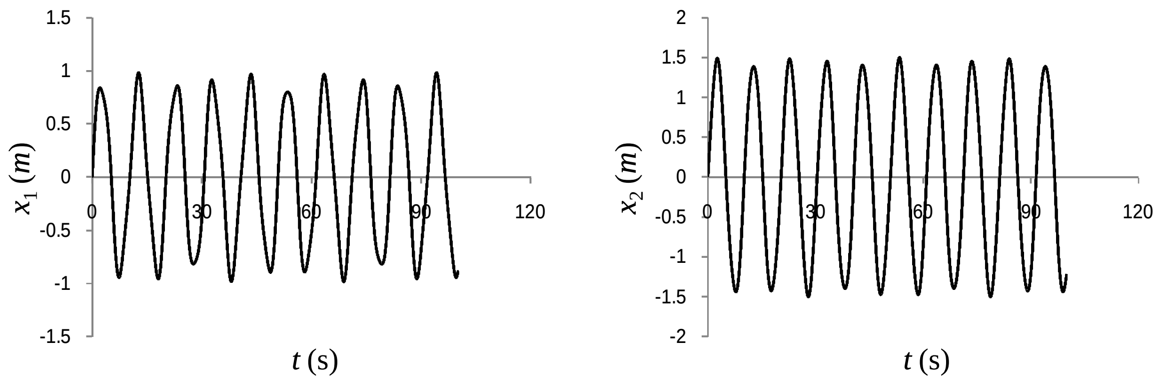

Fig. 4.11(*v*) *x* vs. *t* curves of m_1 and m_2 (for data set (*v*) and for *f(d)*)

[m_1=100kg, m_2= 100kg, k_1=100 N/m, k_2=100 N/m,α_1=0.1 N/m, α_2=0.1 N/m]

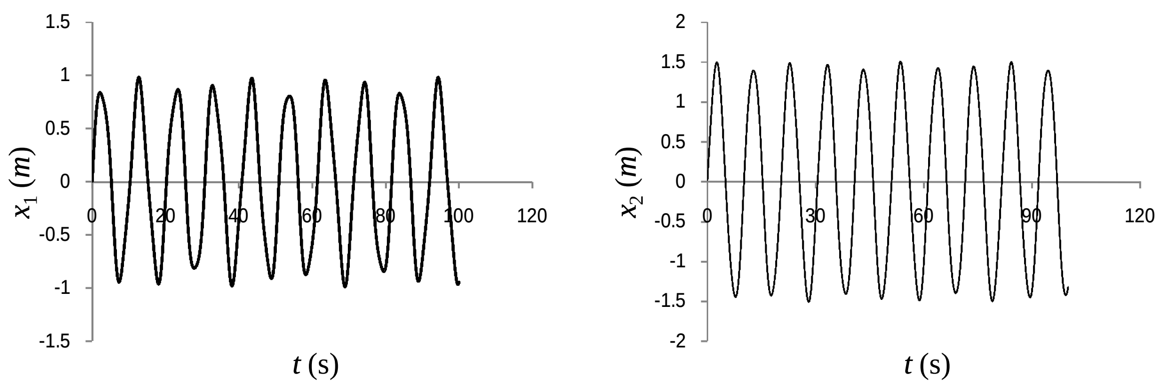

Fig. 4.11(*vi*) *x* vs. *t* curves of m_1 and m_2 (for data set (*vi*) and for *f*(*d*))

[m_1=100kg, m_2= 100kg, k_1=100 N/m, k_2=100 N/m, α_1=0.3 N/m, α_2=0.3 N/m]

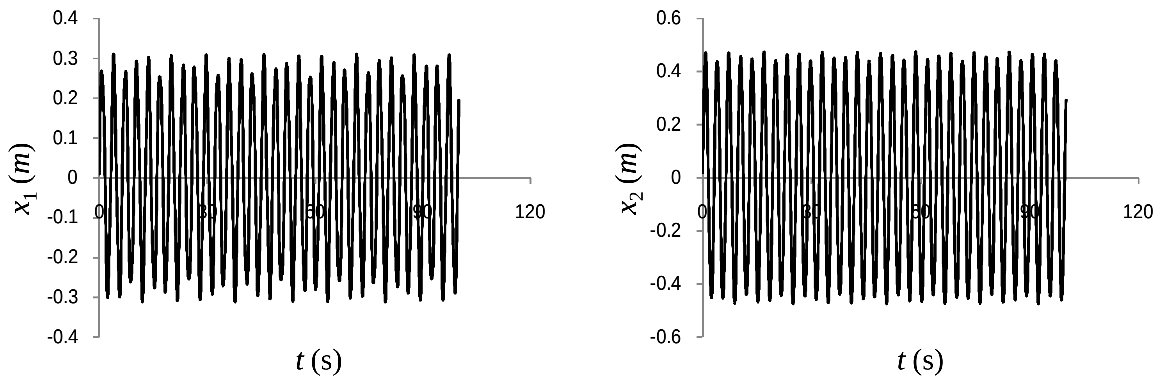

Fig. 4.11(*vii*) x vs. t curves of m_1 and m_2 (for data set (*vii*) and for *f(d)*)
[m_1=100kg, m_2= 100kg, k_1=1000 N/m, k_2=1000 N/m, α_1=0.1 N/m, α_2=0.1 N/m]

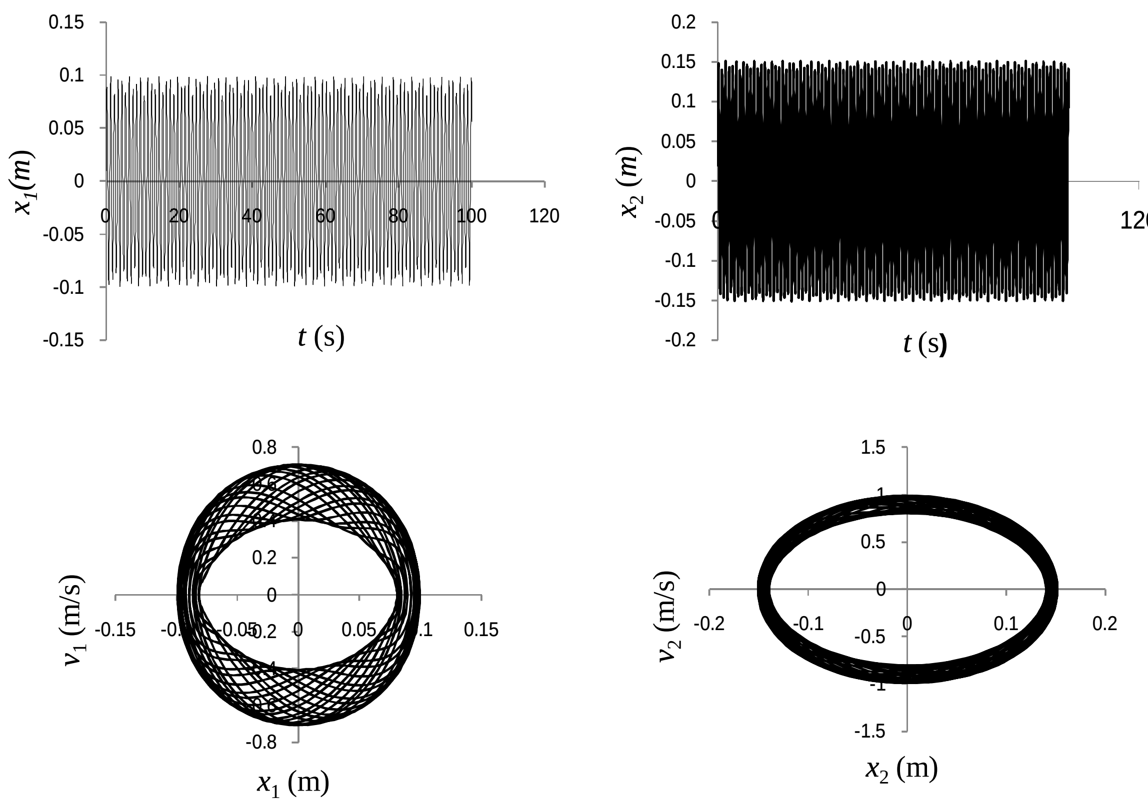

Fig. 4.11(*viii*) x vs. t curves and phase planes of m_1 and m_2 (for data set (*viii*) and for *f(d)*).
[m_1=10kg, m_2= 10kg, k_1=1000 N/m, k_2=1000 N/m, α_1=0.1 N/m, α_2=0.1 N/m**]**

4.4 Analysis of Damped Self-excited Vibration of 2DOFS

This section includes effect of non-linearity on the system's response. For analyzing the damped self-excited vibration of 2DOFS, BVP method has been used to determine the responses for self-excited vibration of 2DOFS. Four different combinations (1-4) from Table 8 of both linear and nonlinear springs and dampers have been considered for analysis. For each combination, four different cases ((*a*)-(*d*)) from Table 2 are incorporated into calculation. Calculations have been performed using two sets of data for various parameters (Table 10).

4.4.1 Response of 2DOFS for the combination of linear springs and linear dampers [*Figures 4.12(a)-4.12(d) and Figures 4.13(a)-4.13(d)]*

For data set 1 of Table 10 and cases (*a*) – (*d*) from Table 2, the response of damped self-excited vibration of 2DOFS has been shown through amplitude of vibration with time in figures 4.12(a) to 4.12(d) and phase planes for cases (*a*), (*c*) and (*d*) are also drawn.

Figure 4.12(a) for *f(d)* shows that m_1 vibrates with smaller amplitude and gradually approaches to stability. Within the time span of 100 seconds, x_1 finally reaches to 0.00289 m and in this way, the system's amplitude tends to zero after certain time. So for this condition,

the system becomes stable. On the other hand, m_2 in figure 4.12(a) vibrates at higher amplitude than m_1. However, the amplitude gradually decreases and hence the system approaches to stability although more time is required to be stable.

Similar types of response are found for all other three cases [(*b)* – *(d*) of Table 2] when combination of linear springs and linear dampers are used. Figures from 4.12(b) to 4.12(d) show the *x-t* curves for these three cases.

For data set 2 of Table 10, the responses of damped self-excited vibration of 2DOFS for four cases [(*a) - (d)* from Table 2] are shown in figures. 4.13(a) to 4.13(d) through *x* vs. *t* curves and phase planes for both m_1 and m_2. In figure 4.13(a) for *f(d)*, the amplitude of m_1 is very high initially but gradually it decreases and after 40 seconds, the system finally reaches to stability. Although the m_1 is same here, but due to increase of spring constant in data set 2 of Table 10, the system approaches to stability very soon. The amplitude of vibration is noticed to be high for data set 2. From figure 4.13(a), it is clear that although amplitude is higher at first, but within small time, the system approaches stability. But figure 4.12(a) for data set 1 reveals that the system takes much time to be stable. For data set 2, similar response for other three cases [(*b*),(*c*) & (*d*)] are observed for m_1 as shown in figures 4.13(b) and 4.13(c).

But for data set 2 for this combination of linear springs and linear dampers, m_2 shows an irregular behavior as seen from figure 4.13(a). From figure 4.13(a) for m_2 For first 20 seconds, m_2 vibrates with high frequency. However, later m_2 starts to vibrate at relatively lower amplitude and with lower frequency and then gradually reaches stable condition.

Figure 4.13(b) for *f(v)* indicates that the amplitude of m_2 is quite low relative to other cases. Response of m_2 is similar to other two cases as shown in figures 4.13(c) and 4.13(d). In figure 4.13(d), m_2 vibrates in an irregular fashion for first 20 seconds. After 20 seconds, m_2 maintains stable amplitude of vibration and up to 40 seconds, the system maintains steady vibration.

For *f(n)*, the responses of damped self-excited vibration of m_1 and m_2 are shown only for 40 seconds as the developed computer code for the chosen conditions does not give the regular values after more than 40 seconds. This is due to that fact that considered numerical technique can't solve after that period of time and hence abnormal results are shown. Therefore, figure 4.13(d) for *f(n)* are drawn for only 40 seconds. That means the system's response for *f(n)* can be drawn for only 40 seconds with the results obtained from developed computer code for considered values of parameters.

Having analyzed *x-t* curves for this combination of linear springs and linear dampers, it would be easy to comprehend the effect of spring nonlinearity on the system's response by comparing with the result for the combination of non-linear spring and linear dampers.

4.4.2 Response of 2DOFS for the combination of linear springs and non-linear dampers. [*Figures 4.14(a) and 4.14(b)]*

Only for *f(n)* and data set 1of Table 10, the response of the system is shown in figure 4.14(a). Again for *f(n)* and data set 2 of Table 10, the response is shown in figure 4.14(b). For other three cases (*a* - *c*), figures [B(1) –B(3) for data set 1 and B(4)-B(6) for data set 2] are given in Appendix B.

In figure 4.14(a) for *f(n)*, the amplitude of vibration of m_1 varies from 0.5 m to .008 m. Initially amplitude is high, but after 5 seconds, it decreases to around 0.2 m and gradually reaches to very low amplitude. This implies that the system approaches to stability after the period of 100 seconds. On the other hand, m_2 vibrates with relatively higher amplitude ranging from 0.5m to 0.05 m. This implies that m_2 takes much time to be stable.

Figure 4.14(b) for data set 2 and *f(n)* shows the responses of the system for the combination of linear springs and non-linear dampers. Here the figures are drawn with the results of computer program for 40 seconds.

In figure 4.14(b), m_1 vibrates with high frequency for first 10 seconds, then its frequency decreases and maintains steady vibration with lower amplitude. On the other hand, m_2 vibrates in a different way rather than m_1. The response of m_2 for *f(n)* is shown in figure 4.14(b). The amplitude of vibration of m_2 is quite low for this case.

However, for *f(n)*, m_2 in figure 4.14(b) maintains a steady vibration and with time its amplitude does not show the decreasing trend. Therefore, for this case, m_2 continues its vibration throughout the entire period.

4.4.3 Response of 2DOFS for the combination of non-linear springs and linear dampers. [*Figures 4.15(a) and 4.15(b)]*

Only for *f(n)* and data set 1of Table 10, the response of the system is shown in figure 4.15(a). Again for *f(n)* and data set 2 of Table 10, the response is shown in figure 4.15(b). For other three cases (*a* - *c*), figures [B(7) –B(9) for data set 1 and B(10)-B(12) for data set 2] are given in Appendix B.

In figure 4.15(a), m_1 starts vibrating with the amplitude of 0.05 m and then finally decreases to 0.01 m. Finally, the vibration of m_1 moves towards stability after the period of 100 seconds. m_2 also vibrates in a similar fashion. But the amplitude of vibration of m_2 decreases more slowly than that of m_1. The response of m_2 is just like as in combination of linear springs and linear dampers. Amplitude of vibration of m_2 also varies from 0.05 m to 0.01 m.

So for *f(n)*, the responses of both m_1 and m_2 [figure 4.15(a)] are quite similar.

For data set 2 and *f(n)*, the responses of both m_1 and m_2 are shown in figure 4.15(b).

In figure 4.15(b) , m_1 vibrates with higher frequency and amplitude range of 0.07 m to 0.017 m for first 15 seconds. Then m_1 maintains steady vibration with the reduction of amplitude and frequency. On the other hand, m_2 continues vibration in steady state mood. m_2 maintains almost constant amplitude of 0.025 m throughout the entire period. Therefore, for *f(n)*, m_2 never reaches to stability.

4.4.4 Response of 2DOFS for the combination of non-linear springs & non-linear dampers. [*Figures 4.16(a)-4.16(d) and Figures 4.17(a)-4.17(d)]*

For cases *(a)* to *(d)* from Table 2 and data set 1 of Table 10, the responses of the system are shown in figures 4.16(a) to 4.16(d). Figures from 4.17(a) to 4.17(b) show the responses of the system for data set 2.

From figure 4.16(a), it is seen that m_1 vibrates with very low amplitude and frequency. Though initially m_1 starts to vibrate with amplitude of 0.04 m, but within few seconds, the amplitude of vibration suddenly drops to 0.0026 m and moves toward stability. But suddenly becomes unstable at t = 100 seconds.

Similarly in figure 4.16(a), m_2 also vibrates with very small amplitude and approaches to stability. The amplitude of vibration for m_2 is higher than that of m_1. This is due to the combination of nonlinear springs and nonlinear dampers.

In figure 4.16(b) for *f(v)*, amplitudes of vibration of both m_1 and m_2 are higher than in *f(d)*. But for both m_1 and m_2, the system approaches to stability after a certain period.

Similar types of response for both m_1 and m_2 are found in figure 4.16(c) for *f(dv)* and figure 4.16(d) for *f(n)* for data set 1. In every case (*a-d*) for data set 1, the system reaches to stable condition.

For data set 2 and all four cases (a - d) for this combination of non-linear springs and non-linear dampers, different types of responses for both m_1 and m_2 are found from the figures 4.17(a) to 4.17(d).

From figures 4.17(a) to 4.17(d) , it is clear that for all cases from *(a)* to *(d)*, m_1 vibrates with high frequency for first 15 seconds and then gradually its frequency decreases. The amplitude of vibration of m_1 starts from 0.06 m and gradually it decreases and hence moves toward steady vibration. In figure 4.17(d) for *f(n)*, the amplitude of m_1 is very small compare to other three cases.

On the other hand, for the combination of non-linear springs and non-linear dampers and for all four cases (a – d), m_2 maintains a steady vibration throughout the entire period. The amplitude of vibration of m_2 remains almost fixed at 0.02 m for cases *(a)* and *(b)* as shown in figures 4.17(a) and 4.17(b). But in figures 4.17(c) and 4.17(d) for cases *(c)* and *(d)*, amplitude of m_2 is much lower than in previous two cases (a - b). For cases *(c)* and *(d)*, amplitude of m_2 remains almost fixed at 0.002 m for the whole period. So for the combination of non-linear springs and non-linear damper and data set 2, the system never reaches to stability rather continues vibration although amplitude is very small.

4.5 Comparison among the responses for four combinations (1- 4 of Table 8) of damped self-excited vibration of 2DOFS

For damped self-excited vibration of 2DOFS, four combinations (1- 4 of Table 8) of springs and dampers depending on nonlinearity and four cases (a - d from Table 2) depending on the type of self-excited vibration function (Table 2) are considered. For two sets of data from Table 10, responses of self-excited vibration of 2DOF have been drawn according to the sequence of combinations of springs and dampers from Table 8.

4.5.1 Combination of linear springs and linear dampers [*Figures 4.12(a)-4.12(d) and 4.13(a)-4.13(d)*]

For combination of linear springs and linear dampers, almost similar response is found for all four cases (a - d) when data set 1 from Table 10 is used for calculation. Figures 4.12(a) to 4.12(d) show that the amplitude of vibration is mostly similar for every case for both m_1 and m_2. For data set 1, the system approaches to stability quickly.

But for data set 2 from Table 10, the system's response for this combination is different from the response for data set 1. The amplitude of vibration of m_1 quickly diminishes. It just takes 20 seconds to reduce the vibration to almost zero. On the other hand, m_2 presents high frequency vibration up to 20 seconds and then it maintains steady state vibration of very lower amplitude. So after few seconds, the system will become stable. This is due to the use of both linear springs and dampers. With increase of spring constant in data set 2 of Table 10, the amplitude of vibration diminishes very quickly.

4.5.2 Combination of linear springs and non-linear dampers [*Figures 4.14(a) & 4.14(b) and Figures B(1)-B(6) from Appendix B*]

For the combination of linear springs and non-linear dampers and for data set 1 from Table 10, the amplitudes of vibration of both m_1 and m_2 in figures B(1)-B(3) and figure 4.14(a) are analogous to those for data set 1 and the combination of linear springs and dampers. This implies that damper nonlinearity has no such apparent effect on the response of self-excited vibration of the system. But for data set 2 and the combination of linear springs and non-linear dampers, the response of the system as shown in figures B(4)-B(6) and figure 4.14(b) is quite similar to that for the *f(n)* for combination of linear springs and linear dampers. Except in the figure 4.14(b) for *f(n)*, the system shows very similar type of vibration. This implies that for combination of linear soft springs and non-linear soft dampers, the response of the system is independent of the self-excited force function whether it is function of displacement, velocity or both of displacement and velocity. Figure 4.17(b) for the *f(n)* shows that the system exhibits steady vibration and hence maintains instability. The different phenomenon for *f(n)* is mainly due to the nonlinear displacement term.

4.5.3 Combination of non-linear springs and linear dampers [*Figures 4.15(a) & 4.15(b) and Figures B(7)-B(12) from Appendix B*]

For the combination of non-linear springs and linear dampers and data set 1 of Table 10, the system, in figures B(7) & B(8) for both *f*(*d*) and *f*(*v*), shows high frequency vibration for first few seconds and then approaches to stability with lower frequency as shown for the combination of linear springs and linear dampers or linear springs and non-linear dampers. But for *f(dv)* and (*d*) and for data set 1, the figures show shooting after the considered period of 100 seconds. The numerically developed code does not show the response of the system after that period. But if more segments are considered for calculation, then the response will be obtained after this period. But for data set 2 for the combination of non-linear springs and linear dampers, the system in figures B(10) - B(12) and figure 4.15(b) shows the response just like the *f(n)* of combination of linear springs and non-linear dampers and for data set 2. This implies that soft springs with non-linearity (from data set 2 of Table 10) lead to the more unstable state of the system although the spring constant is of higher value (k =1000 N/m). Comparison of the system's response between the combination of linear spring and non-linear dampers [figures 4.14(a) & 4.14(b) and figures B(1)-B(6) from Appendix B] and non-linear spring and linear dampers [figures 4.15(a) & 4.15(b) and figures B(7)-B(12) from Appendix B] shows that spring non-linearity causes more instability of the system than the damper non-linearity.

4.5.4 Combination of non-linear springs and non-linear dampers [*Figures 4.16(a)-4.16(d) & 4.17(a)-4.17(d)*]

For the combination of non-linear springs and non-linear dampers and for data set 1 from Table 10, the vibration of both m_1 and m_2 in figures 4.16(a) to 4.16(d) follows the similar fashion as for the combination of linear springs and linear dampers or combination of linear springs and non-linear dampers for data set 1. So the system's response, for hard springs and hard dampers (data set 1 from Table 10), is independent not only of combination of springs and dampers but also of the function of self-excited force.

Again for this combination and for data set 2, pattern and amplitude of vibration in figures 4.17(a) to 4.17(d) are exactly same as for the combination of non-linear springs and dampers for data set 2. This clearly implies that spring non-linearity is dominant over damper non-linearity for soft springs and dampers.

Figures of damped self-excited vibration of 2DOFS (BVP)

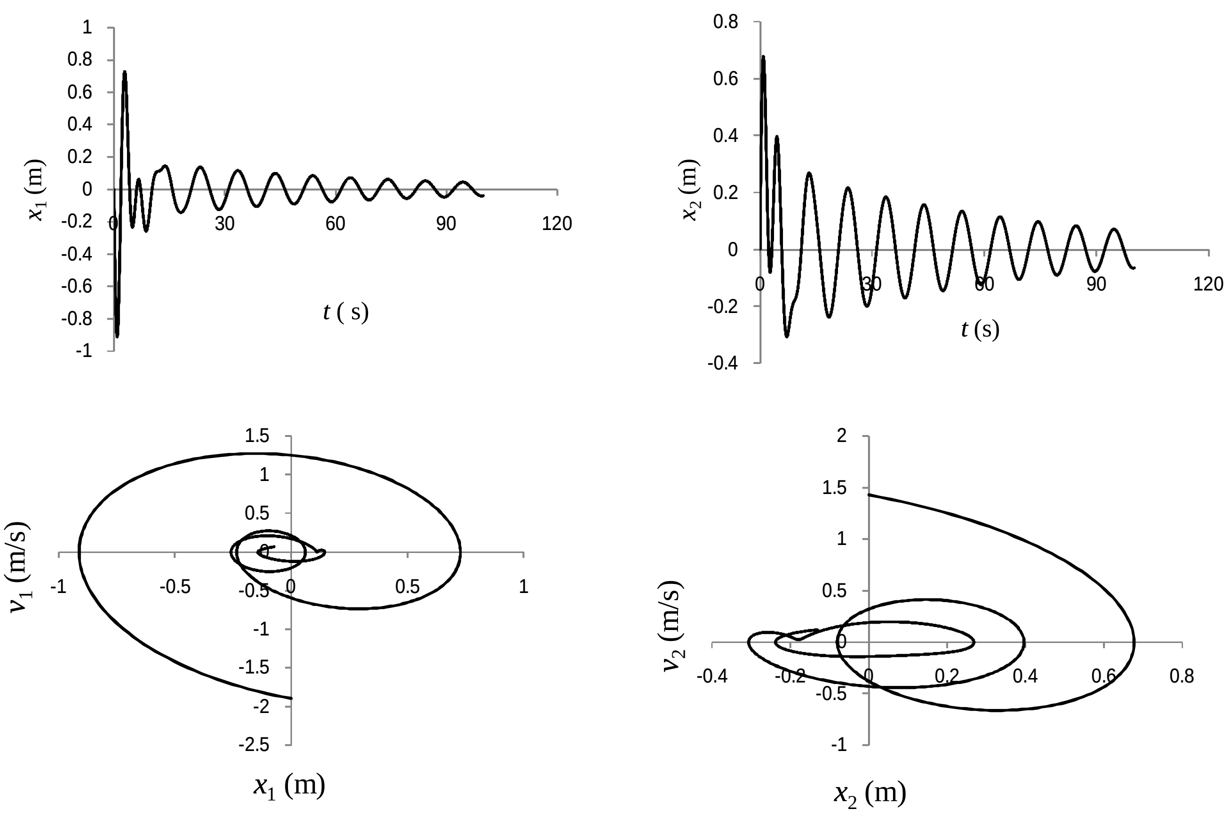

Fig. 4.12(a) x vs. t curves and phase planes of m_1 and m_2 for *f(d)* using data set 1 of Table 10 for combination of linear springs and linear dampers [m_1=100 kg, m_2 =100 kg, k_1=100 N/m, k_2 =100 N/m, c_1= 0.03 Ns/m, c_2 = 30.0 Ns/m, α_1 = 0.20 N/m, α_2 = 0.25 N/m]

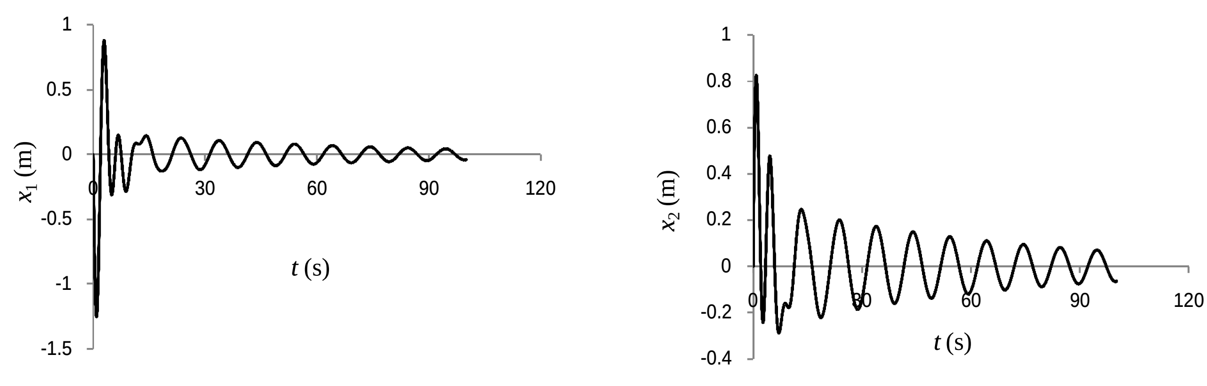

Fig. 4.12(b) x vs. t curves of m_1 and m_2 for *f(v)* of Table 2 using data set 1 of Table 10 for combination of linear springs and linear dampers [m_1=100 kg, m_2 =100 kg, k_1=100 N/m, k_2 =100 N/m, c_1= 0.03 Ns/m, c_2 = 30.0 Ns/m, β_1 = 0.10 Ns/m, β_2 = 0.20 Ns/m]

Figures of damped self-excited vibration of 2DOFS (BVP)

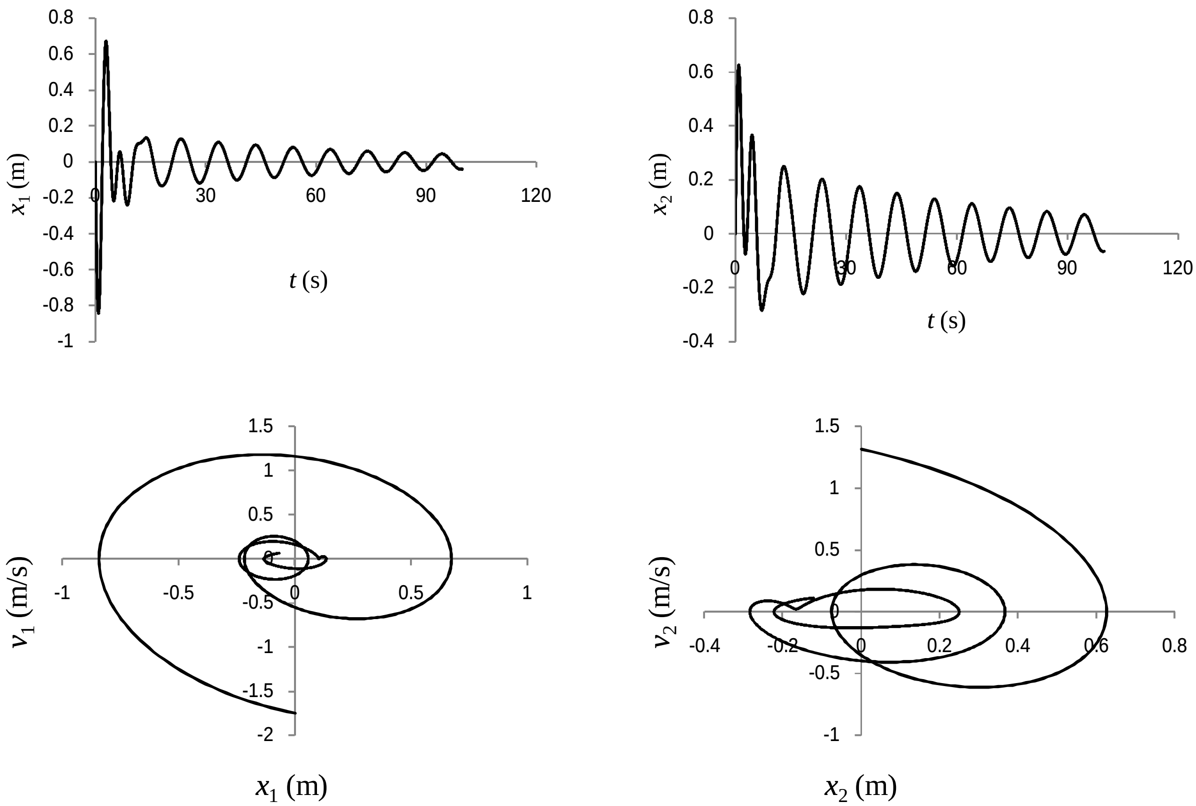

Fig. 4.12(c) x vs. t curves and phase planes of m_1 and m_2 for $f(dv)$ of Table 2 using data set 1 of Table 10 for combination of linear springs and linear dampers [m_1=100 kg, m_2 =100 kg, k_1=100 N/m, k_2 =100 N/m, c_1= 0.03 Ns/m, c_2 = 30.0 Ns/m, α_1 = 0.20 N/m, α_2 = 0.25 N/m, β_1 = 0.10 Ns/m, β_2 = 0.20 Ns/m]

Figures of damped self-excited vibration of 2DOFS (BVP)

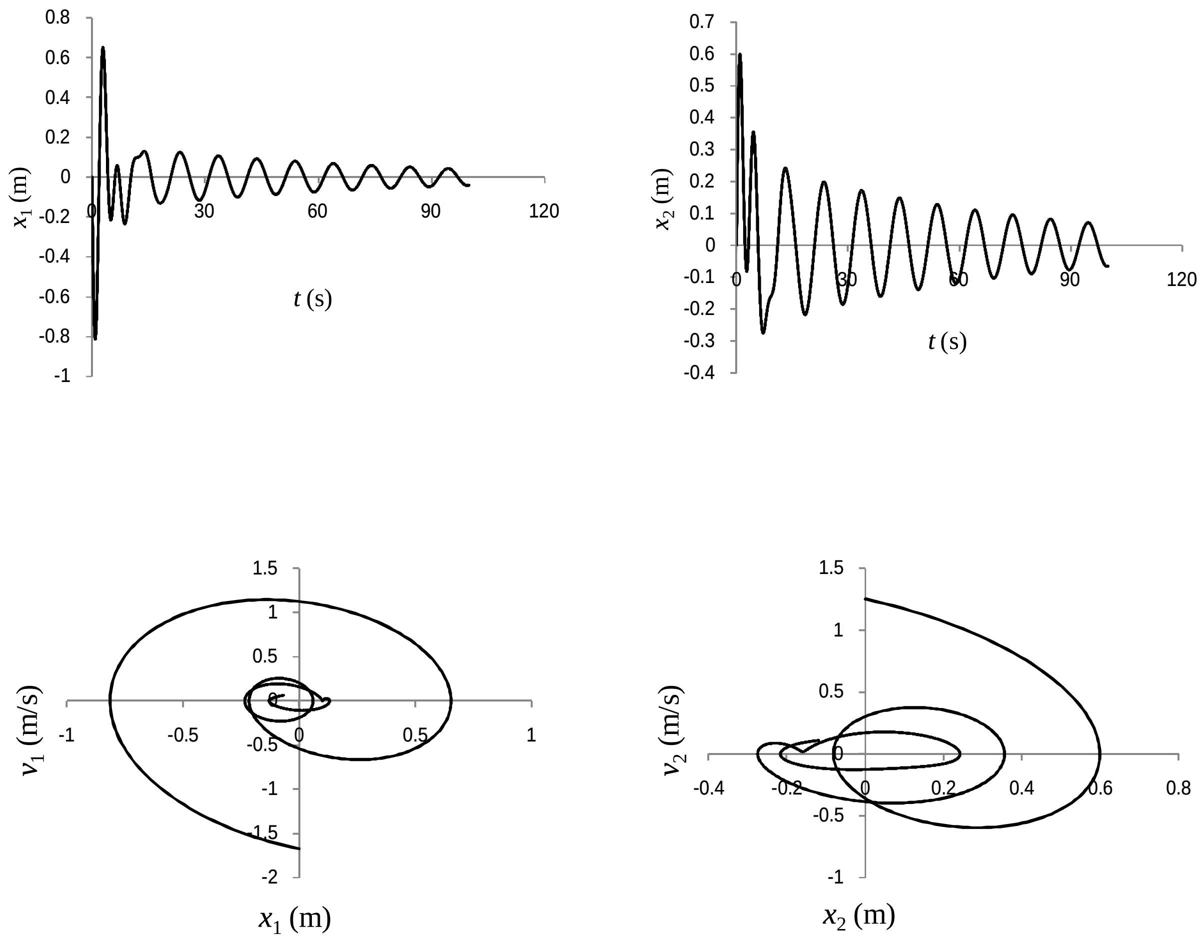

Fig. 4.12(d) x vs. t curves and phase planes of m_1 and m_2 for $f(n)$ of Table 2 using data set 1 of Table 10 for combination of linear springs and linear dampers [m_1=100 kg, m_2 =100 kg, k_1=100 N/m, k_2 =100 N/m, c_1= 0.03 Ns/m, c_2 = 30.0 Ns/m, α_1 = 0.20 N/m, α_2 = 0.25 N/m, β_1 = 0.10 Ns/m, β_2 = 0.20 Ns/m , γ_1 = 0.001 Ns/m^3, γ_2 = 0.002 Ns/m^3].

Figures of damped self-excited vibration of 2DOFS (BVP)

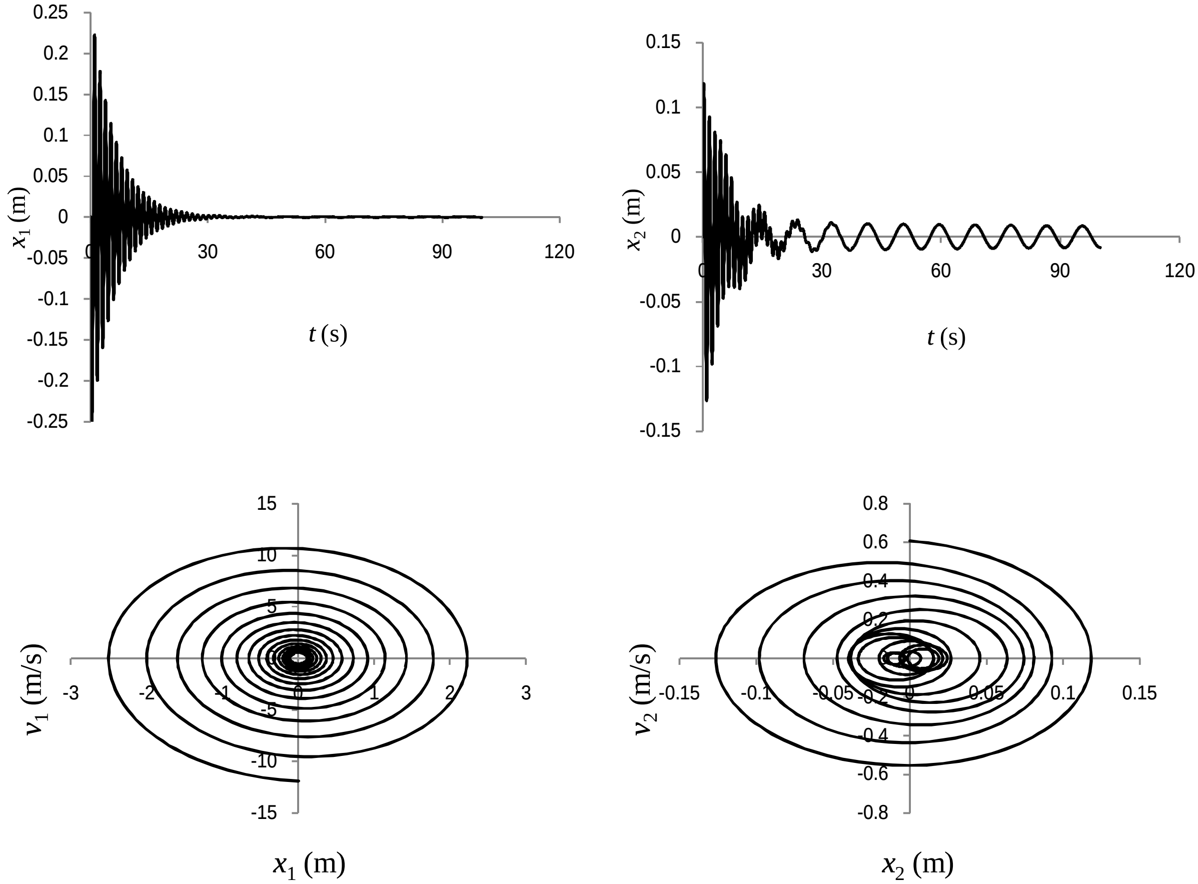

Fig. 4.13(a) x vs. t curves and phase planes of m_1 and m_2 for *f(d)* of Table 2 using data set 2 of Table 10 for combination of linear springs and linear dampers [m_1=100 kg, m_2 =1000 kg, k_1=1000 N/m, k_2 =1000 N/m, c_1= 0.03 Ns/m, c_2 = 30.0 Ns/m, α_1 = 0.15 N/m, α_2 = 0.20 N/m]

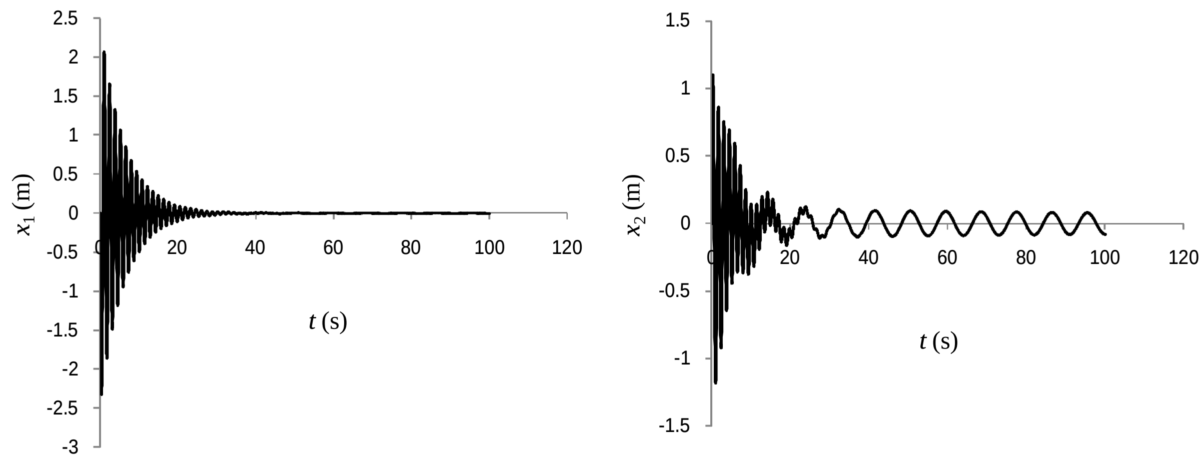

Fig. 4.13(b) x vs. t curves of m_1 and m_2 for *f(v)* of Table 2 using data set 2 of Table 10 for combination of linear springs and linear dampers [m_1=100 kg, m_2 =1000 kg, k_1=1000 N/m, k_2 =1000 N/m, c_1= 0.03 Ns/m, c_2 = 30.0 Ns/m, β_1 = 0.15 Ns/m, β_2 = 0.25 Ns/m].

Figures of damped self-excited vibration of 2DOFS (BVP)

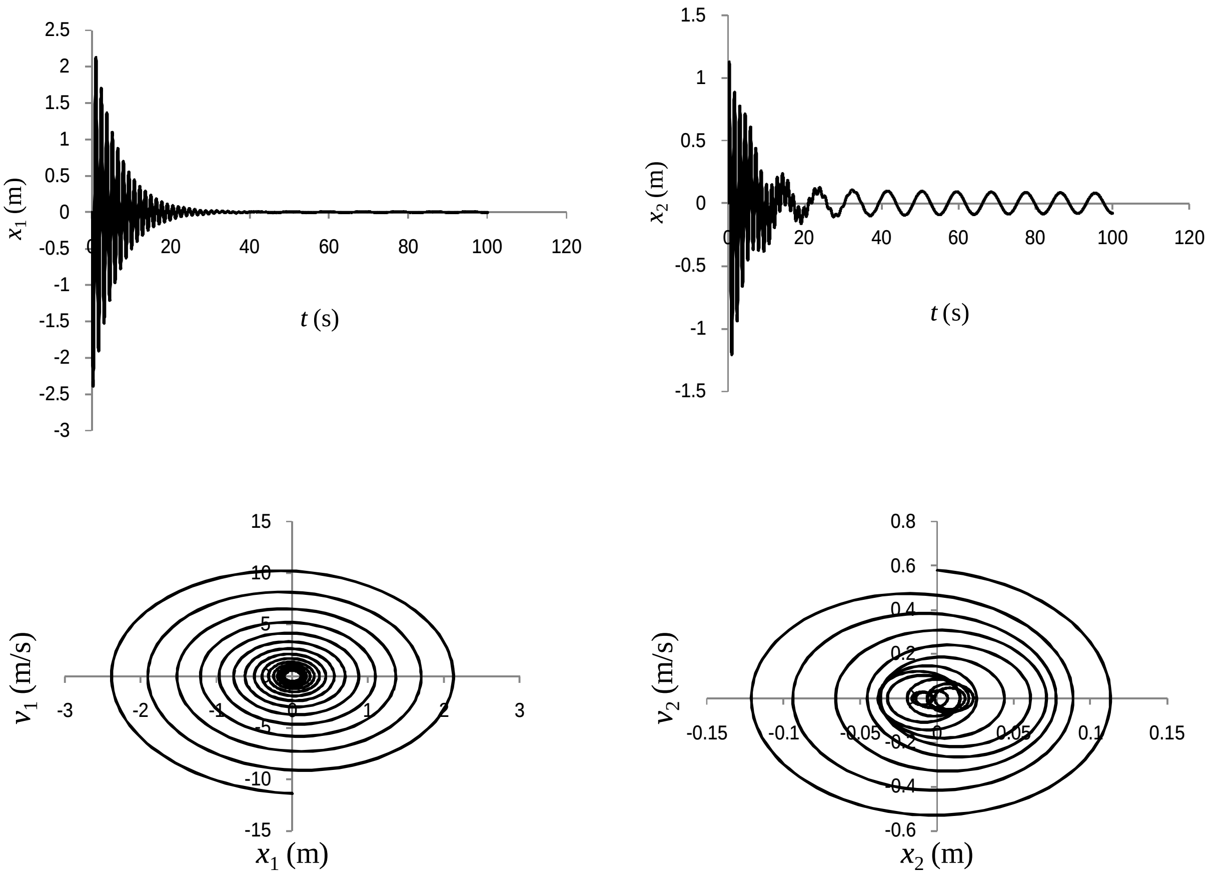

Fig. 4.13(c) x vs. t curves and phase planes of m_1 and m_2 for *f(dv)* of Table 2 using data set 2 of Table 10 for combination of linear springs and linear dampers [m_1=100 kg, m_2 =1000 kg, k_1=1000 N/m, k_2 =1000 N/m, c_1= 0.03 Ns/m, c_2 = 30.0 Ns/m, α_1 = 0.15 N/m, α_2 = 0.20 N/m, β_1 = 0.15 Ns/m, β_2 = 0.25 Ns/m]

Figures of damped self-excited vibration of 2DOFS (BVP)

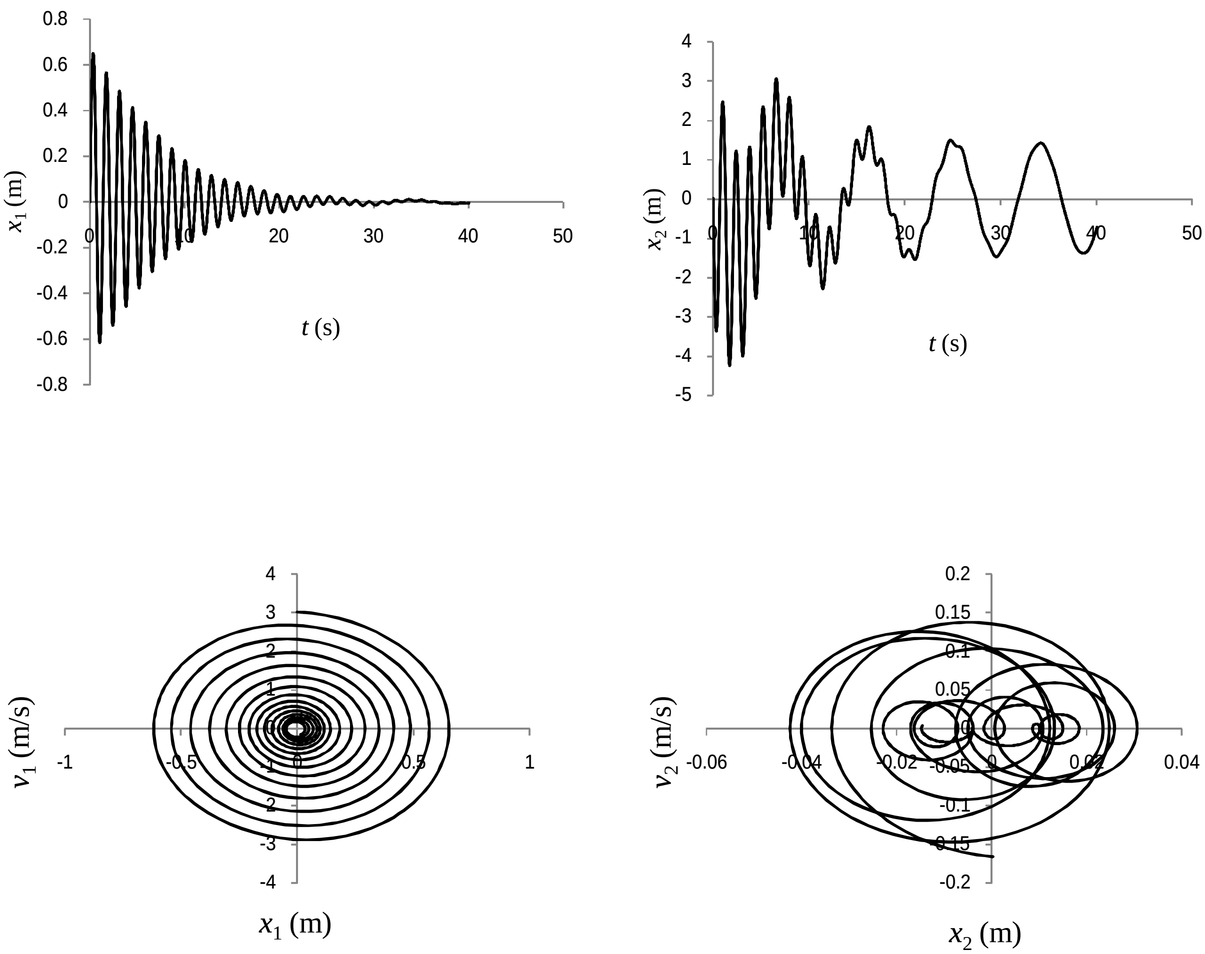

Fig. 4.13(d) x vs. t curves and phase planes of m_1 and m_2 for *f(n)* of Table 2 using data set 2 of Table 10 for combination of linear springs and linear dampers [m_1=100 kg, m_2 =1000 kg, k_1=1000 N/m, k_2 =1000 N/m, c_1= 0.03 Ns/m, c_2 = 30.0 Ns/m, α_1 = 0.15 N/m, α_2 = 0.20 N/m, β_1 = 0.15 Ns/m, β_2 = 0.25 Ns/m, γ_1 = 0.015 Ns/m^3, γ_2 = 0.025 Ns/m^3].

Figures of damped self-excited vibration of 2DOFS (BVP)

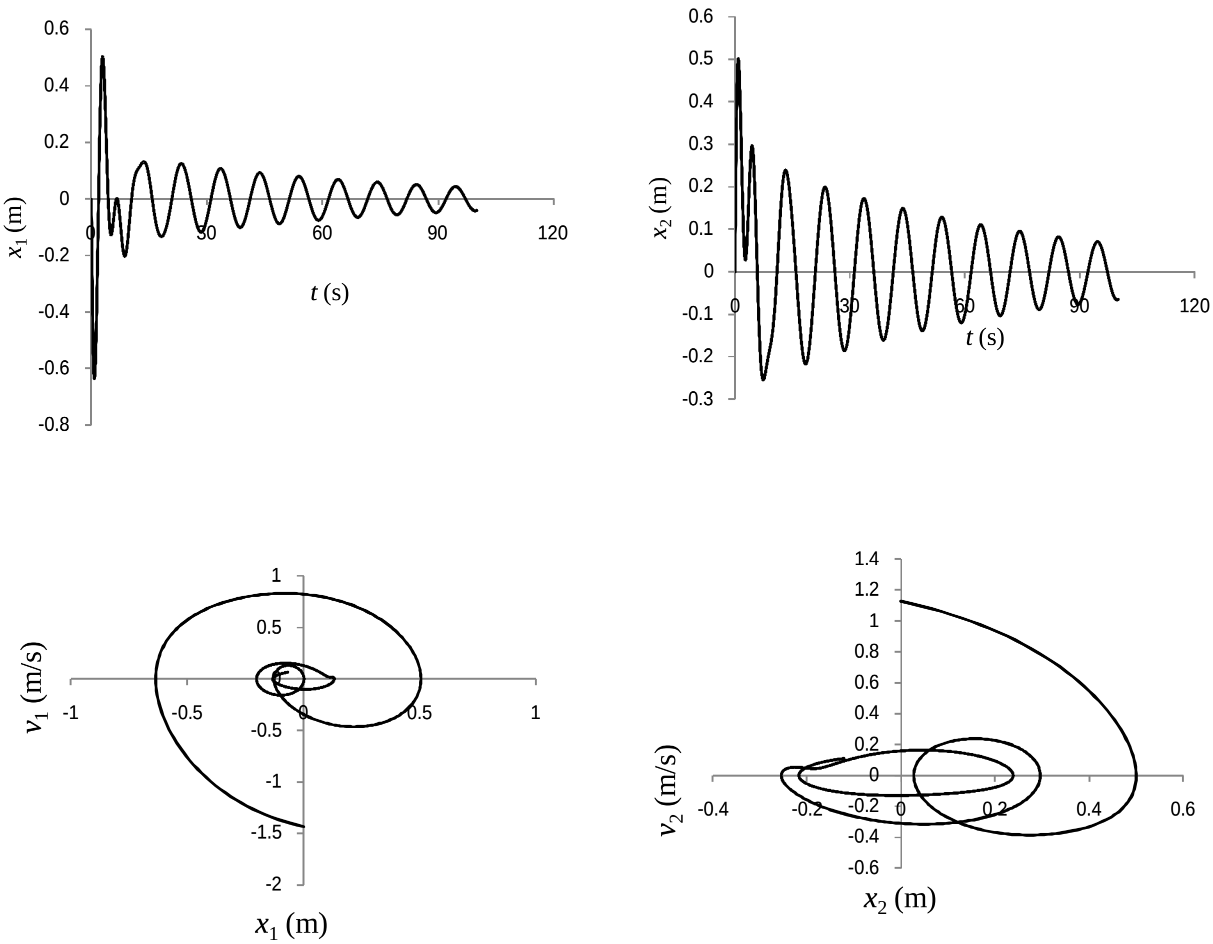

Fig. 4.14(a) x vs. t curves and phase planes of m_1 and $m_2$for $f(n)$ of Table 2 using data set 1 of Table 10 for combination of linear springs and non-linear dampers [m_1=100 kg, m_2 =100 kg, k_1=100 N/m, k_2 =100 N/m, c_1= 0.03 Ns/m, c'_1 = 0.003 Ns/m^3, c_2 = 30.0 Ns/m, c'_2 = 0.003 Ns/m^3, α_1 = 0.20 N/m, α_2 = 0.25 N/m, β_1 = 0.10 Ns/m, β_2 = 0.20 Ns/m, γ_1 = 0.001 Ns/m^3, γ_2 = 0.002 Ns/m^3].

Figures of damped self-excited vibration of 2DOFS (BVP)

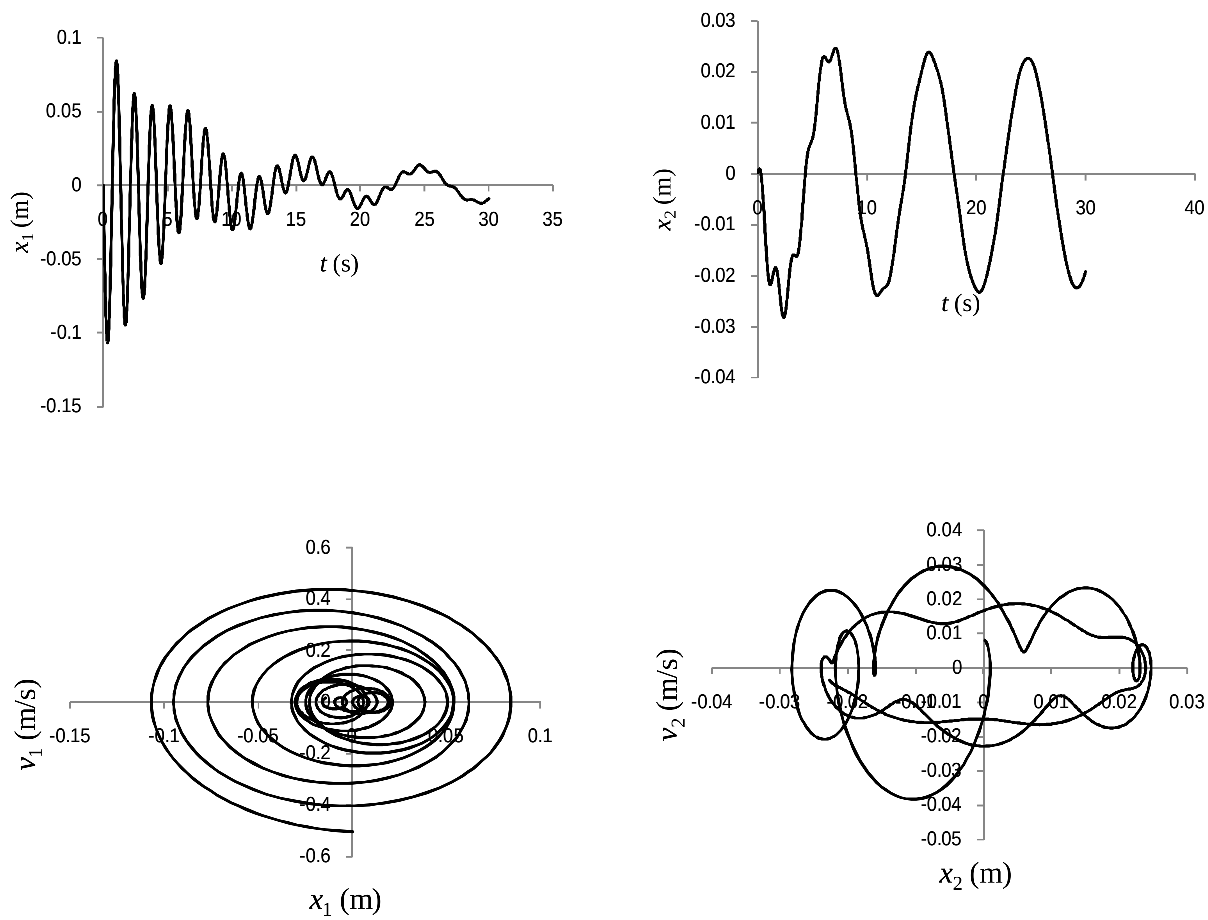

Fig. 4.14(b) x vs. t curves and phase planes of m_1 and m_2 for $f(n)$ of Table 2 using data set 2 of Table 10 for combination of linear springs and non-linear dampers [m_1=100 kg, m_2 =1000 kg, k_1=1000 N/m, k_2 =1000 N/m, c_1= 0.03 Ns/m, c'_1 = -0.003 Ns/m^3, c_2 = 30.0 Ns/m, c'_2 = -0.003 Ns/m^3, α_1 = 0.15 N/m, α_2 = 0.20 N/m, β_1 = 0.15 Ns/m, β_2 = 0.25 Ns/m, γ_1 = 0.015 Ns/m^3, γ_2 = 0.025 Ns/m^3]

Figures of damped self-excited vibration of 2DOFS (BVP)

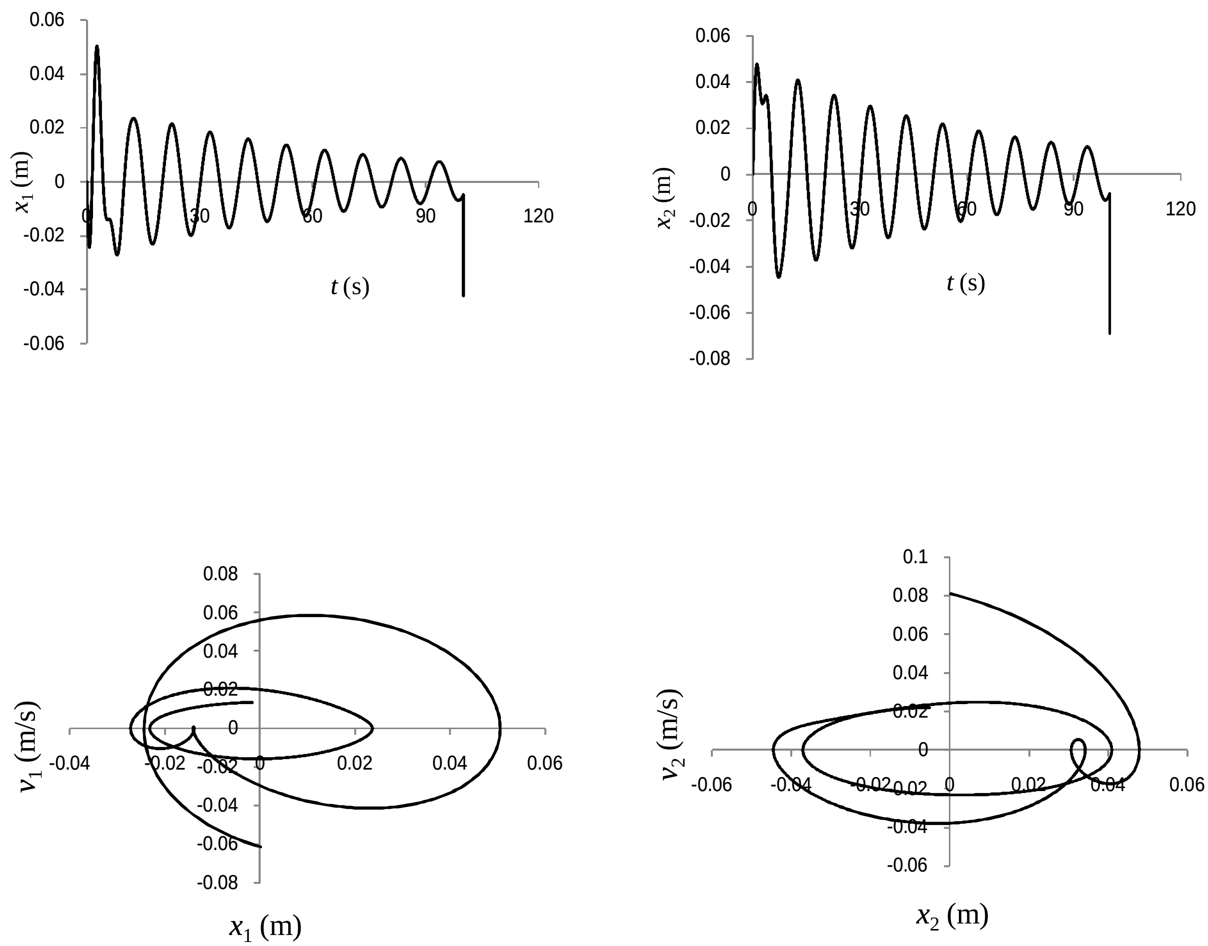

Fig. 4.15(a) *x* vs. *t* curves and phase planes of m_1 and m_2 for *f(n)* of Table 2 using data set 1 of Table 10 for combination of non-linear springs and linear dampers [m_1=100 kg, m_2 =100 kg, k_1=100 N/m, k'_1= 0.3 N/m^3, k_2 =100 N/m, k'_2 = 0.3 N/m^3, c_1= 0.03 Ns/m, c_2 = 30.0 Ns/m, α_1 = 0.20 N/m, α_2 = 0.25 N/m, β_1 = 0.10 Ns/m, β_2 = 0.20 Ns/m, γ_1 = 0.001 Ns/m^3, γ_2 = 0.002 Ns/m^3]

Figures of damped self-excited vibration of 2DOFS (BVP)

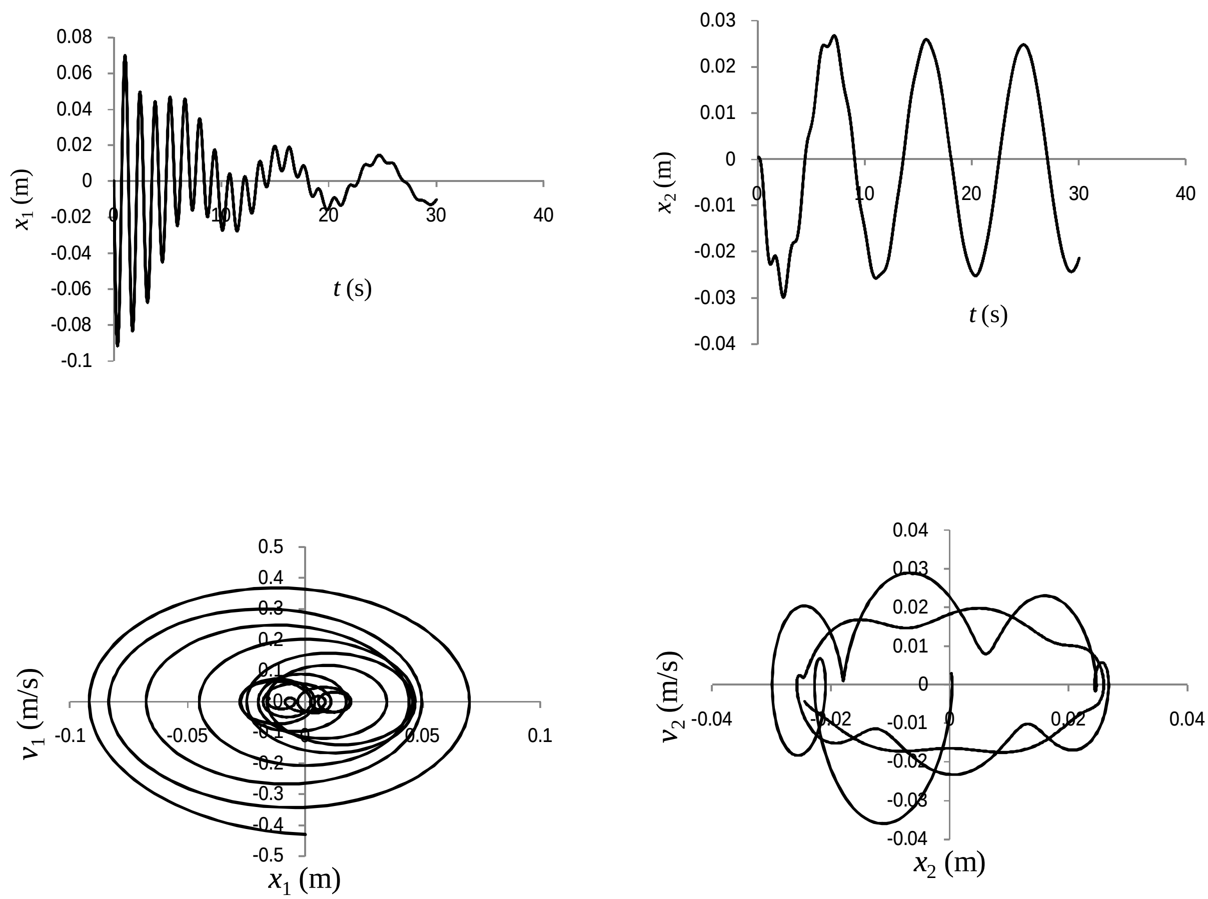

Fig. 4.15(b) x vs. t curves and phase planes of m_1 and m_2 for *f(n)* of Table 2 using data set 2 of Table 10 for combination of non-linear springs and linear dampers [m_1=100 kg, m_2 =1000 kg, k_1=1000 N/m, k'_1= -0.3 N/m^3, k_2 =1000 N/m, k'_2 = -0.3 N/m^3, c_1= 0.03 Ns/m, c_2 = 30.0 Ns/m, α_1 = 0.15 N/m, α_2 = 0.20 N/m, β_1 = 0.15 Ns/m, β_2 = 0.25 Ns/m, γ_1 = 0.015 Ns/m^3, γ_2 = 0.025 Ns/m^3].

Figures of damped self-excited vibration of 2DOFS (BVP)

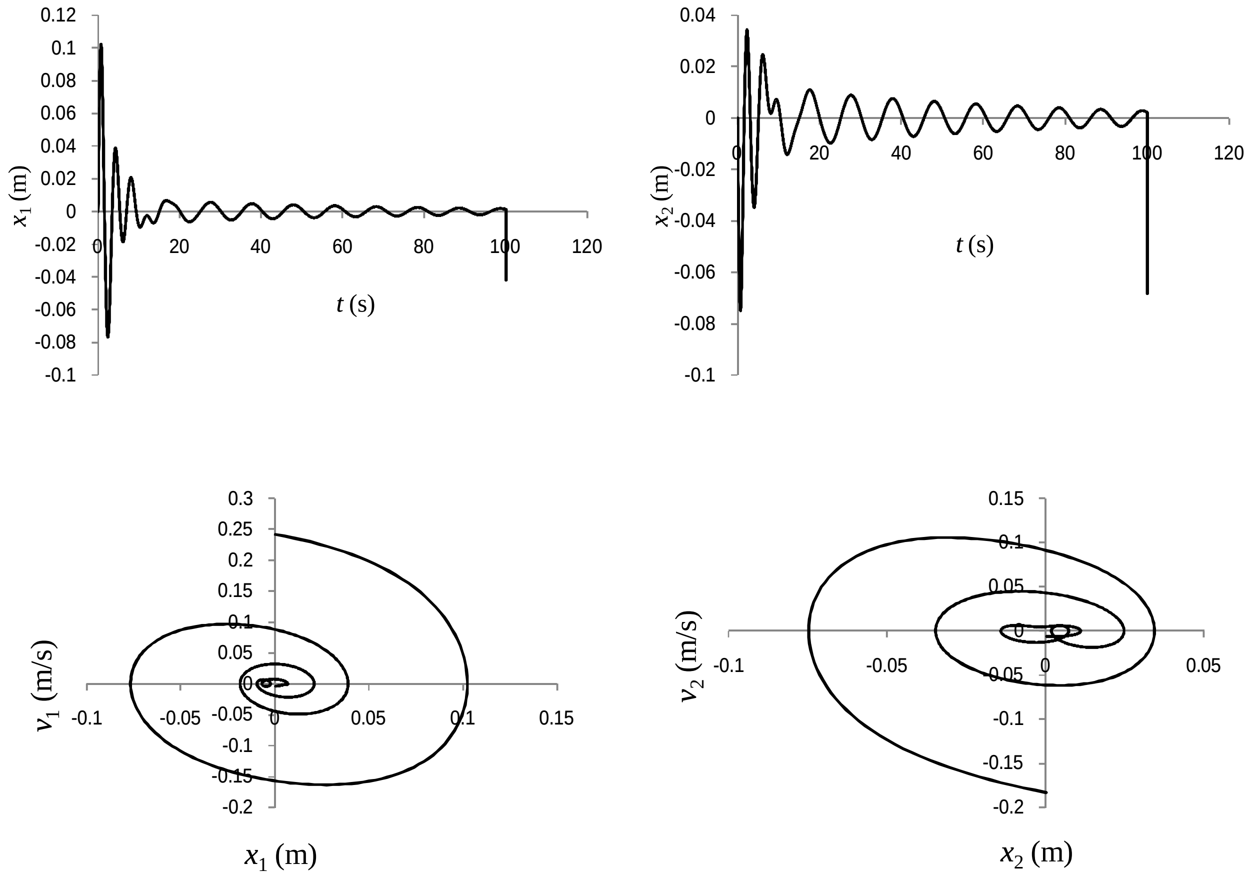

Fig. 4.16(a) x vs. t curves and phase planes of m_1 and m_2 for *f(d)* of Table 2 using data set 1 of Table 10 for combination of non-linear springs and non-linear dampers [m_1=100 kg, m_2 =100 kg, k_1=100 N/m, k'_1= 0.3 N/m^3, k_2 =100 N/m, k'_2 = 0.3 N/m^3, c_1= 0.03 Ns/m, c'_1 = 0.003 Ns/m^3, c_2 = 30.0 Ns/m, c'_2 = 0.003 Ns/m^3, α_1 = 0.20 N/m, α_2 = 0.25 N/m]

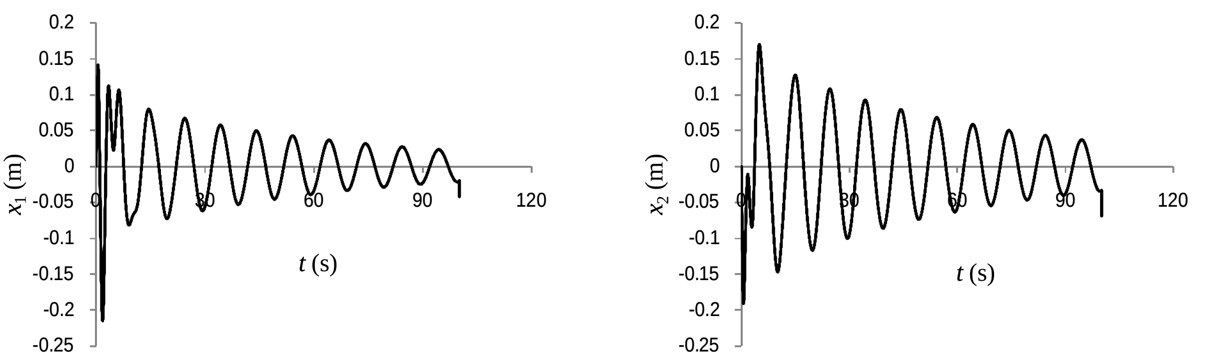

Fig. 4.16(b) x vs. t curves of m_1 and m_2 for *f(v)* of Table 2 using data set 1 of Table 10 for combination of non-linear springs and non-linear dampers [m_1=100 kg, m_2 =100 kg, k_1=100 N/m, k'_1= 0.3 N/m^3, k_2 =100 N/m, k'_2 = 0.3 N/m^3, c_1= 0.03 Ns/m, c'_1 = 0.003 Ns/m^3, c_2 = 30.0 Ns/m, c'_2 = 0.003 Ns/m^3, β_1 = 0.10 Ns/m, β_2 = 0.20 Ns/m]

Figures of damped self-excited vibration of 2DOFS (BVP)

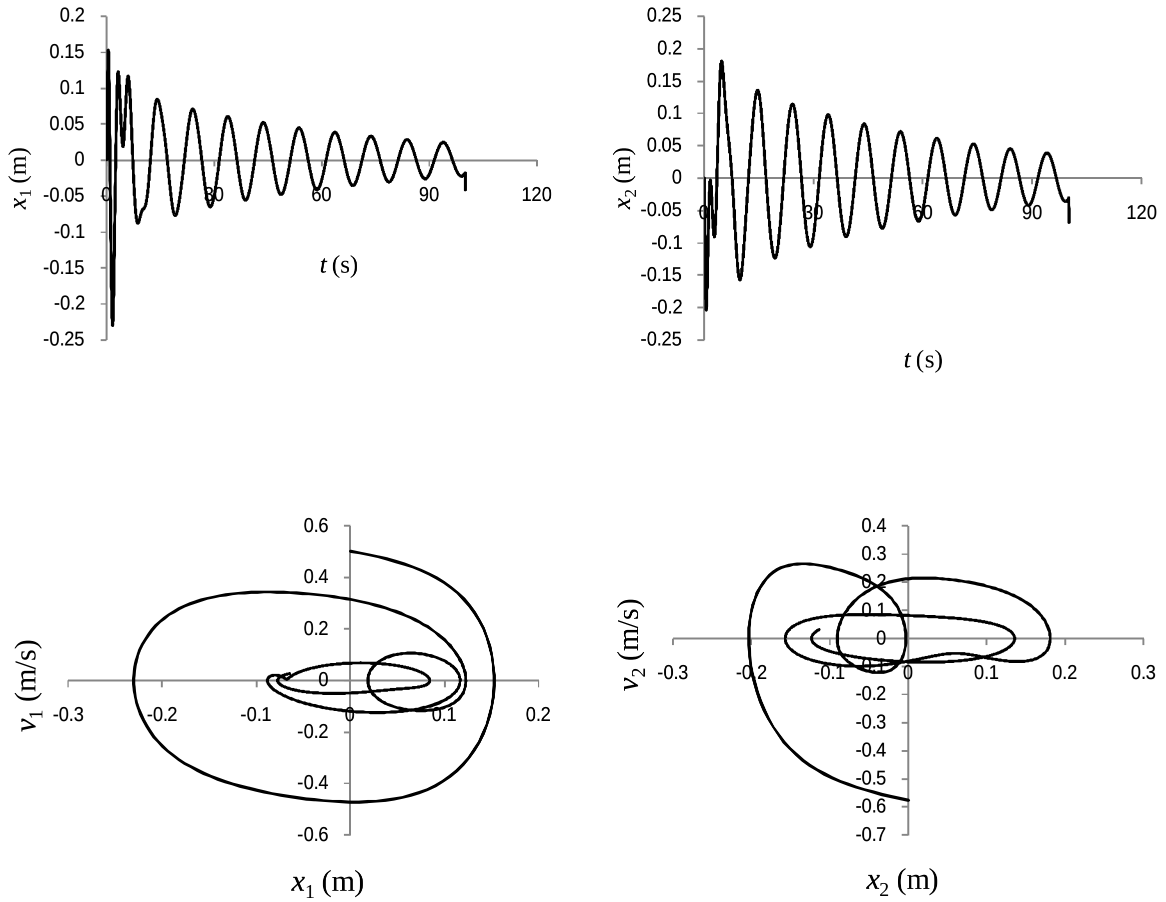

Fig. 4.16(c) x vs. t curves and phase planes of m_1 and m_2 for $f(dv)$ of Table 2 using data set 1 of Table 10 for combination of non-linear springs and non-linear dampers [m_1=100 kg, m_2 =100 kg, k_1=100 N/m, k'_1= 0.3 N/m^3, k_2 =100 N/m, k'_2 = 0.3 N/m^3, c_1= 0.03 Ns/m, c'_1 = 0.003 Ns/m^3, c_2 = 30.0 Ns/m, c'_2 = 0.003 Ns/m^3, α_1 = 0.20 N/m, α_2 = 0.25 N/m, β_1 = 0.10 Ns/m, β_2 = 0.20 Ns/m]

Figures of damped self-excited vibration of 2DOFS (BVP)

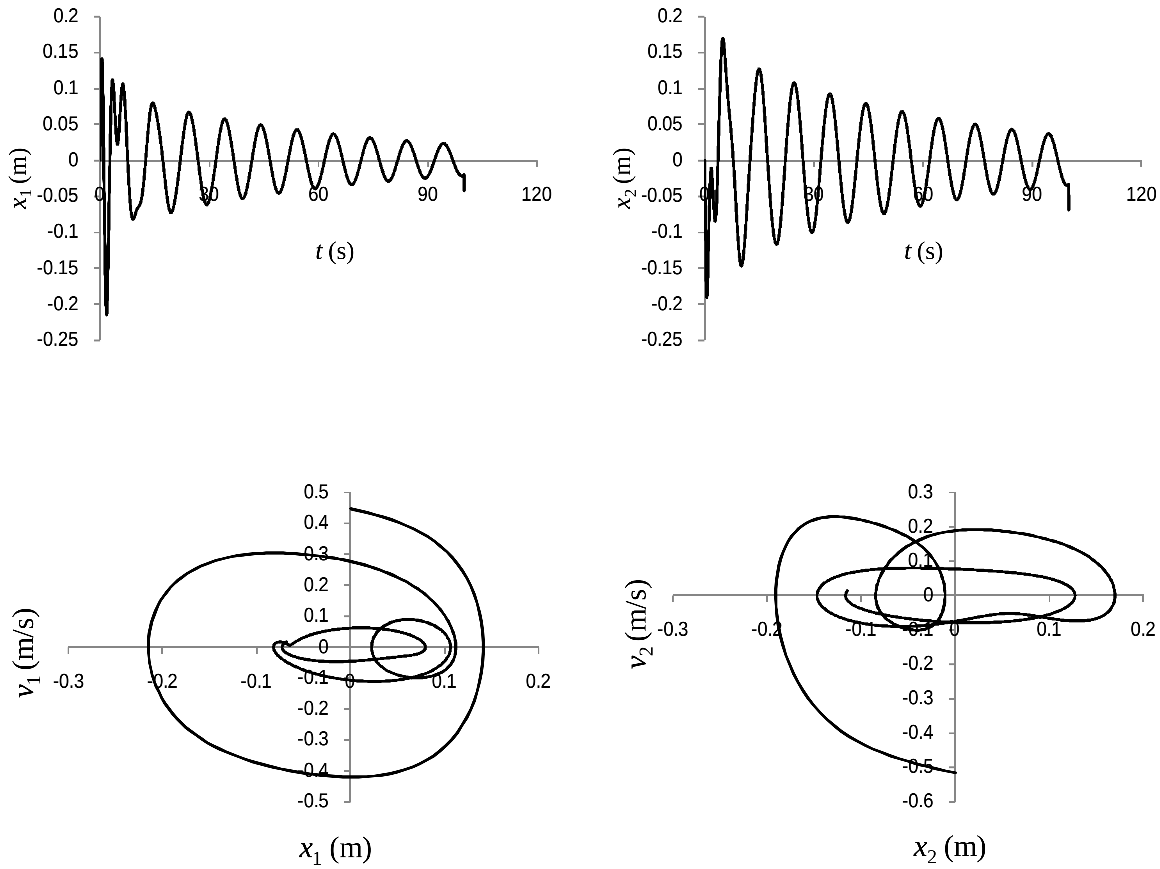

Fig. 4.16(d) x vs. t curves and phase planes of m_1 and m_2 for *f(n)* of Table 2 using data set 1 of Table 10 for combination of non-linear springs and non-linear dampers [m_1=100 kg, m_2 =100 kg, k_1=100 N/m, k'_1= 0.3 N/m^3, k_2 =100 N/m, k'_2 = 0.3 N/m^3, c_1= 0.03 Ns/m, c'_1 = 0.003 Ns/m^3, c_2 = 30.0 Ns/m, c'_2 = 0.003 Ns/m^3, α_1 = 0.20 N/m, α_2 = 0.25 N/m, β_1 = 0.10 Ns/m, β_2 = 0.20 Ns/m, γ_1 = 0.001 Ns/m^3, γ_2 = 0.002 Ns/m^3]

Figures of damped self-excited vibration of 2DOFS (BVP)

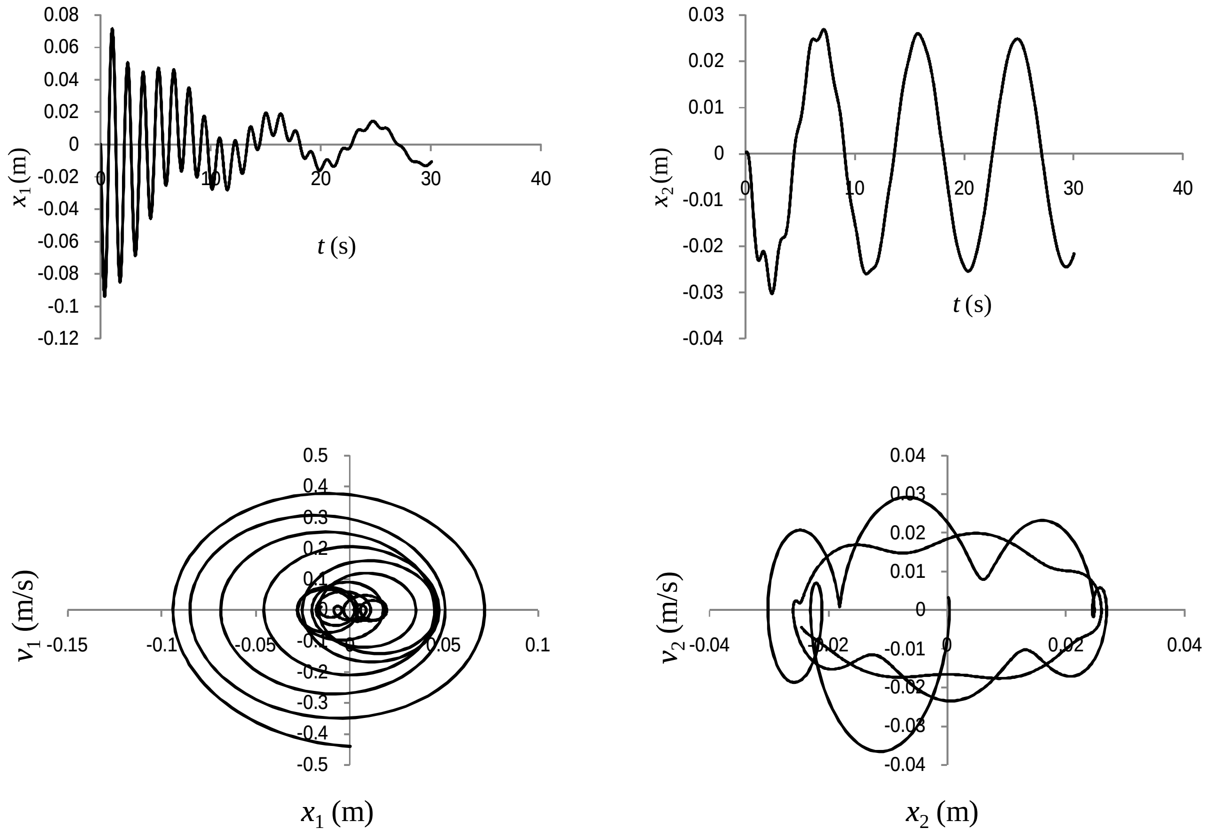

Fig. 4.17(a) *x* vs. *t* curves and phase planes of m_1 and m_2 for *f(d)* of Table 2 using data set 2 of Table 10 for combination of non-linear springs and non-linear dampers [m_1=100 kg, m_2 =1000 kg, k_1=1000 N/m, k'_1= -0.3 N/m^3, k_2 =1000 N/m, k'_2 = -0.3 N/m^3, c_1= 0.03 Ns/m, c'_1 = -0.003 Ns/m^3, c_2 = 30.0 Ns/m, c'_2 = -0.003 Ns/m^3, α_1 = 0.15 N/m, α_2 = 0.20 N/m]

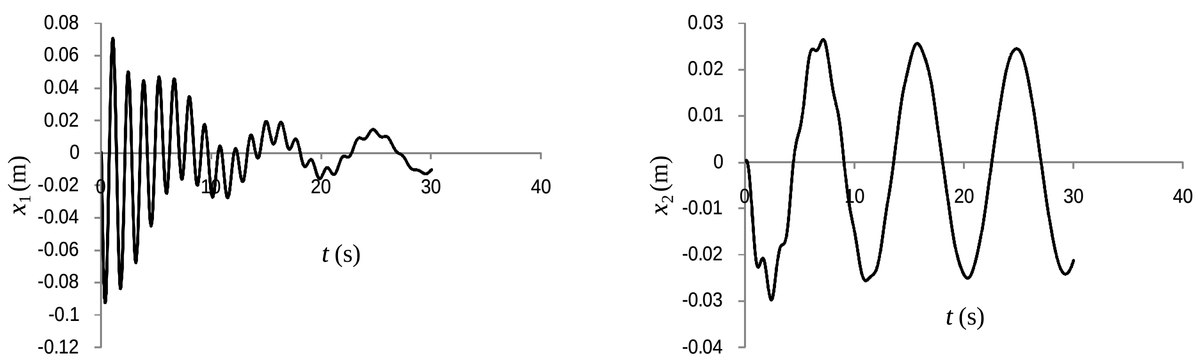

Fig. 4.17(b) *x* vs. *t* curves of m_1 and m_2 for *f(v)* of Table 2 using data set 2 of Table 10 for combination of non-linear springs and non-linear dampers [m_1=100 kg, m_2 =1000 kg, k_1=1000 N/m, k'_1= -0.3 N/m^3, k_2 =1000 N/m, k'_2 = -0.3 N/m^3, c_1= 0.03 Ns/m, c'_1 = -0.003 Ns/m^3, c_2 = 30.0 Ns/m, c'_2 = -0.003 Ns/m^3, β_1 = 0.15 Ns/m, β_2 = 0.25 Ns/m]

Figures of damped self-excited vibration of 2DOFS (BVP)

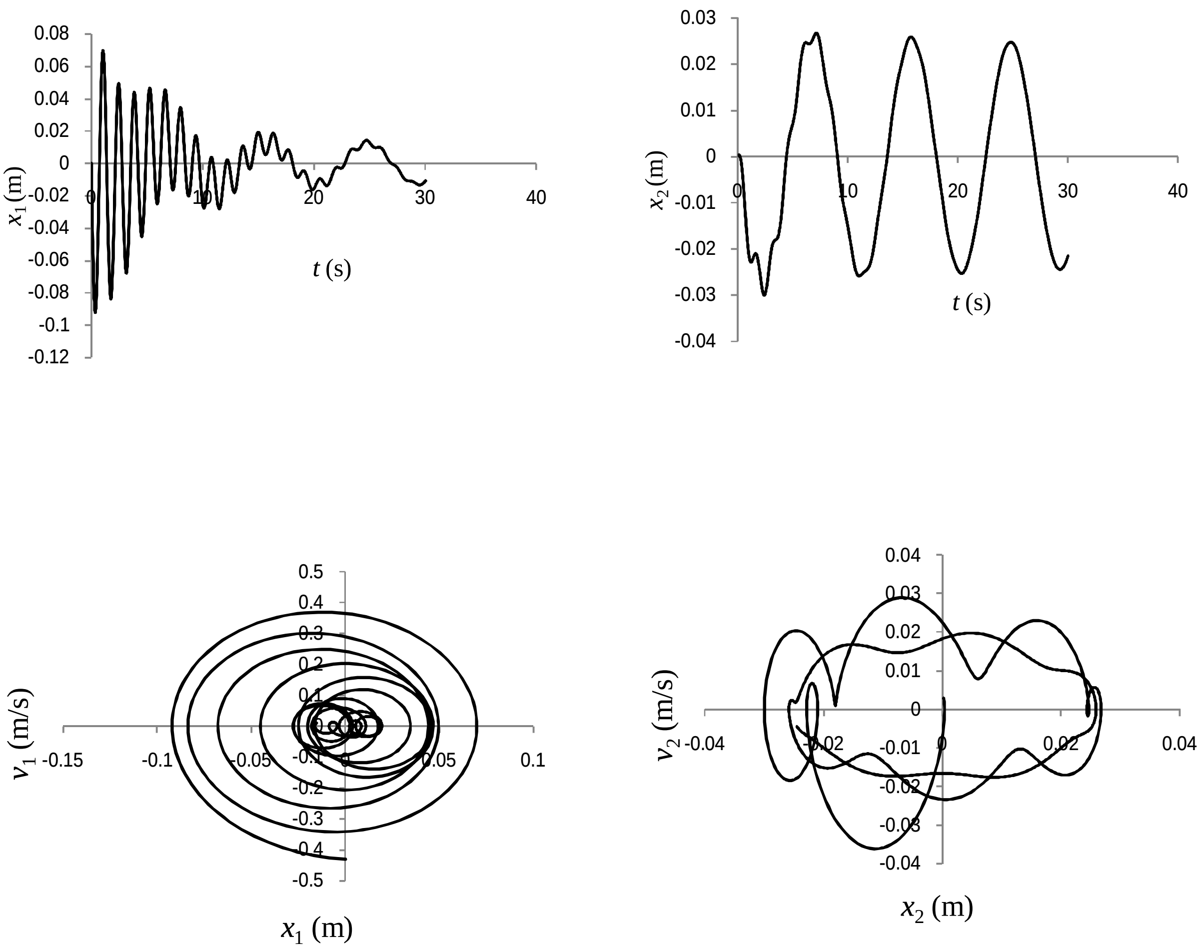

Fig. 4.17(c) x vs. t curves and phase planes of m_1 and m_2 for *f(dv)* of Table 2 using data set 2 of Table 10 for combination of non-linear springs and non-linear dampers [m_1=100 kg, m_2 =1000 kg, k_1=1000 N/m, k'_1= -0.3 N/m^3, k_2 =1000 N/m, k'_2 = -0.3 N/m^3, c_1= 0.03 Ns/m, c'_1 = -0.003 Ns/m^3, c_2 = 30.0 Ns/m, c'_2 = -0.003 Ns/m^3, α_1 = 0.15 N/m, α_2 = 0.20 N/m, β_1 = 0.15 Ns/m, β_2 = 0.25 Ns/m].

Figures of damped self-excited vibration of 2DOFS (BVP)

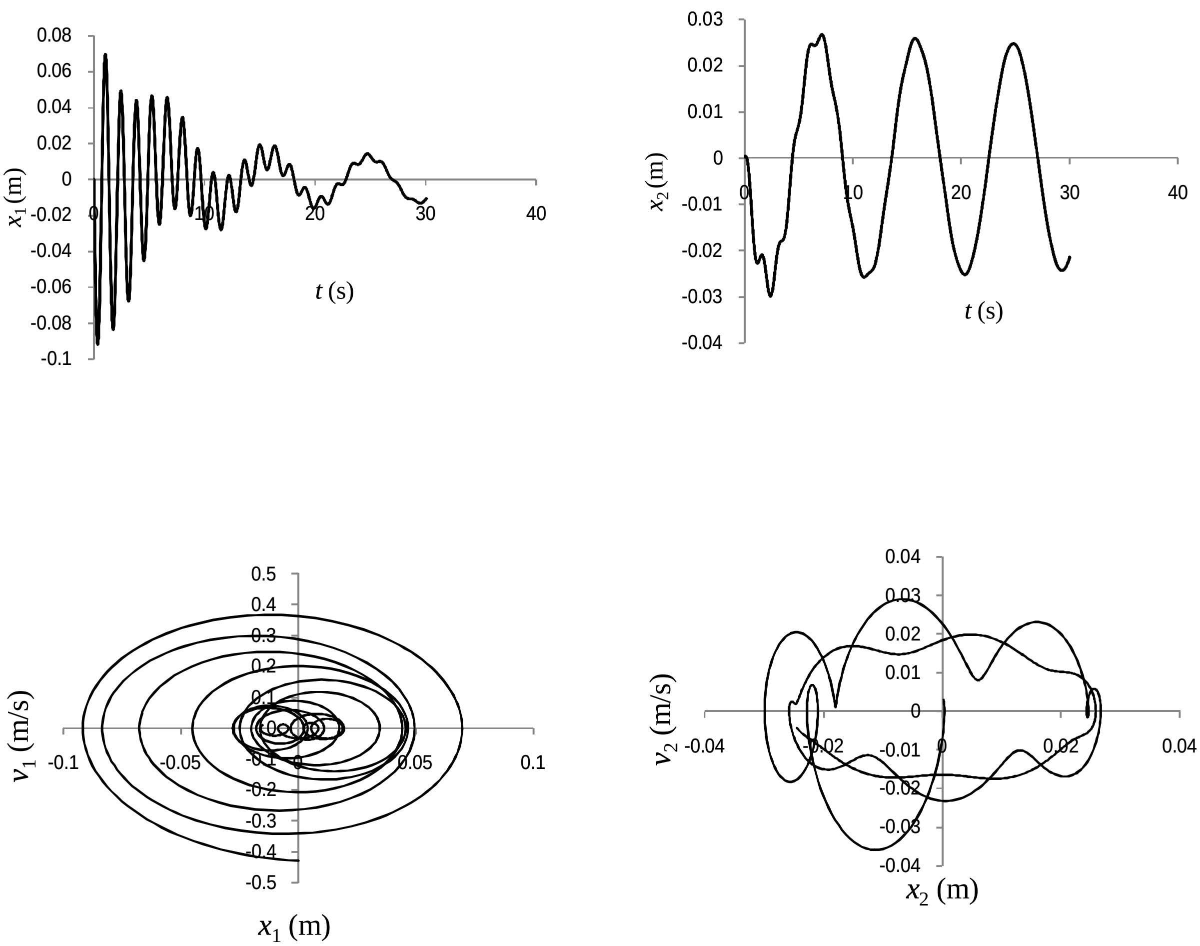

Fig. 4.17(d) *x* vs. *t* curves and phase planes of m_1 and m_2 for *f(n)* of Table 2 using data set 2 of Table 10 for combination of non-linear springs and non-linear dampers [m_1=100 kg, m_2 =1000 kg, k_1=1000 N/m, k'_1= -0.3 N/m^3, k_2 =1000 N/m, k'_2 = -0.3 N/m^3, c_1= 0.03 Ns/m, c'_1 = -0.003 Ns/m^3, c_2 = 30.0 Ns/m, c'_2 = -0.003 Ns/m^3, α_1 = 0.15 N/m, α_2 = 0.20 N/m, β_1 = 0.15 Ns/m, β_2 = 0.25 Ns/m, γ_1 = 0.015 Ns/m^3, γ_2 = 0.025 Ns/m^3]

4.6 Damped self-excited vibration for 3DOFS

For the analysis of damped self-excited vibration of 3DOFS, the responses of the system for data from Table 12 and for the combination of non-linear springs and linear dampers and the combination of non-linear springs and non-linear dampers are given here in figures 4.18(a) to 4.18(d) and 4.19(a) to 4.19(d). Figures from C(1) to C(8) for cases (*a* - *b*) are given in Appendix C.

For observing the responses of the system, four different cases (*a* - *d*) are chosen depending on the self-excited force function. Boundary value problem analysis method has been applied to find out the responses of 3DOF system for cases (*a*) to (*d*) and four combinations (1-4 of Table 8) of springs and dampers..

In figure 4.18(a) for *f(d)*, the amplitudes of m_1, m_2 and m_3 and trajectory for m_1 are given. Maximum amplitude of m_1 from the figure can be seen as 0.07 m. From the trend of the curve, it can be concluded that the amplitude is gradually decreasing and finally attain stability.

For m_2 and m_3, amplitudes of vibration are much higher than that of m_1. However, for both m_2 and m_3, amplitude is decreasing and approaching to stability. The system gains stability after a certain period. From the trajectory of m_1, it is clear that velocity of m_1 along with amplitude decreasing gradually and finally reaches stability.

Similar responses of m_1, m_2 and m_3 are also found in figure 4.19(a) for the combination of non-linear springs and non-linear dampers in *f(d)*. So for 3DOF system, the effect of nonlinear displacement term upon the response of the system is not so intelligible.

For the *f(v)*, the response of the system and trajectory for m_2 is shown in figures 4.18(b). From these curves, it is clear that velocity plays an important role in self-excited force. Due to damped condition, the amplitudes of all three masses are very low. Therefore, the system will attain stability very quickly if required damping is provided. For other combinations of non-linear springs and non-linear dampers and *f(v)*, the response of the system shown in figure 4.19(b) is congruent to the response for *f(v)* and combination of nonlinear springs and linear dampers.

However, when both displacement and velocity (case *c*) are taken into consideration for self-excited force, the effect of displacement becomes dominant. This is clear from the response curves of m_1, m_2 and m_3 and trajectory for m_3 shown in figure 4.18(c). It is also true for combination of non-linear springs and non-linear dampers as shown in figure 4.19(c).

In addition, the effect of nonlinear displacement on self-excited force is not so great. This is shown in figures 4.18(d) and 4.19(d). The amplitudes of vibration for all three masses are nearly similar to that for cases *(a)* & *(c)* of combination 3.

4.7 Comparison among the responses for four combinations (1- 4 of Table 8) of damped self-excited vibration of 3DOFS [*Figures 4.18(a)-4.18(d) , 4.19(a)-4.19(d) and Figures C(1)-C(8) from Appendix C*]

For all the combinations of springs and dampers either linear or non-linear and for all cases from (*a*) to (*d*) of Table 2, 3DOFS shows similar type of response. For every case, the system approaches to stability after gradual decrement of amplitude of vibration. It is also observed that the amplitude of vibration varies due to variation of the self-excited force function.

In figures C(1), C(5), 4.18(a) and 4.19(a) for the *f(d)* and for all combinations of springs and dampers, the amplitude of vibration is higher than that for the *f(v)*. So for 3DOFS, damper non-linearity affects the amplitude of vibration significantly. For *f(d)* and all combinations springs and dampers, m_1 starts vibration with the amplitude of about 0.07m and gradually reduces to be stable. m_2 and m_3 both show the amplitude of around 0.15m. But in figures C(2), C(6), 4.18(b) and 4.19(b) for *f(v)* and all combinations of springs and dampers, m_1 , m_2 and m_3 start the vibration with the amplitude of 0.04m, 0.07m and 0.08m respectively. This phenomenon is seen for all other combinations also.

Similarly for other two combinations (3 - 4) of springs and dampers, and for *f(dv)* and (*d*), the system's response is quite similar to the response for *f(d)*. This indicates that for 3DOFS, the system's response is different for only the case of the self-excited force being function of only velocity. For other cases, the system's response is independent on the chosen cases and combinations. Phase planes for various masses also show this phenomenon clearly.

Figures of damped self-excited vibration of 3DOFS

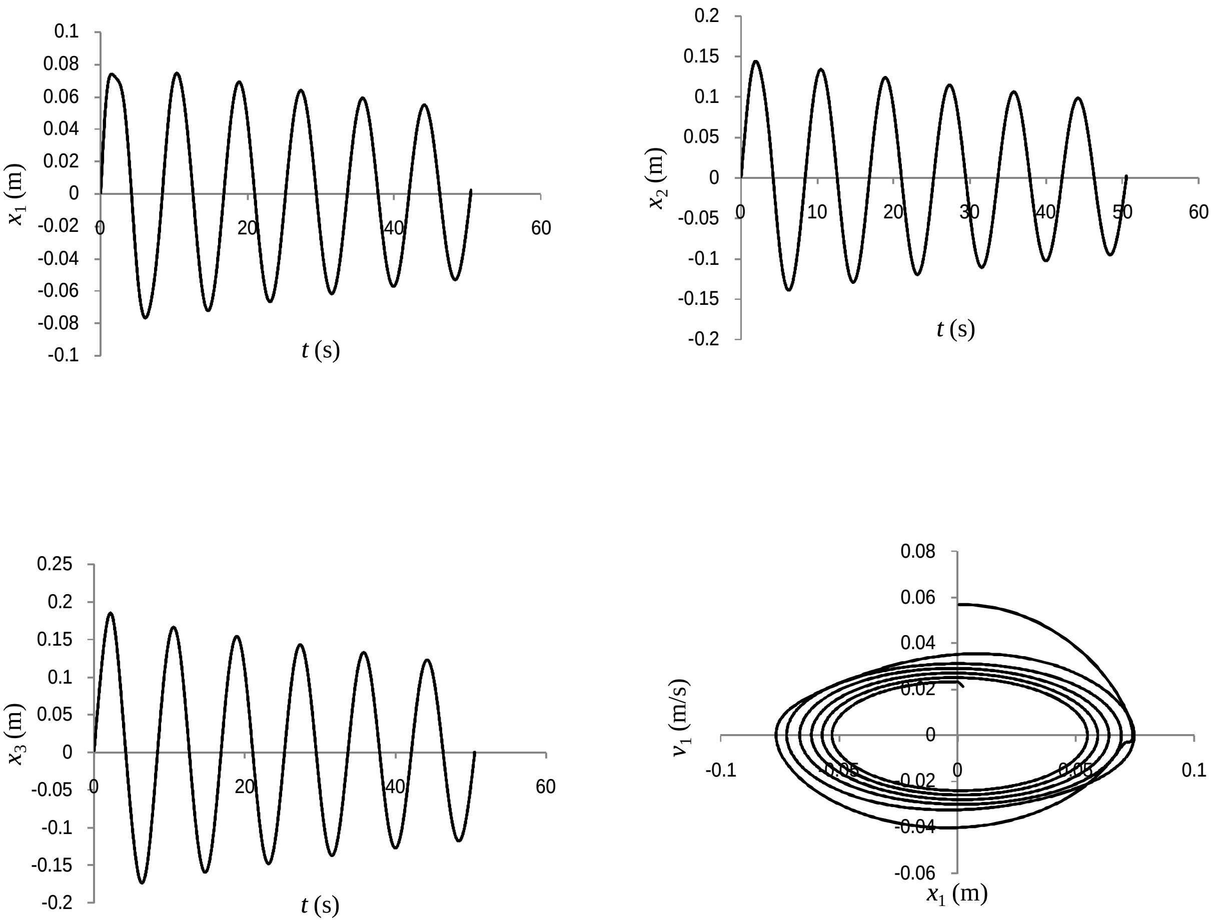

Fig. 4.18(a) x vs. t curves of m_1 , m_2 and m_3 and trajecotory for m_1 for *f(d)* of Table 2 using data of Table 12 for combination of non-linear springs and linear dampers [m_1 =100 kg, m_2 =100 kg, m_3 =100 kg, k_1 =100 N/m, k'_1 =0.30 N/m^3 , k_2 =100 N/m, k'_2 =0.30 N/m^3 , k_3 =100 N/m, k'_3 =0.30 N/m^3 , c_1 =0.03 Ns/m, c_2 =10.0 Ns/m, c_3 =30.0 *Ns/m* , α_1 =0.20 *N/m* , α_2 =0.25 *N/m* , α_3 =0.23 *N/m*]

Figures of damped self-excited vibration of 3DOFS

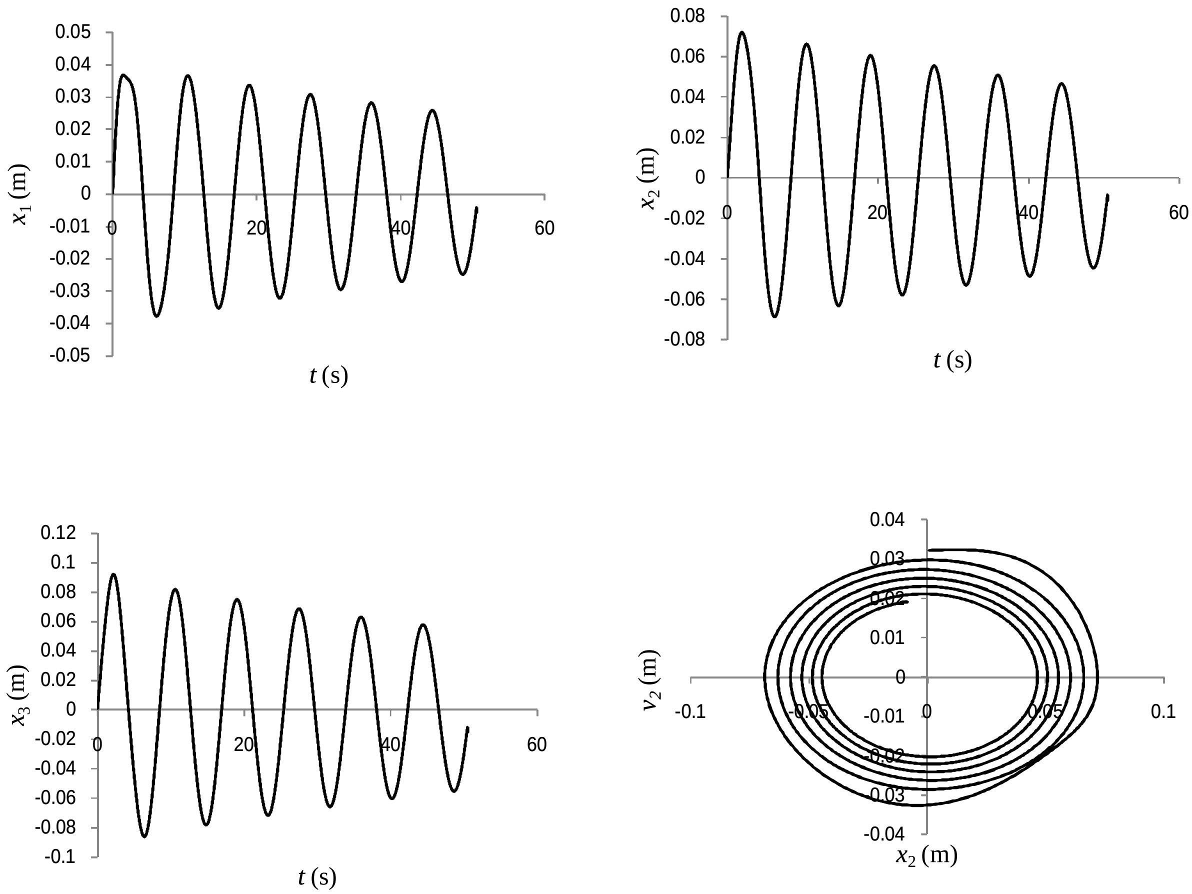

Fig. 4.18(b) *x* vs. *t* curves of m_1, m_2 and m_3 and trajecotory for m_2 for *f(v)* of Table 2 using data of Table 12 for combination of non-linear springs and linear dampers [m_1 =100 kg, m_2 =100 kg, m_3 =100 kg, k_1 =100 N/m, k'_1 =0.30 N/m^3 , k_2 =100 N/m, k'_2 =0.30 N/m^3 , k_3 =100 N/m, k'_3 =0.30 N/m^3 , c_1 =0.03 Ns/m, c_2 =10.0 Ns/m, c_3 =30.0 *Ns/m* , β_1 =0.10 *Ns/m* , β_2 =0.20 *Ns/m* , β_3 =0.15 *Ns/m*]

Figures of damped self-excited vibration of 3DOFS

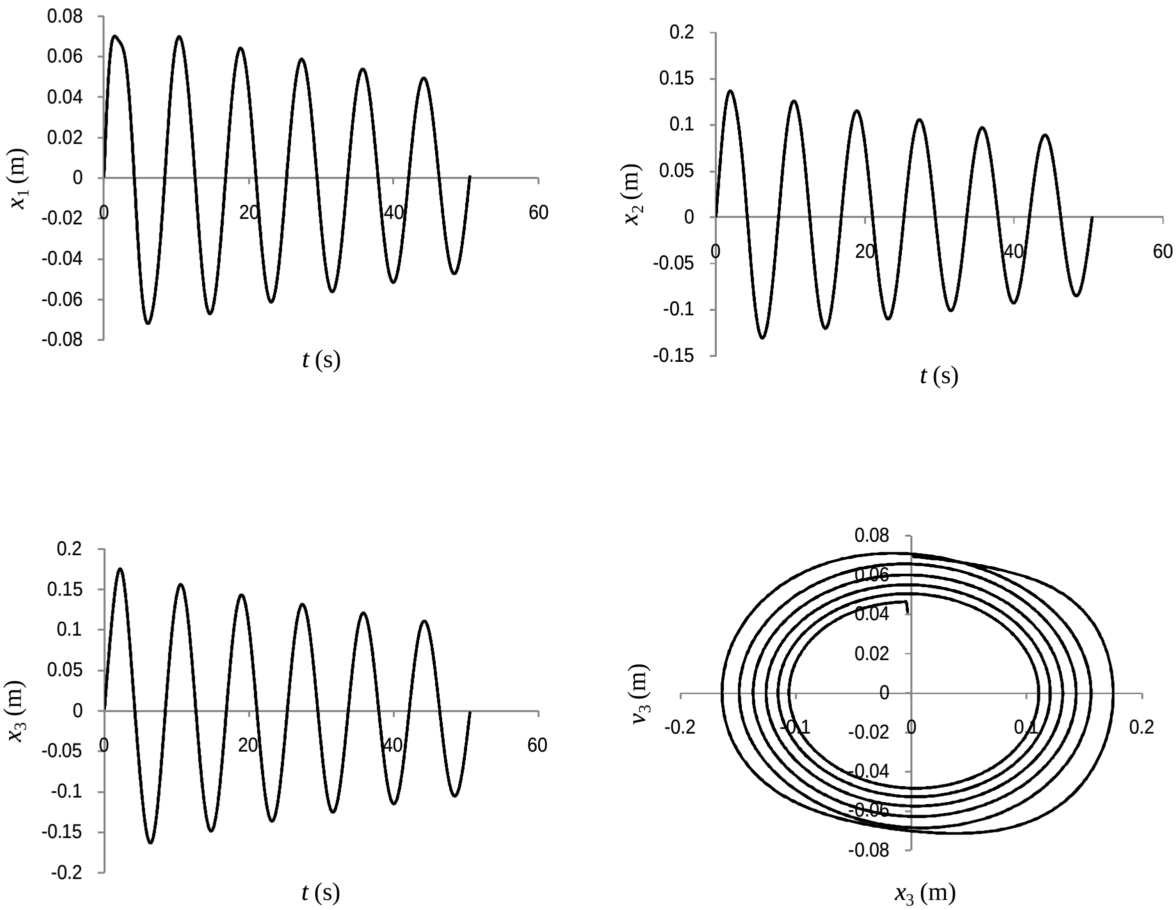

Fig. 4.18(c) x vs. t curves of m_1, m_2 and m_3 and trajecotory for m_2 for *f(dv)* of Table 2 using data of Table 12 for combination of non-linear springs and linear dampers [m_1 =100 kg, m_2 =100 kg, m_3 =100 kg, k_1 =100 N/m, k'_1 =0.30 N/m^3 , k_2 =100 N/m, k'_2 =0.30 N/m^3 , k_3 =100 N/m, k'_3 =0.30 N/m^3 , c_1 =0.03 Ns/m, c_2 =10.0 Ns/m, c_3 =30.0 *Ns/m* , α_1 =0.20 *N/m* , α_2 =0.25 *N/m* , α_3 =0.23 *N/m* , β_1 =0.10 *Ns/m* , β_2 =0.20 *Ns/m* , β_3 =0.15 *Ns/m*].

Figures of damped self-excited vibration of 3DOFS

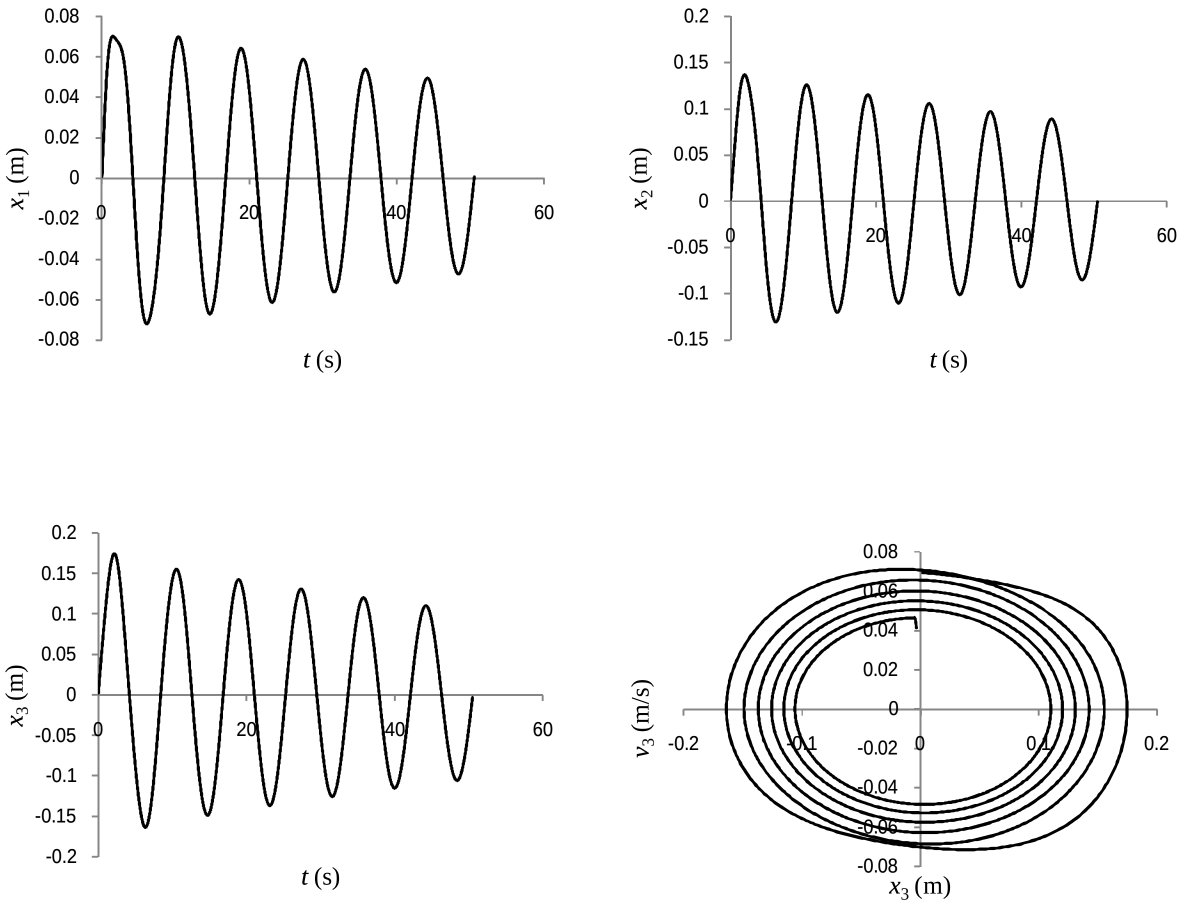

Fig. 4.18(d) x vs. t curves of m_1 , m_2 and m_3 and trajecotory for m_3 for *f(n)* of Table 2 using data of Table 12 for combination of non-linear springs and linear dampers [m_1 =100 kg, m_2 =100 kg, m_3 =100 kg, k_1 =100 N/m, k'_1 =0.30 N/m^3 , k_2 =100 N/m, k'_2 =0.30 N/m^3 , k_3 =100 N/m, k'_3 =0.30 N/m^3 , c_1 = 0.03 Ns/m, c_2 =10.0 Ns/m, c_3 =30.0 *Ns/m* , α_1 =0.20 *N/m* , α_2 =0.25 *N/m* , α_3 =0.23 *N/m* , β_1 =0.10 *Ns/m* , β_2 =0.20 *Ns/m* , β_3 =0.15 *Ns/m* , γ_1 = 0.001*Ns/m*^{3} , γ_2 =0.002 *Ns/m*^{3} , γ_3 =0.025 *Ns/m*^{3}].

Figures of damped self-excited vibration of 3DOFS

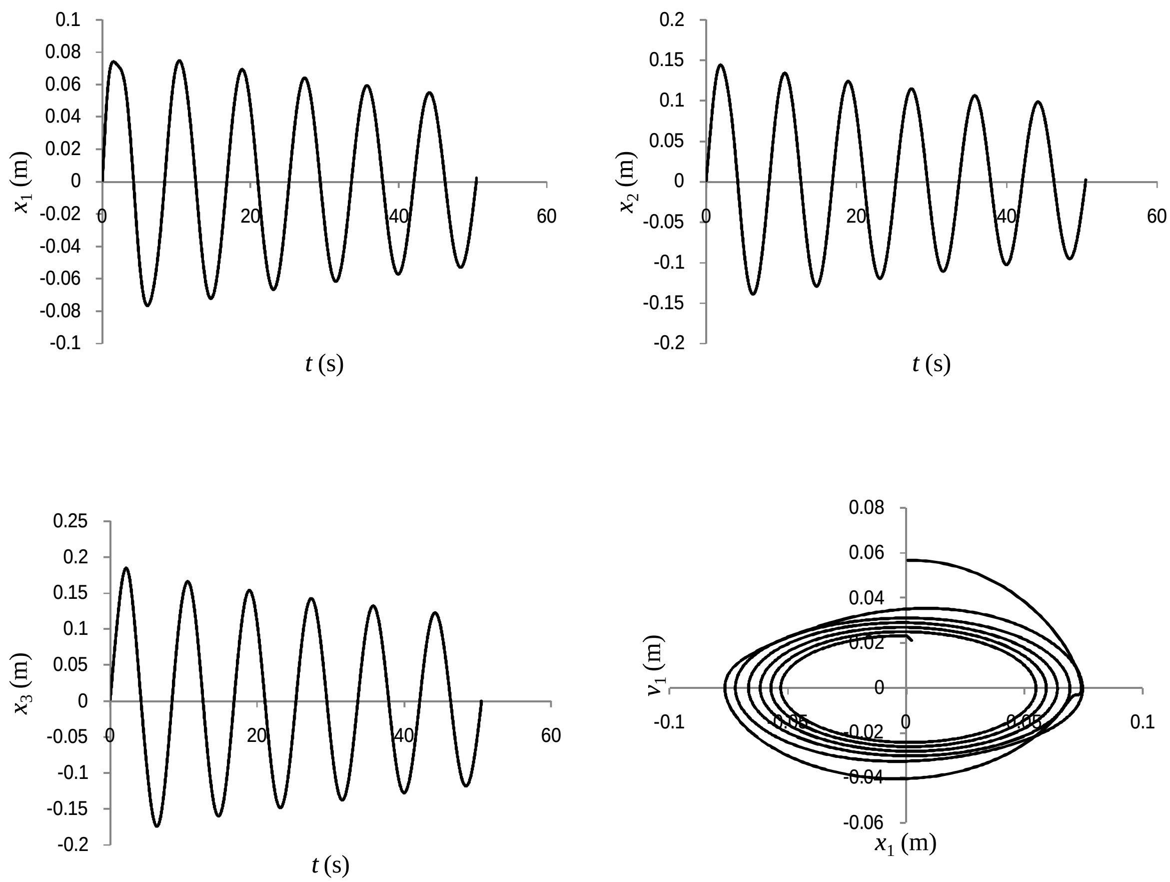

Fig. 4.19(a) x vs. t curves of m_1 , m_2 and m_3 and trajecotory for m_1 for $f(d)$ of Table 2 using data of Table 12 for combination of non-linear springs and non-linear dampers [m_1 =100 kg, m_2 =100 kg, m_3 =100 kg, k_1 =100 N/m, k'_1 =0.30 N/m^3 , k_2 =100 N/m, k'_2 =0.30 N/m^3 , k_3 =100 N/m, k'_3 =0.30 N/m^3 , c_1 =0.03 Ns/m, c'_1 =0.003 Ns/m^3 , c_2 =10.0 Ns/m, c'_2 =0.003 Ns/m^3 , c_3 =30.0 Ns/m , c'_3 =0.003 Ns/m^3 , α_1 =0.20 N/m , α_2 =0.25 N/m , α_3 =0.23 N/m]

Figures of damped self-excited vibration of 3DOFS

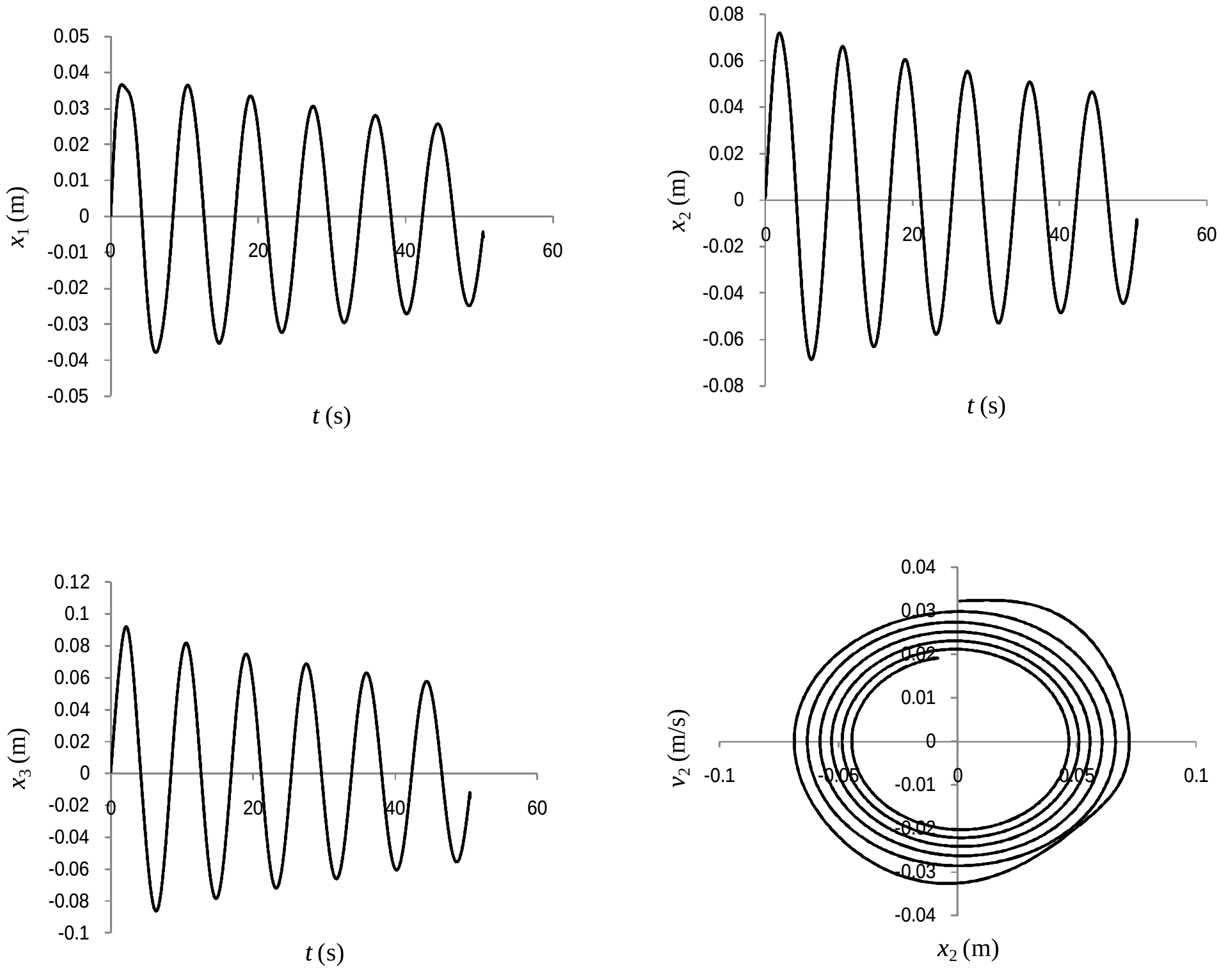

Fig. 4.19(b) x vs. t curves of m_1 , m_2 and m_3 and trajecotory for m_2 for *f(v)* of Table 2 using data of Table 12 for combination of non-linear springs and non-linear dampers [m_1 =100 kg, m_2 =100 kg, m_3 =100 kg, k_1 =100 N/m, k'_1 =0.30 N/m^3 , k_2 =100 N/m, k'_2 =0.30 N/m^3 , k_3 =100 N/m, k'_3 =0.30 N/m^3 , c_1 =0.03 Ns/m, c'_1 =0.003 Ns/m^3 , c_2 =10.0 Ns/m, c'_2 =0.003 *Ns/m*^{3} , c_3 =30.0 *Ns/m* , c'_3 =0.003 *Ns/m*^{3} , β_1 =0.10 *Ns/m* , β_2 =0.20 *Ns/m* , β_3 =0.15 *Ns/m*]

Figures of damped self-excited vibration of 3DOFS

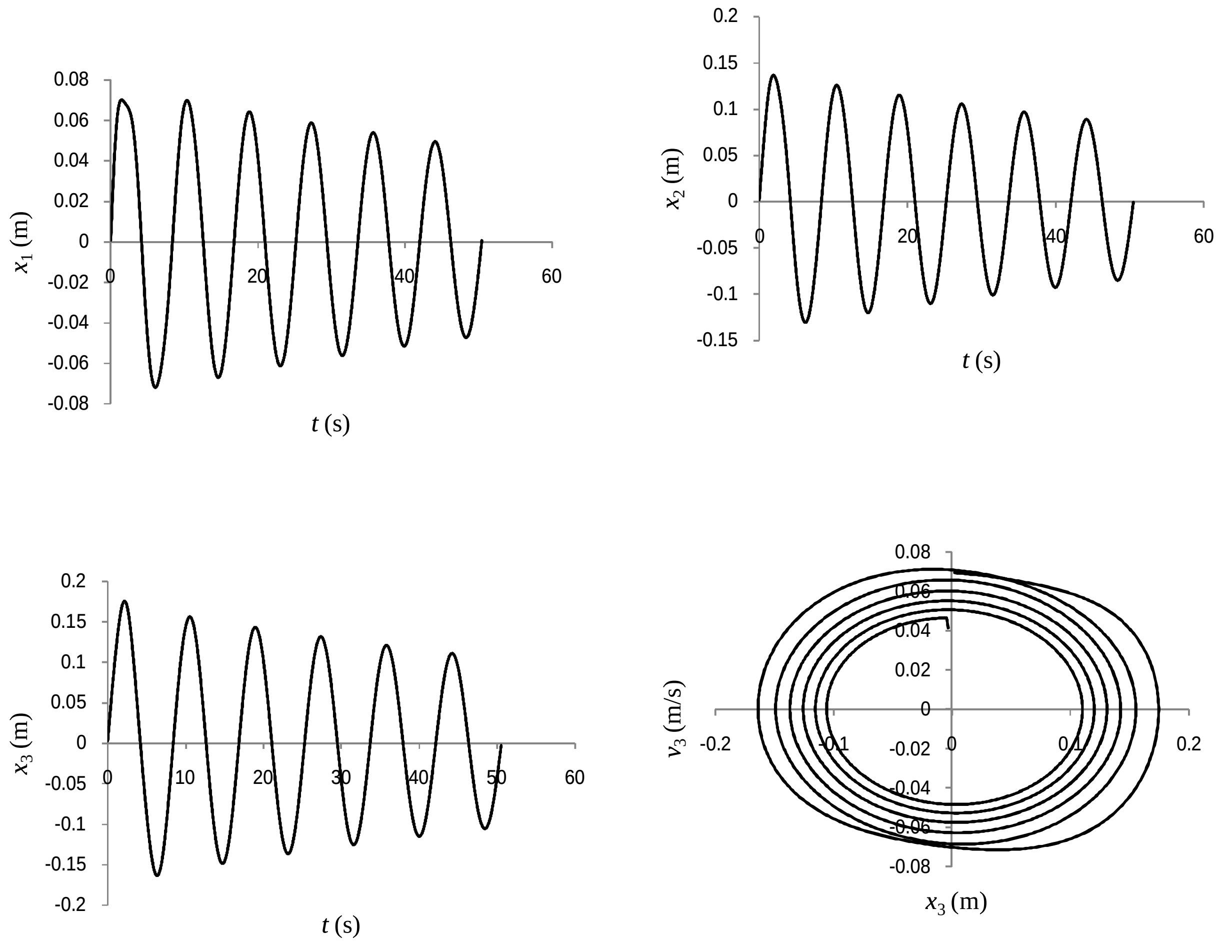

Fig. 4.19(c) x vs. t curves of m_1 , m_2 and m_3 and trajecotory for m_3 for *f(dv)* of Table 2 using data of Table 12 for combination of non-linear springs and non-linear dampers [m_1 =100 kg, m_2 =100 kg, m_3 =100 kg, k_1 =100 N/m, k'_1 =0.30 N/m^3 , k_2 =100 N/m, k'_2 =0.30 N/m^3 , k_3 =100 N/m, k'_3 =0.30 N/m^3 , c_1 =0.03 Ns/m, c'_1 =0.003 Ns/m^3 , c_2 =10.0 Ns/m, c'_2 =0.003 *Ns/m*^{3} , c_3 =30.0 *Ns/m* , c'_3 =0.003 *Ns/m*^{3} , α_1 =0.20 *N/m* , α_2 =0.25 *N/m* , α_3 =0.23 *N/m* , β_1 =0.10 *Ns/m* , β_2 =0.20 *Ns/m* , β_3 =0.15 *Ns/m*]

Figures of damped self-excited vibration of 3DOFS

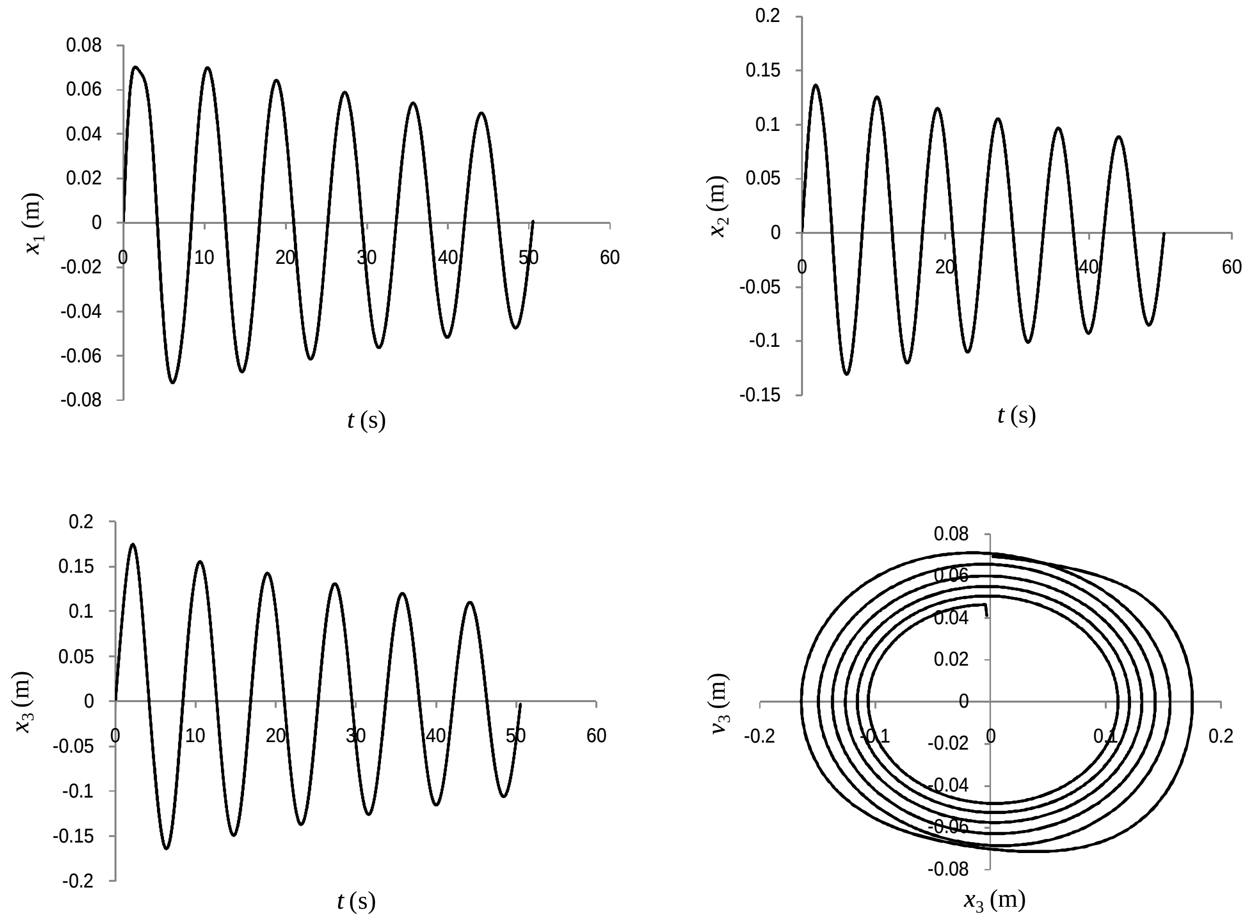

Fig. 4.19(d) x vs. t curves of m_1, m_2 and m_3 and trajecotory for m_3 for $f(n)$ of Table 2 using data of Table 12 for combination of non-linear springs and non-linear dampers [m_1 =100 kg, m_2 =100 kg, m_3 =100 kg, k_1 =100 N/m, k'_1 =0.30 N/m^3 , k_2 =100 N/m, k'_2 =0.30 N/m^3 , k_3 =100 N/m, k'_3 =0.30 N/m^3 , c_1 =0.03 Ns/m, c'_1 =0.003 Ns/m^3 , c_2 =10.0 Ns/m, c'_2 =0.003 *Ns/m*^{3} , c_3 =30.0 *Ns/m* , c'_3 =0.003 *Ns/m*^{3} , α_1 =0.20 *N/m* , α_2 =0.25 *N/m* , α_3 =0.23 *N/m* , β_1 =0.10 *Ns/m* , β_2 =0.20 *Ns/m* , β_3 =0.15 *Ns/m* , γ_1 = 0.001*Ns/m*^{3} , γ_2 =0.002 *Ns/m*^{3} , γ_3 =0.025 *Ns/m*^{3}]

4.8 System's Stability for 2DOFS

In Table 13, few values of various parameters are listed for which the system's stability is ensured. This gives an idea of choosing parameters in practical applications. Responses of the stable systems are shown in figures 4.20(a) to 4.20(f).

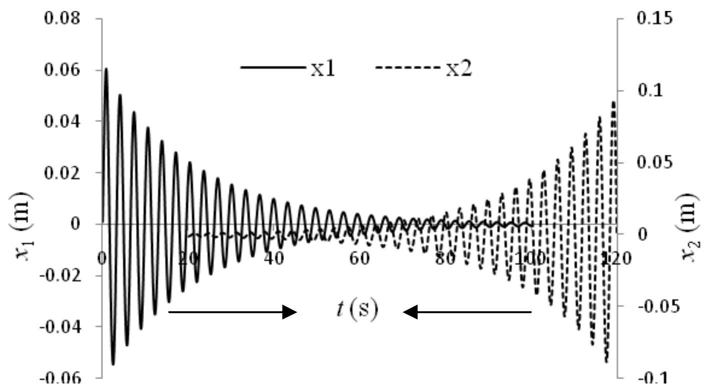

Fig. 4.20(a)

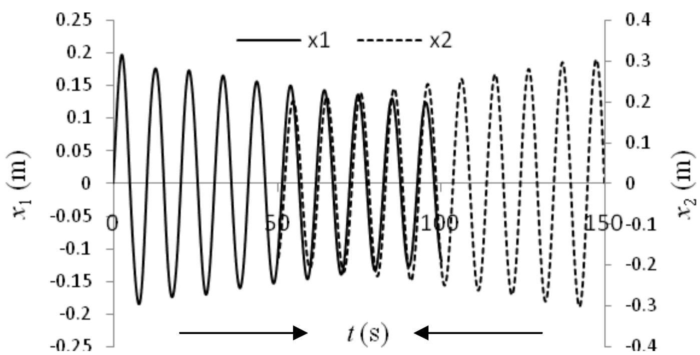

Fig. 4.20(b)

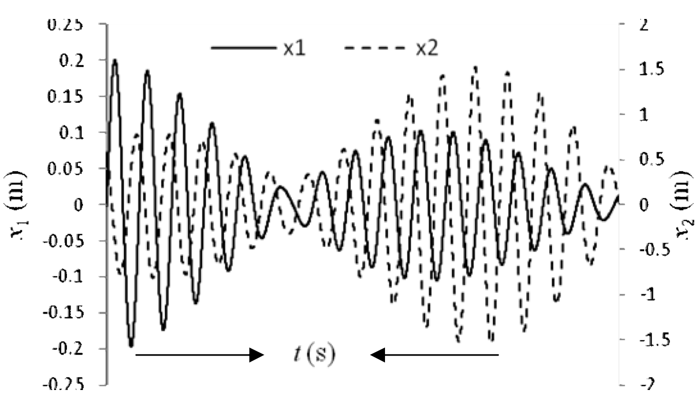

Fig. 4.20(c)

x vs. *t* curves for stability of 2DOFS in case of self-excited vibration

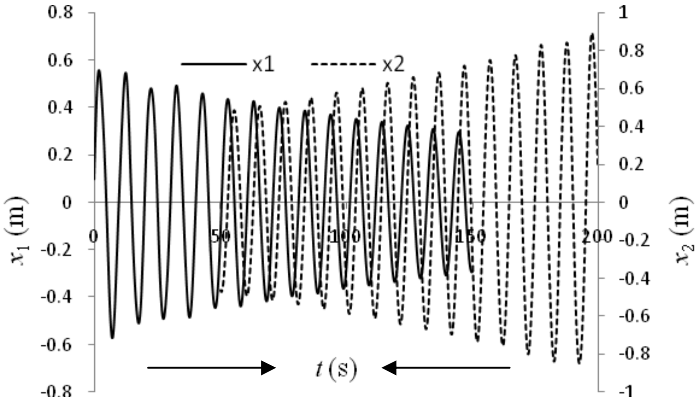

Fig. 4.20(d)

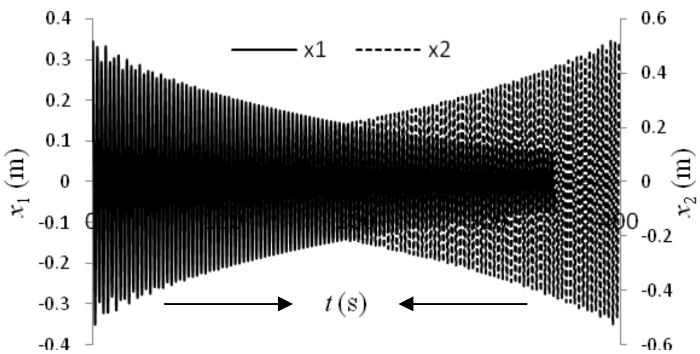

Fig. 4.20(e)

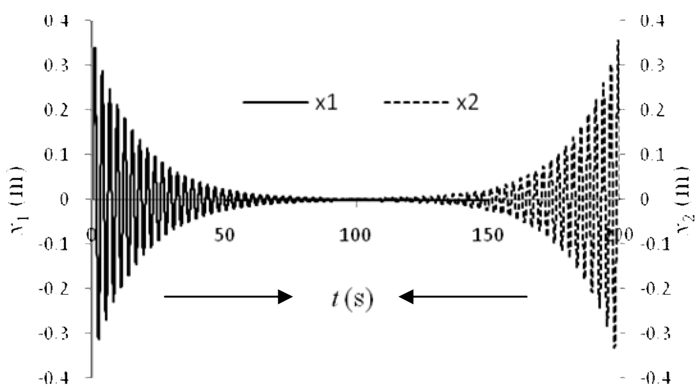

Fig. 4.20(f)

x vs. *t* curves for stability of 2DOFS in case of self-excited vibration

4.9 System's instability for 2DOFS

Using the boundary conditions from Table 16 and considering the case *(d)[f(n)]* from Table 2, two sets of values (given in Table 16) of some parameters are predicted through trial and error method after running the program and checking the system's response after drawing the figures for various combinations of springs and dampers.

For combination of linear springs and linear dampers, unstable response of the system is shown in figures 4.21(a) for data set 3 & 4.21(b) for data set 4.

Figure 4.22(a) show the unstable response of the system for the combination of linear springs and non-linear dampers for data set 3. For data set 4 and same combination, the unstable self-excited vibration is shown in figures 4.22(b).

Similarly figure 4.23(a) for data set 3 and figure 4.23(b) for data set 4 show the unstable response for the combination of non-linear springs and linear dampers.

For the combination of both non-linear springs and non-linear dampers, the responses are shown in figures 4.24(a) for data set 3 and figures 4.24(b) for data set 4.

Figures of instability for self-excited vibration of 2DOFS (BVP)

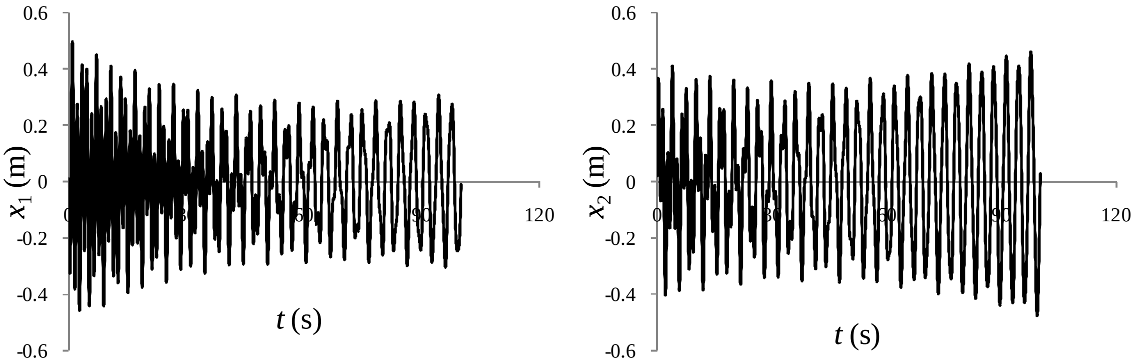

Fig. 4.21(a) x vs. t curves for m_1 and m_2 using data set 3 of Table 16 for combination of linear springs and linear dampers (For *f(n)* of Table 2).[m_1=10 kg, m_2 =10 kg, k_1=100 N/m, k_2 =100 N/m, c_1= 0.03 Ns/m, c_2 = 0.03 Ns/m, α_1 = 0.30 N/m, α_2 = 0.30 N/m, β_1 = 0.30 Ns/m, β_2 = 0.30 Ns/m, γ_1 = 0.001 Ns/m^3, γ_2 = 0.002 Ns/m^3]

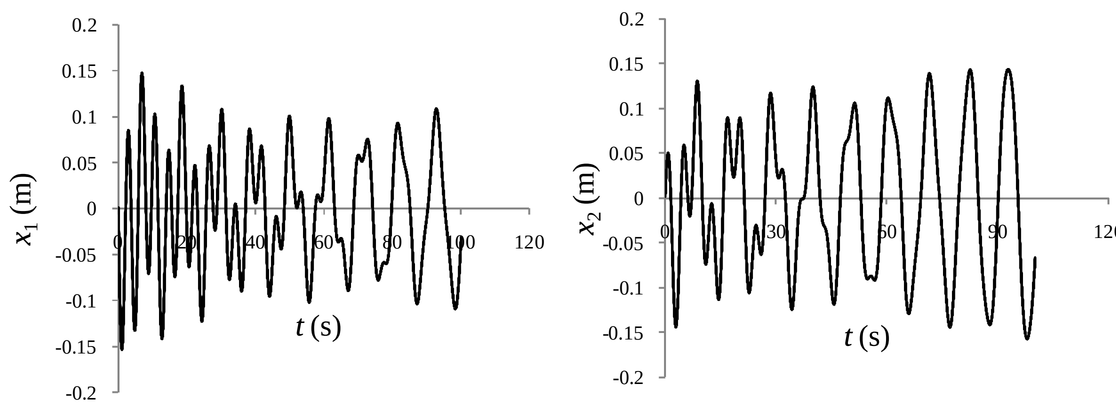

Fig. 4.21(b) x vs. t curves for m_1 and m_2 using data set 4 of Table 16 for combination of linear springs and linear dampers (For *f(n)* of Table 2) [m_1=10 kg, m_2 =10 kg, k_1=10 N/m, k_2 =10 N/m, c_1= 0.03 Ns/m, c_2 = 0.03 Ns/m, α_1 = 0.30 N/m, α_2 = 0.30 N/m, β_1 = 0.30 Ns/m, β_2 = 0.30 Ns/m, γ_1 = 0.001 Ns/m^3, γ_2 = 0.002 Ns/m^3]

Figures of instability for self-excited vibration of 2DOFS (BVP)

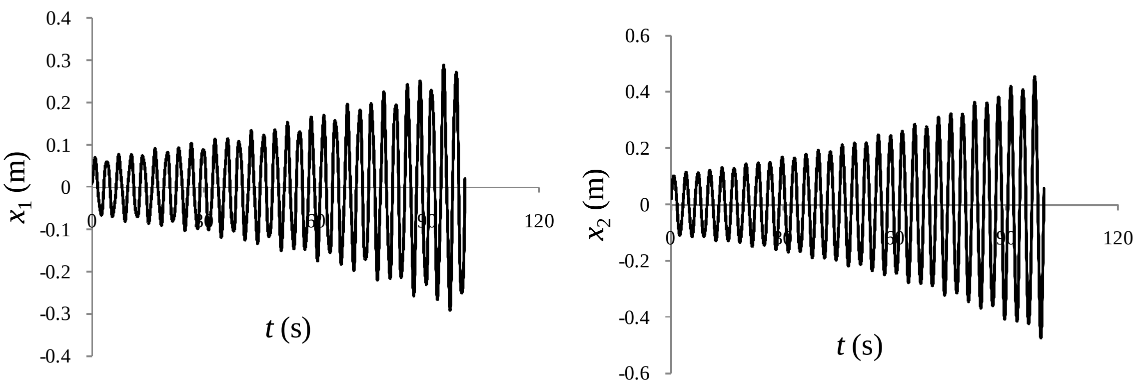

Fig. 4.22(a) *x* vs. *t* curves for m_1 and m_2 using data set 3 of Table 16 for combination of linear springs and non-linear dampers (For *f(n)* of Table 2).[m_1=10 kg, m_2 =10 kg, k_1=100 N/m, k_2 =100 N/m, c_1= 0.003 Ns/m, c'_1 = 0.003 Ns/m^3, c_2 = 0.003 Ns/m, c'_2 = 0.003 Ns/m^3, α_1 = 0.30 N/m, α_2 = 0.30 N/m, β_1 = 0.30 Ns/m, β_2 = 0.30 Ns/m, γ_1 = 0.001 Ns/m^3, γ_2 = 0.002 Ns/m^3]

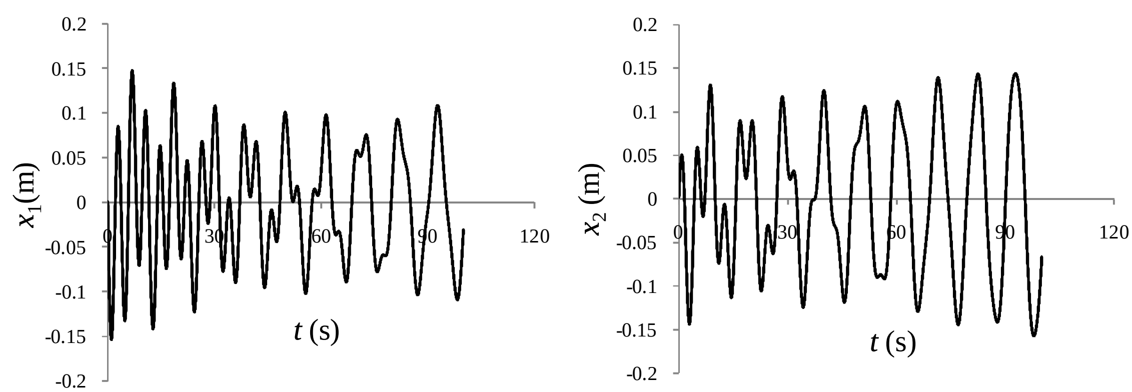

Fig. 4.22(b) *x* vs. *t* curves for m_1 and m_2 using data set 4 of Table 16 for combination of linear springs and non-linear dampers (For *f(n)* of Table 2) [m_1=10 kg, m_2 =10 kg, k_1=10 N/m, k_2 =10 N/m, c_1= 0.30 Ns/m, c'_1 = 0.003 Ns/m^3, c_2 = 0.30 Ns/m, c'_2 = 0.003 Ns/m^3, α_1 = 0.30 N/m, α_2 = 0.30 N/m, β_1 = 0.30 Ns/m, β_2 = 0.30 Ns/m, γ_1 = 0.001 Ns/m^3, γ_2 = 0.002 Ns/m^3]

Figures of instability for self-excited vibration of 2DOFS (BVP)

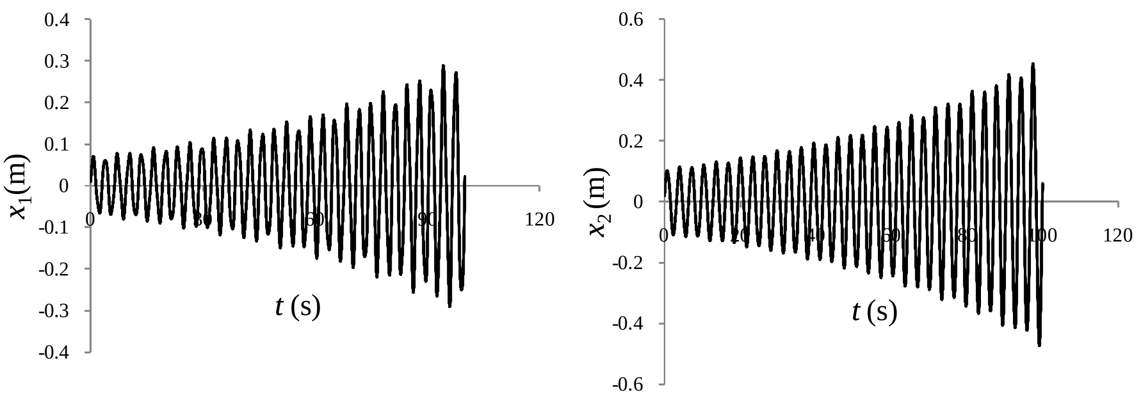

Fig. 4.23(a) x vs. t curves for m_1 and m_2 using data set 3 of Table 16 for combination of non-linear springs and linear dampers (For *f(n)* of Table 2).[m_1=10 kg, m_2 =10 kg, k_1=100 N/m, k'_1= 0.30 N/m^3, k_2 =100 N/m, k'_2 = 0.30 N/m^3, c_1= 0.003 Ns/m, c_2 = 0.003 Ns/m, α_1 = 0.30 N/m, α_2 = 0.30 N/m, β_1 = 0.30 Ns/m, β_2 = 0.30 Ns/m, γ_1 = 0.001 Ns/m^3, γ_2 = 0.002 Ns/m^3]

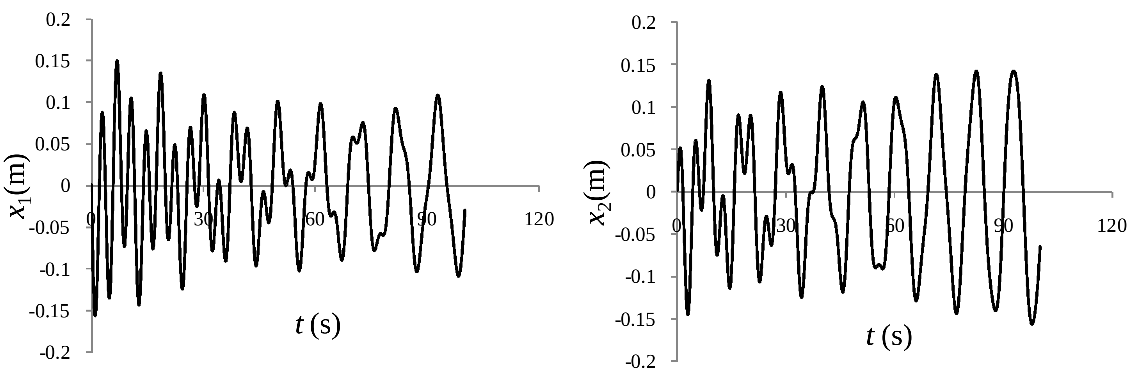

Fig. 4.23(b) x vs. t curves for m_1 and m_2 using data set 4 of Table 16 for combination of non-linear springs and linear dampers (For *f(n)* of Table 2).[m_1=10 kg, m_2 =10 kg, k_1=10 N/m, k'_1= 0.30 N/m^3, k_2 =10 N/m, k'_2 = 0.30 N/m^3, c_1= 0.30 Ns/m, c_2 = 0.30 Ns/m, α_1 = 0.30 N/m, α_2 = 0.30 N/m, β_1 = 0.30 Ns/m, β_2 = 0.30 Ns/m, γ_1 = 0.001 Ns/m^3, γ_2 = 0.002 Ns/m^3]

Figures of instability for self-excited vibration of 2DOFS (BVP)

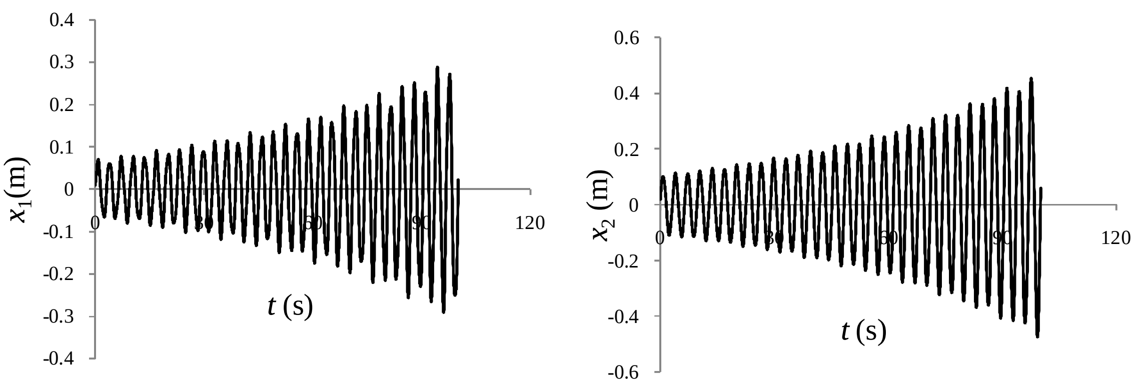

Fig. 4.24(a) x vs. t curves for m_1 and m_2 using data set 3 of Table 16 for combination of non-linear springs and non-linear dampers (For *f(n)* of Table 2).[m_1=10 kg, m_2 =10 kg, k_1=100 N/m, k'_1= 0.30 N/m^3, k_2 =100 N/m, k'_2 = 0.30 N/m^3, c_1= 0.003 Ns/m, c'_1 = 0.003 Ns/m^3, c_2 = 0.003 Ns/m, c'_2 = 0.003 Ns/m^3, α_1 = 0.30 N/m, α_2 = 0.30 N/m, β_1 = 0.30 Ns/m, β_2 = 0.30 Ns/m, γ_1 = 0.001 Ns/m^3, γ_2 = 0.002 Ns/m^3]

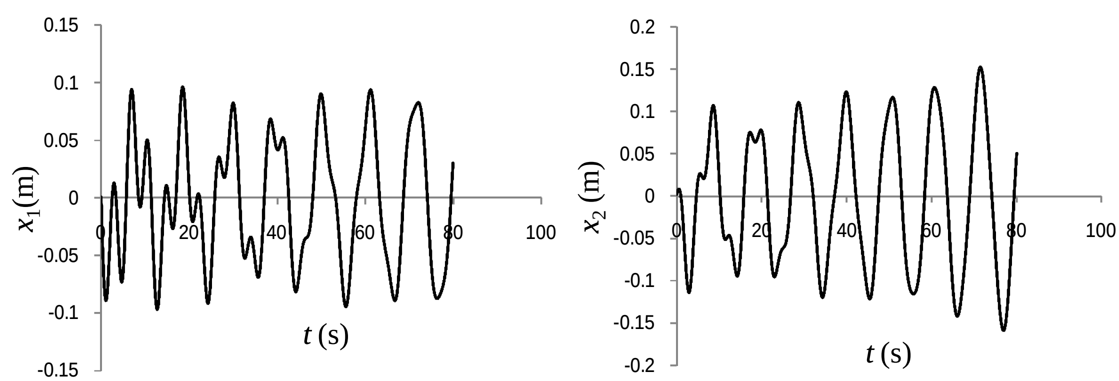

Fig. 4.24(b) x vs. t curves for m_1 and m_2 using data set 4 of Table 16 for combination of non-linear springs and non-linear dampers (For *f(n)* of Table 2).[m_1=10 kg, m_2 =10 kg, k_1=10 N/m, k'_1= 0.30 N/m^3, k_2 =10 N/m, k'_2 = 0.30 N/m^3, c_1= 0.003 Ns/m, c'_1 = 0.30 Ns/m^3, c_2 = 0.30 Ns/m, c'_2 = 0.003 Ns/m^3, α_1 = 0.30 N/m, α_2 = 0.30 N/m, β_1 = 0.30 Ns/m, β_2 = 0.30 Ns/m, γ_1 = 0.001 Ns/m^3, γ_2 = 0.002 Ns/m^3]

CHAPTER 5

CONCLUSIONS AND RECOMMENDATIONS

According to the prearranged targets of the study of self-excited vibrations, analysis of both undamped and damped self-excited vibration for 2DOFS and 3DOFS has been accomplished with the help of BVP and IVP analysis method considering both spring and damper nonlinearities. Soundness of the developed code has been verified through solving Van der Pol's equation and then comparing the obtained results with the available ones. From this study of self-excited vibration, it can be concluded as follows:

5.1 Conclusions for undamped linear self-excited vibration

- Effect of self-exciting force on the system's response is independent of chosen boundary conditions. This happens for both initial value and boundary value problems. For example, the system shows similar deflections for initial value and boundary value problems for *f(d)*.
- Effect of displacement on self-exciting force is not great. When the self-exciting force is considered as function of displacement only, then the system maintains stable vibration throughout the entire period.
- When self-exciting force is considered as a function of both velocity and displacement, then the system approaches more instability throughout the entire period.
- Mass to spring ratio plays a significant role on the maximum deflection of self-exciting vibration system. For the same ratio, system shows almost similar peak amplitudes for various cases.
- Increased spring constant makes the system more unstable and the system vibrates with higher frequency. For example, system for data set (*viii*) from Table 4 shows more instability than that for data set(*iii*) of Table 4(having higher value of spring constant compared to data set (*iii*)).
- From this study, it can be concluded that springs with the higher value of constant along with smaller mass approached more instability.

5.2 Conclusions for damped nonlinear self-excited vibration

- Also for damped condition, effect of self-exciting force on the system's response is independent of chosen boundary conditions.
- Effect of displacement and velocity on damped self-exciting force is almost similar. When the self-exciting force is considered as function of only displacement, then the

system maintains vibration throughout the entire period just like when self-exciting force is considered as function of only velocity.

- When damped self-exciting force is considered as function of both velocity and displacement, then the system approaches stability throughout the entire period.
- For 3DOFS, spring and damper nonlinearity and damped self-exciting force function have very little effect on the system's response.

5.3 Recommendation for Future Work

In future, the developed computer code can be used to study response of similar system having higher degrees of freedom. Practically, this method of vibration analysis will provide handy information for active/passive vibration control of structures. The following recommendations can be made for future works while achieving the set objectives of this thesis:

1. The present analysis should be extended to observe the effect of vibration of the system with higher degrees of freedom.
2. Experimental studies should be carried out to verify the results obtained for the self-excited vibration in any system.
3. This study can be helpful in analyzing flutter that is a self-feeding and potentially destructive vibration where aerodynamic forces on an object coupled with a structure's natural mode of vibration to produce rapid periodic motion.
4. This study is also useful specially, when a self-excited vibration control scheme becomes a boundary value problem and needs to be solved by numerical analysis.

REFERENCES.

1. Ahmed, A. U. (2009). "Stability analysis of vibration absorbers", *M. Sc. Engg. Thesis*, Department of Mechanical Engineering, BUET, Bangladesh.
2. Asfar K. R and Akour **S**. N. (2005). "Optimization Analysis of Impact Viscous Damper for Controlling Self-Excited Vibrations", *Journal of Vibration and Control,* Vol. 11, No. 1, 103-120 (2005).
3. Asfar K.R., Nayfeh A.H. and Mook D.T. (1982). "Response of self-excited two-degree-of-freedom systems to multi-frequency excitations", *Journal of Sound and Vibration*, Volume 84, Issue 2, Pages 199-221.
4. Asrar W. (1991). "Two-degree-of-freedom systems with quadratic non-linearities subjected to parametric and self excitation", *Journal of Sound and Vibration,* Volume 150, Issue 3, Pages 447-456.
5. Bachmann H. (1995). "Vibration Problems in Structures", Birkhauser.
6. Beards C.F (1996). "Structural Vibration: Analysis and Damping (1st Edition)", John Wiley & Sons Inc.
7. Browne M. and Palazzolo A. (2009). "Super harmonic nonlinear lateral vibrations of a segmented driveline incorporating a tuned damper excited by non-constant velocity joints", *Journal of Sound and Vibration*, Volume 323, Issues 1-2, Pages 334-351.
8. Chatterjee S. (2007). "Non-linear control of friction-induced self-excited vibration", *International Journal of Non-Linear Mechanics*, Volume 42, Issue 3, Pages 459-469.
9. Chi M. and Vossoughi J. (1985). "Response of slender structural members in self-excited oscillation", *Journal of Sound and Vibration*, Volume 101, Issue 1, Pages 75-83.
10. Coudeyras N., Sinou J.J. and Nacivet S. (2009). " A new treatment for predicting the self-excited vibrations of nonlinear systems with frictional interfaces: The Constrained Harmonic Balance Method, with application to disc brake squeal", *Journal of Sound and Vibration*, Volume 319, Issues 3-5, Pages 1175-1199.
11. Cveticanin L. (1998). "Self-excited vibrations of the variable mass rotor or fluid system", *Journal of Sound and Vibration*, Volume 212, Issue 4, Pages 685-702.
12. Den Hartog J.P. (1956). "Mechanical Vibrations (4th Edition)", McGraw Hill.
13. Dohnal F. (2007). "Suppressing self-excited vibrations by synchronous and time-periodic stiffness and damping variation", *Journal of Sound and Vibration,* Volume 306, Issues 1-2, Pages 136-152.

14. D'Souza A.F. and Dweib A.H. (1990). “Self-excited vibrations induced by dry friction, part 2: Stability and limit-cycle analysis”, ***Journal of Sound and Vibration*,** Volume 137, Issue 2, Pages 177-190.
15. Dweib A.H. and D'Souza A.F. (1990). “Self-excited vibrations induced by dry friction, part 1: Experimental study”, ***Journal of Journal of Sound and Vibration*,** Volume 137, Issue 2, Pages 163-175.
16. Hilaire A.O. St. (1976). “Analytical prediction of the non-linear response of a self-excited structure”, *Journal of Sound and Vibration*, Volume 47, Issue 2, Pages 185-205.
17. Kalnins, A. and Lestingi, J. E. (1967). “On Nonlinear Analysis of Elastic Shells of Revolution”, *Journal of Applied Mechanics*, Volume 34, Pages 59-64.
18. Kravchenko S. V. (1994). “Active Vibration Isolation Of Self-excited Mechanical Structures”, *Journal of Sound and Vibration*, Volume 178, Issue 5, Pages 621-634.
19. Lieuwen T. C. (2001). “Phase drift characteristics of self-excited, combustion-driven oscillations”, *Journal of Sound and Vibration*, Volume 242, Issue 5, Pages 893-905.
20. Manevitch L. I., Gendelman O., Musienko A. I., Vakakis A. F., and Bergman L. (2003).“Dynamic interaction of a semi-infinite linear chain of coupled oscillators with a strongly nonlinear end attachment”, *Physica D. Nonlinear Phenomena* 178(1-2), pp. 1–18.
21. McMillan A. J. (1997). “A non-linear friction model for self-excited vibrations”, *Journal of Sound and Vibration*, Volume 205, Issue 3, Pages 323-335.
22. Natsiavas S. (1993). “Dynamics of multiple-degree-of-freedom oscillators with colliding components”, *Journal of Sound and Vibration* 165 3, pp. 439-453.
23. Plaut R. H and Limam W. (1991). “Oscillations of weakly non-linear, self-excited systems under multi-frequency parametric excitation”, *Journal of Sound and Vibration*, Volume 144, Issue 2, Pages 197-214.
24. Pust L. and Tondl A. (2008). “System with a non-linear negative self-excitation”, *International Journal of Non-Linear Mechanics*, Volume 43, Issue 6, Pages 497-50.
25. Rahman M. A. and Ahmed A. U. (2009). “Boundary value problem analysis of a tuned vibration absorber having nonlinear springs”, *Int. J. Structural Engineering* (Inderscience Enterprises Ltd., Switzerland) - In press.

26. Rahman M.A., Ahmed A.U. & Uddin M.S. (2009). "Nonlinear analysis of shock absorbers", (ICME09-AM-28) *International Conference on Mechanical Engineering*, Dhaka, Bangladesh.
27. Rudowski J. (1982). "Limit cycles in self-excited multi-degree-of-freedom systems", *Journal of Sound and Vibration*, Volume 81, Issue 1, Pages 33-49.
28. De Silva C W (2005). "*Vibration and Shock Handbook*", CRC press, Taylor and Francis group.
29. Sinou J.J. and Jézéquel L. (2007). "The influence of damping on the limit cycles for a self-exciting mechanism", *Journal of Sound and Vibration*, Volume 304, Issues 3-5, Pages 875-893.
30. Thomson W. T. and Dahleh M.D. (2003). "*Theory of Vibrations with Applications* (*5th Edition*)", Pearson Education, Inc.
31. Thorby D. (2008). "*Structural Dynamics and Vibration in Practice (1st Edition)*", Butterworth-Heinemann Publication.
32. Timoshenko S. (1974). "Vibration Problems in Engineering (4th Edition)", John Wiley & Sons Inc.
33. Tondl A. and Nabergoj N. (2004). "The effect of parametric excitation on a self-excited three-mass system", *International Journal of Non-Linear Mechanics*, Volume 39, Issue 5, Pages 821-832.
34. Tondl, A. (1975). "Quenching of self-excited vibrations: one and two-frequency vibrations", *Journal of Sound and Vibration*, Volume 42, Issue 2, Pages 261-271.
35. Uczko J. (2002). "A geometrically non-linear model of rotating shafts with internal resonance and self-excited vibration", *Journal of Sound and Vibration*, Volume 255, Issue 3, Pages 433-456.
36. Wang Z. and Wang D. (1998). "Method of judging the self-excited vibration of rolling main drive system in rolling slippage", *Journal of Sound and Vibration*, Volume 215, Issue 5, Pages 1135-1143.
37. Zhu S.J., Zheng Y.F. and Fu Y.M. (2004). "Analysis of Non-linear Dynamics of a Two Degree of Freedom Vibration System with Non-linear Damping and Nonlinear Spring", *Journal of Sound and Vibration* 271, pp. 15-24.

LIST OF SYMBOLS AND ABBREVIATIONS

a	=	Initial time reference
b	=	Final time reference
m_1, m_2, m_3	=	Three masses (kg)
c	=	Damping coefficient (N-s/m)
c_1, c_2 , c_3	=	Damping coefficients for m_1 and m_2 and m_3 (N-s/m)
c'	=	Damping nonlinearity index (N-s/m^3)
c'_1, c'_2 , c'_3	=	Damping nonlinearity indexes for m_1 and m_2 and m_3 (N-s/m^3)
k	=	Spring constant (N/m)
k_1, k_2 , k_3	=	Spring constants for m_1 and m_2 and m_3 (N/m)
k'	=	Spring nonlinearity index (N/m^3)
k'_1, k'_2 , k'_3	=	Spring nonlinearity indexes for m_1 and m_2 and m_3 (N/m^3)
t	=	Time (s)
x_1, x_2 , x_3	=	Deflections for m_1 and m_2 and m_3 (m)
y_1, y_3 , y_5	=	x_1, x_2 , x_3 (m)
$\dot{x}_1$, $\dot{x}_2$, $\dot{x}_3$	=	Velocities for m_1 and m_2 and m_3 (m/s)
y_2, y_4 , y_6	=	$\dot{x}_1$, $\dot{x}_2$, $\dot{x}_3$ (m/s)
Spring force	=	$kx \pm k'x^3$
Damping force	=	$c\dot{x} \pm c'\dot{x}x^2$
α	=	Displacement factor for self-excited force.
β	=	Velocity factor for self-excited force.
γ	=	Nonlinear displacement factor for self-excited force.
M	=	Number of segments of the chosen interval.
T	=	A function.
Y	=	Partial derivative term of $y(t)$ with respect to $y(a)$.

TABLES

TABLE 1: Boundary Conditions for solving Van der Pol's equation

y_1 (a) (m)	y_2 (b) (m/s)
0.01	0.70

TABLE 2: Various cases considered for self-excited vibration analysis

Self-excited force is a function of				
	Displacement	Velocity	Both displacement and velocity	Nonlinear displacement term and both displacement velocity
Cases	*a*	*b*	*c*	*d*
	= *f(d)*	= *f(v)*	=*f(dv)*	=*f(n)*

TABLE 3: Arbitrarily chosen boundary conditions for undamped self-excited vibration analysis of 2DOFS (BVP)

Data Set	***i***	***ii***	***iii***	***iv***	***v***	***vi***	***vii***	***viii***
y_1(a) (m)	0.01	0.01	0.01	0.01	0.01	0.01	0.01	0.01
y_3(a) (m)	0.02	0.02	0.02	0.02	0.02	0.02	0.02	0.02
y_2(b) (m/s)	-0.6113	-0.0477	-0.1875	0.372	0.246	0.165	0.277	-0.5745
y_4(b) (m/s)	-0.8557	-0.1780	-0.1999	0.882	0.411	0.290	0.759	-0.605

TABLE 4: Data of parameters for undamped self-excited vibration analysis of 2DOFS (BVP)

Data Set	***i***	***ii***	***iii***	***iv***	***v***	***vi***	***vii***	***viii***
m_1 (kg)	10	10	10	10	100	100	100	10
m_2(kg)	10	10	10	10	100	100	100	10
k_1(N/m)	100	10	10	100	100	100	1000	1000
k_2(N/m)	100	10	10	100	100	100	1000	1000
α_1(N/m)	0.3	0.3	0.1	0.1	0.1	0.3	0.1	0.1
α_2(N/m)	0.3	0.3	0.1	0.1	0.1	0.3	0.1	0.1
β_1(Ns/m)	0.3	0.3	0.1	0.1	0.1	0.3	0.1	0.1
β_2(Ns/m)	0.3	0.3	0.1	0.1	0.1	0.3	0.1	0.1

TABLE 5: Arbitrarily chosen Boundary Conditions for undamped self-excited vibration analysis of 2DOFS (IVP)

y_1 (a) (m)	y_2 (a) (m/s)	y_3 (a) (m)	y_4 (a) (m/s)
0.01	0.70	0.02	0.80

TABLE 6: Data of parameters for undamped self-excited vibration analysis of 2DOFS (IVP)

Data Set	*i*	*ii*	*iii*	*iv*	*v*	*vi*	*vii*	*viii*
m_1 (*kg*)	10	10	10	10	100	100	100	10
m_2 (*kg*)	10	10	10	10	100	100	100	10
k_1 (*N/m*)	100	10	10	100	100	100	1000	1000
k_2 (*N/m*)	100	10	10	100	100	100	1000	1000
α_1 (*N/m*)	0.3	0.3	0.1	0.1	0.1	0.3	0.1	0.1
α_2 (*N/m*)	0.3	0.3	0.1	0.1	0.1	0.3	0.1	0.1

TABLE 7: Ratios of Mass to spring constant (undamped 2DOFS)

Conditions→	*i*	*ii*	*iii*	*iv*	*v*	*vi*	*vii*	*viii*
m_1/ k_1	0.1	1.0	1.0	0.1	1.0	1.0	0.1	0.01
m_2/ k_2	0.1	1.0	1.0	0.1	1.0	1.0	0.1	0.01

TABLE 8: Different combinations of springs and dampers for damped self-excited vibration analysis of 2DOFS & 3DOFS (BVP)

Combinations of spring & Damper				
	1	**2**	**3**	**4**
Springs	Linear	Linear	Nonlinear	Non-linear
Dampers	Linear	nonlinear	linear	Non-linear

TABLE 9: Boundary conditions for damped self-excited vibration analysis of 2DOFS (BVP).

y_1 (a) (m)	y_2 (b) (m/s)	y_3 (a) (m)	y_4 (b) (m/s)
0.01	0.70	0.02	0.80

TABLE 10: Data of parameters for damped self-excited vibration analysis of 2DOFS (BVP)

Parameters	m_1(kg)	m_2(kg)	k_1(N/m)	k'_1(N/m^3)	k_2(N/m)	k'_2(N/m^3)
Data set 1	100	100	100	0.30	100	0.30
Data set 2	100	1000	1000	-0.30	1000	-0.30
Parameters	c_1(Ns/m)	c'_1(Ns/m^3)	c_2(Ns/m)	c'_2(Ns/m^3)	α_1(N/m)	α_2(N/m)
Data set 1	0.03	0.003	30.0	0.003	0.20	0.25
Data set 2	0.03	-0.003	30.0	-0.003	0.15	0.20
Parameters	β_1(Ns/m)	β_2(Ns/m)	γ_1(Ns/m^3)	γ_2(Ns/m^3)		
Data set 1	0.10	0.20	0.001	0.002		
Data set 2	0.15	0.25	0.015	0.025		

TABLE 11: Arbitrarily chosen boundary conditions for damped self-excited vibration analysis of 3DOFS (BVP)

y_1 (a) (m)	y_2 (b) (m/s)	y_3 (a) (m)	y_4 (b) (m/s)	y_5 (a) (m)	y_6 (b) (m/s)
0.01	0.70	0.02	0.80	0.80	0.90

TABLE 12: Data of parameters for damped self-excited vibration analysis of 3DOFS (BVP)

Parameters	m_1(kg)	m_2(kg)	m_3(kg)	k_1(N/m)	k'_1(N/m^3)	k_2(N/m)
Data	100	100	100	100	0.30	100
Parameters	k'_2(N/m^3)	k_3(N/m)	k'_3(N/m^3)	c_1(Ns/m)	c'_1(Ns/m^3)	c_2(Ns/m)
Data	0.30	100	0.30	0.03	0.003	10.0
Parameters	c'_2(Ns/m^3)	c_3(Ns/m)	c'_3(Ns/m^3)	α_1(N/m)	α_2(N/m)	α_3(N/m)
Data	0.003	30.0	0.003	0.20	0.25	0.23
Parameters	β_1(Ns/m)	β_2(Ns/m)	β_3(Ns/m)	γ_1(Ns/m^3)	γ_2(Ns/m^3)	γ_3(Ns/m^3)
Data	0.10	0.20	0.15	0.001	0.002	0.025

TABLE 13: Calculated values of parameters for system's stability of 2DOFS (BVP)

Figures	**Parameters**				
	$m_1(kg)$	$m_2(kg)$	$k_1(N/m)$	$k_2(N/m)$	$c_1(Ns/m)$
4.20 (a)	1	1	10	10	0.5
4.20 (b)	10	10	10	10	0.5
4.20 (c)	1000	10	1000	10	2.5
4.20 (d)	100	100	100	100	2.5
4.20 (e)	100	100	1000	1000	2.5
4.20 (f)	10	10	100	1000	2.5

TABLE 14: Responses of 2DOFS at a glance in case of damped self-excited vibration

Combinations of	**Data Set**	**Stability / Instability**
Linear springs & Linear dampers	1	[*Figures 4.12(a) - 4.12(d)]* The system approaches stability for all cases of the self-excited force function (Table 2).
	2	[*Figures 4.13(a) - 4.13(d)*] m_1 quickly becomes stable within 40 seconds. m_2 also reduces its amplitude of vibration greatly within 40 seconds and continues to vibration with very low amplitude up to 100 seconds. For only case (*d*), m_2 maintains higher amplitude steadily.
Linear springs & Non-linear dampers	1	[*Fig. 4.14(a)* & Appendix A: *Figures 1-3*] The system illustrates stability.
	2	[*Fig. 4.14(b) &* Appendix A: *Figures 4-6*] m_1 becomes stable quickly just within 40 seconds except case (*d*). m_2 maintains steady vibration up to the considered period. Developed code can't show the response after 40seconds for data set 2 due to consideration of one segment for calculation. But the trend shows that it will be stable after a larger period. For case (*d*), though m_1 shows high frequency vibration, but it moves towards stability. From the steady state trend, it can be said that m_2 maintains instability.
Non-linear springs & Linear dampers	1	[*Fig. 4.15(a) &* Appendix A: *Figures 7-9*] The system approaches to stability. But in case (*b*), the system at first shows higher frequency vibration then maintains steady vibration for the considered period of time. The progressing reducing trend indicates the attainment of the system's stability.
	2	[*Fig. 4.15(b) &* Appendix A: *Figures 10-12*] Both m_1 and m_2 continues steady vibration during the period for all cases.
Non-linear springs & Non-linear dampers	1	[*Figures 4.16(a) – 4.16(d)*] The system becomes stable for every case.
	2	[*Figures 4.17(a) – 4.17(d)*] Both m_1 and m_2 maintains steady vibration just like for the combination of non-linear springs and linear dampers for data set 2.

TABLE 15: Responses of 3DOFS at a glance in case of damped self-excited vibration:

Cases	Stability
f(d)	m_1 starts vibration with amplitude of 0.07 m for all four combinations of springs and dampers. Both m_2 and m_3 start to vibrate with amplitude of about 0.15 m for all combinations. For *f*(*d*) the system approaching stability gradually.
f(v)	Both m_1 and m_2 vibrate with very low amplitude and move towards stability. m_3 also ,starting with amplitude of 0.1 m, approaches stability.
f(dv)	The response of the system is quite similar to the response for *f*(*d*). m_1, m_2 and m_3 are showing vibration of gradually reducing amplitude.
f(n)	For all four combinations of springs and dampers, the system for *f*(*n*) shows the response quite similar to the responses for both *f*(*d*) and *f*(*dv*). For this case, the system also showing stability.

TABLE 16: Data of parameters for unstable conditions of 2DOFS (BVP)
[*Only f(n) is considered for calculation*]

Parameters		**Combinations (Table 8) / Data Set**							
		1		***2***		***3***		***4***	
		Set 3	Set 4	Set 3	Set 4	Set 3	Set 4	Set 3	Set 4
m_1	(*kg*)	10		10		10		10	
m_2	(*kg*)	10		10		10		10	
k_1	(*N/m*)	100	10	100	10	100	10	100	10
k'_1	(N/m^3)	0.0		0.0		0.30		0.3	
k_2	(*N/m*)	100	10	100	10	100	10	100	10
k'_2	(N/m^3)	0.0		0.0		0.30		0.3	
c_1	(*Ns/m*)	.03		0.003	0.3	0.003	0.30	0.003	0.30
c'_1	(Ns/m^3)	0.0		0.003		0.0		0.003	
c_2	(*Ns/m*)	0.30		0.003	0.3	0.003	0.30	0.003	0.30
c'_2	(Ns/m^3)	0.0		0.003		0.0		0.003	
α_1	(*N/m*)	0.3		0.3		0.3		0.3	
α_2	(*N/m*)	0.3		0.3		0.3		0.3	
β_1	(*Ns/m*)	0.3		0.3		0.3		0.3	
β_2	(*Ns/m*)	0.3		0.3		0.3		0.3	
γ_1	(Ns/m^3)	0.001		0.001		0.001		0.001	
γ_2	(Ns/m^3)	0.002		0.002		0.002		0.002	

Appendix A

(Figures of undamped self-excited vibration of 2DOFS)

BVP analysis of Undamped Self-excited Vibration of 2DOF for *f(v)* from Table 2
[***Figures A(1) - A(7)***]

Figures A(1) – A(7) for *f(v)* and data sets (*i*) to (*vi*) & (*viii*) from Table 4 show that the system tends to be unstable over the period

But with the higher values of m_1 & m_2, the system maintains stable amplitude throughout the period as shown in figures A(5) & A(6).

For data set *(viii)* with higher values of both m_1 and m_2 and spring constants k_1 and k_2, the amplitude is much lower but gradually the system goes to unstable condition as shown in figure A(7).

.

Figures of undamped self-excited vibration of 2DOFS (BVP)
Figs. A(1)-A(7) drawn using data sets (*i*) - (*vi*) & (*viii*) of **Table 4** for Case. *(b)* of **Table 2**

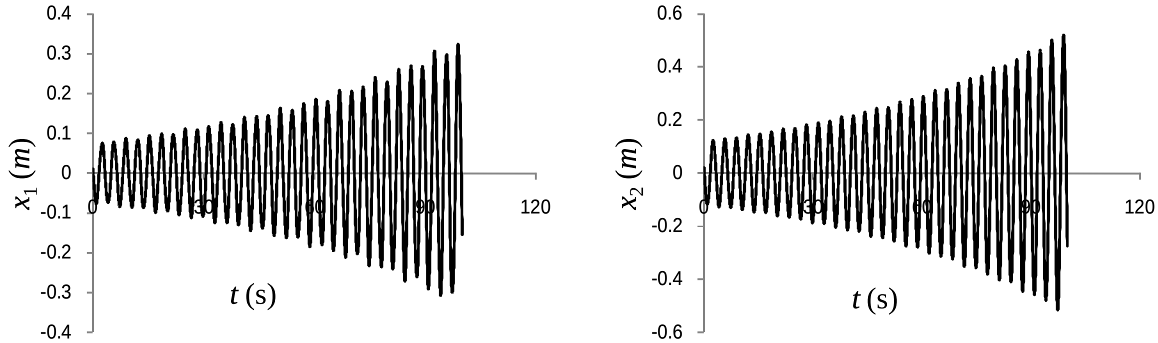

Fig. A(1) x vs. t curves of m_1 and m_2 (for data set (*i*) and for *f(v)*)

[m_1=10kg, m_2= 10kg, k_1=100 N/m, k_2=100 N/m, β_1 = 0.3 Ns/m ,β_2=0.3 Ns/m]

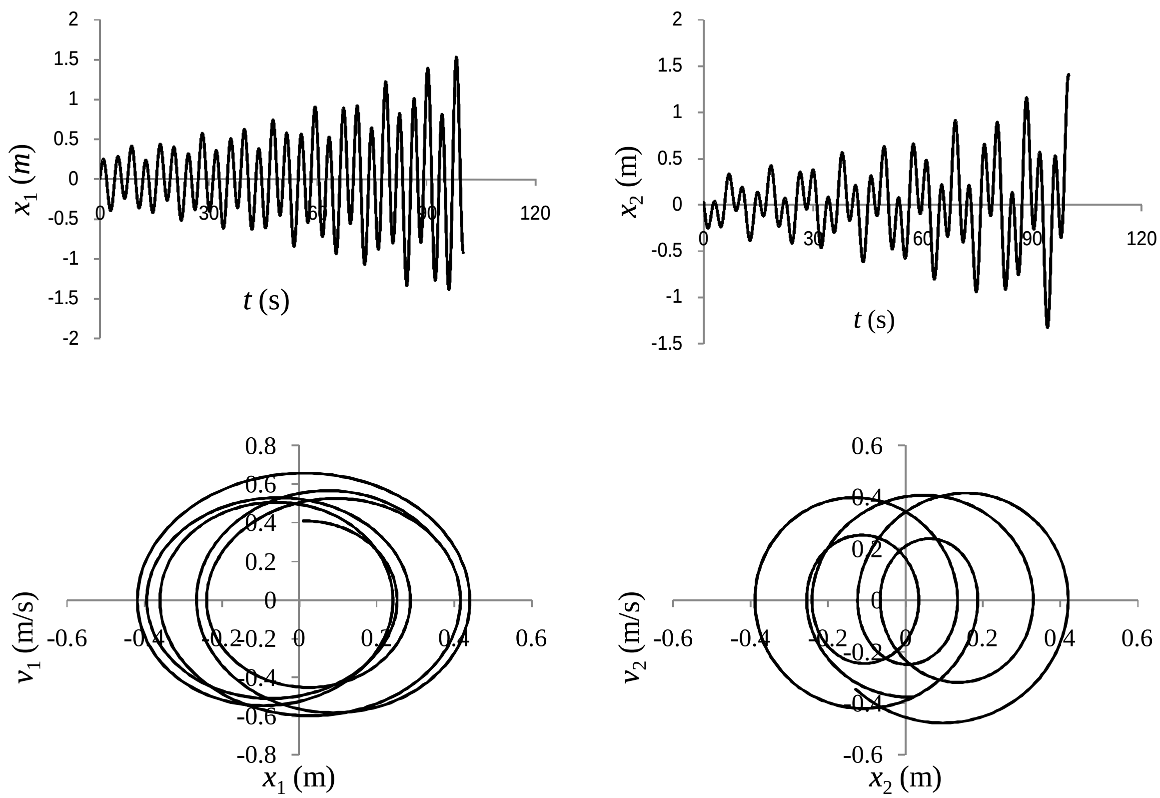

Fig. A(2) x vs. t curves and phase planes of m_1 and m_2 (for data set (*ii*) and for *f(v*)

[m_1=10kg, m_2= 10kg, k_1=10 N/m, k_2=10 N/m, β_1 = 0.3 Ns/m ,β_2=0.3 Ns/m]

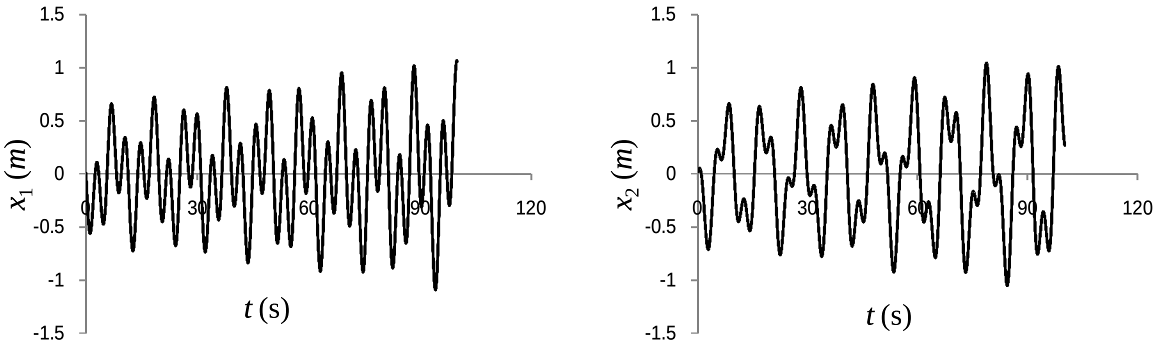

Fig. A(3) x vs. t curves of m_1 and m_2 (for data set (*iii*) and for $f(v)$)
[m_1=10kg, m_2= 10kg, k_1=10 N/m, k_2=10 N/m, β_1 = 0.1 Ns/m ,β_2=0.1 Ns/m]

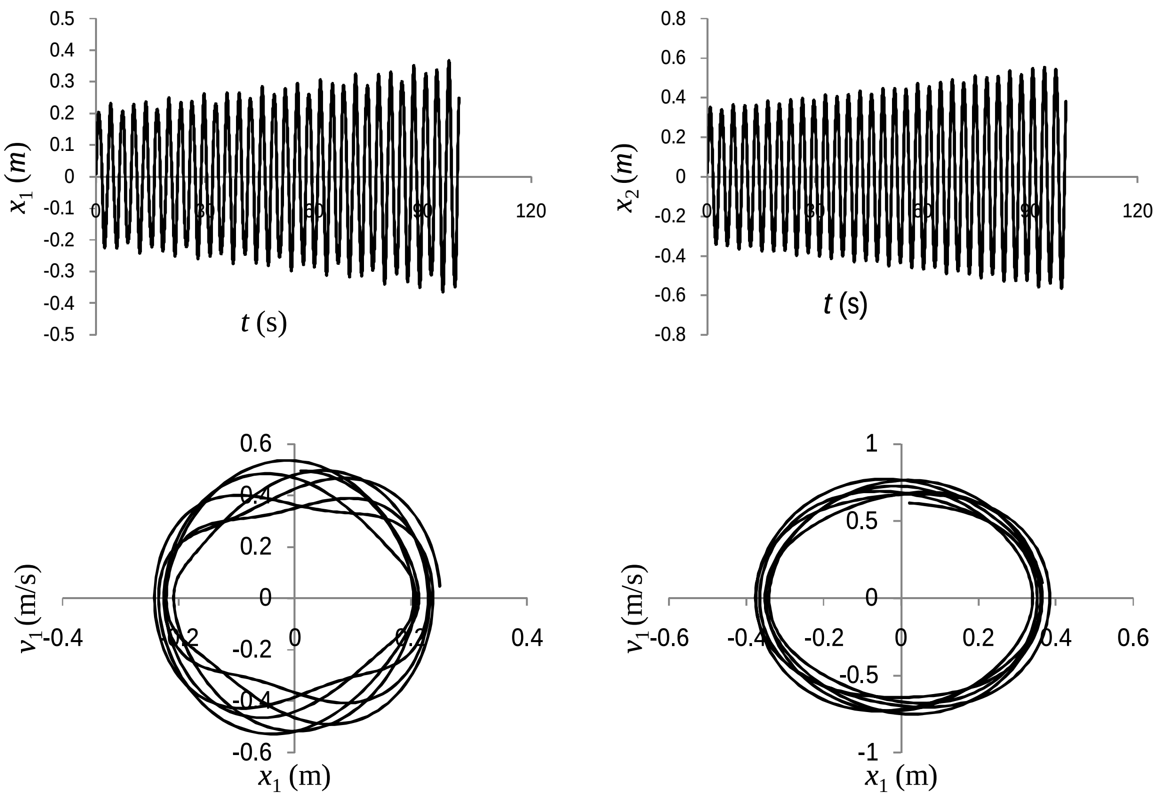

Fig. A(4) x vs. t curves and phase planes of m_1 and m_2 (for data set (*iv*) and for $f(v)$)
[m_1=10kg, m_2= 10kg, k_1=100 N/m, k_2=100 N/m, β_1 = 0.1 Ns/m ,β_2=0.1 Ns/m].

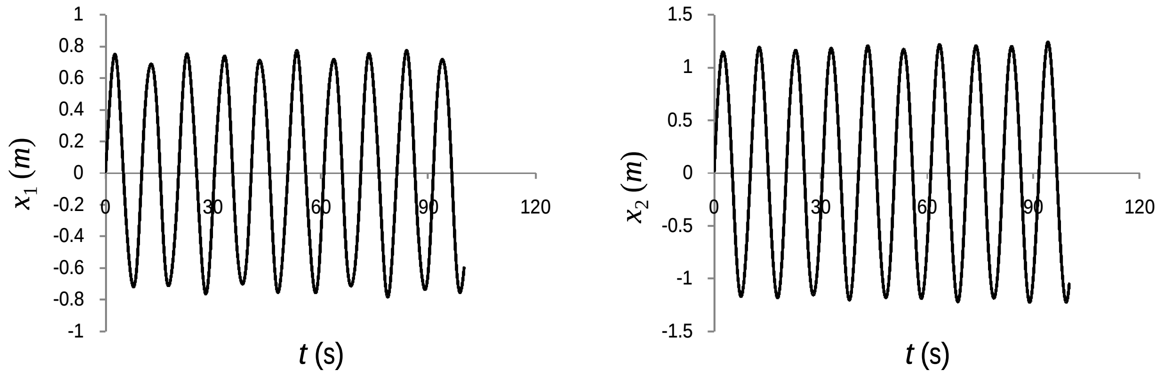

Fig. A(5) x vs. t curves of m_1 and m_2 (for data set (v) and for $f(v)$)

[m_1=100kg, m_2= 100kg, k_1=100 N/m, k_2=100 N/m, β_1 = 0.1 Ns/m ,β_2=0.1 Ns/m]

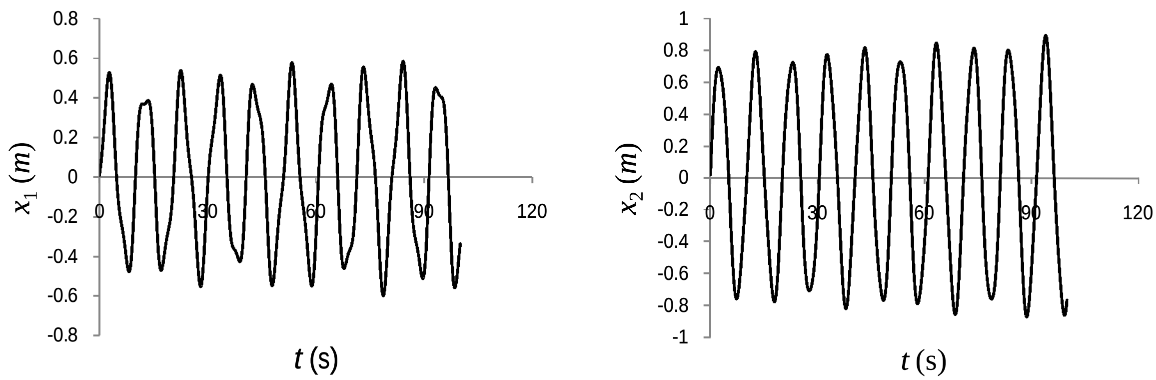

Fig. A(6) x vs. t curves of m_1 and m_2 (for data set (vi) and $f(v)$)

[m_1=100kg, m_2= 100kg, k_1=100 N/m, k_2=100 N/m, β_1 = 0.3 Ns/m ,β_2=0.3 Ns/m]

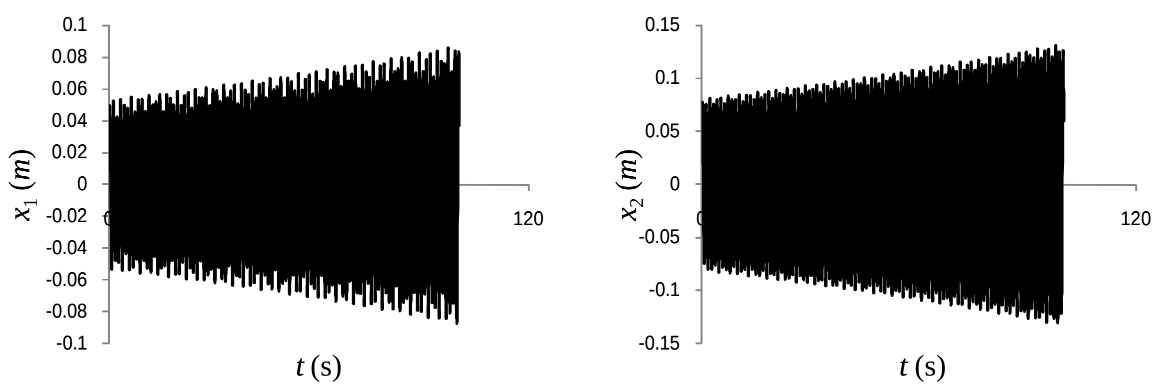

Fig. A(7) x vs. t curves of m_1 and m_2 (for data set ($viii$) and $f(v)$)

[m_1=10kg, m_2= 10kg, k_1=1000 N/m, k_2=1000 N/m, β_1 = 0.1 Ns/m ,β_2=0.1 Ns/m]

APPENDIX B

(Figures of damped self-excited vibration of 2DOFS)

Response of 2DOFS for the combination of linear springs and non-linear dampers
[***Figures B(1) - B(6)]***

For cases (*a*) to (*c*) and data set 1 from Table 10, the response of the system is shown in figures B(1) to B(3). For data set 2 from Table 10, the response is shown in figures B(4) to B(6).

In fig. B(1) for *f(d)*, the amplitude of vibration of m_1 varies from 0.5 m to .008 m. Initially amplitude is high, but after 5 seconds, it decreases to 0.2 m and gradually reaches to very low amplitude. This implies that the system approaches to stability. Similar types of response of m_1 for the same case are seen from figures B(2) and B(3).. All of these figures show that the system is going to be stable after this period of 100 seconds. From these figures, it is clear that for this combination, vibration of m_1 does not differ significantly depending on the values of self-excited force.

On the other hand, m_2 vibrates with relatively higher amplitude ranging from 0.6 m to 0.05 m. This implies that m_2 takes much time to be stable. However, in figure B(2) for *f(v)*, amplitude of m_2 is smaller than case (*a*). This is due to the effect of nonlinear damper and velocity dependent self-excited force. From figure B(2), it is clear that velocity plays an important role in self-excited vibration.

However, when self-excited force is function of both displacement and velocity (case *c*) then amplitude of m_2 in figure B(3) becomes similar to that for *f(d)* for this combination of springs and dampers.

For data set 2 and cases (*a*) to (*c*), the responses of the system are shown in figures B(4) to B(6). Here the figures are drawn with the results of computer program for 40 seconds. For this combination, m_1 vibrates with high frequency and becomes stable quickly. For cases (*a*) to (*c*), m_1 starts vibration with the amplitude of about 0.7 m and then gradually reaches to stability. On the other hand, m_2 vibrates in a different way rather than m_1. The response of m_2 is shown in figures B(4) to B(6). The amplitude of vibration of m_2 is quite low for this combination. m_2 vibrates with high frequency for first 10 seconds. In figure B(4), the amplitude of m_2 varies from 0.045 m to 0.01 m. Hence, it is clear from the response that the system would eventually maintain steady vibration and hence never reaches to stability.

For *f(v)*, the amplitude of m_2 decreases than that for *f(d)*. Due to velocity dependent self-excited force, amplitude decreases and for damper nonlinearity, the magnitude of vibration is quite low. Similar response of m_2 is seen in figures B(5) and B(6).

Figures of damped self-excited vibration of 2DOFS (BVP)

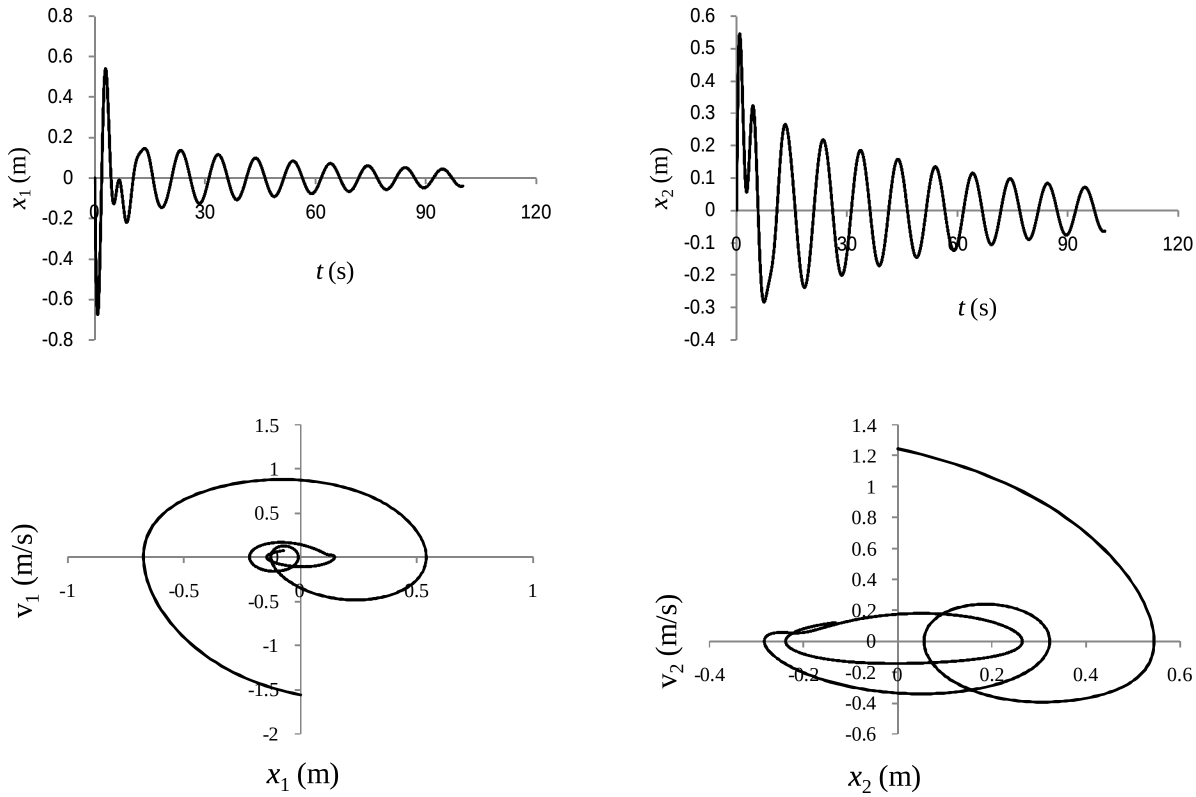

Fig. B(1) x vs. t curves and phase planes of m_1 and m_2 for $f(d)$ of Table 2 using data set 1of Table 10 for combination of linear springs and non-linear dampers [m_1=100 kg, m_2 =100 kg, k_1=100 N/m, k_2 =100 N/m, c_1= 0.03 Ns/m, c'_1 = 0.003 Ns/m^3, c_2 = 30.0 Ns/m, c'_2 = 0.003 Ns/m^3, α_1 = 0.20 N/m, α_2 = 0.25 N/m].

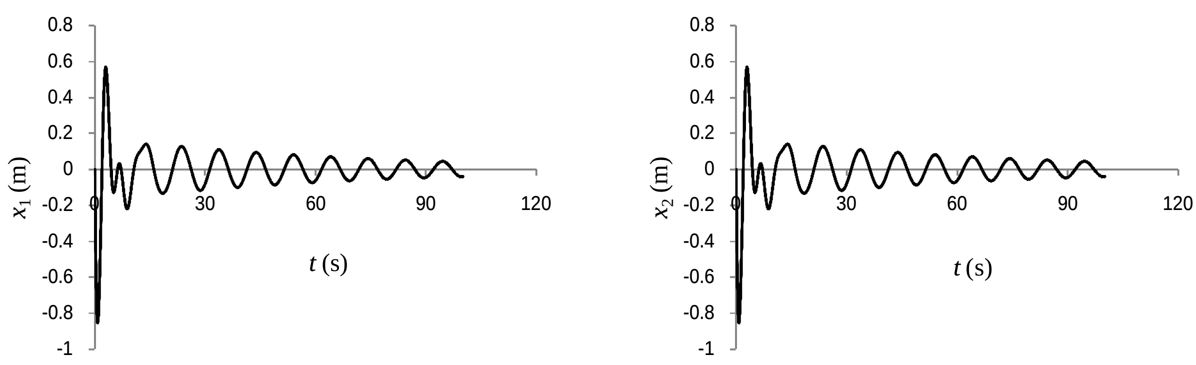

Fig. B(2) x vs. t curves of m_1 and m_2 for $f(v)$ of Table 2 using data set 1 of Table 10 for combination of linear springs and non-linear dampers [m_1=100 kg, m_2 =100 kg, k_1=100 N/m, k_2 =100 N/m, c_1= 0.03 Ns/m, c'_1 = 0.003 Ns/m^3, c_2 = 30.0 Ns/m, c'_2 = 0.003 Ns/m^3, β_1 = 0.10 Ns/m, β_2 = 0.20 Ns/m]

Figures of damped self-excited vibration of 2DOFS (BVP)

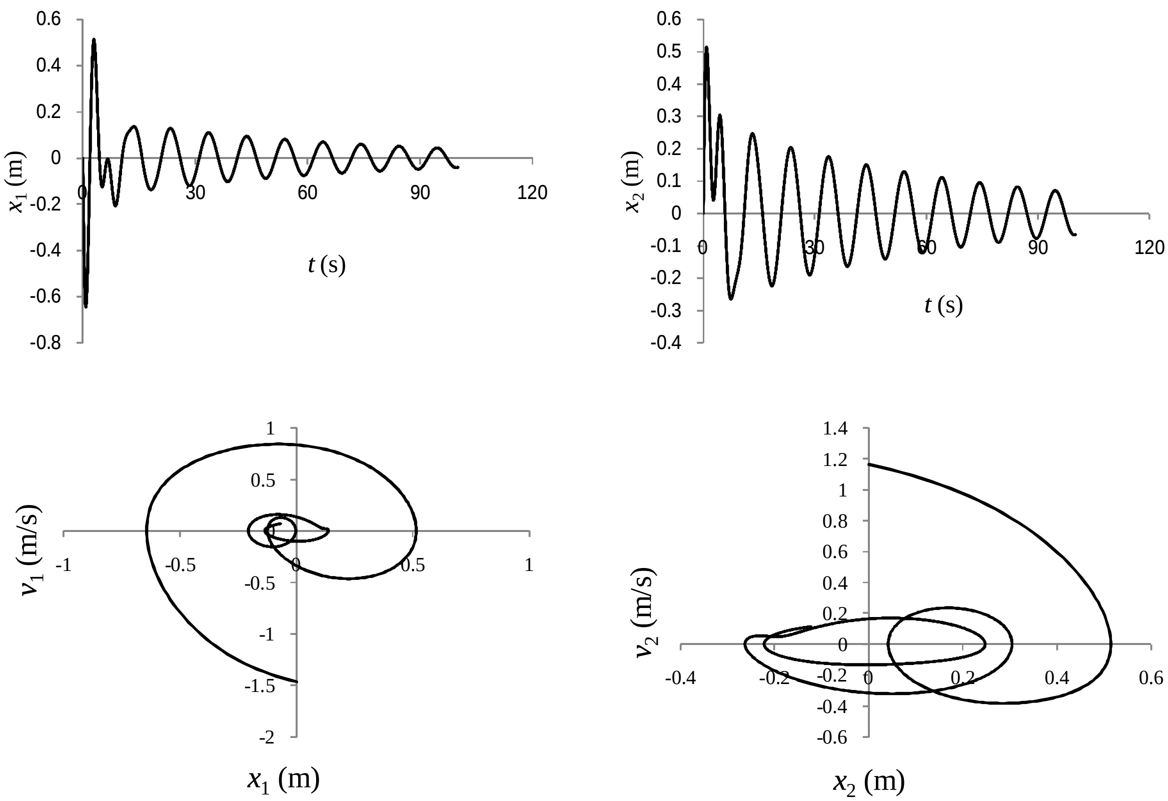

Fig. B(3) x vs. t curves and phase planes of m_1 and m_2 for *f(dv)* of Table 2 using data set 1 of Table 10 for combination of linear springs and non-linear dampers [m_1=100 kg, m_2 =100 kg, k_1=100 N/m, k_2 =100 N/m, c_1= 0.03 Ns/m, c'_1 = 0.003 Ns/m^3, c_2 = 30.0 Ns/m, c'_2 = 0.003 Ns/m^3, α_1 = 0.20 N/m, α_2 = 0.25 N/m, β_1 = 0.10 Ns/m, β_2 = 0.20 Ns/m]

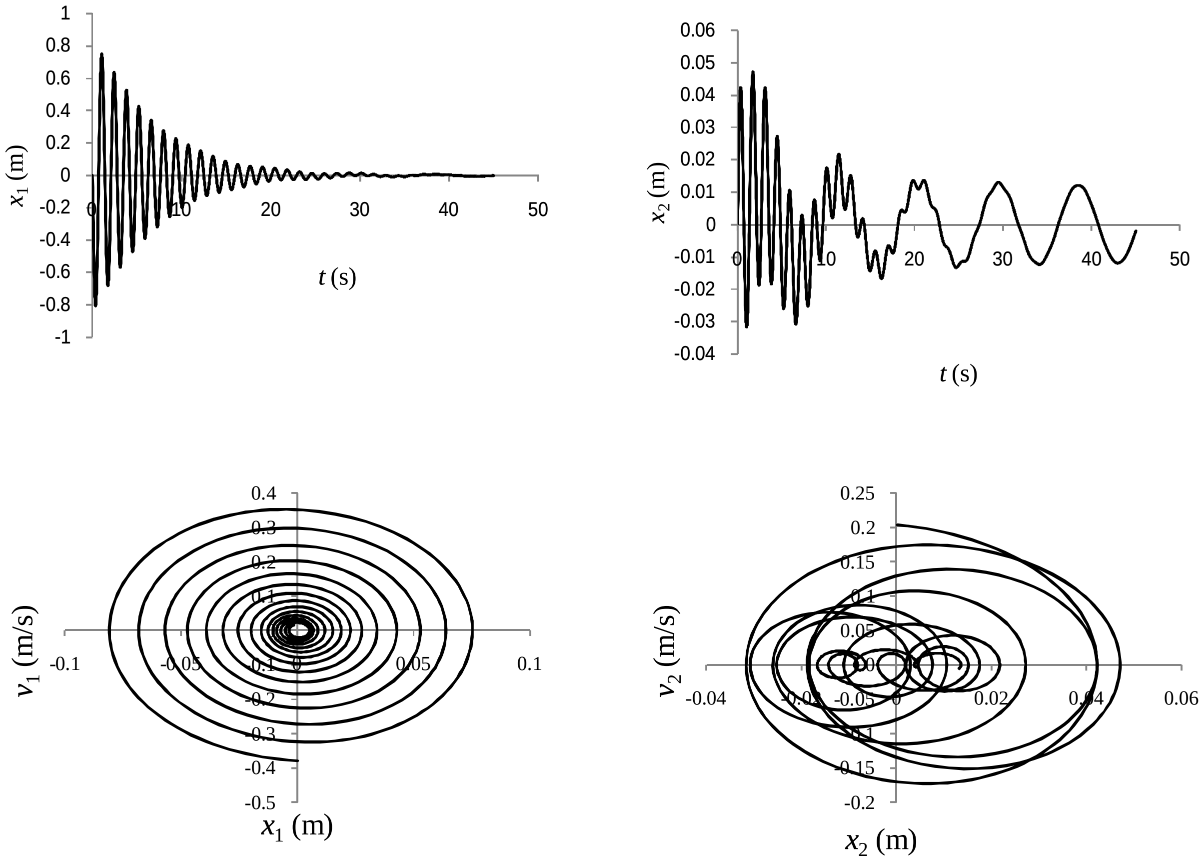

Fig. B(4) *x* vs. *t* curves and phase planes of m_1 and m_2 for *f(d)* of Table 2 using data set 2 of Table 10 for combination of linear springs and non-linear dampers [m_1=100 kg, m_2 =1000 kg, k_1=1000 N/m, k_2 =1000 N/m, c_1= 0.03 Ns/m, c'_1 = -0.003 Ns/m^3, c_2 = 30.0 Ns/m, c'_2 = -0.003 Ns/m^3, α_1 = 0.15 N/m, α_2 = 0.20 N/m]

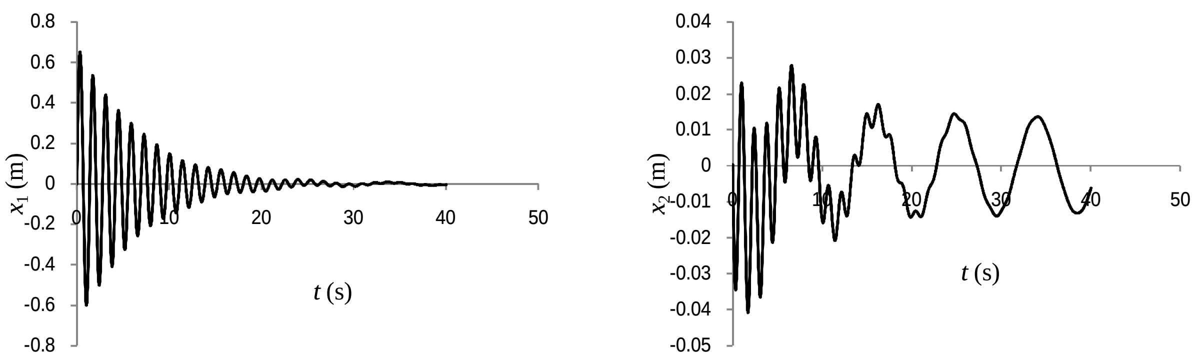

Fig. B(5) *x* vs. *t* curves of m_1 and m_2 for *f(v)* of Table 2 using data set 2 of Table 10 for combination of linear springs and non-linear dampers [m_1=100 kg, m_2 =1000 kg, k_1=1000 N/m, k_2 =1000 N/m, c_1= 0.03 Ns/m, c'_1 = -0.003 Ns/m^3, c_2 = 30.0 Ns/m, c'_2 = -0.003 Ns/m^3, β_1 = 0.15 Ns/m, β_2 = 0.25 Ns/m]

Figures of damped self-excited vibration of 2DOFS (BVP)

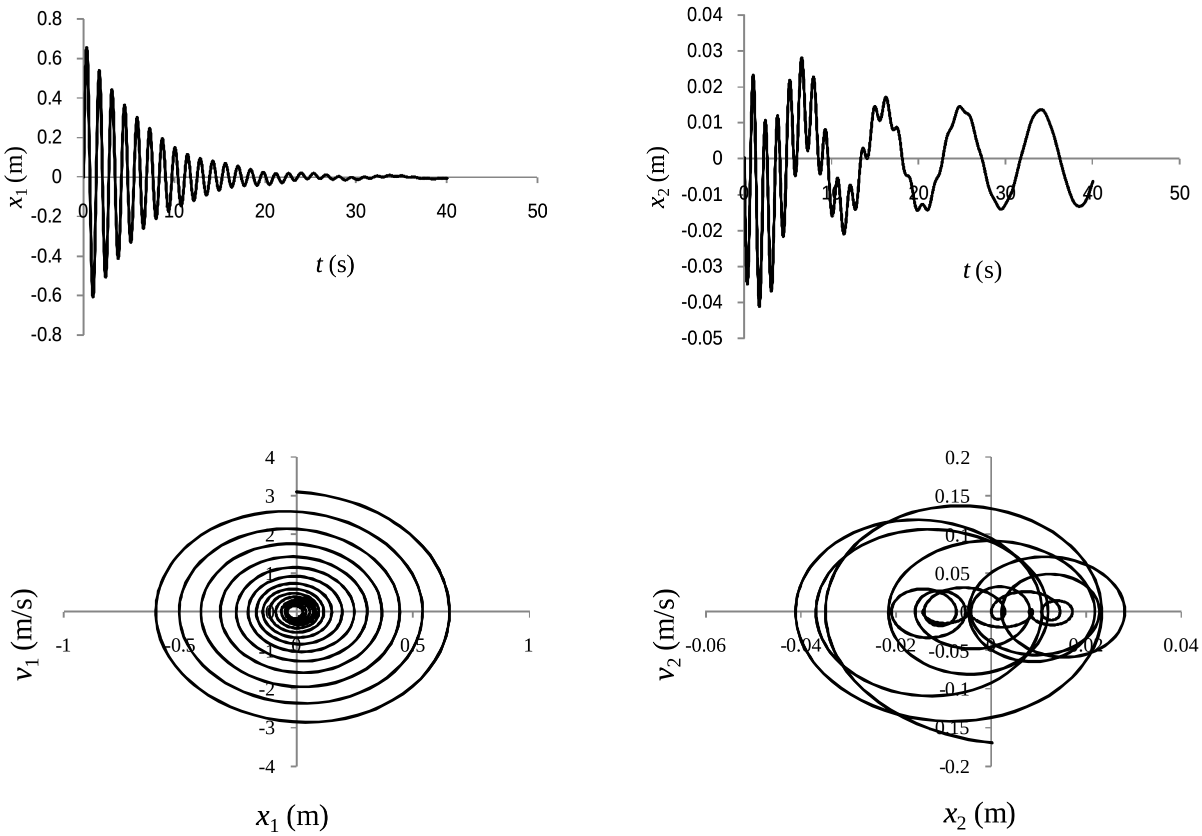

Fig. B(6) x vs. t curves and phase planes of m_1 and m_2 for *f(dv)* of Table 2 using data set 2 of Table 10 for combination of linear springs and non-linear dampers [m_1=100 kg, m_2 =1000 kg, k_1=1000 N/m, k_2 =1000 N/m, c_1= 0.03 Ns/m, c'_1 = -0.003 Ns/m^3, c_2 = 30.0 Ns/m, c'_2 = -0.003 Ns/m^3, α_1 = 0.15 N/m, α_2 = 0.20 N/m, β_1 = 0.15 Ns/m, β_2 = 0.25 Ns/m]

Response of 2DOFS for the combination of non-linear springs and linear dampers [*Figures B(7) - B(12)]*

Figures B(7) to B(9) for cases *(a)* to *(c)* and data set 1 from Table 10, show the responses of the system. In addition, for data set 2, the response of the system is illustrated in figures B910) to B(12).

In figure B97), m_1 vibrates with the amplitude of 0.6 m and then finally decreases to 0.01 m. For first 10 seconds, m_1 vibrates with higher frequency and then its frequency decreases with time. Finally, the vibration of m_1 reaches to stability after certain period. m_2 in figure B(7) also vibrates in a similar fashion. But the amplitude of vibration of m_2 is relatively higher than m_1. Amplitude of vibration of m_2 varies from 0.6 m to 0.01 m. From the figure B(7), it is clear that m_2 reaches to stability after 100 seconds.

For *f(v)*, the responses of both m_1 and m_2 shown in figures B(8) and B(9) are quite different from other cases. For first 10 seconds, both m_1 and m_2 vibrates with higher frequencies. Amplitude of vibration of both m_1 and m_2 starts from 2.5 m and then gradually decreases. After 10 seconds, frequencies of m_1 and m_2 decrease drastically. m_1 approaches to stability more rapidly. But m_2 continues its vibration with steady condition. So for this case, m_2 is unstable.

For *f(dv)* and data set 1, the response of both m_1 and m_2 in figure B(9) is different from the response for *f(v)* due to velocity and displacement dependent self-excited vibration. From figure B99), the effect of such self-excited vibration is clear to understand. Both m_1 and m_2 start vibration with amplitude of about 0.01 m. after maintaining steady vibration for the considered period, the system gradually approaches to stability. After 100 seconds, shooting is observed. This indicates the .limitation of numerical calculation after that period.

Again figures B(10) to B(12) for data set 2 from Table 10 and case *(d)* indicate the responses of both m_1 and m_2 . The responses of m_1 for all three cases [*(a)* to *(c)*] are mostly similar. For first 15 seconds, m_1 vibrates with higher frequency and amplitude range of 0.07 m to 0.017 m. Then m_1 maintains steady vibration with the reduction of amplitude and frequency. This phenomenon is seen in figures B(10) to B(12).

Figures of damped self-excited vibration of 2DOFS (BVP)

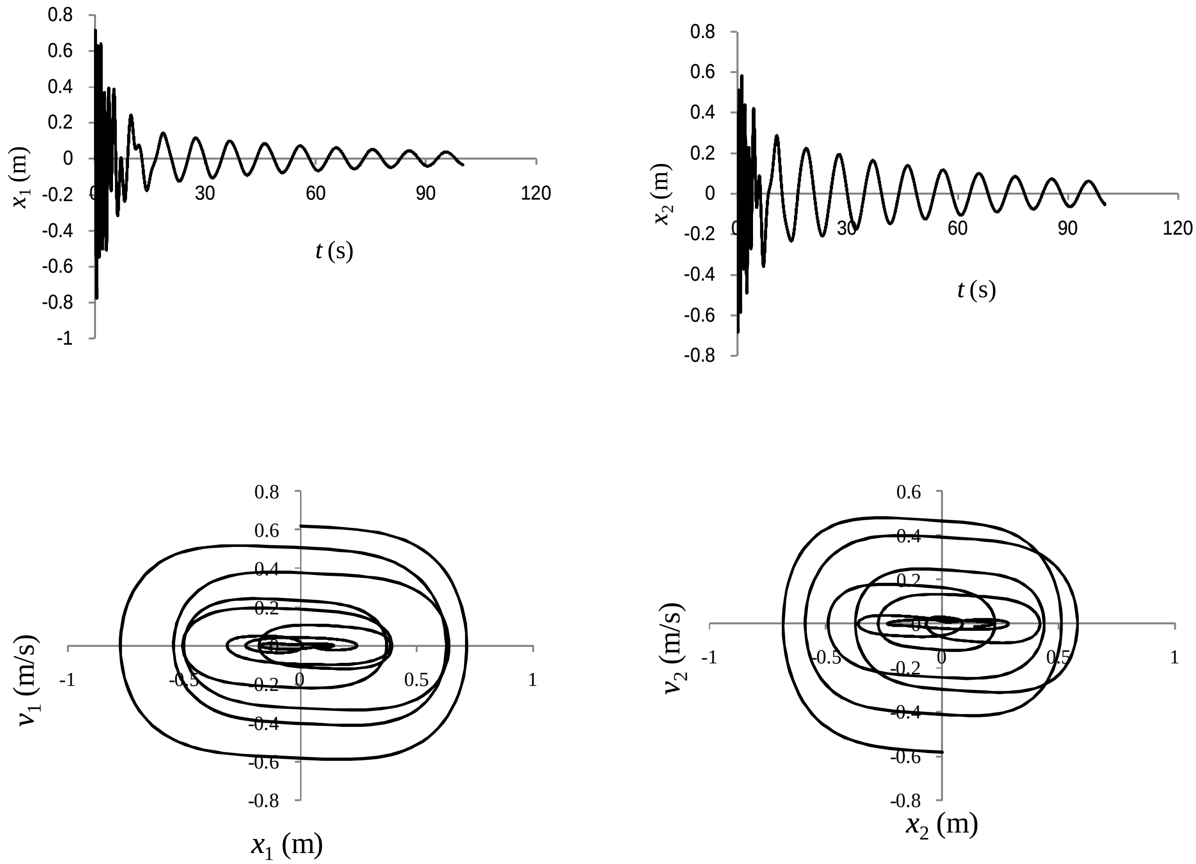

Fig. B(7) x vs. t curves and phase planes for m_1 and m_2 for *f(d)* of Table 2 using data set 1 of Table 10 for combination of non-linear springs and linear dampers [m_1=100 kg, m_2 =100 kg, k_1=100 N/m, k'_1= 0.3 N/m^3, k_2 =100 N/m, k'_2 = 0.3 N/m^3, c_1= 0.03 Ns/m, c_2 = 30.0 Ns/m, α_1 = 0.20 N/m, α_2 = 0.25 N/m]

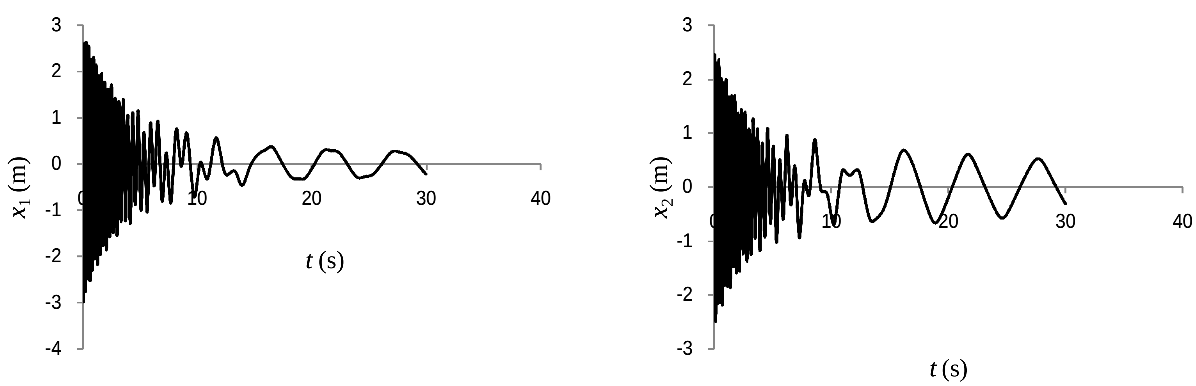

Fig. B(8) x vs. t curves of m_1 and m_2 for *f(v)* of Table 2 using data set 1 of Table 10 for combination of non-linear springs and linear dampers [m_1=100 kg, m_2 =100 kg, k_1=100 N/m, k'_1= 0.3 N/m^3, k_2 =100 N/m, k'_2 = 0.3 N/m^3, c_1= 0.03 Ns/m, c_2 = 30.0 Ns/m, β_1 = 0.10 Ns/m, β_2 = 0.20 Ns/m]

Figures of damped self-excited vibration of 2DOFS (BVP)

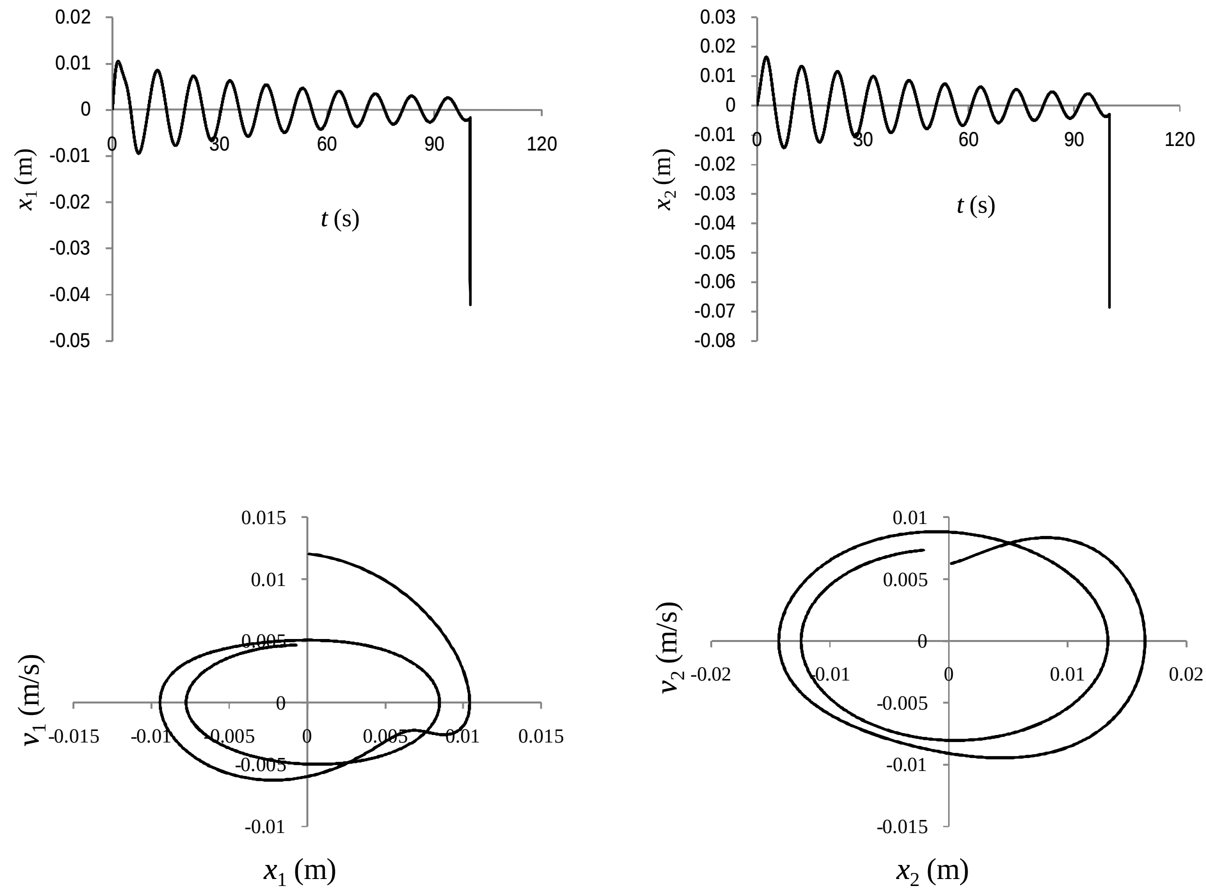

Fig. B(9) x vs. t curves and phase planes of m_1 and m_2 for *f(dv)* of Table 2 using data set 1 of Table 10 for combination of non-linear springs and linear dampers [m_1=100 kg, m_2 =100 kg, k_1=100 N/m, k'_1= 0.3 N/m^3, k_2 =100 N/m, k'_2 = 0.3 N/m^3, c_1= 0.03 Ns/m, c_2 = 30.0 Ns/m, α_1 = 0.20 N/m, α_2 = 0.25 N/m, β_1 = 0.10 Ns/m, β_2 = 0.20 Ns/m]

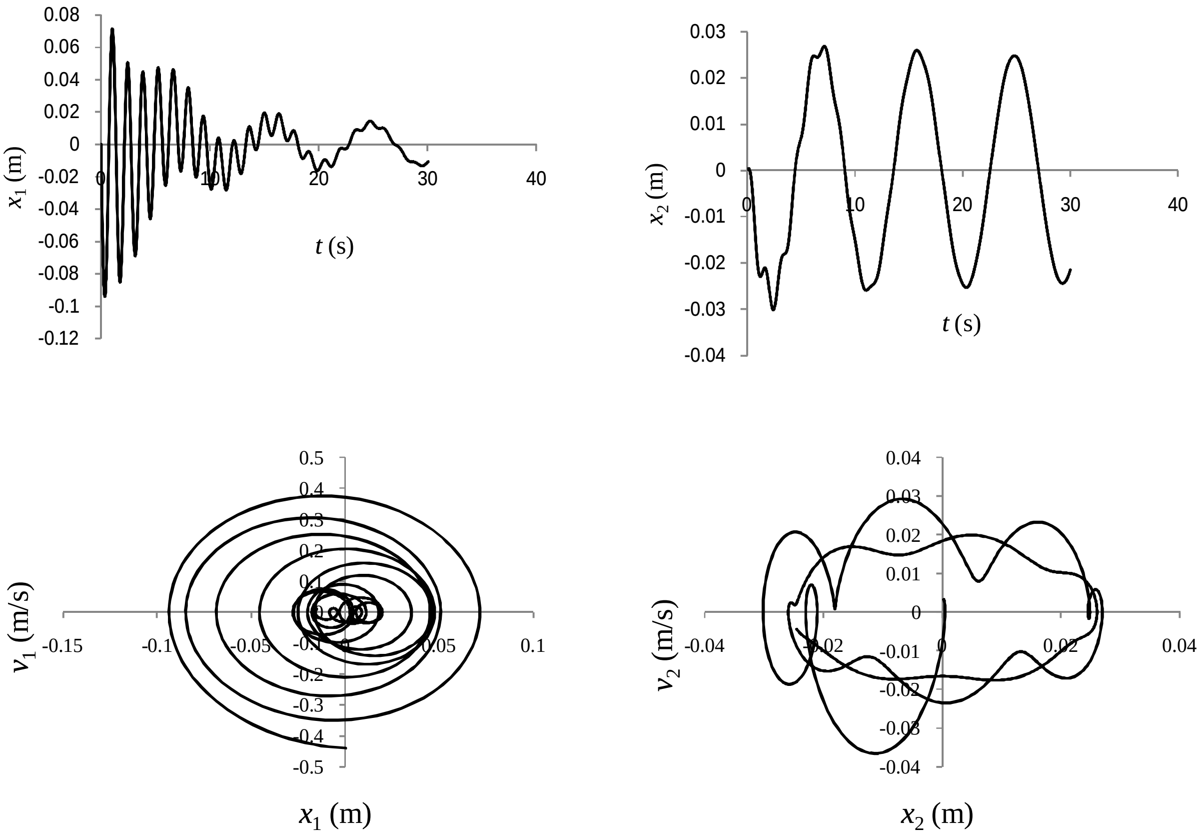

Fig. B(10) x vs. t curves and phase planes of m_1 and m_2 for $f(d)$ of Table 2 using data set 2 of Table 10 for combination of non-linear springs and linear dampers [m_1=100 kg, m_2 =1000 kg, k_1=1000 N/m, k'_1= -0.3 N/m^3, k_2 =1000 N/m, k'_2 = -0.3 N/m^3, c_1= 0.03 Ns/m, c_2 = 30.0 Ns/m, α_1 = 0.15 N/m, α_2 = 0.20 N/m]

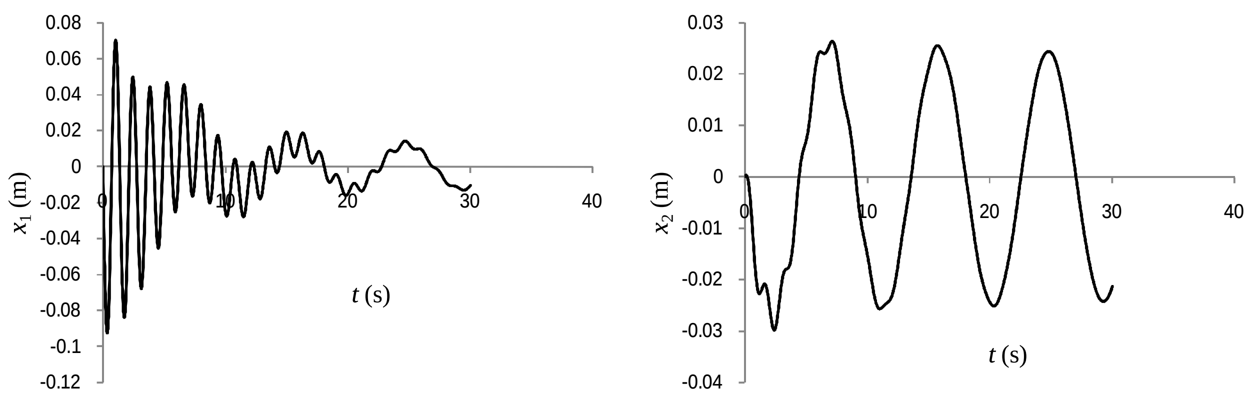

Fig. B(11) x vs. t curves of m_1 and m_2 for $f(v)$ of Table 2 using data set 2 of Table 10 for combination of non-linear springs and linear dampers[m_1=100 kg, m_2 =1000 kg, k_1=1000 N/m, k'_1= -0.3 N/m^3, k_2 =1000 N/m, k'_2 = -0.3 N/m^3, c_1= 0.03 Ns/m, c_2 = 30.0 Ns/m, β_1 = 0.15 Ns/m, β_2 = 0.25 Ns/m]

Figures of damped self-excited vibration of 2DOFS (BVP)

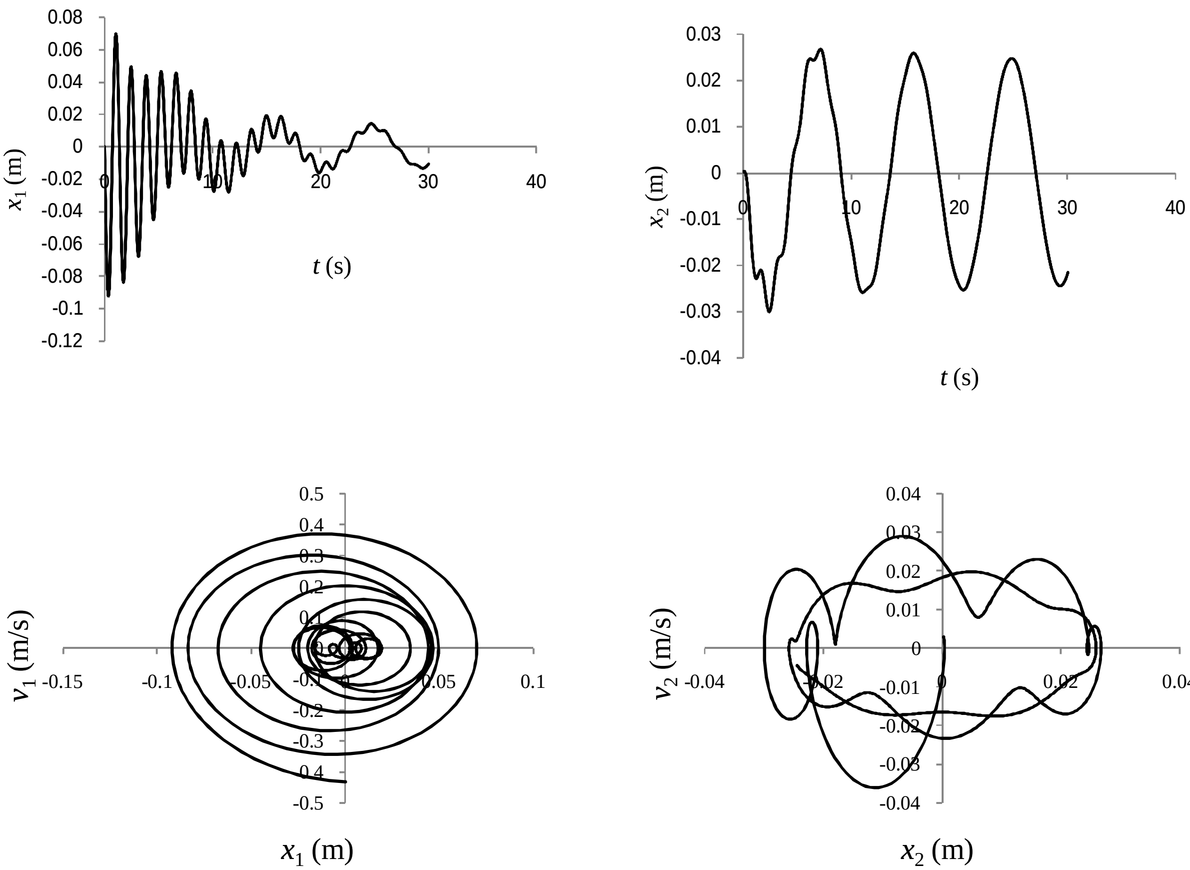

Fig. B(12) x vs. t curves and phase planes of m_1 and m_2 for $f(dv)$ of Table 2 using data set 2 of Table 10 for combination of non-linear springs and linear dampers [m_1=100 kg, m_2 =1000 kg, k_1=1000 N/m, k'_1= -0.3 N/m^3, k_2 =1000 N/m, k'_2 = -0.3 N/m^3, c_1= 0.03 Ns/m, c_2 = 30.0 Ns/m, α_1 = 0.15 N/m, α_2 = 0.20 N/m, β_1 = 0.15 Ns/m, β_2 = 0.25 Ns/m]

APPENDIX C

(Figures of damped self-excited vibration of 3DOFS)

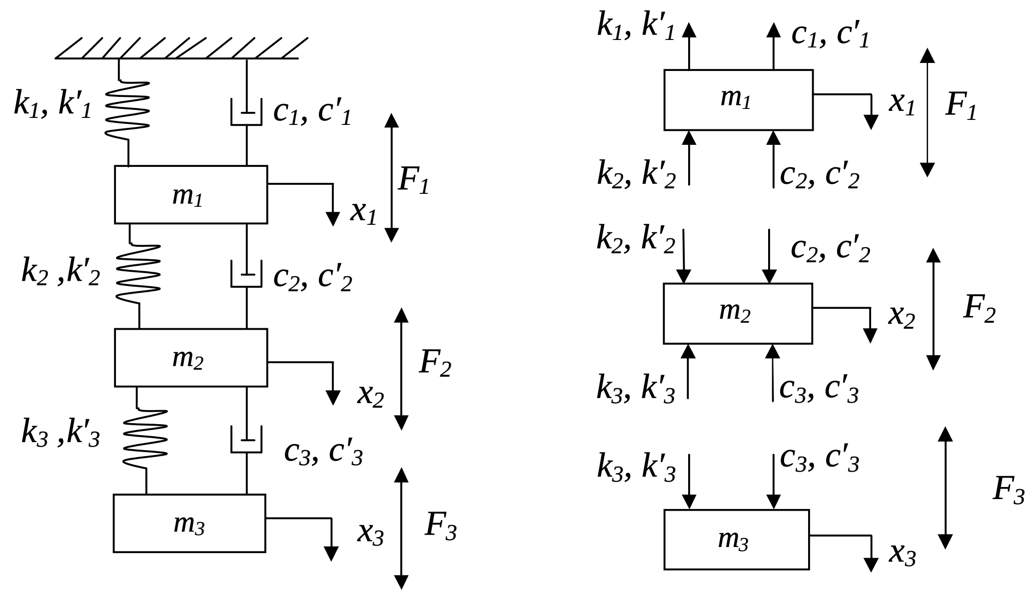

Figure: Arrangement of masses, springs and dampers for self-excited vibration of 3DOF S.

The equations of motion are as follows for m_1, m_2 and m_3, respectively,

$$m_1\ddot{x}_1 + \left(k_1x_1 + k_1'x_1^3\right) + \left(c_1\dot{x}_1 + c_1'\dot{x}_1x_1^2\right) + \left\{k_2(x_1 - x_2) + k_2'(x_1 - x_2)^3\right\} + \left\{c_2(\dot{x}_1 - \dot{x}_2) + c_2'(\dot{x}_1 - \dot{x}_2)(x_1 - x_2)^2\right\} = F_1$$

$$m_2\ddot{x}_2 - \left\{k_2(x_1 - x_2) + k_2'(x_1 - x_2)^3\right\} - \left\{c_2(\dot{x}_1 - \dot{x}_2) + c_2'(\dot{x}_1 - \dot{x}_2)(x_1 - x_2)^2\right\} + \left\{k_3(x_2 - x_3) + k_3'(x_2 - x_3)^3\right\} + \left\{c_3(\dot{x}_2 - \dot{x}_3) + c_3'(\dot{x}_2 - \dot{x}_3)(x_2 - x_3)^2\right\} = F_2$$

$$m_3\ddot{x}_3 + \left\{k_3(x_2 - x_3) + k_3'(x_2 - x_3)^3\right\} + \left\{c_3(\dot{x}_2 - \dot{x}_3) + c_3'(\dot{x}_2 - \dot{x}_3)(x_2 - x_3)^2\right\} = F_3$$

Here self-excited forces F_1 , F_2 and F_3 are the generalized self-excited forces of the considered system.

$$F_1 = \alpha_1 x_1 + \beta_1\dot{x}_1 + \gamma_1 x_1^2\dot{x}_1$$

$$F_2 = \alpha_2 x_2 + \beta_2\dot{x}_2 + \gamma_2 x_2^2\dot{x}_2$$

$$F_3 = \alpha_3 x_3 + \beta_3\dot{x}_3 + \gamma_3 x_3^2\dot{x}_3$$

Damped self-excited vibration for 3DOFS

For observing the responses of the system, two cases (*a* - *b*) are discussed here depending on the self-excited force function.

Figures C(1) for *f(d)*, shows the amplitudes of vibration of m_1, m_2 and m_3 . Trajectory for m_1 is also shown in this figure.

Maximum amplitude of m_1 from the figure C(1) can be seen as 0.07 m. From the trend of the curve, it can be concluded that the amplitude is gradually decreasing and finally attain stability. For m_2 and m_3 in figure C(1) , amplitude of vibration is much higher than that of m_1. However, for both m_2 and m_3, amplitude is decreasing and approaching to stability. Therefore, for damped condition, the system gains stability after a certain period. From the trajectory of m_1, it is clear that velocity of m_1 along with amplitude decreasing gradually and finally reaches stability.

Similar responses are found for other combination of linear springs and non-linear dampers for *f(v)*. These responses are shown in figure C(5).

When self-excited force is function of only velocity (case *b*), the response of the system is shown in figure C(2) and trajectory for m_1 is also shown in this figure. From these curves, it is clear that velocity plays an important role in self-excited force. Due to damped condition, the amplitudes of all three masses are very low. Therefore, the system will attain stability very quickly if required damping is provided. For other combination of linear springs and non-linear dampers for *f(v)*, the response of the system in figure C(6) is congruent to the response for the combination of linear springs and linear dampers for *f(v)* .

However, when both displacement and velocity are taken into consideration for self-excited force (case *c*), the effect of displacement becomes dominant. This is clear from the response curves of three masses in figure C(3) and trajectory for m_2 . It is also true for other combination of linear springs and non-linear dampers as shown in figure C(7).

In addition, the effect of nonlinear displacement term on self-excited force is not so great. This is shown in figures C(4) and C(8). The amplitudes of vibration for all three masses are nearly similar to the amplitudes for cases *(a)* & *(c)* of combination of linear springs and linear dampers.

Figures of damped self-excited vibration of 3DOFS

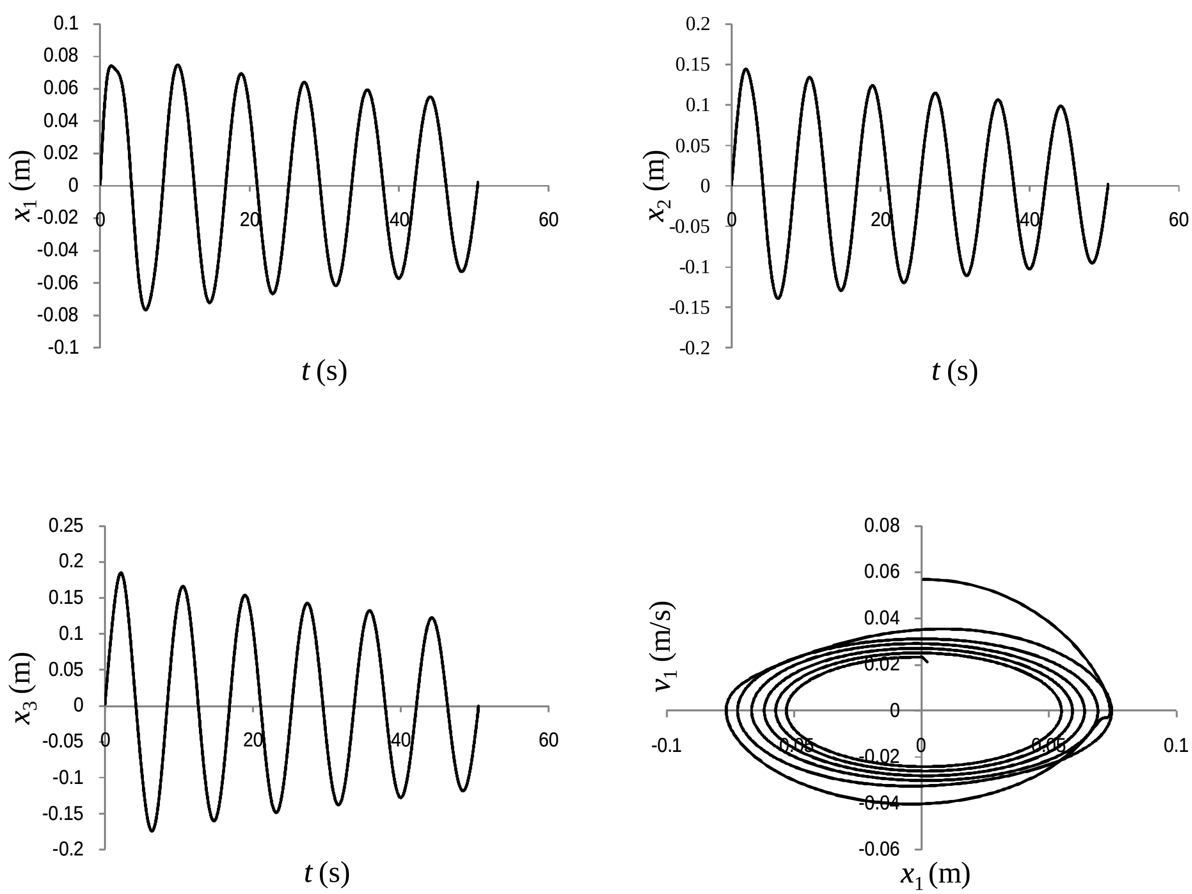

Fig. C(1) *x* vs. *t* curves of m_1 , m_2 and m_3 and trajecotory for m_1 for *f(d)* of Table 2 using data of Table 12 for combination of linear springs and linear dampers [m_1 =100 kg, m_2 =100 kg, m_3 =100 kg, k_1 =100 N/m, k_2 =100 N/m, k_3 =100 N/m, c_1 =0.03 Ns/m, c_2 =10.0 Ns/m, c_3 =30.0 *Ns/m* , α_1 =0.20 *N/m* , α_2 =0.25 *N/m* , α_3 =0.23 *N/m*]

Figures of damped self-excited vibration of 3DOFS

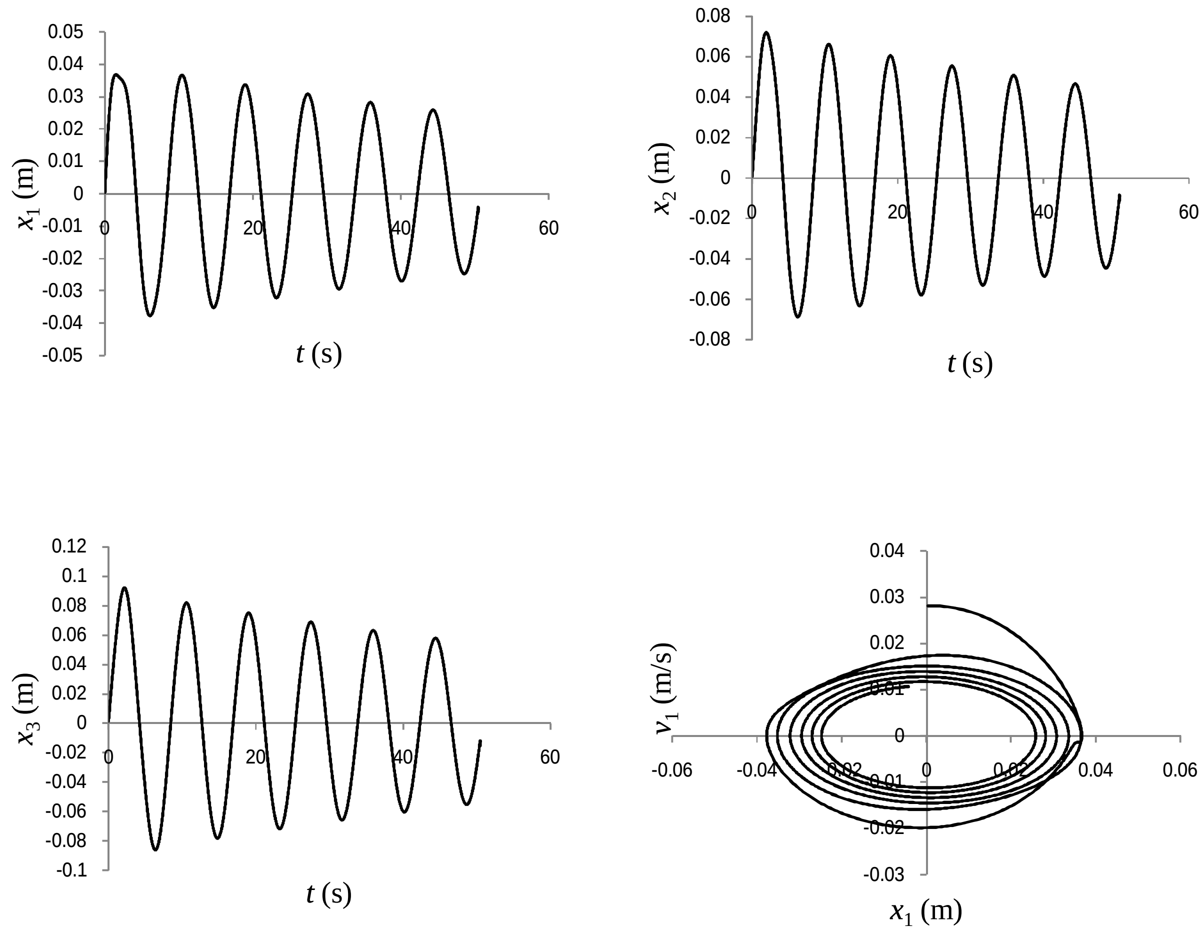

Fig. C(2) x vs. t curves of m_1, m_2 and m_3 and trajecotory for m_1 for $f(v)$ of Table 2 using data of Table 12 for combination of linear springs and linear dampers [m_1 =100 kg, m_2 =100 kg, m_3 =100 kg, k_1 =100 N/m, k_2 =100 N/m, k_3 =100 N/m, c_1 =0.03 Ns/m, c_2 =10.0 Ns/m, c_3 =30.0 *Ns/m* , β_1 =0.10 *Ns/m* , β_2 =0.20 *Ns/m* , β_3 =0.15 *Ns/m*]

Figures of damped self-excited vibration of 3DOFS

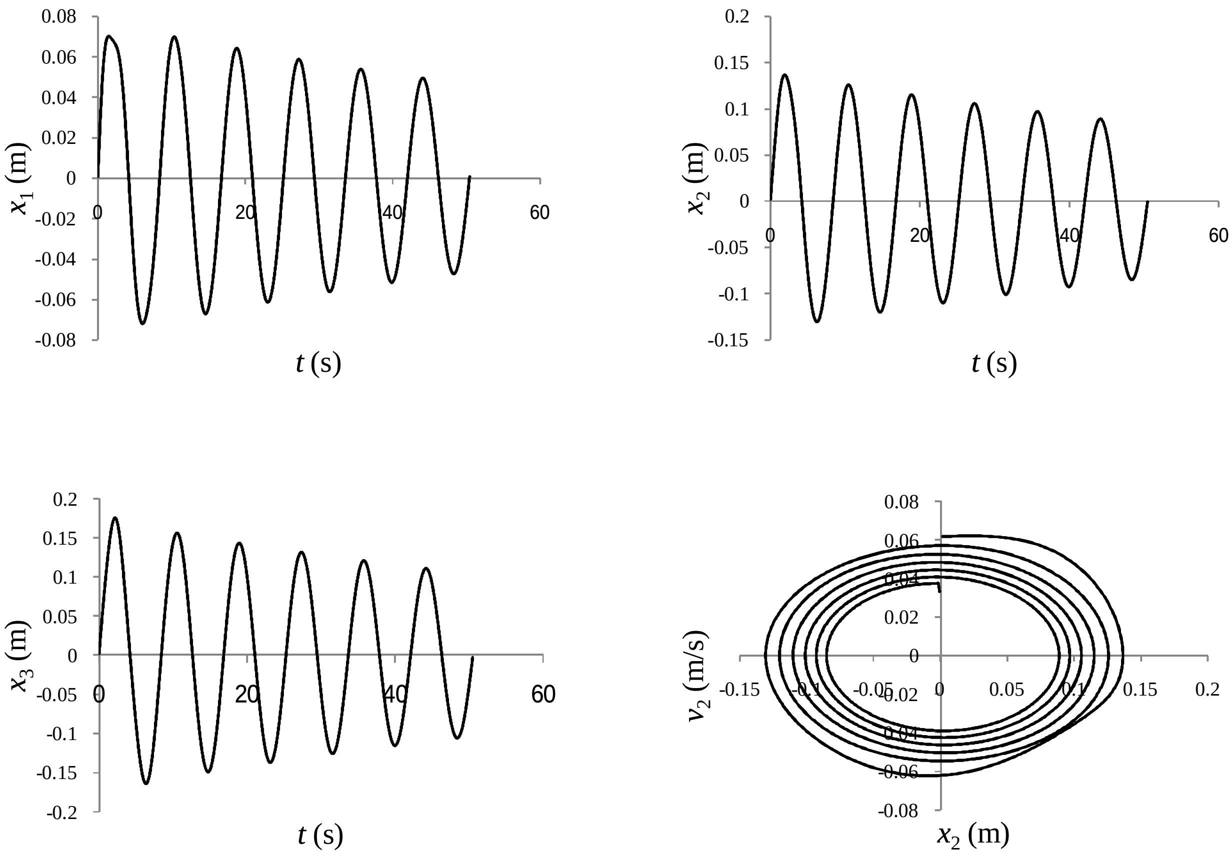

Fig. C(3) x vs. t curves of m_1 , m_2 and m_3 and trajecotory for m_1 for *f(dv)* of Table 2 using data of Table 12 for combination of linear springs and linear dampers [m_1 =100 kg, m_2 =100 kg, m_3 =100 kg, k_1 =100 N/m, k_2 =100 N/m, k_3 =100 N/m, c_1 =0.03 Ns/m, c_2 =10.0 Ns/m, c_3 =30.0 *Ns/m* , α_1 =0.20 *N/m* , α_2 =0.25 *N/m* , α_3 =0.23 *N/m* , β_1 =0.10 *Ns/m* , β_2 =0.20 *Ns/m* , β_3 =0.15 *Ns/m*]

Figures of damped self-excited vibration of 3DOFS

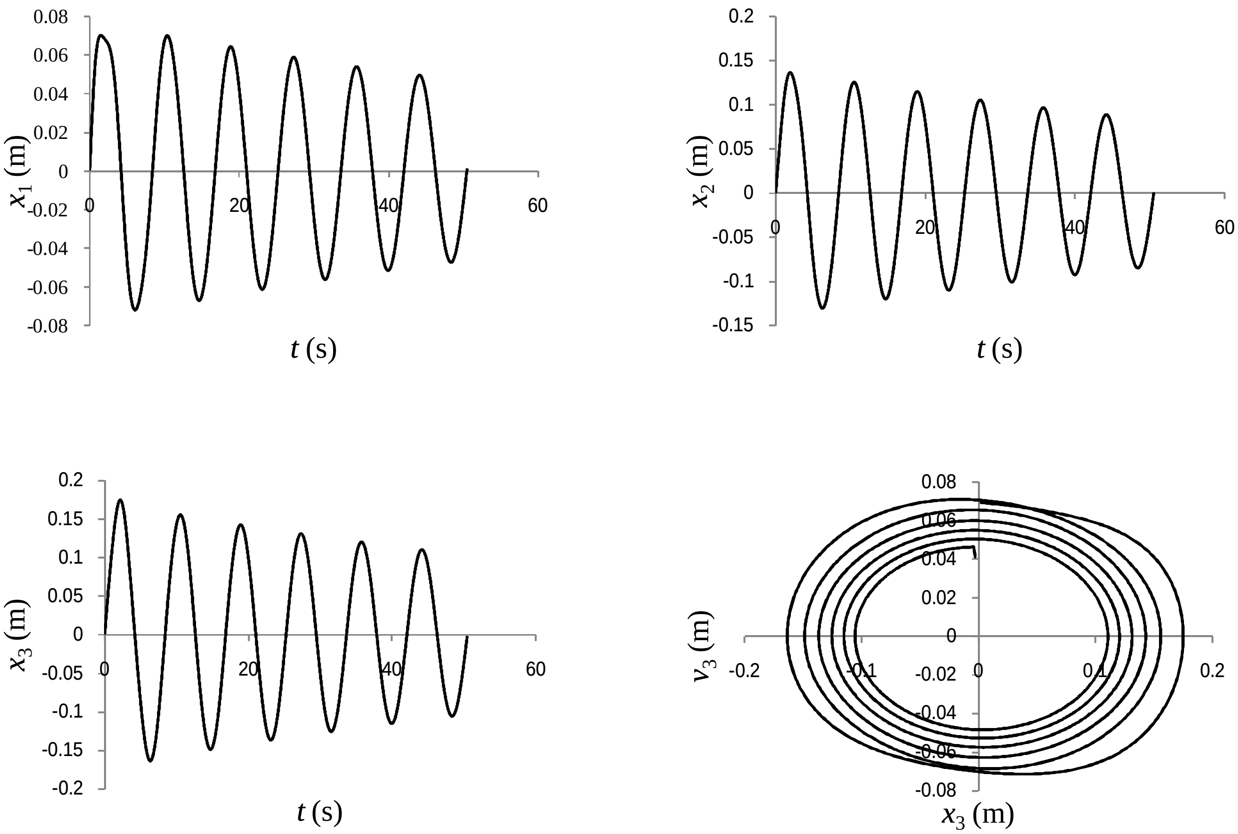

Fig. C(4) x vs. t curves of m_1 , m_2 and m_3 and trajecotory for m_3 for *f(n)* of Table 2 using data of Table 12 for combination of linear springs and linear dampers [m_1 =100 kg, m_2 =100 kg, m_3 =100 kg, k_1 =100 N/m, k_2 =100 N/m, k_3 =100 N/m, c_1 =0.03 Ns/m, c_2 =10.0 Ns/m, c_3 =30.0 *Ns/m* , α_1 =0.20 *N/m* , α_2 =0.25 *N/m* , α_3 =0.23 *N/m* , β_1 =0.10 *Ns/m* , β_2 =0.20 *Ns/m* , β_3 =0.15 *Ns/m* , γ_1 = 0.001Ns/m^3 , γ_2 =0.002 Ns/m^3 , γ_3 =0.025 Ns/m^3]

Figures of damped self-excited vibration of 3DOFS

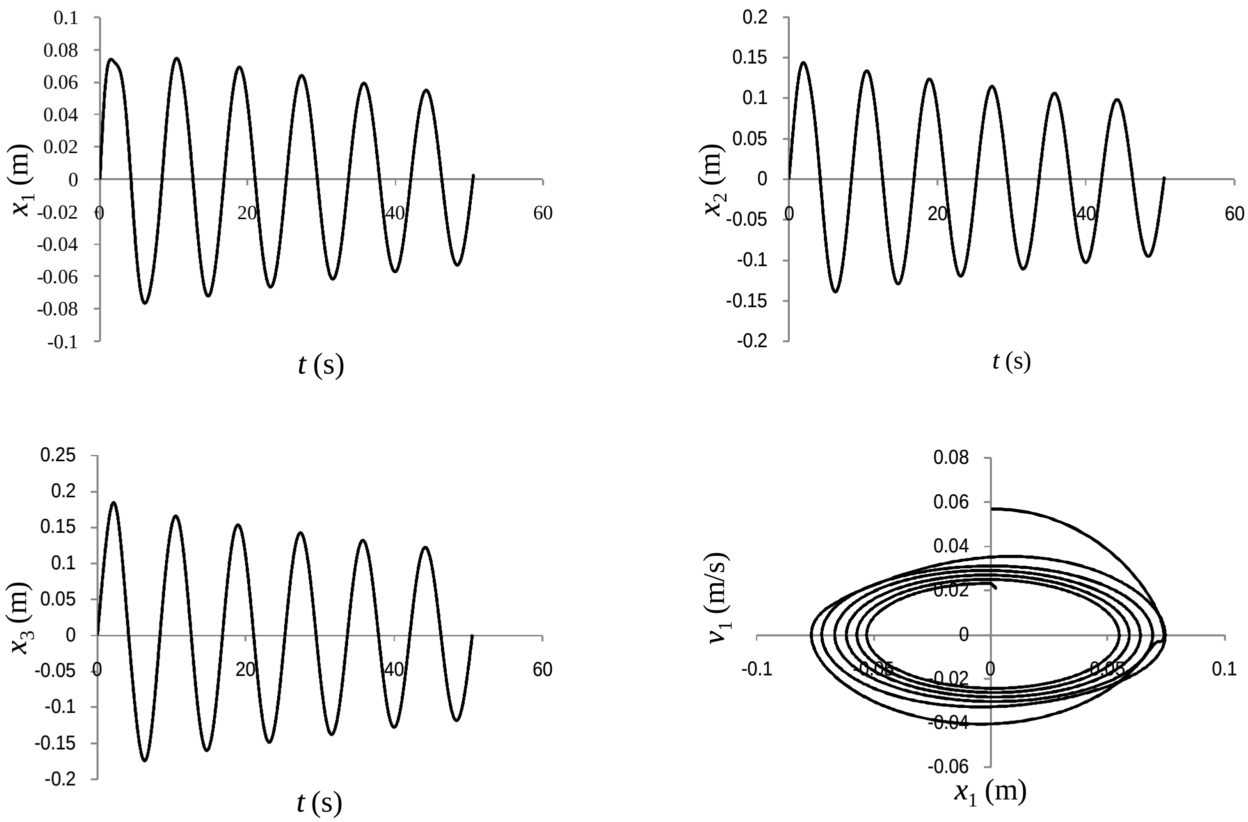

Fig. C(5) x vs. t curves of m_1 , m_2 and m_3 and trajecotory for m_1 for *f(d)* of Table 2 using data of Table 12 for combination of linear springs and non-linear dampers [m_1 =100 kg, m_2 =100 kg, m_3 =100 kg, k_1 =100 N/m, k_2 =100 N/m, k_3 =100 N/m, c_1 =0.03 Ns/m, c'_1 =0.003 Ns/m^3 , c_2 =10.0 Ns/m, c'_2 =0.003 *Ns/m*^{3} ,c_3 =30.0 *Ns/m* , c'_3 =0.003 *Ns/m*^{3} , α_1 =0.20 *N/m* , α_2 =0.25 *N/m* , α_3 =0.23 *N/m*]

Figures of damped self-excited vibration of 3DOFS

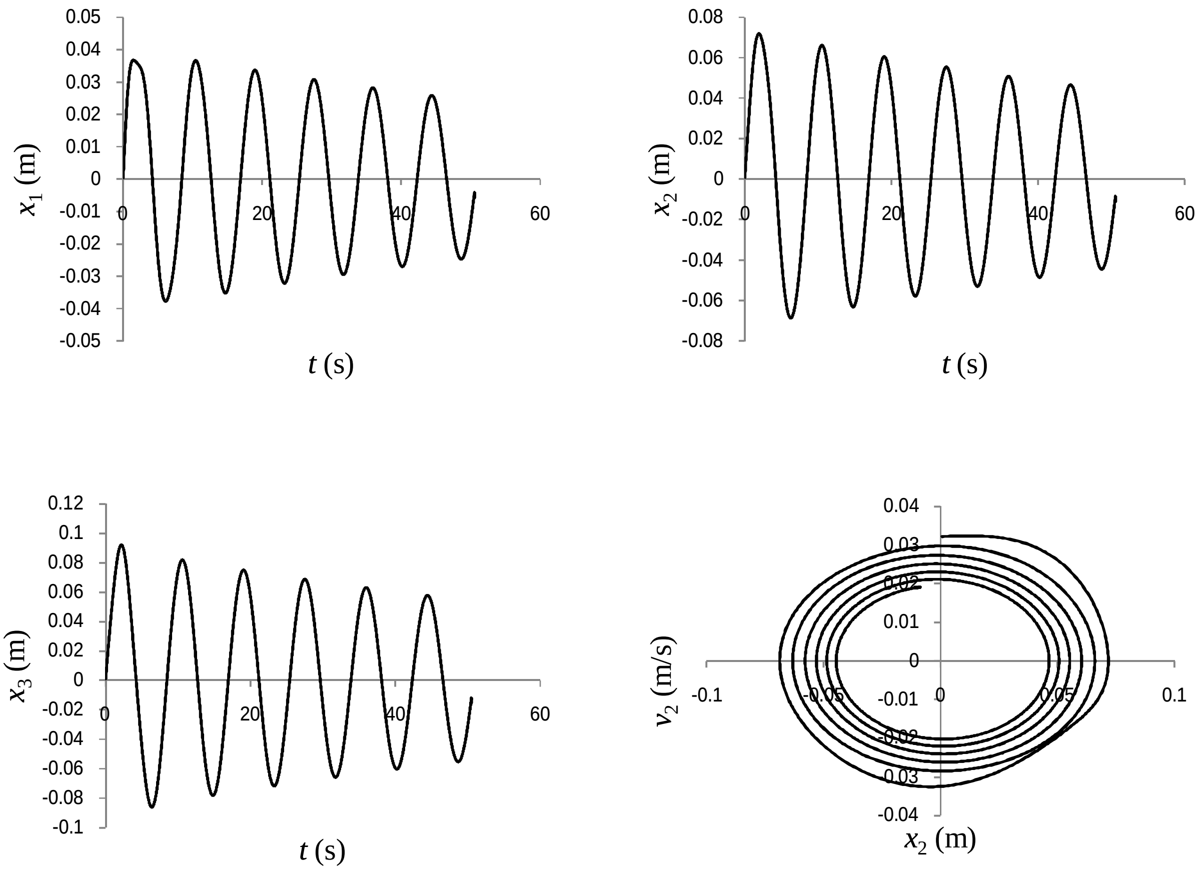

Fig. C(6) x vs. t curves of m_1 , m_2 and m_3 and trajecotory for m_1 for $f(v)$ of Table 2 using data of Table 12 for combination of linear springs and non-linear dampers [m_1 =100 kg, m_2 =100 kg, m_3 =100 kg, k_1 =100 N/m, k_2 =100 N/m, k_3 =100 N/m, c_1 =0.03 Ns/m, c'_1 =0.003 Ns/m^3 , c_2 =10.0 Ns/m, c'_2 =0.003 Ns/m^3 , c_3 =30.0 Ns/m , c'_3 =0.003 Ns/m^3 , β_1 =0.10 Ns/m , β_2 =0.20 Ns/m , β_3 =0.15 Ns/m]

Figures of damped self-excited vibration of 3DOFS

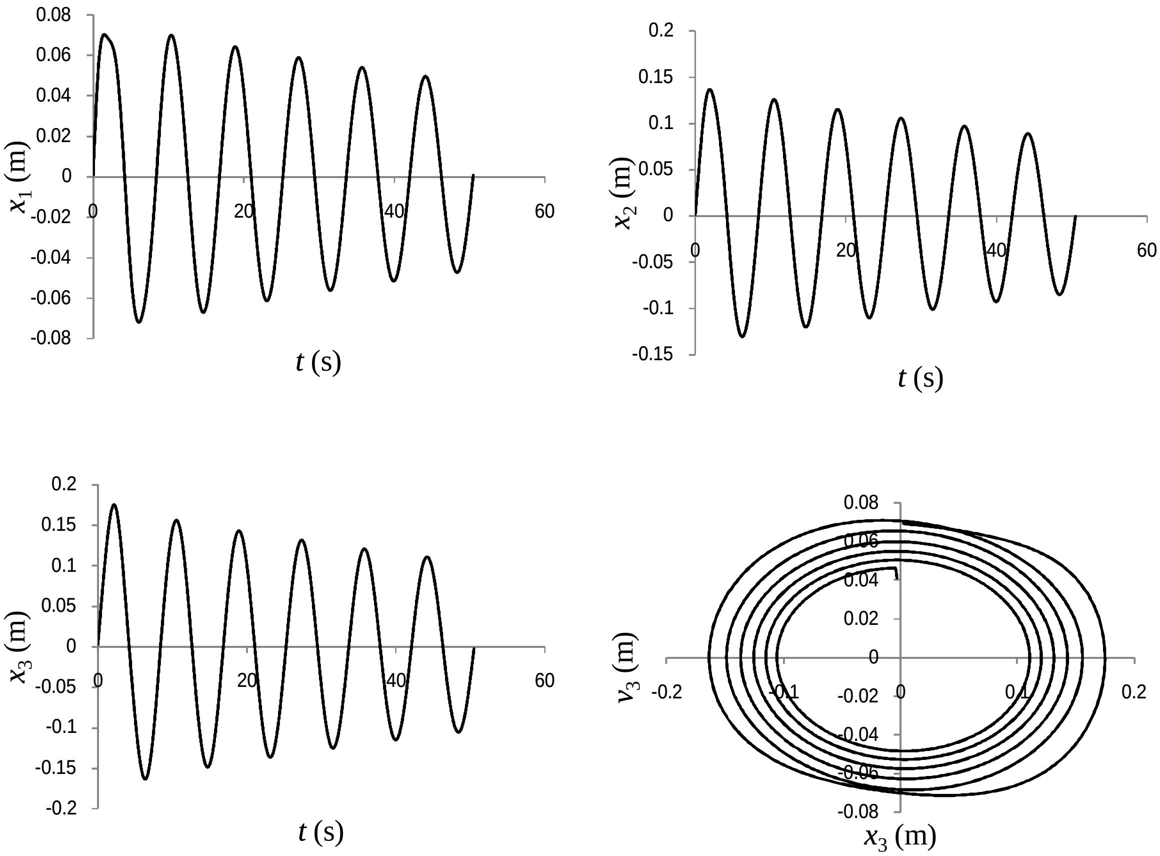

Fig. C(7) x vs. t curves of m_1, m_2 and m_3 and trajecotory for m_3 for *f(dv)* of Table 2 using data of Table 12 for combination of linear springs and non-linear dampers [m_1 =100 kg, m_2 =100 kg, m_3 =100 kg, k_1 =100 N/m, k_2 =100 N/m, k_3 =100 N/m, c_1 =0.03 Ns/m, c'_1 =0.003 Ns/m^3 , c_2 =10.0 Ns/m, c'_2 =0.003 *Ns/m*^{3} , c_3 =30.0 *Ns/m* , c'_3 =0.003 *Ns/m*^{3} , α_1 =0.20 *N/m* , α_2 =0.25 *N/m* , α_3 =0.23 *N/m* ,β_1 =0.10 *Ns/m* , β_2 =0.20 *Ns/m* , β_3 =0.15 *Ns/m*]

Figures of damped self-excited vibration of 3DOFS

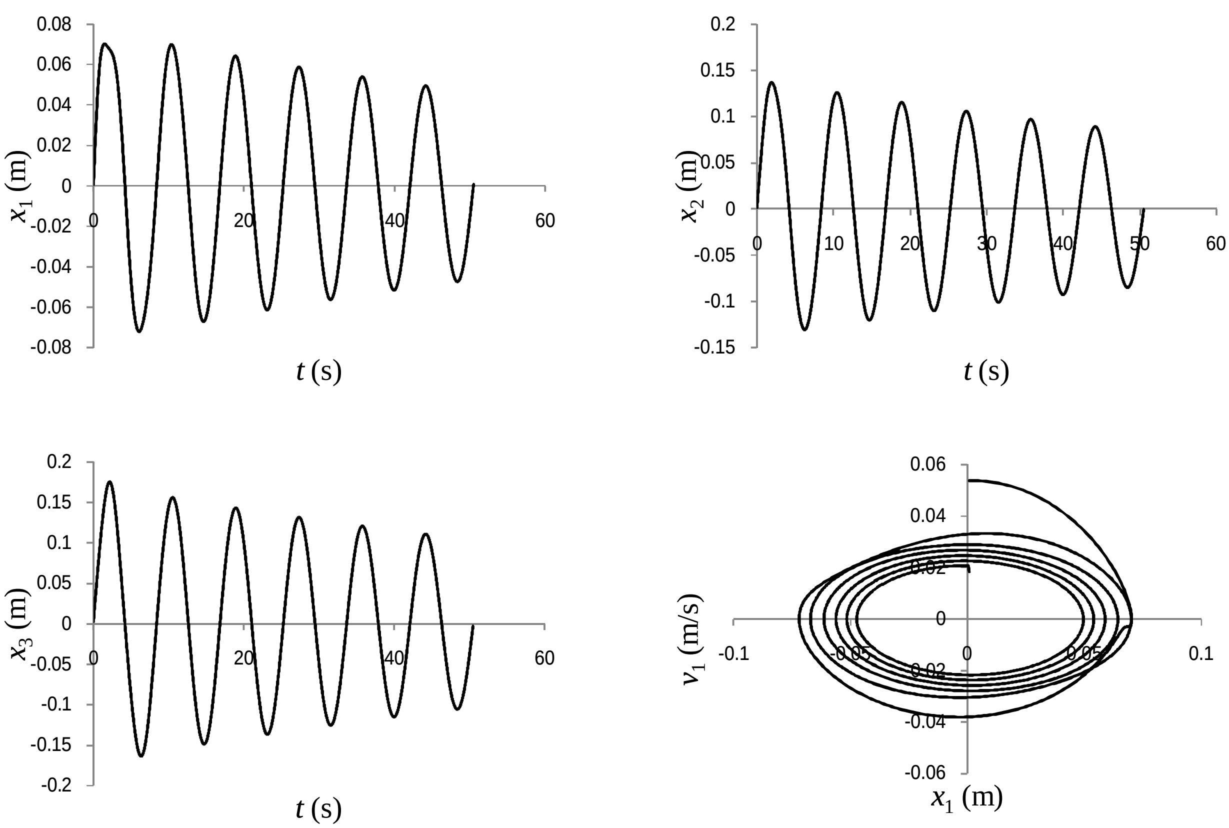

Fig. C(8) x vs. t curves of m_1 , m_2 and m_3 and trajecotory for m_1 for *f(n)* of Table 2 using data of Table 12 for combination of linear springs and non-linear dampers [m_1 =100 kg, m_2 =100 kg, m_3 =100 kg, k_1 =100 N/m, k_2 =100 N/m, k_3 =100 N/m, c_1 =0.03 Ns/m, c'_1 =0.003 Ns/m^3 , c_2 =10.0 Ns/m, c'_2 =0.003 *Ns/m*^{3} , c_3 =30.0 *Ns/m* , c'_3 =0.003 *Ns/m*^{3} , α_1 =0.20 *N/m* , α_2 =0.25 *N/m* , α_3 =0.23 *N/m* ,β_1 =0.10 *Ns/m* , β_2 =0.20 *Ns/m* , β_3 =0.15 *Ns/m*, γ_1 = 0.001*Ns/m*^{3} , γ_2 =0.002 *Ns/m*^{3} , γ_3 =0.025 *Ns/m*^{3}]

APPENDIX D

(Program Code)

```
/*Code for Self-excited Vibration Analysis*/
# include <stdio.h>
# include <conio.h>
# include <math.h>
# include <stdlib.h>
# define n 4
# define mass_1 100.0
# define mass_2 100.0
# define spring_k_1 100.0
# define spring_k_1p 0.50
# define spring_k_2 100.0
# define spring_k_2p 0.50
# define damp_c_1 1.5
# define damp_c_1p 0.20
# define damp_c_2 1.5
# define damp_c_2p 0.20
# define tb 50.01
# define h 0.02
# define w 0.0
# define zero 0.0
# define alpha_1 0.1
# define alpha_2 0.1
# define beta_1 0.1
# define beta_2 0.1
double fnction_1(double t ,double y1,double y2, double y3, double y4, double w1)
{
double z=0.0;
```

```
z= (-(spring_k_1*y1+spring_k_1p*pow(y1,3))-(spring_k_2*(y1-y3)+spring_k_2p*pow((y1-y3),3)) - (damp_c_1*y2+damp_c_1p*y2*pow(y1,2)) - (damp_c_2*(y2-y4)+damp_c_2p*(y2-y4)*pow((y1-y3),2))+alpha_1*y1+beta_1*y2 )/mass_1 ;

return z;

}

double fnction_2(double t, double y1,double y2, double y3, double y4, double w1)

{

double z=0.0;

z= (spring_k_2*(y1-y3)+spring_k_2p*pow((y1-y3),3) + (damp_c_2*(y2-y4)+damp_c_2p*(y2-y4)*pow((y1-y3),2))+alpha_2*y3+beta_2*y4 )/mass_2 ;

return z;

}

float FUHC_1(float t,float Y0,float R1, float Y2, float Y3, float y1, float y2, float y3, float y4)

{

float z=0.0;

z= (-spring_k_1*Y0-spring_k_1p*3*pow(y1,2)*Y0-spring_k_2*(Y0-Y2)-3*spring_k_2p*pow((y1-y3),2)*(Y0-Y2)- damp_c_1*R1- damp_c_1p*R1*pow(y1,2)-2*damp_c_1p*y2*y1*Y0- damp_c_2*(R1-Y3)- damp_c_2p*pow((y1-y3),2)*(R1-Y3)-2*damp_c_2p*(y1-y3)*(y2-y4)*(Y0-Y2)+alpha_1*Y0+beta_1*R1 )/mass_1;

return z;

}

float FUHC_2(float t,float Y0,float R1, float Y2, float Y3, float y1, float y2, float y3, float y4)

{

float z=0.0;

 z= (spring_k_2*(Y0-Y2)+spring_k_2p*3*pow((y1-y3),2)*(Y0-Y2)+ damp_c_2*(R1-Y3)+ damp_c_2p*pow((y1-y3),2)*(R1-Y3)+ 2*damp_c_2p*(y1-y3)*(y2-y4)*(Y0-Y2)+alpha_2*Y2+beta_2*Y3)/mass_2;

return z;

}
```

```
void main()

{

int i,j,n1,l,b,k,u,acc,freq;

double yt[n];

float R1[n][n] ={{1.0},

                        {0.0, 1.0},{0.0,0.0,1.0},{0.0,0.0,0.0,1.0}};

float n2,t,y1new=0.0,y1old=1.0, convgndamp_c_1,
y2new=0.0,y2old=1.0,convgndamp_c_2,y3new=0.0,y3old=1.0,convgnc3,y4new=0.0,y4old=1.0,c
onvgnc4;

double m1[n][n],E[n][n],F[n][n],G[n][n],H[n][n],Y[n][n];

double m2[n][n]={{0.0},{0.0},{0.0},{0.0}};

float m_1[n],m_2[n][n],m_3[n];

float l1[n],q[n][n],r[n],ya[n],yb[n], Yb[n][n];

float
a[n][n],a1[n][n],a2[n][n],a3[n][n],a4[n][n],m1[n][n],m2[n][n],m3[n][n],m4[n],ab1[n][n],ab2[n][n]
,ab3[n][n],inverse[n][n],test[n][n];

float p1,p2,p3,p4,sum,sum_s,freq1;

float yta[n], ytb[n];

float ytini[n]={0.0,0.0,0.0,0.0};

float sum4,sum3,sum2,sum1;

FIFE *fp;

float I[n][n]= {{1.0,0.0,0.0,0.0},

                       {0.0,1.0,0.0,0.0},

                       {0.0,0.0,1.0,0.0},

                       {0.0,0.0,0.0,1.0}} ;

float A[n][n]={{1.0,0.0,0.0,0.0},

                  {0.0,0.0,0.0,0.0},

                  {0.0,0.0,1.0,0.0},
```

```
                {0.0,0.0,0.0,0.0}};


float B[n][n]={{0.0,0.0,0.0,0.0},
                {0.0,1.0,0.0,0.0},
                {0.0,0.0,0.0,0.0},
                {0.0,0.0,0.0,1.0}};
float C[n]={0.01,0.7,0.02,0.8};
float
Gass1,Gass2,Springm1,Springm2,Springm1p,Springm2p,Dampc1,Dampc2,Dampc1p,Dampc2p,
Alpha1,Alpha2,Beta1,Beta2;
Gass1=mass_1;
Gass2=mass_2;
Springm1=spring_k_1;
Springm2=spring_k_2;
Springm1p=spring_k_1p;
Springm2p=spring_k_2p;
Dampc1=damp_c_1;
Dampc2=damp_c_2;
Dampc1p=damp_c_1p;
Dampc2p=damp_c_2p;
Alpha1=alpha_1;
Alpha2=alpha_2;
Beta1=beta_1;
Beta2=beta_2;


t= zero;
n2=((tb-t)/h);
n1=n2;
```

```
 fp=fopen("d:\\output\\flutt.xls","w");

 clrscr();

  for (b=0;b<n;b++)

  {yt[b]=ytini[b];}

convgndamp_c_1=fabs(y1new-y1old);

convgndamp_c_2=fabs(y2new-y2old);

convgnc3=fabs(y3new-y3old);

convgnc4=fabs(y4new-y4old);

  while (0.0001<convgndamp_c_1 && 0.0001<convgndamp_c_2 && 0.0001<convgnc3 &&
0.0001<convgnc4)    /*Starting of checking convergence*/

 {

    yt[0]=0.05;  /*???????*/

    yt[2]=0.07;     /*????????*/

    for (b=0;b<n;b++)

  {yta[b]=ytini[b];

   ytb[b]=ytini[b];

   r[b]=ytini[b];

   l1[b]=ytini[b];

  }

  for (k=0;k<n;k++)

 {  for (b=0;b<n;b++)

  {Yb[k][b]=m2[k][b];

   m2[k][b]=m2[k][b];

   q[k][b]=m2[k][b];

  }}

  for (b=0;b<n;b++)

  {yta[b]=yt[b];}
```

```
sum1=0.0;
sum2=0.0;
sum3=0.0;
sum4=0.0;
sum=0.0;
sum_s=0.0;
p1=0.0;
p2=0.0;
p3=0.0;
p4=0.0;
t=0.0;
for (k=0;k<n;k++)
 {  for (b=0;b<n;b++)
  {m1[k][b]=m2[k][b];
   E[k][b]=m2[k][b];
   F[k][b]=m2[k][b];
   G[k][b]=m2[k][b];
   H[k][b]=m2[k][b];
   Y[k][b]=R1[k][b];
  }}

for (i=0;i<n1;i++)
 {
m1[0][0]=h * yt[1];
m1[0][1]=h * fnction_1(t, yt[0],yt[1], yt[2], yt[3], w);
m1[0][2]=h * yt[3];
m1[0][3]=h * fnction_2(t, yt[0],yt[1], yt[2], yt[3], w);
```

```
m1[1][0]=h * (yt[1]+m1[0][1]/2.0);

m1[1][1]=h * fnction_1(t+h/2.0, yt[0]+m1[0][0]/2.0, yt[1]+m1[0][1]/2.0, yt[2]+m1[0][2]/2.0,
yt[3]+m1[0][3]/2.0, w) ;

m1[1][2]=h * (yt[3]+m1[0][3]/2.0);

m1[1][3]=h * fnction_2(t+h/2.0, yt[0]+m1[0][0]/2.0, yt[1]+m1[0][1]/2.0, yt[2]+m1[0][2]/2.0,
yt[3]+m1[0][3]/2.0, w) ;

m1[2][0]=h * (yt[1]+m1[1][1]/2.0);

m1[2][1]=h * fnction_1(t+h/2.0, yt[0]+m1[1][0]/2.0, yt[1]+m1[1][1]/2.0, yt[2]+m1[1][2]/2.0,
yt[3]+m1[1][3]/2.0, w) ;

m1[2][2]=h * (yt[3]+m1[1][3]/2.0);

m1[2][3]=h * fnction_2(t+h/2.0, yt[0]+m1[1][0]/2.0, yt[1]+m1[1][1]/2.0, yt[2]+m1[1][2]/2.0,
yt[3]+m1[1][3]/2.0, w) ;


m1[3][0]=h * (yt[1]+m1[2][1]);

m1[3][1]=h * fnction_1(t+h, yt[0]+m1[2][0], yt[1]+m1[2][1], yt[2]+m1[2][2], yt[3]+m1[2][3], w)
;

m1[3][2]=h * (yt[3]+m1[2][3]);

m1[3][3]=h * fnction_2(t+h, yt[0]+m1[2][0], yt[1]+m1[2][1], yt[2]+m1[2][2], yt[3]+m1[2][3], w)
;

E[0][0]=h * Y[1][0] ;

E[0][1]=h * FUHC_1(t, Y[0][0], Y[1][0], Y[2][0], Y[3][0], yt[0], yt[1], yt[2], yt[3] ) ;

E[0][2]=h * Y[3][0] ;

E[0][3]=h * FUHC_2(t, Y[0][0], Y[1][0], Y[2][0], Y[3][0], yt[0], yt[1], yt[2], yt[3] ) ;

E[1][0]=h * (Y[1][0]+E[0][1]/2.0) ;

E[1][1]=h * FUHC_1(t+h/2.0, Y[0][0]+E[0][0]/2.0, Y[1][0]+E[0][1]/2.0, Y[2][0]+E[0][2]/2.0,
Y[3][0]+E[0][3]/2.0, yt[0], yt[1], yt[2], yt[3] ) ;

E[1][2]=h * (Y[3][0]+E[0][3]/2.0) ;

E[1][3]=h * FUHC_2(t+h/2.0, Y[0][0]+E[0][0]/2.0, Y[1][0]+E[0][1]/2.0, Y[2][0]+E[0][2]/2.0,
Y[3][0]+E[0][3]/2.0, yt[0], yt[1], yt[2], yt[3] ) ;

E[2][0]=h * (Y[1][0]+E[1][1]/2.0) ;
```

```
E[2][1]=h * FUHC_1(t+h/2.0, Y[0][0]+E[1][0]/2.0, Y[1][0]+E[1][1]/2.0, Y[2][0]+E[1][2]/2.0,
Y[3][0]+E[1][3]/2.0, yt[0], yt[1], yt[2], yt[3] ) ;

E[2][2]=h * (Y[3][0]+E[1][3]/2.0) ;

E[2][3]=h * FUHC_2(t+h/2.0, Y[0][0]+E[1][0]/2.0, Y[1][0]+E[1][1]/2.0, Y[2][0]+E[1][2]/2.0,
Y[3][0]+E[1][3]/2.0, yt[0], yt[1], yt[2], yt[3] ) ;


E[3][0]=h * (Y[1][0]+E[2][1]) ;

E[3][1]=h * FUHC_1(t+h, Y[0][0]+E[2][0], Y[1][0]+E[2][1], Y[2][0]+E[2][2], Y[3][0]+E[2][3],
yt[0], yt[1], yt[2], yt[3] ) ;

E[3][2]=h * (Y[3][0]+E[2][3]) ;

E[3][3]=h * FUHC_2(t+h, Y[0][0]+E[2][0], Y[1][0]+E[2][1], Y[2][0]+E[2][2], Y[3][0]+E[2][3],
yt[0], yt[1], yt[2], yt[3] ) ;


for(l=0;l<n;l++)

{Y[l][0]=Y[l][0]+ (E[0][l]+ 2.0*E[1][l]+ 2.0*E[2][l]+ E[3][l])/6.0 ;}

F[0][0]=h * Y[1][1];

F[0][1]=h * FUHC_1(t, Y[0][1],Y[1][1], Y[2][1], Y[3][1], yt[0], yt[1], yt[2], yt[3] ) ;

F[0][2]=h * Y[3][1];

F[0][3]=h * FUHC_2(t, Y[0][1],Y[1][1], Y[2][1], Y[3][1], yt[0], yt[1], yt[2], yt[3] ) ;


F[1][0]=h * (Y[1][1]+F[0][1]/2.0) ;

F[1][1]=h * FUHC_1(t+h/2.0, Y[0][1]+F[0][0]/2.0, Y[1][1]+F[0][1]/2.0, Y[2][1]+F[0][2]/2.0,
Y[3][1]+F[0][3]/2.0, yt[0], yt[1], yt[2], yt[3] ) ;

F[1][2]=h * (Y[3][1]+F[0][3]/2.0) ;

F[1][3]=h * FUHC_2(t+h/2.0, Y[0][1]+F[0][0]/2.0, Y[1][1]+F[0][1]/2.0, Y[2][1]+F[0][2]/2.0,
Y[3][1]+F[0][3]/2.0, yt[0], yt[1], yt[2], yt[3] ) ;


F[2][0]=h * (Y[1][1]+F[1][1]/2.0) ;

F[2][1]=h * FUHC_1(t+h/2.0, Y[0][1]+F[1][0]/2.0, Y[1][1]+F[1][1]/2.0, Y[2][1]+F[1][2]/2.0,
Y[3][1]+F[1][3]/2.0, yt[0], yt[1], yt[2], yt[3] ) ;
```

```
F[2][2]=h * (Y[3][1]+F[1][3]/2.0) ;

F[2][3]=h * FUHC_2(t+h/2.0, Y[0][1]+F[1][0]/2.0, Y[1][1]+F[1][1]/2.0, Y[2][1]+F[1][2]/2.0,
Y[3][1]+F[1][3]/2.0, yt[0], yt[1], yt[2], yt[3] ) ;


F[3][0]=h * (Y[1][1]+F[2][1] ) ;

F[3][1]=h * FUHC_1(t+h, Y[0][1]+F[2][0], Y[1][1]+F[2][1], Y[2][1]+F[2][2], Y[3][1]+F[2][3],
yt[0], yt[1], yt[2], yt[3] ) ;

F[3][2]=h * (Y[3][1]+F[2][3] ) ;

F[3][3]=h * FUHC_2(t+h, Y[0][1]+F[2][0], Y[1][1]+F[2][1], Y[2][1]+F[2][2], Y[3][1]+F[2][3],
yt[0], yt[1], yt[2], yt[3] ) ;


for(l=0;l<n;l++)

{Y[l][1]=Y[l][1]+ (F[0][l]+ 2.0*F[1][l]+ 2.0*F[2][l]+ F[3][l])/6.0 ;}





G[0][0]=h * Y[1][2] ;

G[0][1]=h * FUHC_1(t, Y[0][2],Y[1][2], Y[2][2], Y[3][2], yt[0], yt[1], yt[2], yt[3] ) ;

G[0][2]=h * Y[3][2] ;

G[0][3]=h * FUHC_2(t, Y[0][2],Y[1][2], Y[2][2], Y[3][2], yt[0], yt[1], yt[2], yt[3] ) ;

G[1][0]=h * (Y[1][2]+G[0][1]/2.0 ) ;

G[1][1]=h * FUHC_1(t+h/2.0, Y[0][2]+G[0][0]/2.0, Y[1][2]+G[0][1]/2.0, Y[2][2]+G[0][2]/2.0,
Y[3][2]+G[0][3]/2.0, yt[0], yt[1], yt[2], yt[3] ) ;

G[1][2]=h * (Y[3][2]+G[0][3]/2.0 ) ;

G[1][3]=h * FUHC_2(t+h/2.0, Y[0][2]+G[0][0]/2.0, Y[1][2]+G[0][1]/2.0, Y[2][2]+G[0][2]/2.0,
Y[3][2]+G[0][3]/2.0, yt[0], yt[1], yt[2], yt[3] ) ;

G[2][0]=h * (Y[1][2]+G[1][1]/2.0) ;
```

```
G[2][1]=h * FUHC_1(t+h/2.0, Y[0][2]+G[1][0]/2.0, Y[1][2]+G[1][1]/2.0, Y[2][2]+G[1][2]/2.0, Y[3][2]+G[1][3]/2.0, yt[0], yt[1], yt[2], yt[3] ) ;

G[2][2]=h * (Y[3][2]+G[1][3]/2.0) ;

G[2][3]=h * FUHC_2(t+h/2.0, Y[0][2]+G[1][0]/2.0, Y[1][2]+G[1][1]/2.0, Y[2][2]+G[1][2]/2.0, Y[3][2]+G[1][3]/2.0, yt[0], yt[1], yt[2], yt[3] ) ;


G[3][0]=h * (Y[1][2]+G[2][1] ) ;

G[3][1]=h * FUHC_1(t+h, Y[0][2]+G[2][0], Y[1][2]+G[2][1], Y[2][2]+G[2][2], Y[3][2]+G[2][3], yt[0], yt[1], yt[2], yt[3] ) ;

G[3][2]=h * (Y[3][2]+G[2][3] ) ;

G[3][3]=h * FUHC_2(t+h, Y[0][2]+G[2][0], Y[1][2]+G[2][1], Y[2][2]+G[2][2], Y[3][2]+G[2][3], yt[0], yt[1], yt[2], yt[3] ) ;

for(l=0;l<n;l++)

{Y[l][2]=Y[l][2]+ (G[0][l]+ 2.0*G[1][l]+ 2.0*G[2][l]+ G[3][l])/6.0 ;}

H[0][0]=h * Y[1][3];

H[0][1]=h * FUHC_1(t, Y[0][3], Y[1][3], Y[2][3], Y[3][3], yt[0], yt[1], yt[2], yt[3] ) ;

H[0][2]=h * Y[3][3];

H[0][3]=h * FUHC_2(t, Y[0][3], Y[1][3], Y[2][3], Y[3][3], yt[0], yt[1], yt[2], yt[3] ) ;

H[1][0]=h * (Y[1][3]+H[0][1]/2.0);

H[1][1]=h * FUHC_1(t+h/2.0, Y[0][3]+H[0][0]/2.0, Y[1][3]+H[0][1]/2.0, Y[2][3]+H[0][2]/2.0, Y[3][3]+H[0][3]/2.0, yt[0], yt[1], yt[2], yt[3] ) ;

H[1][2]=h * (Y[3][3]+H[0][3]/2.0);

H[1][3]=h * FUHC_2(t+h/2.0, Y[0][3]+H[0][0]/2.0, Y[1][3]+H[0][1]/2.0, Y[2][3]+H[0][2]/2.0, Y[3][3]+H[0][3]/2.0, yt[0], yt[1], yt[2], yt[3] ) ;

H[2][0]=h * (Y[1][3]+H[1][1]/2.0);

H[2][1]=h * FUHC_1(t+h/2.0, Y[0][3]+H[1][0]/2.0, Y[1][3]+H[1][1]/2.0, Y[2][3]+H[1][2]/2.0, Y[3][3]+H[1][3]/2.0, yt[0], yt[1], yt[2], yt[3] ) ;

H[2][2]=h * (Y[3][3]+H[1][3]/2.0);

H[2][3]=h * FUHC_2(t+h/2.0, Y[0][3]+H[1][0]/2.0, Y[1][3]+H[1][1]/2.0, Y[2][3]+H[1][2]/2.0, Y[3][3]+H[1][3]/2.0, yt[0], yt[1], yt[2], yt[3] ) ;
```

```
H[3][0]=h * (Y[1][3]+H[2][1] ) ;

H[3][1]=h * FUHC_1(t+h, Y[0][3]+H[2][0], Y[1][3]+H[2][1], Y[2][3]+H[2][2], Y[3][3]+H[2][3],
yt[0], yt[1], yt[2], yt[3] ) ;

H[3][2]=h * (Y[3][3]+H[2][3] ) ;

H[3][3]=h * FUHC_2(t+h, Y[0][3]+H[2][0], Y[1][3]+H[2][1], Y[2][3]+H[2][2], Y[3][3]+H[2][3],
yt[0], yt[1], yt[2], yt[3] ) ;


for(l=0;l<n;l++)

{Y[l][3]=Y[l][3]+ (H[0][l]+ 2.0*H[1][l]+ 2.0*H[2][l]+ H[3][l])/6.0 ;}


   t=t+h;


for (j=0;j<n;j++)

{ yt[j]= yt[j] + (m1[0][j]+ 2.0*m1[1][j]+ 2.0*m1[2][j]+ m1[3][j])/6.0 ; }

      }


  for (i=0;i<n;i++)

 {ytb[i]=yt[i];}

   for (i=0;i<n;i++)

  {for (j=0;j<n;j++)

  {Yb[i][j]=Y[i][j];}}

 for(i=0;i<n;i++)

{ for (j=0;j<n;j++)

  {sum=0.0;

  for (k=0;k<n;k++)

  {sum= sum + Yb[i][k]*yta[k];

  m_1[i]= sum ;

}}}
```

```
for(i=0;i<n;i++)
{ for (j=0;j<n;j++)
  {sum=0.0;
  sum= sum + m_1[i]-ytb[i];
  l1[i]= sum ;
}}
for(i=0;i<n;i++)
{ for (j=0;j<n;j++)
  {sum=0.0;
  for (k=0;k<n;k++)
  {sum= sum + B[i][k]*Yb[k][j];
  m_2[i][j]= sum ;
}}}

for(i=0;i<n;i++)
{ for (j=0;j<n;j++)
  {sum=0.0;
  for (k=0;k<n;k++)
  {sum= sum + B[i][k]*l1[k];
  m_3[i]= sum ;
}}}
for(i=0;i<n;i++)
{ for (j=0;j<n;j++)
  {sum=0.0;
  sum= sum + A[i][j]+m_2[i][j];
  q[i][j]= sum ;
```

```
}}
for(i=0;i<n;i++)
{ for (j=0;j<n;j++)
  {sum=0.0;
  sum= sum + C[i]+m_3[i];
  r[i]= sum ;
}}
for(i=0;i<n;i++)
 {for(j=0;j<n;j++)
 {a[i][j]=q[i][j];
 }}

for(i=0;i<n;i++)
 {for(j=0;j<n;j++)
 {a1[i][j]=a[i][j];
 }}

 for (i=0;i<n;i++)
{sum1=sum1+a1[i][i];
}
p1=sum1/1;
 for (i=0;i<n;i++)
 { for (j=0;j<n;j++)
 {m1[i][j]=p1*I[i][j];}}
 for (i=0;i<n;i++)
 { for (j=0;j<n;j++)
{ sum_s=0.0;
```

```
sum_s=sum_s+a1[i][j]-m1[i][j];
ab1[i][j]=sum_s;}}
    for(i=0;i<n;i++)
{ for (j=0;j<n;j++)
  {sum_s=0.0;
  for (k=0;k<n;k++)
  {sum_s= sum_s + a[i][k]*ab1[k][j];
  a2[i][j]= sum_s ;
}}}
 for (i=0;i<n;i++)
{sum2=sum2+a2[i][i];
}
p2=sum2/2;
  for (i=0;i<n;i++)
 { for (j=0;j<n;j++)
 {m2[i][j]=p2*I[i][j];}}
 for (i=0;i<n;i++)
 { for (j=0;j<n;j++)
{ sum_s=0.0;
sum_s=sum_s+a2[i][j]-m2[i][j];
ab2[i][j]=sum_s;}}
    for(i=0;i<n;i++)
{ for (j=0;j<n;j++)
  {sum_s=0.0;
  for (k=0;k<n;k++)
  {sum_s= sum_s + a[i][k]*ab2[k][j];
  a3[i][j]= sum_s ;
```

```
}}}

 for (i=0;i<n;i++)
{sum3=sum3+a3[i][i];
}
p3=sum3/3;
 for (i=0;i<n;i++)
 { for (j=0;j<n;j++)
 {m3[i][j]=p3*I[i][j];}}
 for (i=0;i<n;i++)
 { for (j=0;j<n;j++)
{ sum_s=0.0;
sum_s=sum_s+a3[i][j]-m3[i][j];
ab3[i][j]=sum_s;}}
    for(i=0;i<n;i++)
{ for (j=0;j<n;j++)
  {sum_s=0.0;
  for (k=0;k<n;k++)
  {sum_s= sum_s + a[i][k]*ab3[k][j];
  a4[i][j]= sum_s ;
}}}
 for (i=0;i<n;i++)
{ sum4= sum4+ a4[i][i];}


 p4= sum4/ 4 ;
  for (i=0;i<n;i++)
```

```
 { for (j=0;j<n;j++)
 {inverse[i][j]=ab3[i][j]/p4;}}
  for(i=0;i<n;i++)
{ for (j=0;j<n;j++)
  {sum_s=0.0;
  for (k=0;k<n;k++)
  {sum_s= sum_s + inverse[i][k]*q[k][j];
  test[i][j]= sum_s ;
}}}
  for(i=0;i<n;i++)
{ for (j=0;j<n;j++)
  {sum_s=0.0;
  for (k=0;k<n;k++)
  {sum_s= sum_s + inverse[i][k]*r[k];
  ya[i]= sum_s ;
}}}
   for(i=0;i<n;i++)
{ for (j=0;j<n;j++)
  {sum_s=0.0;
  for (k=0;k<n;k++)
  {sum_s= sum_s + Yb[i][k]*ya[k];
  m4[i]= sum_s ;
}}}
y1old=yb[0];
y2old=yb[1];
y3old=yb[2];
y4old=yb[3];
```

```
 for (i=0;i<n;i++)
 { for (j=0;j<n;j++)
{ sum_s=0.0;
sum_s=sum_s+m4[i]-l1[i];
 yb[i]=sum_s;}}
y1new=yb[0]  ;
y2new=yb[1]  ;
y3new=yb[2]  ;
y4new=yb[3]  ;
 for (b=0;b<n;b++)
  {yt[b]=ya[b];}
 convgndamp_c_1= fabs(y1new-y1old) ;
 convgndamp_c_2= fabs(y2new-y2old) ;
 convgnc3= fabs(y3new-y3old) ;
 convgnc4= fabs(y4new-y4old) ;
 }
 for (b=0;b<n;b++)
  {yt[b]=ya[b];}
t=0.0;
for (k=0;k<n;k++)
 {  for (b=0;b<n;b++)
  {m1[k][b]=m2[k][b];}}
for (k=0;k<n;k++)
 {  for (b=0;b<n;b++)
  {E[k][b]=m2[k][b];}}
for (k=0;k<n;k++)
 {  for (b=0;b<n;b++)
```

```
  {F[k][b]=m2[k][b];}}
for (k=0;k<n;k++)
 {  for (b=0;b<n;b++)
  {G[k][b]=m2[k][b];}}
for (k=0;k<n;k++)
 {  for (b=0;b<n;b++)
  {H[k][b]=m2[k][b];}}
for (k=0;k<n;k++)
 {  for (b=0;b<n;b++)
  {Y[k][b]=R1[k][b];}}

 fputs (" t(s)\t y1(x1)(m)\t y2(m/s)\t y3(x2)(m)\t y4(m/s) \n",fp);
 fprintf(fp,"  %f\t   %f\t  %f\t %f\t %f \n ",t,yt[0],yt[1],yt[2],yt[3]);
for (i=0;i<(n1-1);i++)
 {
m1[0][0]=h * yt[1];
m1[0][1]=h * fnction_1(t, yt[0],yt[1], yt[2], yt[3], w);
m1[0][2]=h * yt[3];
m1[0][3]=h * fnction_2(t, yt[0],yt[1], yt[2], yt[3], w);
m1[1][0]=h * (yt[1]+m1[0][1]/2.0);
m1[1][1]=h * fnction_1(t+h/2.0, yt[0]+m1[0][0]/2.0, yt[1]+m1[0][1]/2.0, yt[2]+m1[0][2]/2.0,
yt[3]+m1[0][3]/2.0, w) ;
m1[1][2]=h * (yt[3]+m1[0][3]/2.0);
m1[1][3]=h * fnction_2(t+h/2.0, yt[0]+m1[0][0]/2.0, yt[1]+m1[0][1]/2.0, yt[2]+m1[0][2]/2.0,
yt[3]+m1[0][3]/2.0, w) ;

m1[2][0]=h * (yt[1]+m1[1][1]/2.0);
```

```
m1[2][1]=h * fnction_1(t+h/2.0, yt[0]+m1[1][0]/2.0, yt[1]+m1[1][1]/2.0, yt[2]+m1[1][2]/2.0,
yt[3]+m1[1][3]/2.0, w) ;

m1[2][2]=h * (yt[3]+m1[1][3]/2.0);

m1[2][3]=h * fnction_2(t+h/2.0, yt[0]+m1[1][0]/2.0, yt[1]+m1[1][1]/2.0, yt[2]+m1[1][2]/2.0,
yt[3]+m1[1][3]/2.0, w) ;


m1[3][0]=h * (yt[1]+m1[2][1]);

m1[3][1]=h * fnction_1(t+h, yt[0]+m1[2][0], yt[1]+m1[2][1], yt[2]+m1[2][2], yt[3]+m1[2][3], w)
;

m1[3][2]=h * (yt[3]+m1[2][3]);

m1[3][3]=h * fnction_2(t+h, yt[0]+m1[2][0], yt[1]+m1[2][1], yt[2]+m1[2][2], yt[3]+m1[2][3], w)
;

E[0][0]=h * Y[1][0] ;

E[0][1]=h * FUHC_1(t, Y[0][0], Y[1][0], Y[2][0], Y[3][0], yt[0], yt[1], yt[2], yt[3] ) ;

E[0][2]=h * Y[3][0] ;

E[0][3]=h * FUHC_2(t, Y[0][0], Y[1][0], Y[2][0], Y[3][0], yt[0], yt[1], yt[2], yt[3] ) ;


E[1][0]=h * (Y[1][0]+E[0][1]/2.0) ;

E[1][1]=h * FUHC_1(t+h/2.0, Y[0][0]+E[0][0]/2.0, Y[1][0]+E[0][1]/2.0, Y[2][0]+E[0][2]/2.0,
Y[3][0]+E[0][3]/2.0, yt[0], yt[1], yt[2], yt[3] ) ;

E[1][2]=h * (Y[3][0]+E[0][3]/2.0) ;

E[1][3]=h * FUHC_2(t+h/2.0, Y[0][0]+E[0][0]/2.0, Y[1][0]+E[0][1]/2.0, Y[2][0]+E[0][2]/2.0,
Y[3][0]+E[0][3]/2.0, yt[0], yt[1], yt[2], yt[3] ) ;

E[2][0]=h * (Y[1][0]+E[1][1]/2.0) ;

E[2][1]=h * FUHC_1(t+h/2.0, Y[0][0]+E[1][0]/2.0, Y[1][0]+E[1][1]/2.0, Y[2][0]+E[1][2]/2.0,
Y[3][0]+E[1][3]/2.0, yt[0], yt[1], yt[2], yt[3] ) ;

E[2][2]=h * (Y[3][0]+E[1][3]/2.0) ;

E[2][3]=h * FUHC_2(t+h/2.0, Y[0][0]+E[1][0]/2.0, Y[1][0]+E[1][1]/2.0, Y[2][0]+E[1][2]/2.0,
Y[3][0]+E[1][3]/2.0, yt[0], yt[1], yt[2], yt[3] ) ;
```

```
E[3][0]=h * (Y[1][0]+E[2][1]) ;

E[3][1]=h * FUHC_1(t+h, Y[0][0]+E[2][0], Y[1][0]+E[2][1], Y[2][0]+E[2][2], Y[3][0]+E[2][3],
yt[0], yt[1], yt[2], yt[3] ) ;

E[3][2]=h * (Y[3][0]+E[2][3]) ;

E[3][3]=h * FUHC_2(t+h, Y[0][0]+E[2][0], Y[1][0]+E[2][1], Y[2][0]+E[2][2], Y[3][0]+E[2][3],
yt[0], yt[1], yt[2], yt[3] ) ;


for(l=0;l<n;l++)

{Y[l][0]=Y[l][0]+ (E[0][l]+ 2.0*E[1][l]+ 2.0*E[2][l]+ E[3][l])/6.0 ;}


F[0][0]=h * Y[1][1];

F[0][1]=h * FUHC_1(t, Y[0][1],Y[1][1], Y[2][1], Y[3][1], yt[0], yt[1], yt[2], yt[3] ) ;

F[0][2]=h * Y[3][1];

F[0][3]=h * FUHC_2(t, Y[0][1],Y[1][1], Y[2][1], Y[3][1], yt[0], yt[1], yt[2], yt[3] ) ;

F[1][0]=h * (Y[1][1]+F[0][1]/2.0) ;

F[1][1]=h * FUHC_1(t+h/2.0, Y[0][1]+F[0][0]/2.0, Y[1][1]+F[0][1]/2.0, Y[2][1]+F[0][2]/2.0,
Y[3][1]+F[0][3]/2.0, yt[0], yt[1], yt[2], yt[3] ) ;

F[1][2]=h * (Y[3][1]+F[0][3]/2.0) ;

F[1][3]=h * FUHC_2(t+h/2.0, Y[0][1]+F[0][0]/2.0, Y[1][1]+F[0][1]/2.0, Y[2][1]+F[0][2]/2.0,
Y[3][1]+F[0][3]/2.0, yt[0], yt[1], yt[2], yt[3] ) ;

F[2][0]=h * (Y[1][1]+F[1][1]/2.0) ;

F[2][1]=h * FUHC_1(t+h/2.0, Y[0][1]+F[1][0]/2.0, Y[1][1]+F[1][1]/2.0, Y[2][1]+F[1][2]/2.0,
Y[3][1]+F[1][3]/2.0, yt[0], yt[1], yt[2], yt[3] ) ;

F[2][2]=h * (Y[3][1]+F[1][3]/2.0) ;

F[2][3]=h * FUHC_2(t+h/2.0, Y[0][1]+F[1][0]/2.0, Y[1][1]+F[1][1]/2.0, Y[2][1]+F[1][2]/2.0,
Y[3][1]+F[1][3]/2.0, yt[0], yt[1], yt[2], yt[3] ) ;

F[3][0]=h * (Y[1][1]+F[2][1] ) ;

F[3][1]=h * FUHC_1(t+h, Y[0][1]+F[2][0], Y[1][1]+F[2][1], Y[2][1]+F[2][2], Y[3][1]+F[2][3],
yt[0], yt[1], yt[2], yt[3] ) ;

F[3][2]=h * (Y[3][1]+F[2][3] ) ;
```

```
F[3][3]=h * FUHC_2(t+h, Y[0][1]+F[2][0], Y[1][1]+F[2][1], Y[2][1]+F[2][2], Y[3][1]+F[2][3],
yt[0], yt[1], yt[2], yt[3] ) ;

for(l=0;l<n;l++)

{Y[l][1]=Y[l][1]+ (F[0][l]+ 2.0*F[1][l]+ 2.0*F[2][l]+ F[3][l])/6.0 ;}

G[0][0]=h * Y[1][2] ;

G[0][1]=h * FUHC_1(t, Y[0][2],Y[1][2], Y[2][2], Y[3][2], yt[0], yt[1], yt[2], yt[3] ) ;

G[0][2]=h * Y[3][2] ;

G[0][3]=h * FUHC_2(t, Y[0][2],Y[1][2], Y[2][2], Y[3][2], yt[0], yt[1], yt[2], yt[3] ) ;

G[1][0]=h * (Y[1][2]+G[0][1]/2.0 ) ;

G[1][1]=h * FUHC_1(t+h/2.0, Y[0][2]+G[0][0]/2.0, Y[1][2]+G[0][1]/2.0, Y[2][2]+G[0][2]/2.0,
Y[3][2]+G[0][3]/2.0, yt[0], yt[1], yt[2], yt[3] ) ;

G[1][2]=h * (Y[3][2]+G[0][3]/2.0 ) ;

G[1][3]=h * FUHC_2(t+h/2.0, Y[0][2]+G[0][0]/2.0, Y[1][2]+G[0][1]/2.0, Y[2][2]+G[0][2]/2.0,
Y[3][2]+G[0][3]/2.0, yt[0], yt[1], yt[2], yt[3] ) ;

G[2][0]=h * (Y[1][2]+G[1][1]/2.0) ;

G[2][1]=h * FUHC_1(t+h/2.0, Y[0][2]+G[1][0]/2.0, Y[1][2]+G[1][1]/2.0, Y[2][2]+G[1][2]/2.0,
Y[3][2]+G[1][3]/2.0, yt[0], yt[1], yt[2], yt[3] ) ;

G[2][2]=h * (Y[3][2]+G[1][3]/2.0) ;

G[2][3]=h * FUHC_2(t+h/2.0, Y[0][2]+G[1][0]/2.0, Y[1][2]+G[1][1]/2.0, Y[2][2]+G[1][2]/2.0,
Y[3][2]+G[1][3]/2.0, yt[0], yt[1], yt[2], yt[3] ) ;

G[3][0]=h * (Y[1][2]+G[2][1] ) ;

G[3][1]=h * FUHC_1(t+h, Y[0][2]+G[2][0], Y[1][2]+G[2][1], Y[2][2]+G[2][2], Y[3][2]+G[2][3],
yt[0], yt[1], yt[2], yt[3] ) ;

G[3][2]=h * (Y[3][2]+G[2][3] ) ;

G[3][3]=h * FUHC_2(t+h, Y[0][2]+G[2][0], Y[1][2]+G[2][1], Y[2][2]+G[2][2], Y[3][2]+G[2][3],
yt[0], yt[1], yt[2], yt[3] ) ;

for(l=0;l<n;l++)

{Y[l][2]=Y[l][2]+ (G[0][l]+ 2.0*G[1][l]+ 2.0*G[2][l]+ G[3][l])/6.0 ;}

H[0][0]=h * Y[1][3];

H[0][1]=h * FUHC_1(t, Y[0][3], Y[1][3], Y[2][3], Y[3][3], yt[0], yt[1], yt[2], yt[3] ) ;
```

```
H[0][2]=h * Y[3][3];

H[0][3]=h * FUHC_2(t, Y[0][3], Y[1][3], Y[2][3], Y[3][3], yt[0], yt[1], yt[2], yt[3] ) ;

H[1][0]=h * (Y[1][3]+H[0][1]/2.0);

H[1][1]=h * FUHC_1(t+h/2.0, Y[0][3]+H[0][0]/2.0, Y[1][3]+H[0][1]/2.0, Y[2][3]+H[0][2]/2.0,
Y[3][3]+H[0][3]/2.0, yt[0], yt[1], yt[2], yt[3] ) ;

H[1][2]=h * (Y[3][3]+H[0][3]/2.0);

H[1][3]=h * FUHC_2(t+h/2.0, Y[0][3]+H[0][0]/2.0, Y[1][3]+H[0][1]/2.0, Y[2][3]+H[0][2]/2.0,
Y[3][3]+H[0][3]/2.0, yt[0], yt[1], yt[2], yt[3] ) ;

H[2][0]=h * (Y[1][3]+H[1][1]/2.0);

H[2][1]=h * FUHC_1(t+h/2.0, Y[0][3]+H[1][0]/2.0, Y[1][3]+H[1][1]/2.0, Y[2][3]+H[1][2]/2.0,
Y[3][3]+H[1][3]/2.0, yt[0], yt[1], yt[2], yt[3] ) ;

H[2][2]=h * (Y[3][3]+H[1][3]/2.0);

H[2][3]=h * FUHC_2(t+h/2.0, Y[0][3]+H[1][0]/2.0, Y[1][3]+H[1][1]/2.0, Y[2][3]+H[1][2]/2.0,
Y[3][3]+H[1][3]/2.0, yt[0], yt[1], yt[2], yt[3] ) ;

H[3][0]=h * (Y[1][3]+H[2][1] ) ;

H[3][1]=h * FUHC_1(t+h, Y[0][3]+H[2][0], Y[1][3]+H[2][1], Y[2][3]+H[2][2], Y[3][3]+H[2][3],
yt[0], yt[1], yt[2], yt[3] ) ;

H[3][2]=h * (Y[3][3]+H[2][3] ) ;

H[3][3]=h * FUHC_2(t+h, Y[0][3]+H[2][0], Y[1][3]+H[2][1], Y[2][3]+H[2][2], Y[3][3]+H[2][3],
yt[0], yt[1], yt[2], yt[3] ) ;

for(l=0;l<n;l++)

{Y[l][3]=Y[l][3]+ (H[0][l]+ 2.0*H[1][l]+ 2.0*H[2][l]+ H[3][l])/6.0 ;}

  t=t+h;

for (j=0;j<n;j++)

{ yt[j]= yt[j] + (m1[0][j]+ 2.0*m1[1][j]+ 2.0*m1[2][j]+ m1[3][j])/6.0 ; }

 printf("\n at t=%f   y1=%f\t  y3=%f\t  \n",t,yt[0],yt[2]);

   fprintf(fp,"  %f\t   %f\t  %f\t %f\t %f \n ",t,yt[0],yt[1],yt[2],yt[3]);


      }
```

```
  fprintf(fp,"  %f\t   %f\t  %f\t %f\t %f \n ",t+h,yb[0],yb[1],yb[2],yb[3]);


fputs("\n\n",fp);

fputs("Gass_1\tGass_2\tSpring_m1\t Spring_m1p\t Spring_m2\t Spring_m2p\t Damp_c1\t
Damp_c1p\t Damp_c2\t Damp_c2p \n",fp);

fprintf(fp,"%f\t %f\t %f\t %f\t %f\t %f\t %f\t %f\t %f\t
%f\n",Gass1,Gass2,Springm1,Springm1p,Springm2,Springm2p,Dampc1,Dampc1p,Dampc2,Dam
pc2p);

fputs("\n\n",fp);

fputs("alpha1\t alpha2\t beta1\t beta2\n",fp);

fprintf(fp,"%f\t %f\t %f\t %f\n",Alpha1,Alpha2,Beta1,Beta2);

fputs("\n\n",fp);

fputs("Boundary Conditions:\n",fp);

fputs("y1(a)\t y2(b)\t y3(a)\t y4(b)\n",fp);

fprintf(fp,"%f\t %f\t %f\t %f\n",C[0],C[1],C[2],C[3]);

 fclose(fp);



getch();


}
```